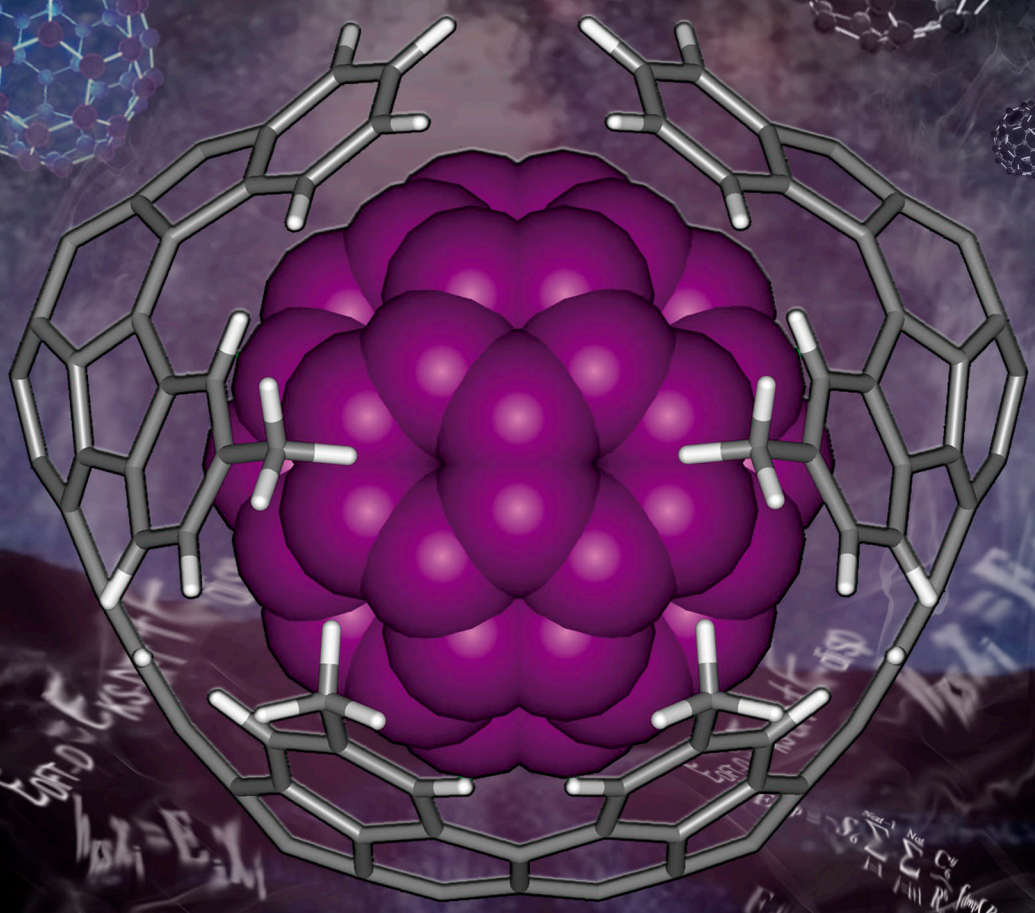
USC
UNIVERSIDADE DE SANTIAGO DE COMPOSTELA
FACULTADE DE QUÍMICA
DEPARTAMENTO DE QUÍMICA-FÍSICA

TAILORING BUCKYBOWLS FOR FULLERENE RECOGNITION



TESE DE DOUTORAMENTO

Daniela Josa

UNIVERSIDADE DE SANTIAGO DE COMPOSTELA

FACULTADE DE QUÍMICA

DEPARTAMENTO DE QUÍMICA-FÍSICA

PhD Thesis

Tailoring buckybowls for fullerene recognition

Daniela Josa

Santiago de Compostela, Mayo 2015

Los Dres. JESÚS RODRÍGUEZ OTERO y ENRIQUE MANUEL CABALEIRO LAGO, Profesores titulares del Departamento de Química Física de la Universidade de Santiago de Compostela, autorizan la presentación de la tesis doctoral titulada **"Tailoring buckybowls for fullerene recognition"** realizada por Dña. Daniela Josa, Licenciada en Química, para optar al Grado de Doctora en Química.

Y para que así conste, firmamos el presente documento en Santiago de Compostela, a 8 de Mayo de 2015.

Fdo.: Dr. Jesús Rodríguez Otero

Fdo.: Dr. Enrique M. Cabaleiro Lago

Agradecimientos

If I have seen further it is by standing on the shoulders of giants.

Sir Isaac Newton

Quiero expresar mi más sincero agradecimiento

A Dios por la vida, la salud y la fuerza para seguir adelante. Gracias Señor, por direccionar mis pasos, por hacer posible el desarrollo de esta tesis, sobre todo por poner personas tan maravillosas en mi vida que me han amado, apoyado y enseñado. Además no podría dejarte de darte las gracias por concederme la beca FPU, sin ella seria imposible llevar a cabo este trabajo.

A mis directores de tesis, Jesús y Enrique por guiarme en el reto de realizar una tesis. En especial a Jesús, por concederme el privilegio de trabajar en su grupo, por depositar su confianza en mí, ofreciéndome libertad y también apoyo constante, y sobre todo por sus sabios consejos.

A la profesora Ángeles por la supervisión de mis primeros trabajos en el grupo.

Al Ministerio de Educación de España por haberme concedido una beca FPU y al proyecto INCITE09209103PR de la Xunta de Galicia por el soporte económico.

Al Centro de Supercomputación de Galicia (CESGA) por el uso de sus ordenadores.

Al Centro Singular de Investigación en Química Biológica y Materiales Moleculares (CIQUS) por el apoyo económico.

Al profesor Hélio y su grupo de investigación, en especial al Dr. Maurício por la introducción al método SCC-DFTB-D.

Al profesor Teodorico y al graduado Lucas por la colaboración en parte de los trabajos de esta tesis.

A mis compañeros de laboratorio, en especial, Iván y Marcos por las contribuciones directas o indirectas a esta tesis.

A los profesores Saulo, María Merced y María Carmen por las enseñanzas y apoyo en las clases prácticas en las que he colaborado como monitora y contratada FPU.

A mis profesores de la carrera (Teodorico, Elaine, Matheus, Ruy, Luís, Joaquim y Maria do Carmo) y del doctorado (Antonio, Jesús, Iñaki y Vicent) por sus excelentes clases e importante contribución a mi formación.

A mis directores de iniciación científica en la carrera, Teodorico y Elaine, en especial a Teo por concederme el privilegio de trabajar en su grupo, por los trabajos confiados, su gran apoyo y sobre todo por sus valiosos consejos y motivación.

A mis compañeras de piso Daniely y Michele que hicieron mi adaptación en Santiago mucho más sencilla y agradable. Gracias chicas, por vuestro apoyo en los momentos difíciles.

A Silvana por tu amistad tan valiosa, por el apoyo, ánimo y un montón de buenos momentos compartidos desde la facultad.

A toda mi gran familia, padres, esposo, suegros, abuelos, tíos, hermanos, cuñados, primos y sobrinos, por todo vuestro amor, apoyo y comprensión. Sois maravillosos, os quiero mucho.

En especial quiero agradecer a mis padres Daniel y Denise por el amor incondicional, por las palabras de consuelo y ánimo en los momentos difíciles, por todos sus esfuerzos para que yo pudiera alcanzar mis objetivos.

A mi esposo André, por todo su amor, compañerismo, comprensión y consejos, por estar a mi lado en todas las etapas de mi doctorado, por su constante fuerza y ánimo en los momentos difíciles. Gracias por hacer mi vida más repleta y feliz.

En fin, a todas las personas que directa o indirectamente han contribuido para el desarrollo de esta tesis.

A mis padres, Daniel y Denise,
y a mi esposo André

Contents

RESUMEN ..... **I**

CHAPTER 1: THESIS OVERVIEW **1**

1.1. MOTIVATION 1
1.2. THESIS OBJECTIVES 3
1.3. THESIS ORGANIZATION 3
1.4. PUBLICATIONS 5
1.5. REFERENCES 7

CHAPTER 2: INTRODUCTION **9**

2.1. SUPRAMOLECULAR CHEMISTRY 9
2.2. INTERMOLECULAR INTERACTIONS 10
2.2.1. Long-range interactions *12*
2.2.2. Short-range interactions *13*
2.3. INTERACTIONS INVOLVING CURVED POLYCYCLIC AROMATIC SYSTEMS 13
2.4. FULLERENES 17
2.5. BUCKYBOWLS 19
2.5.1. Interest of buckybowls *20*
2.5.2. Structural studies of buckybowls *21*
2.5.3. Interactions with buckybowls *22*
2.6. MOLECULAR TWEEZERS 23
2.6.1. Molecular tweezers with buckybowls pincers *26*
2.6.2. Applications of molecular tweezers with buckybowls pincers *27*
2.7. REFERENCES 29

CHAPTER 3: METHODOLOGY **35**

3.1. INTRODUCTION 35
3.2. DENSITY FUNCTIONAL THEORY (DFT) 37
3.2.1. Hohenberg and Kohn theorems *37*
3.2.2. Kohn-Sham method *38*
3.3. EXCHANGE-CORRELATION FUNCTIONALS 42
3.4. DISPERSION-CORRECTED DENSITY FUNCTIONAL THEORY (DFT-D) 43
3.4.1. DFT-D2 ..... *43*
3.5. REDUCING COMPUTATIONAL COST 44
3.5.1. Resolution of the identity density functional theory *45*
3.6. DENSITY FUNCTIONAL BASED TIGHT-BINDING 47
3.6.1. The Self-Consistent Charge Correction: SCC-DFTB *51*
3.6.2. Dispersion-Corrected (SCC-) DFTB *52*
3.7. BASIS SETS 53
3.8. SUPERMOLECULE METHOD 56
3.9. BASIS SET SUPERPOSITION ERROR (BSSE) 57
3.9.1. Counterpoise correction including monomer deformation *58*
3.10. PYRAMIDALIZATION ANGLE (π-ORBITAL AXIS VECTOR, POAV) 58
3.11. MOLECULAR ELECTROSTATIC POTENTIAL (MEP) MAPS 59
3.12. NON-COVALENT INTERACTIONS (NCI) METHOD 61

3.12.1. Identifying non-covalent interactions *62*
3.12.2. Identifying interaction types *62*
3.12.3. Type of calculations *64*
3.13. REFERENCES 65

CHAPTER 4: SUBSTITUENT EFFECTS IN CORANNULENE DIMERS 71
4.1. INTRODUCTION 71
4.2. COMPUTATIONAL DETAILS 73
4.3. RESULTS AND DISCUSSION 74
4.3.1. Corannulene monomers *74*
4.3.2. Corannulene dimers *75*
4.3.3. Substituted corannulene dimers *79*
4.4. CONCLUSIONS 81
4.5. REFERENCES 82

CHAPTER 5: ANALYSIS OF THE PERFORMANCE OF DFT-D, M05-2X AND M06-2X FUNCTIONALS FOR STUDYING Π···Π INTERACTIONS 85
5.1. INTRODUCTION 85
5.2. COMPUTATIONAL DETAILS 86
5.3. RESULTS AND DISCUSSION 87
5.3.1. Complexes from the S22 benchmark database *87*
5.3.2. Complexes with eclipsed planar complexes *88*
5.3.3. Complexes with curved monomers *90*
5.3.4. Mixed Complexes *93*
5.4. CONCLUSIONS 94
5.5. REFERENCES 95

CHAPTER 6: SUBSTITUTED CORANNULENES AND SUMANENES AS FULLERENE RECEPTORS 97
6.1. INTRODUCTION: 97
6.2. COMPUTATIONAL DETAILS 98
6.3. RESULTS AND DISCUSSION 99
6.3.1. Unsubstituted complexes *100*
6.3.2. Substituted complexes *100*
6.4. CONCLUSIONS 110
6.5. REFERENCES 110

CHAPTER 7: RING-ANNELATED CORANNULENES AS FULLERENE RECEPTORS 113
7.1. INTRODUCTION 113
7.2. COMPUTATIONAL DETAILS 114
7.3. RESULTS AND DISCUSSION 115
7.4. CONCLUSIONS 124
7.5. REFERENCES 125

CHAPTER 8: IN SEARCH OF BUCKYBOWLS FOR FULLERENE RECOGNITION 127
8.1. INTRODUCTION 127
8.2. COMPUTATIONAL DETAILS 128
8.3. RESULTS AND DISCUSSION 129

8.3.1. Performance of B97-D2//SCC-DFTB-D for studying π···π interactions..130
8.3.2. Stacking interactions between buckybowls and fullerenes C_{60}, C_{70}, and C_{40} 133
8.4. CONCLUSIONS 141
8.5. REFERENCES 142

CHAPTER 9: FULLERENE RECOGNITION WITH MOLECULAR TWEEZERS MADE UP OF EFFICIENT BUCKYBOWLS 145
9.1. INTRODUCTION 145
9.2. COMPUTATIONAL DETAILS 148
9.3. RESULTS AND DISCUSSION 149
9.3.1. Analysis of B97-D2/TZVP//SCC-DFTB-D performance regarding to B97-D2/TZVP 149
9.3.2. Improving the ability of buckycatcher $C_{60}H_{28}$ for catching C_{60} 153
9.4. CONCLUSIONS 159
9.5. REFERENCES 160

CHAPTER 10: GENERAL CONCLUSIONS 163

APPENDIX A: SUPPORTING INFORMATION FOR CHAPTER 6 167
A.1. MODIFIED FIGURE 6.3 167
A.2. DISPERSION CONTRIBUTION VS. INTERACTION ENERGY 168
A.3. MEP OF C_{60} AND C_{70} 169

APPENDIX B: SUPPORTING INFORMATION FOR CHAPTER 7 171
B.1. WHY 4···C_{60} IS MORE STABLE IN THE STAGGERED CONFORMATION? 171
B.2. NCIPLOTS 175
B.3. NBO CALCULATIONS 176

APPENDIX C: SUPPORTING INFORMATION FOR CHAPTER 8 177
C.1. FULLERENE FACES 177
C.2. SCHEME FOR "BUILDING" THE COMPLEXES 178
C.3. COMPLETE INTERACTION ENERGIES 179
C.4. INTERACTION ENERGY VS. EQUILIBRIUM DISTANCE 181
C.5. FLEXIBILITY OF FLAPS 182
C.6. MEPS OF COMPOUNDS 2, 3, 10, AND 11 183
C.7. NCIPLOTS 184

APPENDIX D: SUPPORTING INFORMATION FOR CHAPTER 9 191
D.1. INTERACTION ENERGIES USING DIFFERENT DFT-D METHODS 191
D.2. BSSE 193
D.3. B97-D2/TZVP//SCC-DFTB-D VS. B97-D2/TZVP INTERACTION ENERGY 194
D.4. B97-D2/TZVP//SCC-DFTB-D RESULTS 195
D.5. NCIPLOTS 196

Resumen

El descubrimiento de una nueva forma de carbono elemental, los fulerenos, a mediados de los años 80 del siglo pasado inició una actividad investigadora sin precedentes en el campo de la física, la química y la ciencia de materiales. Además, este descubrimiento ha conducido a un especial interés acerca de los hidrocarburos aromáticos policíclicos (*polycyclic aromatic hydrocarbons*, PAH) que poseen superficies curvadas de carbonos π, comúnmente conocidos como *buckybowls*.

Los *buckybowls* se destacan por su arquitectura única en forma de cuenco molecular que proporciona dos caras distintas, una cóncava y otra convexa lo cual amplía de manera notable su potencialidad con respecto a los PAHs estándar. Sus representantes más sencillos son el coranuleno ($C_{20}H_{10}$) y el sumaneno ($C_{21}H_{12}$), los cuales corresponden a un trozo del buckminsterfulereno (C_{60}). Por esta razón también reciben el nombre de fragmentos de fulereno.

En los últimos años, el coranuleno ha sido objeto de intensos estudios experimentales y teóricos. Cabe destacar que recientemente el grupo de Jay Siegel ha optimizado el proceso de síntesis del coranuleno a escala de kilogramos (J. S. Siegel *et al.*, *Org. Process Res. Dev.* **2012**, *16*, 664). Sin duda, la producción de coranuleno a escala de kilogramo marca la transición del coranuleno desde un compuesto de interés académico a una entidad química con un potencial futuro comercial.

El mayor interés de los *buckybowls* es el relacionado con la formación de complejos intermoleculares de diversa naturaleza. Este es el ámbito de la química supramolecular, que implica el uso de interacciones no covalentes para el ensamblaje de moléculas en estructuras estables, bien definidas, denominadas supramoléculas. Así, los *buckybowls* pueden exhibir interacciones intermoleculares con un variado espectro de diferentes especies, tales como metales de transición, cationes metálicos y aniones. Además, si interaccionan con otras superficies curvadas ello puede dar lugar a un tipo muy interesante de interacción conocido como interacción cóncavo-convexa de tipo π···π. Esta interacción puede tener una enorme utilidad práctica como es el caso de las pinzas moleculares que pueden retener especies de gran interés, como por ejemplo los fulerenos; en este caso los *buckybowls* pueden ser utilizados como uno de los más eficientes *buckycatchers*.

Mientras que las interacciones π···π de compuestos aromáticos planos han sido bien estudiadas, no ocurre lo mismo con los compuestos curvados. Por lo tanto, el objetivo de esta tesis es estudiar extensivamente las interacciones π···π cóncavo-convexas a fin de averiguar los principales factores que controlan este tipo de interacciones.

Hoy en día, uno de los campos más activos en la química de los fulerenos es la búsqueda de receptores moleculares capaces de formar agregados estables con ellos. Además de la importancia de los receptores de fulerenos para separar los fulerenos de los demás componentes del hollín, también permiten desarrollar nuevos materiales para la conversión de la energía solar, la optoelectrónica, la catálisis y los interruptores moleculares. De este modo, el diseño y la síntesis de receptores de fulereno ha sido un

tema de gran importancia en los últimos años, y una variedad de compuestos han sido explorados en busca de receptores de fulerenos más eficaces y/o selectivos.

Dado que las fuerzas de dispersión parecen predominantes en el reconocimiento molecular de los fulerenos, utilizar la complementariedad cóncavo-convexa es sin duda una estrategia muy prometedora para el diseño de nuevos receptores de fulerenos, tanto en términos de la estabilidad como de la selectividad de los complejos formados.

Desafortunadamente, los ejemplos de receptores cóncavos de fulerenos son relativamente escasos dado que las moléculas curvadas no son siempre un objetivo sintético fácil debido a sus estructuras fuertemente tensionadas. En este contexto, el diseño y la síntesis de receptores moleculares de fulerenos que incorporen *buckybowls* en su estructura parece muy prometedor, dado que la superficie cóncava de los *buckybowls* se ajusta muy bien a la superficie convexa de los fulerenos y que, además, varios *buckybowls* han sido sintetizados en los últimos años.

La primera evidencia definitiva de fuertes interacciones π···π entre el coranuleno y el C_{60} fue publicada en 2007, cuando Sygula y col. sintetizaron una pinza molecular ($C_{60}H_{28}$, un *buckycatcher*) formada por dos unidades de coranuleno que puede atrapar un fulereno (A. Sygula *et al. J. Am. Chem. Soc.* **2007**, *129*, 3842). El estudio experimental sugiere que la fuerza de la interacción proviene de interacciones π···π puras entre el fulereno convexo y las caras cóncavas de las dos subunidades de coranuleno convenientemente orientadas. Desde entonces, predecir cómo modificar este *buckycatcher* para mejorar su eficiencia y/o selectividad se ha convertido en un tema de gran interés.

Aunque muchos de los más importantes usos de los *buckycatchers* están aún por descubrir, su aplicación real a corto plazo se puede concretar fundamentalmente en dos campos: como fase estacionaria para la separación de fulerenos y como complejos *buckycatcher*-fulereno en dispositivos fotovoltaicos.

Sin lugar a dudas, el diseño y síntesis de nuevas pinzas moleculares es un tema de gran interés. Sin embargo, el esquema clásico para sintetizar pinzas moleculares es un proceso largo y costoso, que incluye seleccionar los brazos y espaciadores que parecen probables candidatos para maximizar la interacción con los fulerenos; sintetizar varias pinzas moleculares, y a continuación probar su capacidad para el reconocimiento molecular en disolución y en estado sólido. En este contexto, la utilización de modelos computacionales para diseñar e identificar objetivos sintéticos que maximicen las interacciones π···π es altamente recomendable. Por tanto, el objetivo final de esta tesis doctoral es averiguar cómo modificar la pinza molecular propuesta por Sygula y col. para mejorar su eficacia y/o selectividad. Con este fin, seis estudios teóricos detallados de las interacciones π···π cóncavo-convexo entre *buckybowls* y fulerenos fueron llevados a cabo (capítulos 4-9).

Cabe destacar que el éxito en el diseño de sistemas eficientes requiere un conocimiento en profundidad de las características de la interacción π···π. Cálculos precisos mediante funciones de onda basadas en cálculos *ab initio* de alto nivel, como CCSD(T), dan lugar a un gran nivel de exactitud cuando se utilizan bases de gran tamaño, pero este procedimiento tiene un coste prohibitivo incluso para sistemas relativamente pequeños. Métodos más económicos, tales como el MP2, siguen siendo

inviables para sistemas grandes y, además, tienden a sobrestimar la magnitud de la energía de interacción. Por lo tanto, la opción más viable sería utilizar la teoría del funcional de la densidad (DFT), que permite tratar sistemas grandes con un coste computacional razonable. Desafortunadamente, los métodos DFT convencionales fallan completamente en el tratamiento de los efectos dispersivos. Para resolver este problema, recientemente se han desarrollado dos tipos de estrategias. La primera de ellas consiste en el desarrollo de un nuevo tipo de funcionales como los M05 y M06. La segunda estrategia consiste en tratar de corregir las deficiencias de los funcionales existentes, añadiendo un término empírico para representar la dispersión: éstos son los denominados métodos DFT-D.

A pesar de los progresos logrados en los últimos años, la evaluación teórica rigurosa de la fortaleza de las interacciones π···π cóncavo-convexo, todavía está en una fase muy poco avanzada. De este modo para la pinza sintetizada por Sygula, la estimación de la energía de interacción abarca un gran rango que va desde 21 hasta 43 kcal/mol, dependiendo del modelo DFT utilizado. En este contexto, conocer el rango de aplicación y limitación de las nuevas variantes DFT para el estudio de las interacciones π···π cóncavo-convexo es sin duda un paso fundamental para el éxito en el diseño de las pinzas moleculares. Por lo tanto, el rendimiento de una serie de funcionales DFT-D, M05-2X y M06-2X para estudiar las interacciones π···π cóncavo-convexo fue evaluado a lo largo de los capítulos 4 y 5.

En el **capítulo 4** se llevó a cabo un estudio de los efectos de los sustituyentes y de la curvatura en dímeros de coranuleno. Las moléculas de coranuleno fueron sustituidos con cinco unidades alternadas de Br, Cl, CH_3, C_2H o CN. En este estudio una "copia del fulereno" denominada C_{60}-like, coranuleno con la curvatura del buckminsterfulereno (C_{60}) fue incluida a fin de imitar la interacción cóncavo-convexa entre los coranulenos sustituidos y el fulereno C_{60}. Las energías de interacción entre los monómeros fueron calculadas utilizando los funcionales M06-2X, B97-D y ωB97X-D y el conjunto de función de base 6-31+G*. Los efectos de los sustituyentes fueron evaluados en base a la contribución de la dispersión y mediante mapas del potencial electrostático molecular (MEP). Otro objetivo de este estudio fue evaluar el rendimiento de los funcionales M06-2X, B97-D y ωB97X-D para una serie de dímeros de coranuleno. Los resultados fueron comparados con los obtenidos por Sygula y Saebø al nivel SCS-MP2/cc-pVTZ (A. Sygula and S. Saebø, *Int. J. Quant. Chem.*, **2009**, *109*, 65). Los resultados indican que los cálculos con los métodos DFT-D, utilizando los funcionales B97-D y ωB97X-D producen mejores energías de interacción para los dímeros de coranuleno que el funcional M06-2X, comparado con el método SCS-MP2. Todos los coranulenos penta-sustituidos evaluados se comportan como un mejor *buckycatcher* que el coranuleno no sustituido. La capacidad de los *buckybowls* sustituidos para atrapar la copia del fulereno está directamente relacionada con el carácter dador/aceptor de los sustituyentes. Los resultados de los MEPs indican que la introducción de sustituyentes que retiran carga electrónica como el Br, Cl y CN y que hacen el lado cóncavo del *bowl* (interior) más positivo, permiten una mejor interacción con el MEP negativo de la cara convexa (exterior) de la copia del fulereno. El efecto más notable fue producido por la sustitución con grupos CN, que presentó un aumento de 9,12 kcal/mol en la energía de interacción con relación al coranuleno original. Por otra parte hay que destacar que no sólo las interacciones electrostáticas son suficientes para explicar la diferente capacidad de interacción de los

buckybowls sustituidos con los fulerenos. Las dos contribuciones, electrostática y dispersión son importantes para analizar el efecto de los sustituyentes en las interacciones de apilamiento π···π en los sistemas curvados.

El **capítulo 5** se centra en un análisis más detallado del rendimiento de una variedad de funcionales DFT-D, M06-2X y M05-2X para estudiar las interacciones π···π. El rendimiento de los funcionales B97-D, PBE-D, B-LYP-D, BP86-D, M06-2X y M05-2X fue evaluado para cuatro grupos representativos de complejos con interacciones π···π: (1) complejos de la base de datos S22 (P. Jurecka *et al.*, *Phys. Chem. Chem. Phys.* **2006**, *8*, 1985); (2) complejos con PAHs planos eclipsados; (3) complejos con PAHs curvados; (4) complejos mixtos (compuesto por PAHs planos y curvados). Los resultados fueron comparados con los obtenidos previamente mediante cálculos CCSD(T) y QCISD(T). Los resultados indican que el funcional B97-D parece el más indicado entre los funcionales evaluados para el estudio de las interacciones π···π. Por lo tanto, este funcional ha sido utilizado en los estudios posteriores.

Una vez elegido el nivel de cálculo, el próximo paso de este trabajo fue estudiar extensivamente los efectos que pueden reforzar la interacción entre los *buckybowls* y los fulerenos y/o hacer que ésta sea selectiva. Sin duda, el conocimiento de los efectos de la curvatura y de los sustituyentes en los *buckybowls* podría aportar informaciones relevantes para el diseño de nuevos receptores de fulerenos. Por lo tanto, dichos efectos fueron estudiados en los capítulos 4, 6, 7 y 8.

Cabe resaltar que los dos fulerenos más populares C_{60} y C_{70}, son bastante similares, pero muestran ciertas propiedades únicas. De este modo, sería muy interesante separar estas estructuras similares por medio de las pinzas moleculares. Desafortunadamente, estudios recientes muestran energías de interacción muy similares para los complejos entre la pinza molecular tradicional con el C_{60} y el C_{70}. Así, encontrar *buckybowls* capaces de discriminar C_{60} del C_{70} es un tema de gran interés. Por lo tanto, ambos fulerenos fueron estudiados en los capítulos 6-8 de esta tesis.

En el **capítulo 6** se estudiaron las interacciones de apilamiento entre *buckybowls* sustituidos (coranuleno y sumaneno) con fulerenos (C_{60} y C_{70}). Los monómeros de coranuleno y sumaneno fueron sustituidos con cinco y seis unidades de Br, Cl, CH_3, C_2H o CN, respectivamente. El principal objetivo de este trabajo ha sido complementar los resultados obtenidos en el capítulo 4, donde una copia del fulereno (C_{60}-like) fue utilizada en las interacciones de apilamiento con los coranulenos sustituidos. Otro objetivo de este trabajo ha sido ampliar nuestro estudio, introduciendo sumanenos sustituidos y el fulereno C_{70}. Los resultados muestran que todos los *buckybowls* sustituidos evaluados se comportan como un *buckycatcher* mejor que los *buckybowls* no sustituidos. El sumaneno sustituido con seis grupos CH_3 da lugar al complejo más favorable. Las interacciones CH···π son en gran parte responsables de este resultado. Además, los resultados de este trabajo muestran que el C_{60}-like, utilizado en el capitulo 4, no parece comportarse correctamente en la reproducción de las interacciones π···π cóncavo-convexa entre *buckybowls* y fulerenos. La debilidad del C_{60}-like proviene de la incapacidad de esta estructura para reproducir las características electrostáticas del C_{60} completo. Sin embargo, los resultados utilizando C_{60}-like no son completamente fallidos porque esta

estructura simplificada es capaz de reproducir bastante bien el efecto dispersivo (que es la contribución más importante) del C_{60} real.

En el **capítulo 7** se aborda el estudio de las interacciones de apilamiento π···π entre coranulenos anillados y los fulerenos C_{60} y C_{70}. Para este propósito anillos saturados e insaturados de tres, cuatro, y cinco miembros fueron añadidos a los cinco enlaces periféricos del coranuleno (enlaces *rim*). Además, se evaluaron los efectos de sustitución de unidades de NH, O y S en cada uno de los cinco anillos saturados de cinco miembros anillados a los enlaces *rim* del coranuleno. Los coranulenos anillados parecen estructuras adecuadas para el estudio adicional de la capacidad de los coranulenos como receptores de fulerenos. Además de que la anillación en los enlaces *rim* del coranuleno aplana gradualmente el *bowl* también introduce grupos CH_2 en la estructura del *bowl* los cuales pueden interaccionar con los fulerenos mediante interacciones CH···π. Los resultados muestran energías de coordinación más grandes que la del coranuleno para todos los casos estudiados; en el mejor de los casos se encontró un aumento de casi el 90%. De acuerdo con los resultados, el aumento de la energía de los complejos está directamente relacionado con el aumento de la contribución de la dispersión, donde las interacciones CH···π juegan un papel muy importante. Por otra parte, la inclusión de heteroátomos en los anillos saturados de cinco miembros tienen un efecto bastante pequeño, de modo que las interacciones CH···π permanecen como la característica principal.

Aunque varios *buckybowls* con diferentes propiedades geométricas y electrónicas han sido sintetizados en los últimos años, la mayoría de los estudios de interacción de apilamiento entre *buckybowls* y fulerenos han estado centrados en el coranuleno y sus derivados. Por otro lado, el cambio de los coranulenos que constituyen la mayor parte del tradicional *buckycatcher* por otros *buckybowls* parece una estrategia muy prometedora para mejorar su eficiencia. Por lo tanto, el objetivo del **capitulo 8** es probar una serie de *buckybowls* con diferente tamaños y estructuras como posibles receptores de fulerenos C_{60}, C_{70} y C_{40}. Un estudio exhaustivo teniendo en cuenta las diferentes orientaciones de los fulerenos fue llevado a cabo con el fin de obtener la disposición más favorable para la interacción con los *bowls*. Aunque B97-D2 parece un buen enfoque para el estudio de las interacciones π···π, este método es todavía muy costoso para ser empleado en una búsqueda metódica de sistemas adecuados para mejorar la eficiencia y/o la selectividad de los receptores de fulerenos. Por lo tanto, otro objetivo de este trabajo fue evaluar el rendimiento de una metodología más "económica", la B97-D2//SCC-DFTB-D, y comparar los resultados con los obtenidos usando B97-D2 en cuatro grupos de complejos con interacciones π···π: (1) complejos con PAHs plano-eclipsados; (2) complejos con PAHs curvados; (3) complejos mixtos (compuestos por PAHs planos y curvados); (4) complejos formados por PAHs curvados y el C_{60}. Los resultados muestran que los cálculos B97-D2/TZVP//SCC-DFTB-D son una herramienta muy útil para una rápida selección de las posibles estrategias para el diseño racional de las pinzas moleculares. En cuanto a la capacidad de *catching* de los diferentes *buckybowls*, se puede concluir que la forma del *buckybowl* juega un papel crucial en su éxito. De este modo, la introducción de "solapas" en la estructura de los *buckybowls* mediante la *benzannelation* del *rim* de los *buckybowls* parece una estrategia muy prometedora para el diseño de nuevos receptores de fulerenos. Esta estrategia, además de aumentar el tamaño del sistema π también aumenta el número de átomos de hidrógeno que pueden interactuar con los fulerenos a través de interacciones CH···π. Con el fin de comprobar esta estrategia, fue propuesto en este

estudio un derivado curvado del hexabenzocoroneno ($C_{72}H_{24}$). Como era esperado, este *buckybowl* ideado muestra la mejor capacidad para atrapar a los fulerenos C_{60}, C_{70} y C_{40} entre los *buckybowls* evaluados. Cabe destacar que su interacción con el C_{60} es tres veces la correspondiente al *buckybowl* prototípico, el coranuleno. Por otra parte, cuanto más rígido y compacto sea un *buckybowl*, éste presenta una capacidad menor para interactuar con los fulerenos.

Todas las interacciones de apilamiento entre los *buckybowls* evaluados en esta tesis con el fulereno C_{60} muestran valores de energía de coordinación bastante similares a los obtenidos con el fulereno C_{70}. Por lo tanto, no se espera que estos *buckybowls* se unan específicamente a uno de los fulerenos cuando se expongan a una mezcla de fulerenos C_{60}/C_{70}. Por otro lado, los complejos con el C_{40} sí que presentaron una disminución significativa en la energía de interacción con respecto a C_{60} y C_{70}. Las mayores diferencias se producen para el pentaindenocoranuleno ($C_{50}H_{20}$) y el derivado curvado de hexabenzocoroneno ($C_{72}H_{24}$) que muestran una disminución de 3,43 y 4,56 kcal/mol con respecto al C_{60}, respectivamente. Curiosamente, estos son los únicos *buckybowls* estudiados (con C_{40}) que tienen "solapas" en su estructura. De este modo, la introducción de "solapas" en el borde del *bowl* quizás también podría ser una estrategia útil para el diseño de *buckybowls* destinados a la separación selectiva de mezclas de fulerenos.

Finalmente, el **capítulo 9** se centra en el diseño teórico de nuevas pinzas moleculares como potenciales receptores de fulereno C_{60}. En este estudio fueron evaluadas tres estrategias para mejorar la eficiencia del tradicional *buckycatcher* sintetizado por Sygula y col.: (1) cambiar los brazos de la pinza formados por coranulenos por otros *buckybowls*; (2) cambiar el espaciador tetrabencil ciclooctatetraeno por uno de tipo *buckybowl*; (3) introducir sustituyentes metilos en la estructura del *buckycatcher*. Cálculos de nivel B97-D2/TZVP//SCC-DFTB-D fueron empleados en este estudio con el fin de obtener una rápida selección de las estrategias adecuadas para el diseño de nuevos *buckycatchers*. Además, todos los complejos fueron optimizaron posteriormente al nivel B97-D2/TZVP con el fin de obtener resultados más precisos. Todas las estrategias propuestas en este estudio proporcionan un aumento notable en la interacción con el C_{60}. Así, la combinación de estas tres estrategias parece un camino prometedor para el diseño de nuevas pinzas moleculares. La mejor pinza molecular modelada en este estudio presentó una energía de coordinación 2,6 veces mayor que la obtenida por la pinza molecular tradicional.

Chapter 1

Thesis Overview

This Chapter provides an overview of the research works presented in this thesis. It describes the motivation to carry out this work, objectives, structure of the thesis and publications obtained from the studies performed herein.

1.1. Motivation

Nearly 30 years after their discovery, fullerenes, the third allotrope of carbon, remain attracting the interest of many researches worldwide due to their unique properties and applications in wide-ranging fields from material science to medicine. [1-3]

Nowadays, one of most active fields in fullerene chemistry is the search for molecular receptors able to form stable associates with them.[4] Besides the importance of fullerene receptors to separate fullerene of the soot, it also enables to develop new materials for solar energy conversion, optoelectronics, catalysis and switching.[3, 5, 6] So, the design and synthesis of fullerene receptors has been a subject of big significance in recent years and a variety of hosts have been explored with the goal of finding more effective and selective fullerene receptors.[7-23]

A promising strategy to design new molecular receptors for fullerenes is using the concave-convex complementarity. Nevertheless, the examples of concave fullerenes receptors are relatively scarce given that curved molecules are not always an easy synthetic target due to their tensioned structures.[24] In this context, bowl-shaped polycyclic aromatic hydrocarbons, commonly known as buckybowls or fullerene fragments seem very attractive, given that several buckybowls have been synthetized in recent years[25-32] and their concave surface can fit adequately to the convex surface of the fullerenes through concave-convex "ball-and-socket" π···π interactions.

In 2007, Sygula and co-workers have synthesized a well-known molecular tweezers (a buckycatcher, $C_{60}H_{28}$)[33] made up by two units of corannulene (the smallest buckybowl, $C_{20}H_{10}$) that can trap fullerenes. Thenceforth, predicting how to modify this buckycatcher to improve its efficiency and/or selectivity has become a subject of great interest.

The usefulness of buckycatchers could be very wide. Sygula and Collier envision future applications for the buckycatchers as stationary phases in liquid chromatography for the separation of fullerenes and as buckycatcher-fullerene complexes in photovoltaic devices.[34] On the other hand, theoretical studies have already predicted potential applications for the complex $C_{60}H_{28}\cdots C_{60}$, such as a two-photon absorption active (TPA)[35] and charge-transfer mediating material with attractive applications in nanoelectronic devices.[36] In addition, supramolecular complexes made up by buckycatcher $C_{60}H_{28}$ and endohedral nitrogen fullerene ($N@C_{60}$) could be a candidate for quantum-information processing (QIP) as qubit.[37]

Undoubtedly, the design and synthesis of buckycatchers with more ability and/or selectivity than buckycatcher $C_{60}H_{28}$ is a task of great interest. However, the classic approach to synthesize these buckycatchers is a hard and expensive task which includes (1) selecting tethers and pincers that appear likely to maximize binding of the target guests with the host, (2) synthesizing many molecular tweezers, and then (3) testing their molecular recognition abilities in solution and in the solid state. In this context, the utilization of computational models to design and identify synthetic targets with desired π···π interactions could be crucial for saving cost and time.

In addition, it is noteworthy that the number of theoretical studies of concave-convex π···π interactions between buckybowls and fullerenes is limited due to the recent discovery of these structures, to their large size and, especially, to the fact that until a few years ago there were no satisfactory options for the precise calculation of the non-covalent interactions between large molecules.

The main groups devoted to the study of concave-convex π···π interactions between buckybowls and fullerenes are run by A. Sygula at the Mississippi State University, USA, and by P. A. Denis at University of the Oriental Republic of Uruguay. The first group is essentially an experimental group, engaged fundamentally to the synthesis of buckybowls and to the study of their interactions.[25, 33, 37-50] This group performs theoretical calculations in some isolated cases, but only as a support for their experimental elucidations. The second group is devoted exclusively to theoretical study and has performed several works in recent years.[11-14] However, in our opinion their works might provide not enough consistent results to obtain good conclusions, since they use the M06-2X functional coupled with the People's 6-31G basis set, unprovided of polarization and diffuse functions. In addition, it is known that M06-2X functional provides a considerable underestimation of the interaction energy for systems with concave-convex π···π interactions.[42, 51, 52] P. A. Denis claims that using this weak level compensates very well the non-inclusion of the basis set superposition error (BSSE), but we believe that this strategy does not guarantee the reliability of results.

For all these reasons, it is a very advisable issue to carry out a detailed theoretical study of the concave-convex π···π interactions between a series of buckybowls and fullerenes to gain more insight into the characteristics of these systems. Undoubtedly, our calculations could provide important guides for future experiments and development of new technologies related to supramolecular chemistry.

1.2. Thesis objectives

The present doctoral thesis is focused in the detailed theoretical study of the concave-convex π···π interactions between buckybowls and fullerenes with the ultimate goal of designing new molecular tweezers based on buckybowls for fullerene recognition. To this end, the objectives of this thesis are:

1. Selecting a reliable level of calculation to study concave-convex π···π interactions (Chapter 4 and 5).

2. Evaluating the effects that can enhance the interaction between buckybowls and fullerenes. In particular, the addition of substituents and the curvature effects are evaluated (Chapters 4-8).

3. Evaluating the performance of the B97-D2//SCC-DFTB-D calculations regarding B97-D2 ones in order to obtain a rapid tool for selecting suitable strategies for the rational design of molecular tweezers (Chapters 8 and 9).

4. Trying to answer the key question: How to modify the buckycatcher $C_{60}H_{28}$ to improve its efficiency and/or selectivity? (Chapter 9).

1.3. Thesis organization

The structure of this thesis is shown in Figure 1.1.

Chapter 2 introduces the main issues concerned in this thesis: supramolecular chemistry, intermolecular interactions, fullerenes, buckybowls, and molecular tweezers.

In **Chapter 3** an overview of the theoretical methods and computational tools employed is included: density functional theory (DFT), dispersion-corrected DFT, resolution of the identity (RI) approach, SCC-DFTB method, basis sets, supermolecule method, basis set superposition error (BSSE), pyramidalization angle (POAV), molecular electrostatic potential (MEP) maps and non-covalent interactions (NCI) approach.

Chapter 4 presents a DFT study of the substituent effects in corannulene dimers. Corannulene is substituted with five alternating Br, Cl, CH_3, C_2H or CN units. Moreover, corannulene dimers with different curvature are also studied for evaluating the effect of curvature in the stacking of bowls. In this Chapter, a "fullerene copy", C_{60}-like (a corannulene with the curvature of the buckminsterfullerene, C_{60}) is incorporated for imitating the concave-convex interaction between corannulene and buckminsterfullerene. Substituent effects are evaluated based on the contribution of dispersion and MEP maps. Intermolecular BSSE corrected interaction energies are obtained using M06-2X, B97D and ωB97XD functionals with the 6-31+G* basis set. Results are compared with those obtained by Sygula and Saebø at the SCS-MP2/cc-pVTZ level.[40]

Chapter 5 is focused on the analysis of the performance of a variety of DFT-D functionals with empirical dispersion correction (B97-D, PBE-D, B-LYP-D, BP86-D) and specialized functionals for the treatment of non-covalent interactions (M06-2X and M05-2X). Four representative groups of complexes with π···π interactions are evaluated: (1) dispersion–dominated complexes taken from the S22 database;[53] (2) complexes with eclipsed planar polycyclic aromatic hydrocarbons, PAHs; (3) complexes with curved PAHs; (4) mixed complexes made up by planar and curved PAHs.

Chapter 6 is devoted to the study of the stacking interactions between substituted buckybowls (corannulene and sumanene) and fullerenes (C_{60} and C_{70}). Corannulene and sumanene monomers are substituted with five and six Br, Cl, CH_3, C_2H or CN units, respectively. The main goal of this work is supplementing the results obtained in Chapter 4, where the substituent effects in stacking interactions with substituted corannulene were evaluated using C_{60}-like. Another objective of this study was to expand our previous study by the addition of substituted sumanenes and the fullerene C_{70}. All calculations are performed at the B97-D/TZVP level. In addition, NCI calculations are used in order to obtain more detailed information about the substituent effects.

Chapter 7 is the study of the π···π stacking between ring-annelated corannulenes and fullerenes C_{60} and C_{70}. For this purpose three-, four-, and five-membered rings (saturated and unsaturated) are annelated to the five *rim* bonds of corannulene. Substitution effects with NH, O and S units on each one of the five saturated five-membered rings annelated to the *rim* of corannulene are also evaluated. The calculations are performed at the B97-D/TZVP level. Besides that ring annelation to the *rim* of corannulene gradually flattens the bowl it also introduces CH_2 groups in the bowl structure. So, ring-annelated corannulenes seem suitable structures for evaluating the effects of curvature and the CH···π interactions in the recognition the fullerenes. Ring-annelation effects are evaluated based on the contribution of dispersion, MEPs and NCI calculations.

In **Chapter 8** a series of buckybowls with different size and structure are tested as potential receptors of fullerenes C_{60}, C_{70} and C_{40}. Among these buckybowls are corannulene ($C_{20}H_{10}$), sumanene ($C_{21}H_{12}$), pinakene ($C_{28}H_{14}$), hemifullerene ($C_{30}H_{12}$), circumtriindene ($C_{36}H_{12}$), pentaindenocorannulene ($C_{50}H_{20}$) and bowl-shaped hexabenzocoronene derivatives. An exhaustive study taking into account different orientations of the fullerenes is performed to obtain the most favourable arrangement for interacting with the bowls. Complexes are optimized at the SCC-DFTB-D level and interaction energies are obtained at the B97-D2/TZVP level including BSSE corrections. Furthermore, the performance of the B97-D2//SCC-DFTB-D calculations is compared with that of B97-D2 for four groups of complexes with π···π interactions: (1) complexes with eclipsed planar polycyclic aromatic hydrocarbons, PAHs; (2) complexes with curved PAHs; (3) mixed complexes made up of planar and curved PAHs; (4) complexes made up of curved PAHs and C_{60}. Buckybowls are evaluated based on the contribution of dispersion, MEPs and NCI calculations.

Chapter 9 is devoted to the computational design of molecular tweezers based on buckybowls as fullerene receptors. The ultimate goal of this chapter is to attempt to

answer the key question: how to modify the buckycatcher $C_{60}H_{28}$ designed by Sygula and co-workers to improve its efficiency and/or selectivity? Three strategies to modify this buckycatcher are evaluated: (1) changing the corannulene pincers by others buckybowls; (2) changing the tether part by a buckybowl; (3) introducing methyl substituents on the buckycatcher. B97-D2/TZVP//SCC-DFTB-D calculations are used in this study in order to get a rapid selection of suitable strategies for designing new buckycatchers. Furthermore, all complexes are optimized at the B97-D2/TZVP level to obtain more accurate results.

Finally, **Chapter 10** provides the general conclusions of the work carried out in this thesis.

1.4. Publications

Each of Chapters 4-9 corresponds to an article that has been already published. Their references are:

- Chapter 4: D. Josa, J. Rodríguez Otero, E. M. Cabaleiro Lago, *Phys. Chem. Chem. Phys.* **2011**, *13*, 21139.
- Chapter 5: D. Josa, J. Rodríguez Otero, E. M. Cabaleiro Lago, M. Rellán-Piñeiro, *Chem. Phys. Lett.* **2013**, *557*, 170.
- Chapter 6: D. Josa, J. Rodríguez Otero, E. M. Cabaleiro Lago, L. A. Santos, T. C. Ramalho, *J. Phys. Chem. A* **2014**, *118*, 9521.
- Chapter 7: D. Josa, L. A. Santos, I. González-Veloso, J. Rodríguez Otero, E. M. Cabaleiro Lago, T. C. Ramalho, *RSC. Adv.* **2014**, *4*, 29826.
- Chapter 8: D. Josa, I. González-Veloso, J. Rodríguez Otero, E. M. Cabaleiro Lago, *Phys. Chem. Chem. Phys.* **2015**, *17*, 6233.
- Chapter 9: D. Josa, J. Rodríguez Otero, E. M. Cabaleiro Lago, *Phys. Chem. Chem. Phys.* **2015**, *17*, 13206.

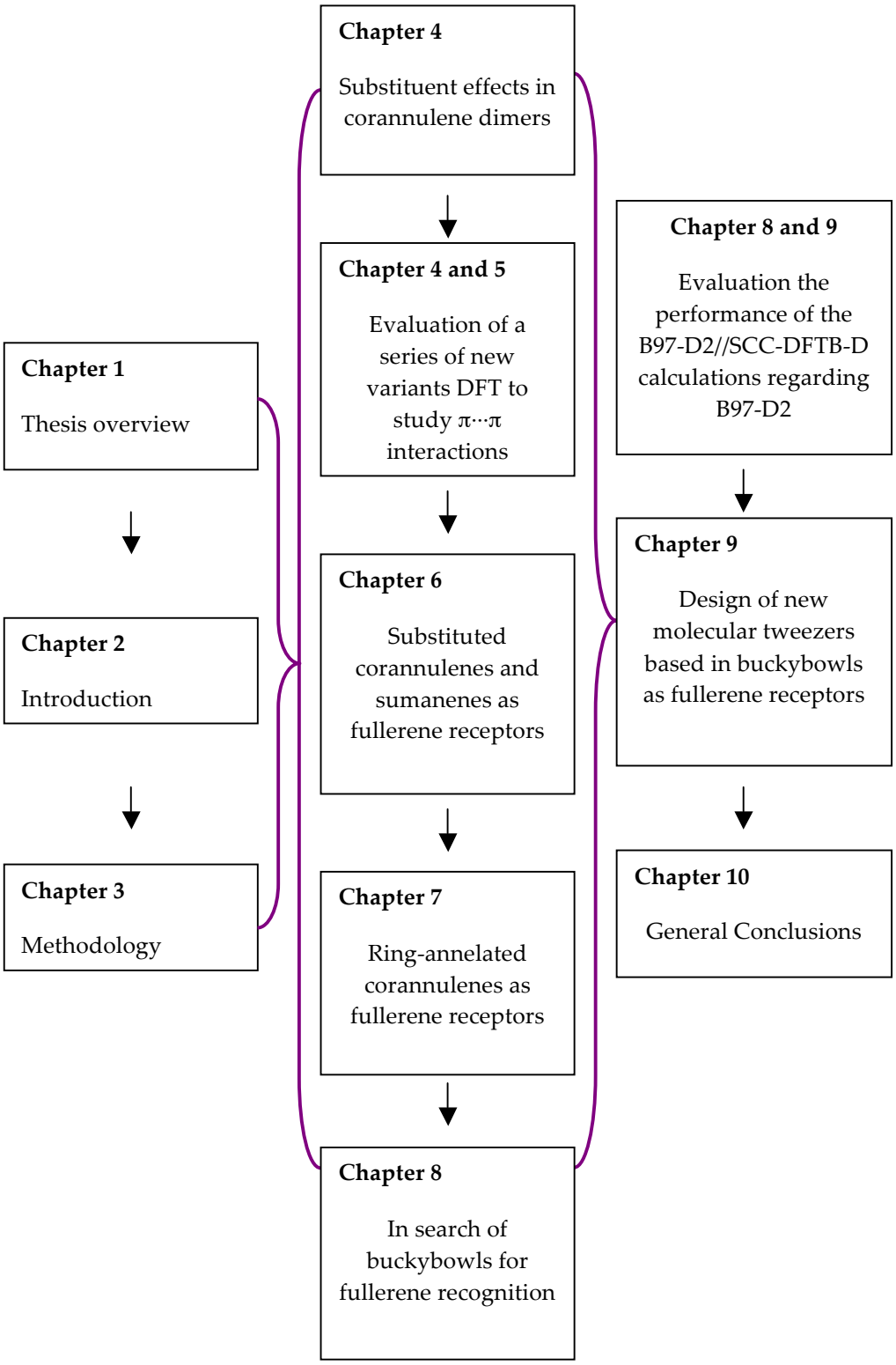


Figure 1.1: Thesis organization roadmap.

1.5. References

1. A. Bianco and T. Ros, Biological Applications of Fullerenes in *Fullerenes Principles and Applications. Ed. Fernando Langa and Jean-François Nierengarten.* Cambridge: RSC Publ., 2008.
2. R. Bakry, R. M. Vallant, M. Najam-ul-Haq, M. Rainer, Z. Szabo, C. W. Huck and K. B. Günther, *Int. J. Nanomedicine*, 2007, **2**, 639–649.
3. A. M. López and A. Mateo-Alonso, Fullerenes for materials Science in *Fullerenes Principles and Applications.* Ed. Fernando Langa and Jean-François Nierengarten. Cambridge: RSC Publ., 2008, ch. 7, pp. 191-220.
4. E. M. Pérez and N. Martín, *Pure Appl. Chem.*, 2010, **82**, 523-533.
5. F. D'Souza and O. Ito, *Chem. Commun.*, 2009, 4913-4928.
6. H. Imahori and S. Fukuzumi, *Adv. Funct. Mater.*, 2004.
7. J. Wang, S. G. Bodige, W. H. Watson and C. D. Gutsche, *J. Org. Chem.*, 2000, **65**, 8260-8263.
8. J. C. Iglesias-Sánchez, A. Fragoso, J. Mendoza and P. Prados, *Org. Lett.*, 2006, **8**, 2571-2574.
9. O. D. Fox, J. Cookson, E. J. S. Wilkinson, M. G. B. Drew, E. J. MacLean, S. J. Teat and P. D. Beer, *J. Am. Chem. Soc.*, 2006, **128**, 6990-7002.
10. E. Huerta, H. Isla, E. M. Pérez, C. Bo, N. Martín and J. de Mendoza, *J. Am. Chem. Soc.*, 2010, **132**, 5351–5353.
11. P. A. Denis, *Chem. Phys. Lett.*, 2014, **591**, 323–327.
12. P. A. Denis, *New J. Chem.*, 2014.
13. P. A. Denis, *RSC Adv.*, 2013, **3**, 25296-25305.
14. P. A. Denis, *Chem. Phys. Lett.*, 2011, **516**, 82-87.
15. I. Welsh and M. Lein, *J. Comput. Chem.*, 2014, **35**, 181-191.
16. P. E. Georghiou, A. H. Tran, S. Mizyed, M. Bancu and L. T. Scott, *J. Org. Chem.*, 2005, **70**, 6158-6163.
17. D. Josa, J. Rodríguez-Otero, E. M. Cabaleiro-Lago, L. A. Santos and T. C. Ramalho, *J. Phys. Chem. A*, 2014, **118**, 9521-9528.
18. D. Josa, L. Azevedo dos Santos, I. González-Veloso, J. Rodríguez-Otero, E. M. Cabaleiro-Lago and T. de Castro Ramalho, *RSC Adv.*, 2014, **4**, 29826-29833.
19. T. Kawase, N. Fujiwara, M. Tsutumi, M. Oda, Y. Maeda, T. Wakahara and T. Akasaka, *Angew. Chem. Int. Ed.* , 2004, **43**, 5060-5062.
20. T. Kawase and H. Kurata, *Chem. Rev.*, 2006, **106**, 5250-5273.
21. E. M. Pérez, A. L. Capodilupo, G. Fernandez, L. Sanchez, P. M. Viruela, R. Viruela, E. Orti, M. Bietti and N. Martín, *Chem. Commun.*, 2008, 4567-4569.
22. E. M. Pérez, L. Sanches, G. Fernández and N. Martín, *J. Am. Chem. Soc.*, 2006, **128**, 7172-7173.
23. K. Tashiro and T. Aida, *Chem. Soc. Rev.*, 2007, **36**, 189-197.
24. E. M. Pérez and N. Martín, *Chem. Soc. Rev.*, 2008, **37**, 1512-1519.
25. A. Sygula, *Eur. J. Org. Chem.*, 2011, **2011**, 1611-1625.
26. A. C. Whalley, K. N. Plunkett, A. A. Gorodetsky, C. L. Schenck, C.-Y. Chiu, M. L. Steigerwald and C. Nuckolls, *Chem. Sci.*, 2011, **2**, 132-135.
27. E. A. Jackson, B. D. Steinberg, M. Bancu, A. Wakamiya and L. T. Scott, *J. Am. Chem. Soc.*, 2007, **129**, 484-485.

28. T. C. Wu, M. K. Chen, Y. W. Lee, M. Y. Kuo and Y. T. Wu, *Angew. Chem. Int. Ed.*, 2013, **52**, 1289-1293.
29. H. Sakurai, T. Daiko and T. Hirao, *Science*, 2003, **301**, 1878.
30. S. Higashibayashi and H. Sakurai, *Chem. Lett.*, 2011, **40**, 122-128.
31. W. E. Barth and R. G. Lawton, *J. Am. Chem. Soc.*, 1966, **88**, 380-381.
32. L. T. Scott, M. S. Bratcher and S. Hagen, *J. Am. Chem. Soc.*, 1996, **118**, 8743-8744.
33. A. Sygula, F. R. Fronczek, R. Sygula, P. W. Rabideau and M. M. Olmstead, *J. Am. Chem. Soc.*, 2007, **129**, 3842-3843.
34. A. Sygula and W. E. Collier, Molecular Clips and Tweezers with Corannulene Pincers, in *Fragments of Fullerenes and Carbon Nanotubes: Designed Synthesis, Unusual Reactions, and Coordination Chemistry* (eds M. A. Petrukhina and L. T. Scott), John Wiley & Sons, Inc., Hoboken, NJ, USA., 2011, ch. 1, pp. 1-40.
35. S. Chakrabarti and K. Ruud, *J. Phys. Chem. A*, 2009, **113**, 5485–5488.
36. A. A. Voityuk and M. Duran, *J. Phys. Chem. C*, 2008, **112**, 1672-1678.
37. J. Yang, P. Feng, A. Sygula, W. Harneit, J.-H. Su and J. Du, *Phys. Lett. A*, 2012, **376**, 1748-1751.
38. A. Sygula, R. Sygula, A. Ellern and P. W. Rabideau, *Org. Lett.*, 2003, **5**, 2595-2597.
39. A. Sygula, R. Sygula and P. W. Rabideau, *Org. Lett.*, 2005, **7**, 4999-5001.
40. A. Sygula and S. Saebø, *Int. J. Quantum Chem.*, 2009, **109**, 65-72.
41. A. Sygula, M. Yanney, W. P. Henry, F. R. Fronczek, A. V. Zabula and M. A. Petrukhina, *Cryst. Growth Des.*, 2014, **14**, 2633–2639.
42. T. Janowski, P. Pulay, A. A. Sasith Karunarathna, A. Sygula and S. Saebø, *Chem. Phys. Lett.*, 2011, **512**, 155-160.
43. L. Kobryn, W. P. Henry, F. R. Fronczek, R. Sygula and A. Sygula, *Tetrahedron Lett.*, 2009, **50**, 7124-7127.
44. A. Sygula, G. Xu, Z. Marcinow and P. W. Rabideau, *Tetrahedron*, 2001, **57**, 3637-3644.
45. G. Xu, A. Sygula, Z. Marcinow and P. W. Rabideau, *Tetrahedron Lett.*, 2000, **41**, 9931–9934.
46. A. H. Abdourazak, A. Sygula and P. W. Rabideau, *J. Am. Chem. Soc.*, 1993, **115**, 3010-3011.
47. A. Sygula and P. W. Rabideau, *J. Am. Chem. Soc.*, 2000, **122**, 6323-6324.
48. A. Sygula, R. Sygula and P. W. Rabideau, *Org. Lett.*, 2006, **8**.
49. A. Sygula, R. Sygula and L. Kobryn, *Org. Lett.*, 2008, **10**, 3927-3929.
50. C. Mück-Lichtenfeld, S. Grimme, L. Kobryn and A. Sygula, *Phys. Chem. Chem. Phys.*, 2010, **12**, 7091-7097.
51. D. Josa, J. Rodríguez Otero and E. M. Cabaleiro Lago, *Phys. Chem. Chem. Phys.*, 2011, **13**, 21139-21145.
52. D. Josa, J. Rodríguez-Otero, E. M. Cabaleiro-Lago and M. Rellán-Piñeiro, *Chem. Phys. Lett.*, 2013, **557**, 170-175.
53. P. Jurecka, J. Sponer, J. Cerny and P. Hobza, *Phys. Chem. Chem. Phys.*, 2006, **8**, 1985-1993.

Chapter 2

Introduction

In this Chapter an introduction of the main issues involved in this thesis is presented: supramolecular chemistry, intermolecular interactions, fullerenes, buckybowls and molecular tweezers.

2.1. Supramolecular Chemistry

Supramolecular chemistry has been defined by one of its major proponents, Jean-Marie Lehn[1] as the "chemistry of molecular assemblies and of the intermolecular bond". More commonly it is expressed as "chemistry beyond the molecule". Others definitions include phrases such as "the chemistry of the non-covalent bond", "non-molecular chemistry" or even "Lego chemistry".[2, 3]

Fundamentally, supramolecular chemistry examines the weak non-covalent interactions that hold groups of molecules together. These forces include hydrogen bonding, metal coordination, hydrophobic forces, van der Waals forces, π···π interactions or electrostatic effects.

Originally, supramolecular chemistry was defined in terms of non-covalent interactions between a host and a guest molecule (Figure 2.1). Commonly the host is a large molecule such as an enzyme or a synthetic cyclic compound possessing an adequate cavity, while the guest may be a cation, an anion, or more sophisticated molecules such as a hormone or fullerenes. More formally, Donald Cram has defined the

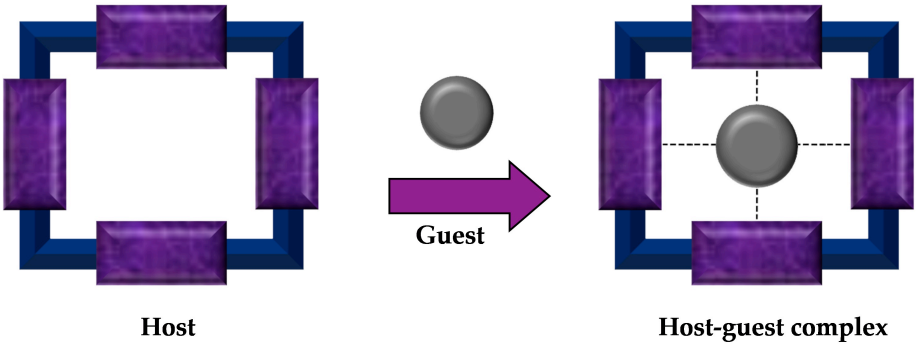


Figure 2.1: Schematic diagram of host-guest complexation.

host and guest as molecular entities possessing convergent and divergent binding sites, respectively.[4]

The concept of host-guest chemistry pre-empted with Emil Fischer in 1894,[5] when this author proposed that enzymes interact with their substrate as a key does with its lock. Another important step in the developing the supramolecular chemistry was the discovery of crown ether in 1967 by Charles J. Pedersen[6] that opened the door for researching on artificial host molecules. Following this work, other researchers such as Donalds J. Cram[7, 8], Jean-Marie Lehn[9, 10] and Fritz Vogtle[11] became active in synthesizing shape- and ion-selective receptors.

Finally, the importance of the supramolecular chemistry was established in 1987 with Nobel Prize for Chemistry awarded to Donald J. Cram, Jean-Marie Lehn, and Charles J. Pedersen in recognition of their work in this area. Thenceforth, supramolecular chemistry has been one of the fastest-growing fields of chemical research, crossing a range of subjects from biological chemistry to materials science.

The first works involving supramolecular chemistry sought to understand the formation of supermolecules of two components, a host and a guest, which interact among them non-covalently. Nowadays, these studies have progressed to include understanding and mimicking of biological processes, molecular recognition, molecular self-assembly, catalysis, materials, medicinal chemistries and dynamic covalent chemistry.[3, 12] Thereby, it is not surprising that supramolecular chemistry shows several important applications such as drug delivery,[13, 14] sensors,[15] molecular machines[16] and molecular architectures to remove hazardous materials from the environment.[17]

In this context, a deep knowledge of the intermolecular interactions is crucial to understanding existing supramolecular systems and to guide the design of new more effective and/or selective systems.

2.2. Intermolecular interactions

When molecules are close together forces of attraction and repulsion come into play. These forces arising from the interactions between electrons and nuclei of different molecules are known as intermolecular interactions.

Boscovich first enunciated the concept that molecules are subject to attractive and repulsive forces in 1783. Afterwards, Clausius established that molecules repel at short distances and attract at long distances. This concept was then incorporated by Maxwell and Van der Waals to the description of the kinetic behaviour of gases and function of state for real gases, respectively.[18] Although, since the end of the century XIX there was a wide speculation about the origin and characteristics of the intermolecular interactions, an understanding of the nature of intermolecular forces was not reached until 1930, after the principles of quantum mechanics were established.

Intermolecular forces control a broad range of physical, chemical and biological processes that are very relevant in the nature, such as the existence of liquids and solids, the chemical reactivity of compounds, the crystal packing, the melting and boiling points of substances, the stability and conformation of biomolecules like DNA and proteins, the muscle contractions and the enzymatic catalysis. In fact, in their absence our world would be a uniform ideal gas.[19]

It is convenient to express the interaction between two molecules in terms of intermolecular potential energy, *U(R)*. Figure 2.2 shows the typical form of the potential energy as a function of distance between molecules. As can be seen, this curve is the result of the combination of attractive and repulsive interactions. A strongly repulsive interaction (positive) happens at short distances and an attractive (negative) interaction takes place at long distances. Furthermore, the potential energy curve is characterized by two main parameters: the diameter of collision, σ, distance at which the potential energy is zero; and the separation R_m, distance whose energy has a minimum value, -ε.

The intermolecular interactions can be grouped into two main types: long-range or attractive, where the energy of interaction behave as an inverse power of *R* (being *R* the intermolecular distance) and short-range or repulsive, where the energy decreases exponentially with distance.

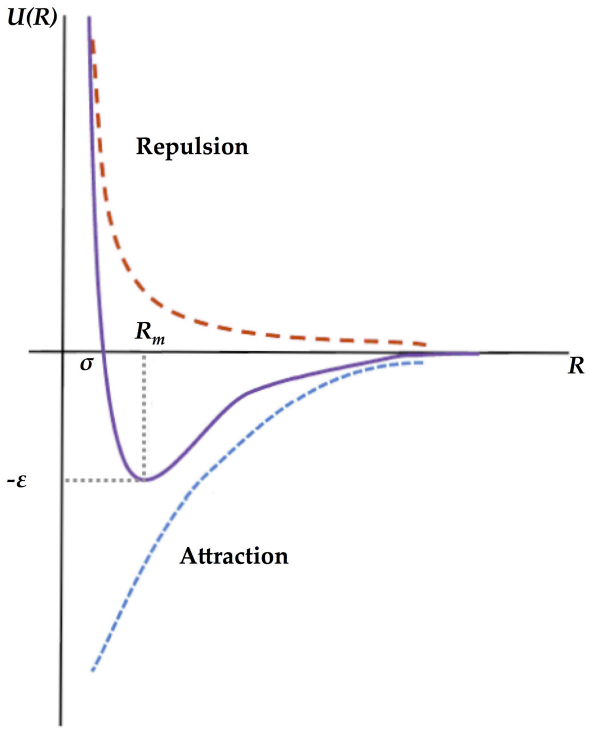


Figure 2.2: A typical intermolecular potential energy function.

2.2.1. Long-range interactions

Long-range interactions can be divided in three types: electrostatic, induction and dispersion.

i. Electrostatic

This interaction is established between charged species and/or neutral species without net charge but that show a permanent multipolar moment. The electrostatic contribution is a coulombic interaction that depends on the separation between molecules and the relative orientation of these molecules. The charge distribution of a molecule is described in terms of the multipole moments. They are strictly pairwise additive and may be either attractive or repulsive. In general, the dependence of the interaction energy with the distance is $R^{-(l1+l2+1)}$ where $l1$ and $l2$ are the order of the multipoles (0 for monopoles, 1 for dipoles, 2 for quadrupoles, etc.). Thus, the electrostatic contribution can show a large variety: R^{-1} for two punctual charges, R^{-2} for a molecule with dipole and a punctual charge, R^{-3} for two molecules with dipole...

ii. Induction

The charge distribution of a system can be affected by external electric fields, for example neighbouring molecules. This charge redistribution is known as polarization. Its first consequence is that a dipole moment is induced and a new type of interaction called induction energy is generated. Induction is non-additive because the fields of several neighbouring molecules may reinforce each other or cancel out. The induction interaction, induced by dipole moments varies according R^{-6} for two neutral species.

iii. Dispersion

In contrast to the previous two contributions, dispersion cannot be explained by the use of classical phenomena. It is a contribution of exclusively quantum nature, which has its origin in the correlation of the fluctuations of electron charge clouds of the molecules due to the movement of electrons. However, a classical description can help to understand them. Classically, these interactions can be explained considering that a molecule due to continuous electronic motion can generate an instantaneous dipole moment. This dipole moment will induce a dipole moment in a neighbouring molecule and as classical induction forces the net effect will be the attraction. Due its dependence on the polarizability, the size and molecular shape are the factors that control the relative strength of the dispersion interactions. Thereby, the dispersion interactions between the π-systems are relatively strong, since π-electrons in conjugated systems are easily polarizable. Finally, it is worth mentioning that dispersion energy is present in all kinds of molecules.

2.2.2. Short-range interactions

When molecules are very close to each other, the interactions between them begin to be dominated by electronic and nuclear repulsions. The repulsive interactions can be explained by the Pauli exclusion principle, which limits the possibility that two electrons can occupy the overlapping regions of the electron clouds of two molecules that are very close. Thus, the electron density is reduced in the area of overlap and cores are not as well protected against the remaining cores, and these repel mutually. Thereby, the repulsion between molecules arises in part from the electrostatic repulsion between the cores and the interelectronic repulsion.

2.3. Interactions involving curved polycyclic aromatic systems

This section shows a brief description of usual interactions between buckybowls and fullerenes.

π···π interactions

This class of interactions that involves direct attraction between aromatic rings plays an outstanding role in biochemistry, material science, molecular engineering, host-guest complexes and packing of aromatic molecules in crystals.[20-23] In addition, many drugs, including anticancer agents that intercalate into DNA[24], utilize π···π interactions in their binding.

Unfortunately, as it will be seen in detail in Chapter 3, accurate description of π···π interactions is a challenging task for quantum chemistry methods in general. In addition, it is worth mentioning that experimentalists and theoreticians are still not in complete agreement on the structure of the most stable complexes formed by prototypical aromatic molecule, the benzene.[25]

π···π interactions were not extensively studied until about 1990, when Hunter and Sanders began to investigate this intriguing interaction.[23] These researchers proposed an electrostatic model to explain the geometries for interactions between aromatic molecules. The key feature of their model was to consider separately the systems σ and π, which are formed by three layers: one central constituted by a σ frame with +1 relative charge, and two layers with -1/2 charge corresponding to the π system. Through this simple model, these researchers justified the attractive interactions for the T-shaped and the parallel-displaced configurations and the repulsive interaction for the sandwich configuration (Figure 2.3).

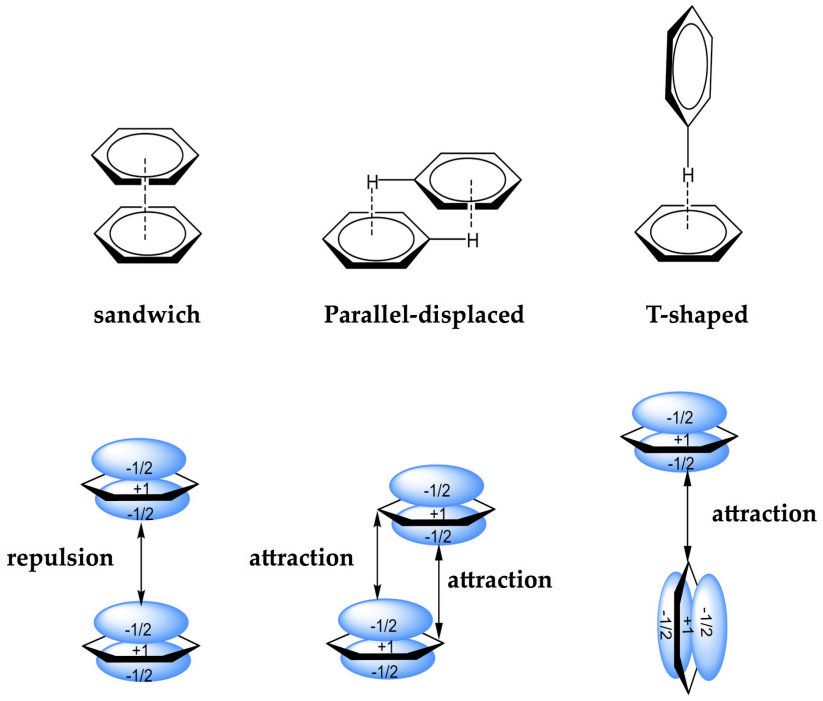


Figure 2.3: Benzene dimer configurations and π-quadrupoles.

On the other hand, nowadays, the benzene dimer is considered a typical van der Waals complex in which the long-range dispersion interactions play the major role.

Consequently, the dimer is unbound at the uncorrelated Hartree-Fock and many density functional theory (DFT) levels.[26] This more refined view is increasingly replacing the Hunter's model of π···π interactions,[23] which (over)emphasizes the main quadrupole-quadrupole electrostatic component of the interaction in benzene-type systems.[27]

Currently, π···π interactions of aromatic planar systems have been broadly studied by several research groups; among them, that run by C. David Sherrill can be highlighted. According to several works carried by this group the substituents play an important role in the π···π interaction of benzene dimer.[22, 28-32]

Concave-convex π···π interactions

Recent progress in fullerene chemistry introduced a novel aspect to the π···π stacking interactions, that is, interactions of curved π-conjugated molecular networks also known as concave-convex π···π interactions.

Concave-convex π···π interactions are responsible for column packing in the crystal structure of buckybowls[33] and in the formation of dimers[34] (Figure 2.4). Furthermore, this kind of interaction may have a huge practical value as in the case of molecular tweezers for catching species of interest, such as fullerenes.[35] In this case, buckybowls can be used as one of the most efficient buckycatchers.

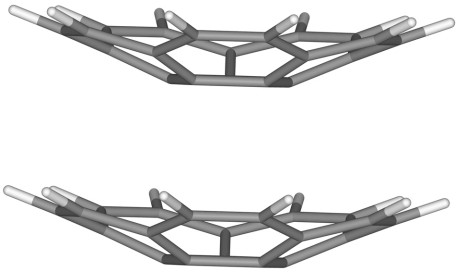


Figure 2.4: Concave-convex π···π interactions between corannulene monomers.

According to Haddon's initial predictions the concave-convex π···π interaction should be different from the interaction between flat graphene sheets, because curved π systems such as fullerenes would be polarized regarding to the convex and concave sides, owing to the unsymmetrical nature of their *p* orbitals (Figure 2.5). [36-38]

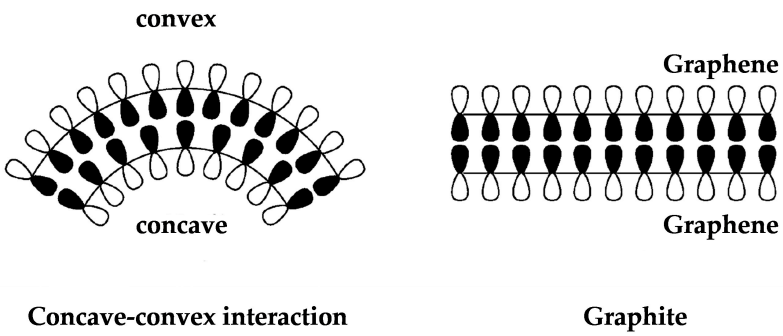


Figure 2.5: Schematic comparison between the arrangement of *p* orbitals for concave-convex and for flat graphene interactions.

In 2009, Sygula and Saebø performed an interesting research about π···π stacking of corannulene dimers[34] that enabled to begin exploration of curvature effects on π···π interactions. Their calculations led to three important conclusions:

- At least, part of the interaction energy in the stacked curved systems can be attributed to the electrostatic dipole-dipole interaction that is absent in planar dimers.

- The interactions between curved π-systems are of comparable magnitude to those of planar systems of the same size.

- Corannulene dimers prefer an eclipsed conformation, while planar dimers prefer a staggered conformation.

Recently, Kennedy *et al.*[39] have carried out a more detailed study of the effect of curvature on π···π interactions. Their results indicated that curvature affects to all four major components of non-covalent interactions (dispersion, electrostatics, exchange, and induction) and that an increase of curvature in concave-convex π···π interactions leads to more favourable interaction energies, except at short distances where the most highly curved systems are less favourable as exchange repulsion terms begin to dominate the interaction.

Despite recent advances in concave-convex π···π interactions, still there is much to know. Therefore, the goal of this thesis is to study the main factors that control the stacking interactions between buckybowls and fullerenes.

On the other hand, the addition of substituents to buckybowls is also a subject of great interest because it may exert a modulatory effect that can enable a better concave-convex π···π interaction with fullerenes. Therefore, the effect of substituents on stacking interactions of curved systems also has been extensively studied in this thesis. As can be seen in detail in Chapter 6 and 7, alkyl substituents can contribute significantly to enhance the interactions with fullerenes through CH···π interactions.

CH···π interactions

The CH···π interaction is a weak hydrogen bond formed between a soft acid CH and a soft base π-system (Figure 2.6). This interaction plays an important role in supramolecular chemistry, crystal packing, drug design and selectivity in organic reactions.[40]

CH···π interactions can be either dispersion or electrostatic dominated depending of the acidity of C-H group. Recent theoretical calculations show that the energy of one CH···π hydrogen bond is *ca.* 1.5-2.5 kcal/mol for typical cases involving aliphatic and aromatic CH groups as the hydrogen donor and the C6 aromatic ring as CH-acceptor. For these cases, the dispersion energy is the most important contribution. On the other hand, CH···π bonds involving activated or acidic C-H groups are comparable to conventional hydrogen bonds. So, the energy of a CH···π hydrogen bond involving acetylene or chloroform has been estimated to be *ca.* 3-5 kcal/mol.[41] Finally, it is noteworthy that proportion of the electrostatic energy increases on going from sp^3-CH to sp^2-CH and then to *sp*-CH.[42]

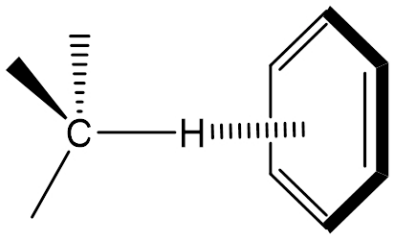


Figure 2.6: Schematic representation of CH···π interaction.

2.4. Fullerenes

Fullerenes are molecule composed entirely of carbon, in the form of a hollow sphere, ellipsoid or tube. Spherical fullerenes are also referred to as 'buckyballs', and they resemble the balls used in football (soccer). Cylindrical ones are called carbon nanotubes. In this thesis, we focused in the study of the buckyballs, especially the fullerenes C_{60} and C_{70} given in Figure 2.7.

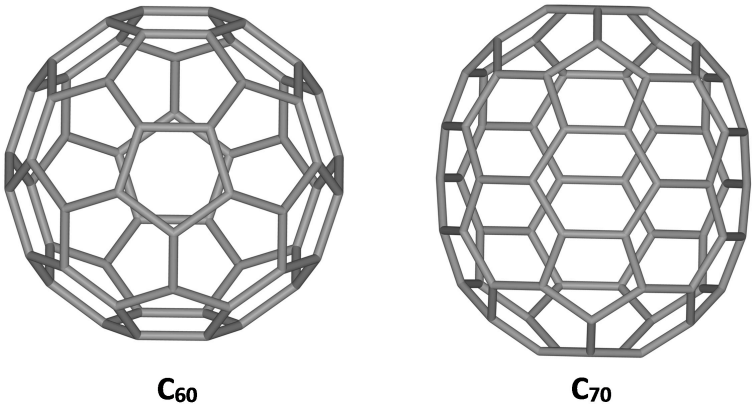


Figure 2.7: Structure of the fullerenes C_{60} and C_{70}.

Fullerenes and in particular the buckminsterfullerene C_{60}, the third allotrope of carbon, were first discovered in 1985 by Richard Smalley, Robert Curl, James Heath, Sean O'Brien, and Harold Kroto.[43] Few years later, these researchers were awarded the 1996 Nobel Prize[44] in Chemistry for their roles in the discovery of this class of molecules.

Buckminsterfullerene (C_{60}) was named in homage to American architect Richard Buckminster Fuller, whom had built geodesic domes based in hexagons and pentagons that have a shape similar to C_{60}.

In 1990, Kräetschmer and co-workers produced the fullerene C_{60} for the first time in multigram quantities *via* arc-discharge method, commonly known as Hufmann-Kräetschmer method.[45] In this method, pure carbon in the form of graphite is heated under a very high temperature (*ca.* 2000°C) by means of graphite electrodes in an inert atmosphere, usually helium. Unfortunately, this method leads to the production of carbon soot, in which the fullerenes have to be separated from. Fullerenes C_{60} and C_{70} are the major isomers obtained in 75 % and 24% respectively. The remaining 1% constitutes a variety of higher order fullerenes ranging from C_{74} to beyond C_{100}.[46]

In this context, undoubtedly, another important step in the development of fullerene science was the isolation, separation and characterization of the fullerenes C_{60} and C_{70} by Taylor *et al*.[47] Besides that this study showed that separation of fullerenes could be possible by using chromatographic methods it also enabled to begin the exploration of the chemistry, spectroscopy and properties of these two fullerenes.

Fullerenes possess important applications in wide ranging fields, from material science to medicine. For example fullerenes show applications in photovoltaic cells to prevent deterioration of the polymers at high temperatures,[48] as organic photovoltaic materials,[49, 50] as part of cosmetics due to their antioxidant character,[51] or as drug and gene delivery.[51, 52] In addition, they show potential antiviral activity for several pathogens as HIV[51, 52] or Ebola[53] and they are potential photosensitizers for photodynamic therapy, which is a treatment for some kind of cancers.[51, 52]

Fullerene Receptors

Nowadays, one of most active fields in fullerene chemistry is the searching for molecular receptors able to form stable associates with them.[54] The first example of macrocyclic fullerene receptors in solution was published by Diederich *et al.* in 1992, using the lipophilic cavity of azacrown ethers to host fullerenes.[55] Shortly thereafter, Andersson and co-workers showed that a water-soluble complex of C_{60} was formed upon refluxing a solution of γ-cyclodextrin with solid C_{60}. [56]

Fullerene receptors are not only important to separate fullerenes of the soot, but they also enable the development of new materials for solar energy conversion, optoelectronics, catalysis and switching.[57] So, the design and synthesis of fullerene receptors has been a subject of great interest in recent years and a variety of hosts have been studied. These include calix[n]arenes,[58-61] resorcarenes[62, 63], cyclotriveratrylenes,[64-66] corannulenes,[67-74] cyclic paraphenyleneacetylenes,[75, 76] π-extended tetrathiafulvalenes,[65, 77-79] and porphyrins.[80-83]

In order to design receptors able to form complexes of high stability and selectivity, it is very important to keep in mind that fullerenes are a peculiar kind of guest. Fullerenes are solely made up by carbon atoms and thus devoid of functionality.

So, as dispersion forces are predominant in the stabilization of the fullerene associates, maximizing concave-convex π···π complementarity represents a crucial element in the construction of successful fullerene receptors.[84]

On the other hand, it is noteworthy that examples of concave fullerene receptors are relatively scarce given that curved molecules are not always an easy synthetic target due their tensioned structures.[84] In this context, bowl-shaped polycyclic aromatic hydrocarbons (PAHs), commonly known as buckybowls or fullerene fragments seem very attractive, given that several buckybowls have been synthetized in last years[85-93] and their concave surface can fit highly to the convex surface of fullerenes through concave-convex "ball-and-socket" π···π interactions.[35]

2.5. *Buckybowls*

As commented above, the discovery of a new form of elemental carbon, buckminsterfullerene (C_{60}), in the mid-80s of last century has promoted a lot of research activities in the fields of physics, chemistry and materials science. In addition, this discovery has conduced to a special interest on buckybowls. In contrast to others PAHs previously discovered the curvature of buckybowls is not a consequence of bulky substituents, but of the impossibility of placing contiguous pentagons and hexagons in a planar sheet.

Buckybowls show a unique bowl-shaped architecture that provide two different faces, one concave and one convex that significantly increase their potential with respect to standard PAHs. As fragments of fullerenes, buckybowls are potential substrates for the synthesis of fullerenes and nanotubes. Therefore, the understanding of the interaction in these systems can be very important in the development of molecular engineering and materials science.

The smallest buckybowl, corannulene ($C_{20}H_{10}$, 1, Figure 2.8) has been subject of intense experimental and theoretical research in last years.[34, 39, 71, 73, 94-100]

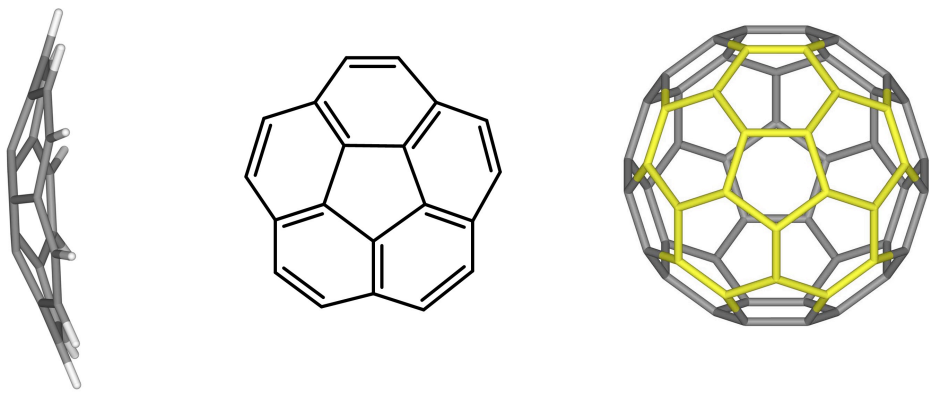


Figure 2.8: Corannulene and its structural relationship with fullerene C_{60}.

Corannulene was first synthesized from acenaphthalene *via* a 17 steps process by Lawton and Barth in 1966.[101] Thenceforth, several alternative synthetic methods have been developed, as well as methods for derivatization of the corannulene framework.[85]

Recently, Siegel's group has optimized the process for synthesis of corannulene on kilogram scale that reduces material costs by over 2 orders of magnitude compared to that for the published gram-scale synthesis.[100] Undoubtedly, this discovery represents a significant step for its future industrial commercialization.

In recent years, several buckybowls have been synthesized; among them sumanene,[89] pentaindenocorannulene[87] and circumtrindene[102] can be highlighted (Figure 2.9). Furthermore these buckybowls may have substituents and/or heteroatoms in their structure.

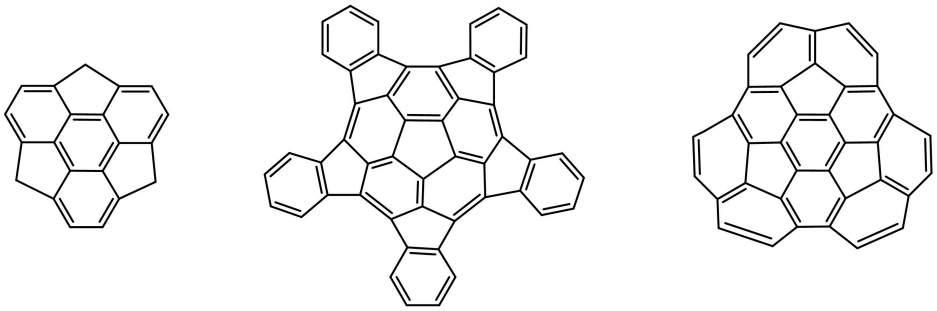


Figure 2.9: Examples of buckybowls synthetized in recent years.

2.5.1. Interest of buckybowls

Besides their pure scientific interest, buckybowls also represent a chemical entity with future potential applications. In fact, there are numerous reasons to study buckybowls:

1. They are potential candidates as fullerene receptors, because the complementarity character between carbon surfaces of buckybowls and fullerenes.

2. They offer unique molecular architectures that can be used as framework for molecular systems of nanometer size including bowls for host/guest chemistry.

3. They are potential substrates for the synthesis of fullerenes and nanotubes.

4. They show a great advantage in modifying their shape compared to fullerene and nanotubes.

5. In contrast to planar aromatic compounds, their curved surfaces provide different physical and chemical environments.

6. In contrast to fullerenes, buckybowls show concave and convex surfaces easily accessible that enable the endo-exo preference.

7. If, as expected, the industrial applications of fullerenes grow, decomposition of fullerenes "residue" can lead to fragmentation, with buckybowls that become part of the environment. Thereby, the knowledge of their chemical and physical properties is imperative.

2.5.2. Structural studies of buckybowls

The structural studies of buckybowls are focused basically on the analysis of the planarity of these species as well as the energy cost of bowl-to-bowl inversion. Corannulene, with a bowl depth of 0.87 Å,[103] gives rise to an inversion process with an energetic cost of about 10 kcal/mol[95] (Figure 2.10). On the other hand, sumanene, with a bowl depth of 1.11 Å[104] shows a much higher inversion barrier: 19.0 kcal/mol.[105]

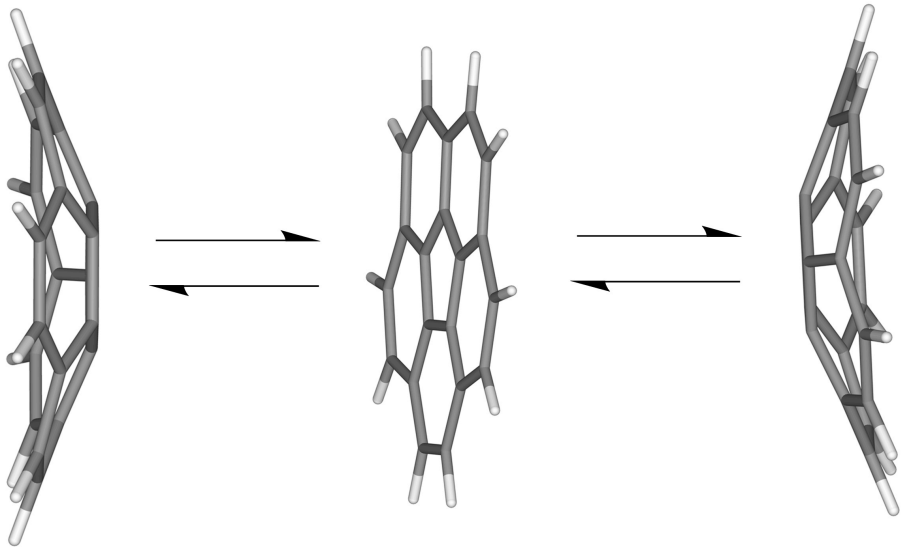


Figure 2.10: Bowl-to-bowl inversion process of corannulene *via* a planar transition state.

According to studies carried out by Seiders *et al*.[95] there is a clear relationship between the depth of the bowl and the inversion barrier. The correlation between structure and barrier can be easily visualized in Figure 2.11. Compounds of the class I

with bulky substituents on *peri* adjacent positions flatten the bowl and produce lesser barrier than that obtained for corannulene. On the other hand, compounds of the class II with substituents bonded in *peri* position lead to a general increase of the barrier.

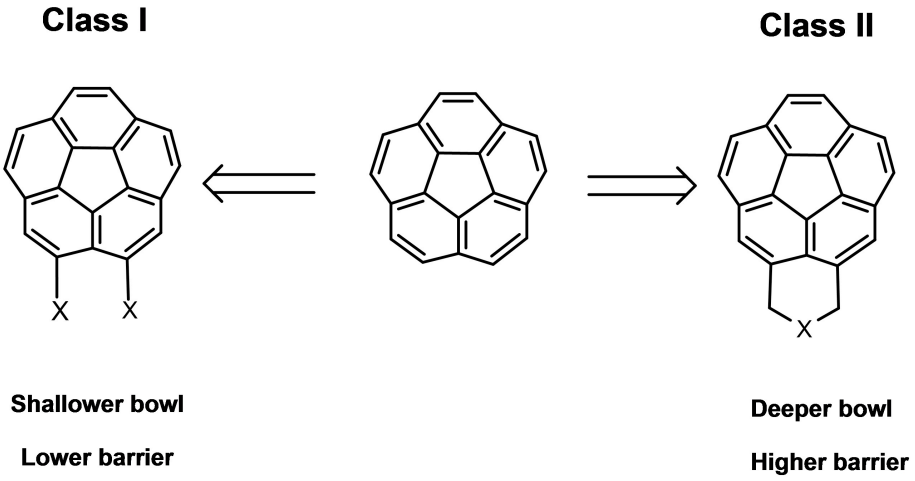


Figure 2.11: Correlation between bowl depth and inversion barrier.

2.5.3. Interactions with buckybowls

The major interest of buckybowls is that related to the formation of intermolecular complexes of different nature. In addition, buckybowls can exhibit intermolecular interactions with a wide range of different species, such as transition metals,[106-109] metal cations[94, 110-112] and anions.[113-115] Also, the interaction with other curved surfaces can lead to an interesting type of interaction known as concave-convex π···π interaction.[34, 35, 70, 72]

Although both C_{60} and corannulene are curved carbon surfaces, they exhibit very different behaviour. In complexes of C_{60} with transition metals, the metal always is bound to two carbons (hapticity 2). On the other hand, in the case of corannulene···transition metal complex, the metal (Ru, Os, Fe, Pd, Pt) is generally linked to the carbons of the six-membered ring with hapticity 6.[107, 108, 116-118]

According to DFT calculations, buckybowls can form complexes with cations such as Li^+ and Na^+ by both the convex and concave sides. However, the convex side is slightly favoured. In addition, it is worth noting that these complexes show interaction energies significantly higher than those for similar planar compounds.[110, 112, 119]

The introduction of substituents on bowls is a subject of great interest, since it allows modulating the molecular electrostatic potential (MEP) of the bowls so they can be tuned for favourable interaction with anions or cations. Recently, Campo-Cacharrón *et al.* has carried out a detailed studied of a series of complexes made up by substituted buckybowls derived from corannulene and sumanene with sodium cation or chloride anion. Corannulene and sumanene monomers were substituted with five and six CH_3, F or CN units, respectively. Their results show that sumanene interacts more strongly than corannulene with both anions and cations. As the substituent becomes more electron-withdrawing the interaction with the anion becomes stronger, closely following the changes in the MEPs of the bowls. So, complexes with chloride anion show interactions ranging from -6 kcal/mol in the methylated corannulene derivative to -45 kcal/mol in the CN-substituted sumanene. By contrast, sodium complexes show interactions going from deeply attractive complexes with the methylated derivatives (-36 kcal/mol with sumanene derivative) to slightly repulsive ones in the CN-substituted bowls (2 kcal/mol in the corannulene derivative).[114]

As already commented, this thesis is focused on the theoretical study of concave-convex π···π interactions between buckybowls and fullerenes. Becker and co-workers reported the first evidence of complexation between corannulene and fullerene C_{60} in 1993. Their gas phase experiments with cationic corannulene and neutral C_{60} evidenced the $[C_{60}\cdots\text{corannulene}]^+$ complex formation. Although this finding was an important advance for the application of buckybowls as fullerene receptors, neutral complexes in solution and solid state are more desirable.[120]

Georghiou and co-workers published the first stacking interaction between fullerenes and corannulene thioether in toluene solution in 2001.[121] In addition, four years later this group also carried out another study involving penta- and decasubstituted corannulenes with C_{60}.[72] Despite the promising results obtained, the experiments did not proved the existence of strong π···π interactions between corannulenes and fullerenes. The association constants obtained were relatively small and highly dependent on substituents, so that one could argue that the true interaction that bound the complex was that taking place between the fullerene and the edge substituents of corannulene and not the π···π interaction between corannulene and fullerene.

Fortunately, two years later, Sygula and co-workers confirmed that the strength of the interaction between buckycatcher $C_{60}H_{28}$ and C_{60} is indeed from pure concave-convex π···π interactions between convex faces of fullerene and concave faces of the two subunits of suitably oriented corannulene.[35] Since then, the interest by concave-convex π···π interactions has revived and several studies involving these interactions have been carried out.[34, 39, 67-71, 73, 74, 122-128]

2.6. Molecular tweezers

Molecular tweezers are noncyclic receptors with an open cavity capable of binding guest molecules through non-covalent interactions. Their basic structure is

composed mainly of two pincers that are held together by a spacer group also called as tether (Figure 2.12).

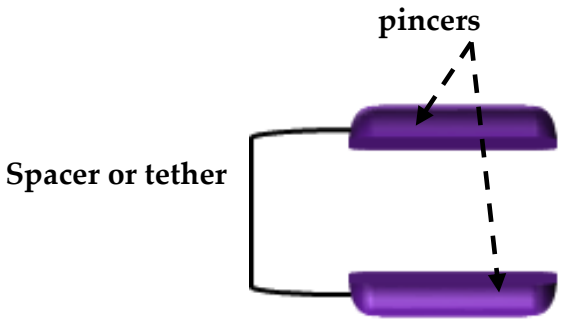


Figure 2.12: General structure of molecular tweezers.

The term "molecular tweezers" was introduced by Chen and Whitlock[129] in 1978 to describe a molecular receptor characterized by two flat, generally aromatic, identical pincers separated by some more or less rigid spacer. In their original publication, Chen and Whitlock proposed the flexible molecular tweezers involving two caffeine molecules separated by an alkyl-diyne spacer (Figure 2.13).

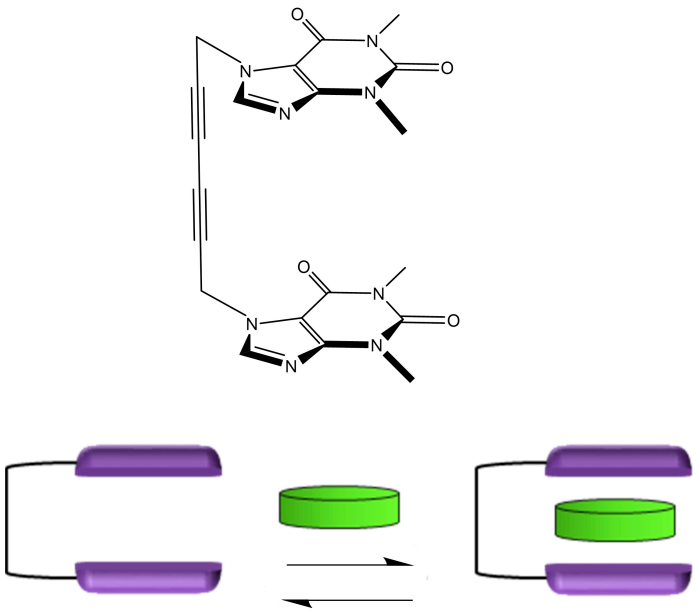


Figure 2.13: Chen and Whitlock's molecular tweezers and their principle for molecular recognition.

Soon afterwards, some criteria were established to define molecular tweezers.[130] These are:

(1) The presence of a spacer that prevents self-association of the arms or pincers.

(2) A spacer that establishes a distance between the pincers of about 7 Å (plane to plane or centroid to centroid), ideal for the inclusion of a single aromatic guest.

(3) A spacer that holds the pincers rigidly in a *syn* conformation. Although, the diene tether of the molecular tweezers introduced by Chen and Whitlock did not meet this third criterion, they were very important for further developments.

Molecular tweezers gained popularity in the mid-1980s to early 1990s with the introduction of a rigid spacer in a *syn* conformation by Zimmerman[131, 132] and later by Klärner and co-workers.[133] Zimmerman *et al.* designed molecular tweezers showing a high degree of pre-organization with a spacer that enforced a *syn* conformation of the binding pincers. However, the tweezers still exhibit a certain degree of conformational mobility since both pincers can potentially rotate around the bond that connecting them to the spacer. Such rotation changes the cavity size, allowing some optimization to take place during the binding process. On the other hand, Klärner and co-workers developed highly rigidified polyarene architectures. Representative examples of these two families of tweezers are depicted in Figure 2.14.

It is noteworthy that design and synthesis of molecular tweezers is an issue of great interest in supramolecular chemistry. In particular, many efforts are devoted to design and synthesis of tweezers appropriate to receiving fullerenes by concave-convex host-guest complementarity and molecular machines that function through host-guest recognition. Both show promising perspectives toward molecular nanodevices.

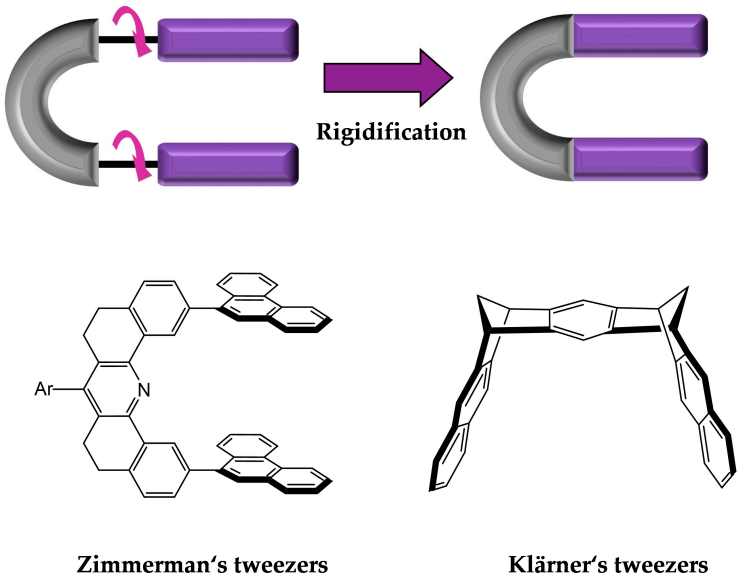


Figure 2.14: Two families of molecular tweezers with different degrees of rigidification.

In recent years several molecular tweezers have been synthesized and a series of reviews with emphasis on a specific aspect of molecular tweezers have been published: Zimmerman in 1991[134] and 1993[135] on rigid molecular tweezers, Nolte in 1995[136] and 1999[137] on glycoluril-based molecular clips, Klärner in 2003 on polyarene molecular clips and tweezers,[133] Harmata in 2004 on chiral molecular tweezers,[130] Martín in 2010 on molecular tweezers for fullerenes[54] and Sallé on molecular clips and tweezers hosting neutral guests in 2011.[12] In addition, in 2011 Leblond published a minireview on the nature and flexibility of the spacer group.[138]

2.6.1. Molecular tweezers with buckybowls pincers

Recently, Sygula and co-workers[35] introduced a novel type of molecular tweezers with buckybowl pincers. These authors showed that accessible concave surfaces of the buckybowls appear to be ideal candidates for recognizing curved-surface fullerenes through concave-convex ball-and-socket interactions. Figure 2.15 shows their famous molecular tweezers $C_{60}H_{28}$ made up by two corannulene pincers and a tetrabenzocyclooctatetraene tether forming a stable inclusion complex with C_{60}.

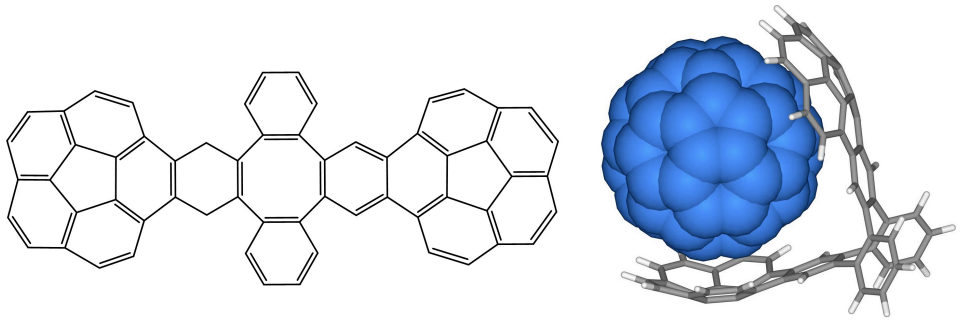


Figure 2.15: Molecular tweezers synthesized by Sygula and co-workers.[35]

The experimental results proved that molecular tweezers $C_{60}H_{28}$ form a stable inclusion complex with C_{60}, both in solid state and in toluene solution. According to those studies, these tweezers can "embrace" a molecule of C_{60} forming a 1:1 inclusion complex through pure concave-convex $\pi\cdots\pi$ interactions. [35]

Undoubtedly, a different functionalization of buckybowls, which constitute the main part of tweezers, could provide selective trapping of different species, thus obtaining a very efficient "buckycatcher". There are two main strategies for the funcionalization of the corannulene pincers: increase the structure of the bowl and introduce substituents groups onto the *rim* of the bowls.

The most basic functionalzation of corannulene is the introduction of alkyl chains to the *rim*. Several alkyl substituted corannulene derivatives have been synthesized in last years.[33, 139, 140] According to theoretical studies, the introduction of methyl groups on a buckycatcher is a good strategy to enhance the fullerene recognition through CH···π interactions.[69, 73, 74]

In recent years, several buckybowls with different geometric and electronic properties have been synthesized.[85-93, 101, 141, 142] In this context, knowing the factors that maximize the concave-convex π···π interaction between buckybowls and fullerenes is crucial in order to design and synthesize more effective molecular tweezers.

2.6.2. Applications of molecular tweezers with buckybowls pincers

Since the search for molecular receptors of fullerenes continues to be a very active field of researches, the utility of molecular tweezers could be very large, especially in separation and materials sciences.

Sygula and Collier envision future applications for the buckycatchers as stationary phases in liquid chromatography for the separation of fullerenes, and as buckycatcher-fullerene complexes in photovoltaic devices.[143]

Recently, Japan and U.S., have begun the industrial scale production of C_{60} in multi-ton quantities.[144] The ability to produce vast quantities of fullerenes in industrial settings makes it a significant occupational hazard. Despite there is no agreement on fullerenes as an occupational hazard or ultimately as a consumer or environmental hazard, recent studies show that fullerenes and their derivatives represent potential health risks.[145, 146] According to Sygula and Collier, in the coming years will surely grow the need for chromatographic separation of fullerenes and their detection at low concentration.[143]

As commented above, molecular tweezers with buckybowl pincers interact with fullerenes through π···π concave-convex stacking of curved carbon networks.[35] So, buckycatchers could be attached to stationary chromatographic phases and they will modify the absorption of fullerenes onto the surface, thereby changing their elution time. Moreover, specific buckycatchers could be synthetized immobilized on silica gel or other porous stationary phases for the separation of fullerene mixtures (Figure 2.16).[143] Once achieved the anchoring of buckycatchers on a solid support, the bilayers composed by buckycatchers (host) and fullerenes deposited above them (guest), are potentially light acceptors for photovoltaic devices (Figure 2.17).[143] That is because fullerenes absorb light very efficiently and are good electron acceptors, facts that have been extensively studied.[37, 147]

On the other hand, recent theoretical studies have already predicted potential applications for the host-guest complex $C_{60}H_{28}\cdots C_{60}$, such as a two-photon absorption active (TPA) material at near IR wavelengths that show application in photodynamic cancer therapy (PDCT)[148] and as a charge-transfer mediating with attracting applications

in nanoelectronic devices.[149] In addition, recent studies show that crystallization of supramolecular complexes made up by buckycatcher $C_{60}H_{28}$ and endohedral nitrogen fullerene ($N@C_{60}$) from toluene provides a solid material with a columnar alignment of fullerene cages that can be a candidate as qubit for quantum-information processing (QIP).[150]

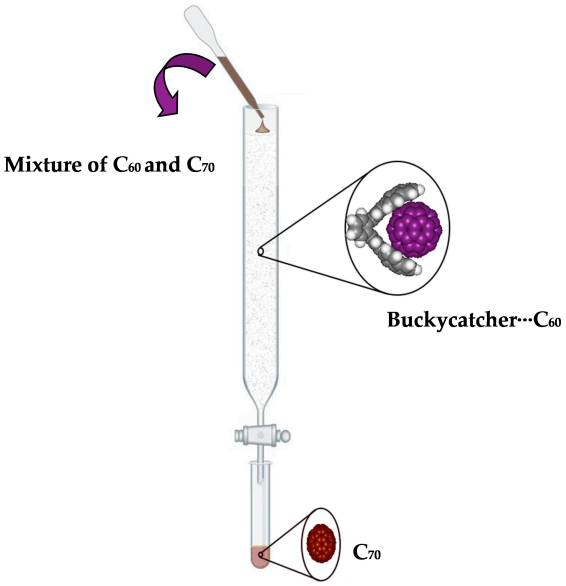


Figure 2.16: A schematic representation of buckycatchers as stationary phase in liquid chromatography for the separation of fullerenes.

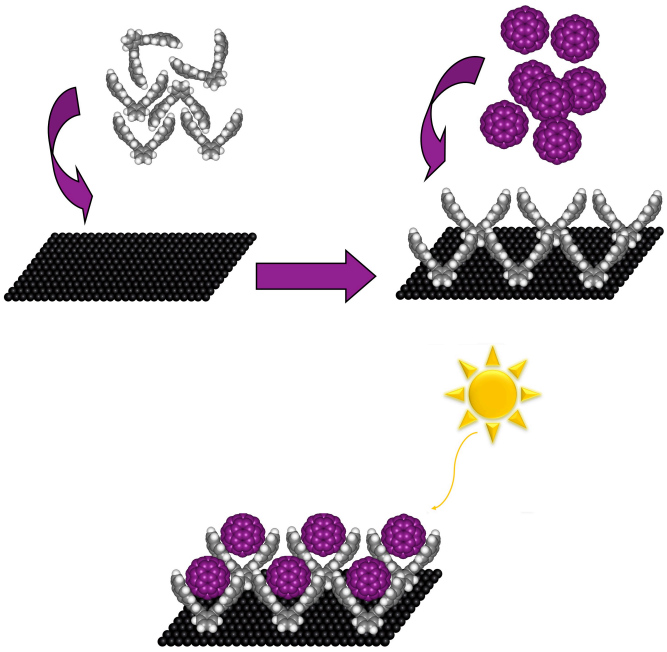


Figure 2.17: A schematic representation of a bilayer formation on a solid support and their applications as potential photovoltaic devices.

2.7. References

1. J. M. Lehn, *Prix Nobel*, 1988, 129-176.
2. J. W. Steed, *Supramolecular Chemistry: Definition, in Encyclopedia of Supramolecular Chemistry,* ed. J. L. Atwood, J. W. Steed, Dekker, New York, 2004.
3. J. W. Steed and J. L. Atwood, *Supramolecular Chemistry,* 2nd Edition, John Wiley & Sons, 2009.
4. E. P. Kyba, R. C. Helgeson, K. Madan, G. W. Gokel, T. L. Tarnowski, S. S. Moore and D. J. Cram, *J. Am. Chem. Soc.*, 1977, **99**, 2564-2571.
5. E. Fischer, *Ber. Dtsch. Chem. Ges.*, 1894, **27**, 2985–2993.
6. C. J. Pedersen, *J. Am. Chem. Soc.*, 1967, **89**, 7017-7035.
7. D. J. Cram and J. M. Cram, *Acc. Chem. Res.*, 1978, **11**, 8-14.
8. D. J. Cram and J. M. Cram, 1997, 1-19.
9. A. Hamilton, J. M. Lehn and J. L. Sessler, *J. Am. Chem. Soc.*, 1986, **108**, 5158-5167.
10. B. Dietrich, Cryptands, *in Encyclopedia of Supramolecular Chemistry,* ed. J. L. Atwood, J. W. Steed, Dekker, New York, 2004.
11. B. Tummler, G. Maass, E. Weber, W. Wehner and F. Vogtle, *J. Am. Chem. Soc.*, 1977, **99**.
12. M. Hardouin-Lerouge, P. Hudhomme and M. Salle, *Chem. Soc. Rev.*, 2011, **40**, 30-43.
13. P. J. Cragg, Supramolecular Terapheutics *in Supramolecular Chemistry from Biological Inspiration to Biological Applications,* Springer, University of Brighton, UK, 2010.
14. D. Nagda, K. S. Rathore, M. Bharkatiya, S. S. Sisodia and R. K. Nema, *J. Chem. Pharm. Res.*, 2010, **2**, 240-248.
15. P. J. Cragg, Supramolecular Sensors *in Supramolecular Chemistry from Biological Inspiration to Biological Applications*, Springer, University of Brighton, UK, 2010.
16. V. Balzoni, M. Gomez-Lopez and J. F. Stoddart, *Acc. Chem. Res.*, 1998, **31**, 405-414.
17. S. Erdemir, M. Bahadir and M. Yilmaz, *J Hazard Mater*, 2009, **168**, 1170-1176.
18. J. M. Lluch, *Química Teórica y Computacional,* Editores: Juan Andrés y Beltrán, Ed. Publicaciones de la Universitat Jaume I, 2000.
19. I. G. Kaplan, *Intermolecular Interactions: Physical Picture, Computational Methods and Model Potentials;* John Wiley and Sons: Mexico, 2006.
20. K. Tiefenbacher and J. Rebek, Jr., *J. Am. Chem.Soc.*, 2012, **134**, 2914-2917.
21. V. Spiwok, P. Hobza and J. Řezáč, *J. Phys. Chem. C*, 2011, **115**, 19455-19462.
22. M. O. Sinnokrot and C. D. Sherrill, *J. Phys. Chem. A*, 2006, **110**, 10656-10668.
23. C. A. Hunter and J. K. M. Sanders, *J. Am. Chem. Soc.*, 1990, **112**, 5525-5534.
24. M. F. Brana, M. Cacho, A. Gradillas, B. Pascual-Teresa and A. Ramos, *Curr. Pharm. Des.*, 2001, **7**, 1745-1780.
25. T. F. Headen, C. A. Howard, N. T. Skipper, M. A. Wilkinson, D. T. Bowron and A. K. Soper, *J. Am. Chem. Soc.*, 2010, **132**, 5735–5742.
26. S. Grimme, J. Antony, T. Schwabe and C. Mück-Lichtenfeld, *Org. Biomol. Chem.*, 2007, **5**, 741-758.
27. S. Grimme, *Angew. Chem. Int. Ed.* , 2008, **47**, 3430-3434.
28. M. O. Sinnokrot and C. D. Sherrill, *J. Phys. Chem. A*, 2003, **107**, 8377-8379.
29. M. O. Sinnokrot and C. D. Sherrill, *J. Am. Chem. Soc.*, 2004, **126**, 7690-7697.

30. A. L. Ringer and C. D. Sherrill, *J. Am. Chem. Soc.*, 2009, **131**, 4574–4575.
31. S. A. Arnstein and C. D. Sherrill, *Phys. Chem. Chem. Phys.*, 2008, **10**, 2646–2655.
32. A. L. Ringer, M. O. Sinnokrot, R. P. Lively and C. D. Sherrill, *Chem. Eur. J.*, 2006, **12**, 3821 – 3828.
33. Y. T. Wu, D. Bandera, R. Maag, A. Linden, K. K. Baldridge and J. S. Siegel, *J. Am. Chem. Soc.*, 2008, **130**, 10729–10739
34. A. Sygula and S. Saebø, *Int. J. Quantum Chem.*, 2009, **109**, 65-72.
35. A. Sygula, F. R. Fronczek, R. Sygula, P. W. Rabideau and M. M. Olmstead, *J. Am. Chem. Soc.*, 2007, **129**, 3842-3843.
36. R. C. Haddon, *Acc. Chem. Res.*, 1992, **25**, 127-133.
37. R. C. Haddon, R. E. Palmer, H. W. Kroto and P. A. Sermon, 1993.
38. R. C. Haddon, *J. Am. Chem. Soc.*, 1997, **119**, 1797-1798.
39. M. R. Kennedy, L. A. Burns and C. D. Sherrill, *J. Phys. Chem. A*, 2012, **116**, 11920-11926.
40. M. Nishio, *Phys. Chem. Chem. Phys.*, 2011, **13**, 13873-13900.
41. M. Nishio, Y. Umezawa, J. Fantini, M. S. Weiss and P. Chakrabarti, *Phys. Chem. Chem. Phys.*, 2014, **16**, 12648-12683.
42. M. Nishio, *J. Mol. Struct.*, 2012, **1018**, 2-7.
43. H. W. Kroto, J. R. Heath, S. C. O'Brien, R. F. Curl and R. E. Smalley, *Nature*, 1985, **318**, 162-163.
44. H. W. Kroto, *Nobel Lecture*, 1996, 44-78.
45. W. Kratschmer, L. D. Lamb, K. Fostiropoulos and D. R. Huffman, *Nature*, 1990, **347**, 354-358.
46. R. Taylor and G. A. Burley, Production, Isolation and Purification of Fullerenes in *Fullerenes Principles and Applications.* Ed. Fernando Langa and Jean-François Nierengarten. Cambridge: RSC Publ., 2008, ch. 1, pp. 1-14.
47. R. Taylor, J. P. Hare, A. K. Abdul-Sada and H. W. Kroto, *J. Chem. Soc., Chem. Commun.*, 1990, 1423-1425.
48. C. Lindqvist, J. Bergqvist, O. Bäcke, S. Gustafsson, E. Wang, E. Olsson, O. Inganäs, M. R. Andersson and C. Müller, *Appl. Phys. Lett.*, 2014, **104**, 153301.
49. P. Hudhomme and J. Cousseau, Plastic Solar Cells Using Fullerene Derivatives *in the Photoactive Layer in Fullerenes Principles and Applications.* Ed. Fernando Langa and Jean-François Nierengarten. Cambridge : RSC Publ., 2008, ch. 8, pp. 221-265.
50. E. Voroshazi, K. Vasseur, T. Aernouts, P. Heremans, A. Baumann, C. Deibel, X. Xue, A. J. Herring, A. J. Athans, T. A. Lada, H. Richter and B. P. Rand, *J. Mater. Chem.*, 2011, **21**, 17345.
51. R. Bakry, R. M. Vallant, M. Najam-ul-Haq, M. Rainer, Z. Szabo, C. W. Huck and K. B. Günther, *Int. J. Nanomedicine*, 2007, **2**, 639–649.
52. A. Bianco and T. Ros, *Biological Applications of Fullerenes in Fullerenes Principles and Applications.* Ed. Fernando Langa and Jean-François Nierengarten. Cambridge: RSC Publ., 2008, ch. 10, pp. 301-328..
53. J. Luczkowiak, A. Munoz, M. Sanchez-Navarro, R. Ribeiro-Viana, A. Ginieis, B. M. Illescas, N. Martín, R. Delgado and J. Rojo, *Biomacromolecules*, 2013, **14**, 431-437.
54. E. M. Pérez and N. Martín, *Pure Appl. Chem.*, 2010, **82**, 523-533.
55. F. Diederich, J. Effing, U. Jonas, L. Jullien, T. Plesnivy, H. Ringsdor, C. Thilgen and D. Weinstein, *Angew. Chem. Int. Ed. Engl.*, 1992, **31**, 1599-1602.

56. T. Andersson, K. Nilsson, M. Sundahl, G. Westman and O. Wennerstrom, *J. Chem. Soc., Chem. Commun.*, 1992, 604-606.
57. F. D'Souza and O. Ito, *Chem. Commun.*, 2009, 4913-4928.
58. J. Wang, S. G. Bodige, W. H. Watson and C. D. Gutsche, *J. Org. Chem.*, 2000, **65**, 8260-8263.
59. J. C. Iglesias-Sánchez, A. Fragoso, J. Mendoza and P. Prados, *Org. Lett.*, 2006, **8**, 2571-2574.
60. M. Makha, M. J. Hardie and C. L. Raston, *Chem. Commun.*, 2002, 1446-1447.
61. S. Bhattacharya, S. K. Nayak, A. Semwal, S. Chattopadhyay and M. Banerjee, *J. Phys. Chem. A*, 2004, **108**, 9064-9068.
62. O. D. Fox, J. Cookson, E. J. S. Wilkinson, M. G. B. Drew, E. J. MacLean, S. J. Teat and P. D. Beer, *J. Am. Chem. Soc.*, 2006, **128**, 6990-7002.
63. F. C. Tucci, D. M. Rudkevich and J. Rebek, Jr., *J. Org. Chem.*, 1999, **64**, 4555-4559.
64. A. M. Bond, W. Miao, C. L. Raston, T. J. Ness, M. J. Barnes and J. L. Atwood, *J. Phys. Chem. B*, 2001, **105**, 1687-1695.
65. E. Huerta, H. Isla, E. M. Pérez, C. Bo, N. Martín and J. de Mendoza, *J. Am. Chem. Soc.*, 2010, **132**, 5351–5353.
66. S. Zhang, A. Palkar, A. Fragoso, P. Prados, J. de Mendoza and L. Echegoyen, *Chem. Mater.*, 2005, **17**, 2063-2068.
67. P. A. Denis, *Chem. Phys. Lett.*, 2014, **591**, 323–327.
68. P. A. Denis, *New J. Chem.*, 2014.
69. P. A. Denis, *RSC Adv.*, 2013, **3**, 25296-25305.
70. P. A. Denis, *Chem. Phys. Lett.*, 2011, **516**, 82-87.
71. I. Welsh and M. Lein, *J. Comput. Chem.*, 2014, **35**, 181-191.
72. P. E. Georghiou, A. H. Tran, S. Mizyed, M. Bancu and L. T. Scott, *J. Org. Chem.*, 2005, **70**, 6158-6163.
73. D. Josa, J. Rodríguez-Otero, E. M. Cabaleiro-Lago, L. A. Santos and T. C. Ramalho, *J. Phys. Chem. A*, 2014, **118**, 9521-9528.
74. D. Josa, L. Azevedo dos Santos, I. González-Veloso, J. Rodríguez-Otero, E. M. Cabaleiro-Lago and T. de Castro Ramalho, *RSC Adv.*, 2014, **4**, 29826-29833.
75. T. Kawase and H. Kurata, *Chem. Rev.*, 2006, **106**, 5250-5273.
76. T. Kawase, N. Fujiwara, M. Tsutumi, M. Oda, Y. Maeda, T. Wakahara and T. Akasaka, *Angew. Chem. Int. Ed.* , 2004, **43**, 5060-5062.
77. E. M. Pérez, L. Sanches, G. Fernández and N. Martın, *J. Am. Chem. Soc.*, 2006, **128**, 7172-7173.
78. E. M. Pérez, A. L. Capodilupo, G. Fernandez, L. Sanchez, P. M. Viruela, R. Viruela, E. Orti, M. Bietti and N. Martin, *Chem. Commun.*, 2008, 4567-4569.
79. E. M. Pérez, M. Sierra, L. Sanchez, M. R. Torres, R. Viruela, P. M. Viruela, E. Orti and N. Martín, *Angew. Chem., Int. Ed.*, 2007, **46**, 1847-1851.
80. K. Tashiro and T. Aida, *Chem. Soc. Rev.*, 2007, **36**, 189-197.
81. H. Sato, K. Tashiro, H. Shinmori, A. Osuka, Y. Murata, K. Komatsu and T. Aida, *J. Am. Chem. Soc.*, 2005, **127**, 13086-13087.
82. M. Yanagisawa, K. Tashiro, M. Yamasaki and T. Aida, *J. Am. Chem. Soc.*, 2007, **129**, 11912-11913.
83. D. Sun, F. S. Tham, C. A. Reed, L. Chaker and P. D. W. Boyd, *J. Am. Chem. Soc.*, 2002, **124**, 6604-6612.
84. E. M. Pérez and N. Martín, *Chem. Soc. Rev.*, 2008, **37**, 1512-1519.

85. A. Sygula, *Eur. J. Org. Chem.*, 2011, **2011**, 1611-1625.
86. A. C. Whalley, K. N. Plunkett, A. A. Gorodetsky, C. L. Schenck, C.-Y. Chiu, M. L. Steigerwald and C. Nuckolls, *Chem. Sci.*, 2011, **2**, 132-135.
87. E. A. Jackson, B. D. Steinberg, M. Bancu, A. Wakamiya and L. T. Scott, *J. Am. Chem. Soc.*, 2007, **129**, 484-485.
88. T. C. Wu, H. J. Hsin, M. Y. Kuo, C. H. Li and Y. T. Wu, *J. Am. Chem. Soc.*, 2011, **133**, 16319-16321.
89. H. Sakurai, T. Daiko and T. Hirao, *Science*, 2003, **301**, 1878.
90. S. Higashibayashi and H. Sakurai, *Chem. Lett.*, 2011, **40**, 122-128.
91. L. T. Scott, *Pure & Appl. Chem.*, 1996, **68**, 291-300.
92. G. Mehta and G. Panda, *Chem. Commun.*, 1997, 2081-2082.
93. T. C. Wu, M. K. Chen, Y. W. Lee, M. Y. Kuo and Y. T. Wu, *Angew. Chem. Int. Ed.*, 2013, **52**, 1289-1293.
94. M. Rellán Piñero, J. Rodríguez Otero, E. M. Cabaleiro Lago and D. Josa, *J. Mol. Model.*, 2013, **19**, 2049-2055.
95. T. J. Seiders, K. K. Baldridge, G. H. Grube and J. S. Siegel, *J. Am. Chem. Soc.*, 2001, **123**, 517-525.
96. K. Kavitha, M. Manoharan and P. Venuvanalingam, *J. Org. Chem.*, 2005, **70**, 2528-2536.
97. A. K. Kandalam, B. K. Rao and P. Jena, *J. Phys. Chem. A*, 2005, **109**, 9220-9225.
98. P. A. Denis, *J. Mol. Struct.:THEOCHEM*, 2008, **865**, 8-13.
99. T. Janowski, P. Pulay, A. A. Sasith Karunarathna, A. Sygula and S. Saebø, *Chem. Phys. Lett.*, 2011, **512**, 155-160.
100. A. M. Butterfield, B. Gilomen and J. S. Siegel, *Org. Process Res. Dev.*, 2012, **16**, 664-676.
101. W. E. Barth and R. G. Lawton, *J. Am. Chem. Soc.*, 1966, **88**, 380-381.
102. R. B. M. Ansems and L. T. Scott, *J. Am. Chem. Soc.*, 2000, **122**, 2719-2724.
103. J. C. Hanson and C. E. Nordman, *Acta Cryst.*, 1976, **B32**, 1147-1153.
104. H. Sakurai, T. Daiko, H. Sakane, T. Amaya and T. Hirao, *J. Am. Chem. Soc.*, 2005, **127**, 11580-11581.
105. T. Amaya, H. Sakane, T. Nakata and T. Hirao, *Pure Appl. Chem.*, 2010, **82**, 969–978.
106. M. A. Petrukhina and L. T. Scott, *Dalton transactions*, 2005, 2969-2975.
107. P. A. Vecchi, C. M. Alvarez, A. Ellern, R. J. Angelici, A. Sygula, R. Sygula and P. W. Rabideau, *Organometallics*, 2005, **24**, 4543-4552.
108. H. Sakane, T. Amaya, T. Moriuchi and T. Hirao, *Angew. Chem.*, 2009, **48**, 1640-1643.
109. A. S. Filatov and M. A. Petrukhina, *Coord. Chem. Rev.*, 2010, **254**, 2234-2246.
110. U. D. Priyakumar and G. N. Sastry, *Tetrahedron Lett.*, 2003, **44**, 6043-6046.
111. J. R. Green and R. C. Dunbar, *J. Phys. Chem. A*, 2011, **115**, 4968-4975.
112. J. A. Carrazana-Garcia, J. Rodriguez-Otero and E. M. Cabaleiro-Lago, *J. Phys. Chem. B*, 2011, **115**, 2774-2782.
113. P. García-Novo, A. Campo-Cacharrón, E. M. Cabaleiro-Lago and J. Rodríguez-Otero, *Phys. Chem. Chem. Phys.*, 2012, **14**, 104-112.
114. A. Campo-Cacharrón, E. M. Cabaleiro-Lago and J. Rodríguez-Otero, *J. Comput. Chem.*, 2014, **35**, 1533-1544.
115. A. Campo-Cacharrón, E. M. Cabaleiro-Lago, I. Gonzalez-Veloso and J. Rodríguez-Otero, *J. Phys. Chem. A*, 2014, **118**, 6112-6124.

116. B. Zhu, A. Ellern, A. Sygula, R. Sygula and R. J. Angelici, *Organometallics*, 2007, **26**, 1721-1728.
117. M. A. Petrukhina, *Angew. Chem.*, 2008, **47**, 1550-1552.
118. A. Y. Rogachev, Y. Sevryugina, A. S. Filatov and M. A. Petrukhina, *Dalton trans.*, 2007, 3871-3873.
119. R. C. Dunbar, *J. Phys. Chem. A*, 2002, **106**, 9809-9819.
120. H. Becker, G. Javahery, S. Petrie, P. C. Cheng, H. Schwarz, L. T. Scott and D. K. Bohme, *J. Am. Chem. Soc.*, 1993, **115**, 11636-11637.
121. S. Mizyed, P. E. Georghiou, M. Bancu, B. Cuadra, A. K. Rai, P. Cheng and L. T. Scott, *J. Am. Chem. Soc.*, 2001, **123**, 12770-12774.
122. B. M. Wong, *J. Comput. Chem.*, 2009, **30**, 51-56.
123. Y. Zhao and D. G. Truhlar, *Phys. Chem. Chem. Phys.*, 2008, **10**, 2813–2818.
124. L. Kobryn, W. P. Henry, F. R. Fronczek, R. Sygula and A. Sygula, *Tetrahedron Lett.*, 2009, **50**, 7124-7127.
125. C. Mück-Lichtenfeld, S. Grimme, L. Kobryn and A. Sygula, *Phys. Chem. Chem. Phys.*, 2010, **12**, 7091-7097.
126. D. Josa, J. Rodríguez Otero and E. M. Cabaleiro Lago, *Phys. Chem. Chem. Phys.*, 2011, **13**, 21139-21145.
127. D. Josa, J. Rodríguez-Otero, E. M. Cabaleiro-Lago and M. Rellán-Piñeiro, *Chem. Phys. Lett.*, 2013, **557**, 170-175.
128. G. Casella and G. Saielli, *New J. Chem.*, 2011, **35**, 1453.
129. C.-W. Chen and H. W. Whitlock Jr., *J. Am. Chem. Soc.*, 1978, **100**, 4921-4922.
130. M. Harmata, *Acc. Chem. Res.*, 2004, **37**, 862-873.
131. S. C. Zimmerman and C. M. VanZyl, *J. Am. Chem. Soc.*, 1987, **109**, 7894-7896.
132. S. C. Zimmerman and W. Wu, *J. Am. Chem. Soc.*, 1989, **111**, 8054-8055.
133. F. G. Klärner and B. Kahlert, *Acc. Chem. Res.*, 2003, **36**, 919-932.
134. S. C. Zimmerman, *Bioorga. Chem. Front.*, 1991, **2**, 33-71.
135. S. C. Zimmerman, *Top. Curr. Chem.*, 1993, **165**, 71-102.
136. R. P. Sijbesma and R. J. M. Nolte, *Top. Curr. Chem.*, 1995, **175**, 25-56.
137. A. E. Rowan, J. A. A. W. Elemans and R. J. M. Nolte, *Acc. Chem. Res.*, 1999, **32**, 995-1006.
138. J. Leblond and A. Petitjean, *ChemPhysChem*, 2011, **12**, 1043-1051.
139. T. J. Seiders, E. L. Elliott, G. H. Grube and J. S. Siegel, *J. Am. Chem. Soc.*, 1999, **121**, 7804-7813.
140. Y. Sevryugina, A. Y. Rogachev, E. A. Jackson, L. T. Scott and M. A. Petrukhina, *J. Org. Chem.*, 2006, **71**, 6615-6618.
141. S. Hagen, M. S. Bratcher, M. S. Erickson, G. Zimmermann and L. T. Scott, *Angew. Chem. Int. Ed. Engl.*, 1997, **36**, 406-408.
142. S. Higashibayashi, *J. Am. Chem. Soc.*, 2008, **130**, 8592–8593.
143. A. Sygula and W. E. Collier, Molecular Clips and Tweezers with Corannulene Pincers, in *Fragments of Fullerenes and Carbon Nanotubes: Designed Synthesis, Unusual Reactions, and Coordination Chemistry* (eds M. A. Petrukhina and L. T. Scott), John Wiley & Sons, Inc., Hoboken, NJ, USA., 2011, ch. 1, pp. 1-40.
144. L. T. Scott, *Angew. Chem. Int. Ed.*, 2004, **43**, 4994-5007.
145. J. Gao, H. L. Wang, A. Shreve and R. Iyer, *Toxicol. Appl. Pharmacol.*, 2010, **244**, 130-143.

146. E. J. Park, H. Kim, Y. Kim, J. Yi, K. Choi and K. Park, *Toxicol. Appl. Pharmacol.*, 2010, **244**, 226-233.
147. A. J. Ferguson, J. L. Blackburn and N. Kopidakis, *Mater. Lett.*, 2013, **90**, 115-125.
148. S. Chakrabarti and K. Ruud, *J. Phys. Chem. A*, 2009, **113**, 5485–5488.
149. A. A. Voityuk and M. Duran, *J. Phys. Chem. C*, 2008, **112**, 1672-1678.
150. J. Yang, P. Feng, A. Sygula, W. Harneit, J.-H. Su and J. Du, *Phys. Lett. A*, 2012, **376**, 1748-1751.

Chapter 3

Methodology

In this Chapter, the theoretical foundations of the methods employed in this thesis will be presented. It is important to emphasize that the aim of this Chapter is neither presenting an exhaustive description of subjects nor discussing the theories with their entire mathematical rigor. The main objective of this Chapter is showing the methodologies employed and their theoretical principles. For a more complete discussion, the suggested references can be consulted.

3.1. Introduction

The objectives proposed in this doctoral thesis have been achieved through the use of quantum chemistry methodology, which has been proved a powerful tool to analyse phenomena of various kinds. This methodology offers valuable interpretive information and it also can provide very useful predictive information to guide the design of new molecules that make use of concave-convex π···π interactions.

Nevertheless, in general it is noteworthy that accurate description of the π···π interactions is a challenging task for quantum chemistry methods.[1, 2] Accurate *ab initio*-correlated wavefunction methods, such as CCSD(T) in combination with a large basis set, give rise to a good level of accuracy. However, this calculation level is prohibitively expensive for large systems. On the other hand, "cheaper" methods, such as MP2, remain unfeasible for large systems, and tend to overestimate the interaction energy, especially for dispersive π···π interactions.[3-9] Density functional theory (DFT), the most widely used methodology for electronic calculations in chemistry and physics, offers the opportunity to study large systems at a reasonable computational cost.[10, 11] However, it is not appropriate for treatment of non-covalent interactions, because conventional DFT techniques fail to treat dispersion effects completely. In order to solve this problem, nowadays, two types of strategies have been developed. The first one is the development of new types of functionals as BMK[12], M05[13] or M06.[14] Variants of the latter two (M05-2X[15] and M06-2X[14]) were recently used to study the concave-convex interaction in the tweezers designed by Sygula *et al*.[16, 17] The second strategy lies in trying to correct the deficiencies of the existing functional adding an empirical term for the dispersion: these are the so-called DFT-D methods.[18-20] The inclusion of empirical dispersion coefficients is a very simple technique, and this kind of approach has been applied

successfully in many applications. Recently, Peverati and Baldridge have tried several methods based on both strategies for the study of a set of polynuclear hydrocarbons.[21] According to their results, both types of procedures can be very promising, especially the latter. Grimme *et al.* also using DFT-D calculations have studied the anthracene dimer and the interaction of corannulene with small molecules (water, ammonia, methane).[22]

Despite the considerable progress in the development of new DFT versions achieved in recent years, theoretical estimates of interaction energy for the molecular tweezers designed by Sygula *et al.* lead to a huge variety of results: from 21 to 43 kcal/mol, depending on the DFT model used.[16, 17, 20, 23] Thus, knowing the range of application and the limitations of the new DFT versions to study concave-convex π···π interaction is a crucial step for the successfully design of new molecular tweezers.

Recently, for the corannulene dimer, Kennedy *et al.*[24] showed that the best results (compared with the benchmark performed at the QCISD(T)/aug-cc-pVTZ level[25]) correspond to B3LYP-D3(BJ), but with a very small advantage over B3LYP-D2, M06-2X and B97-D2 (Figure 3.1). Of these DFT methods, B97-D2 is the best to take advantage of the noticeable reduction of computational cost that allows the resolution of identity approximation (RI) implemented in Turbomole program suite,[26] since for non-hybrid functionals the RI procedure speeds up calculations by a factor 10 at least (as compared to conventional treatments) without sacrificing accuracy. In addition, calculations using B97-D2 method also provide very good results as can be observed in several previous works.[19, 23, 25, 27-30]

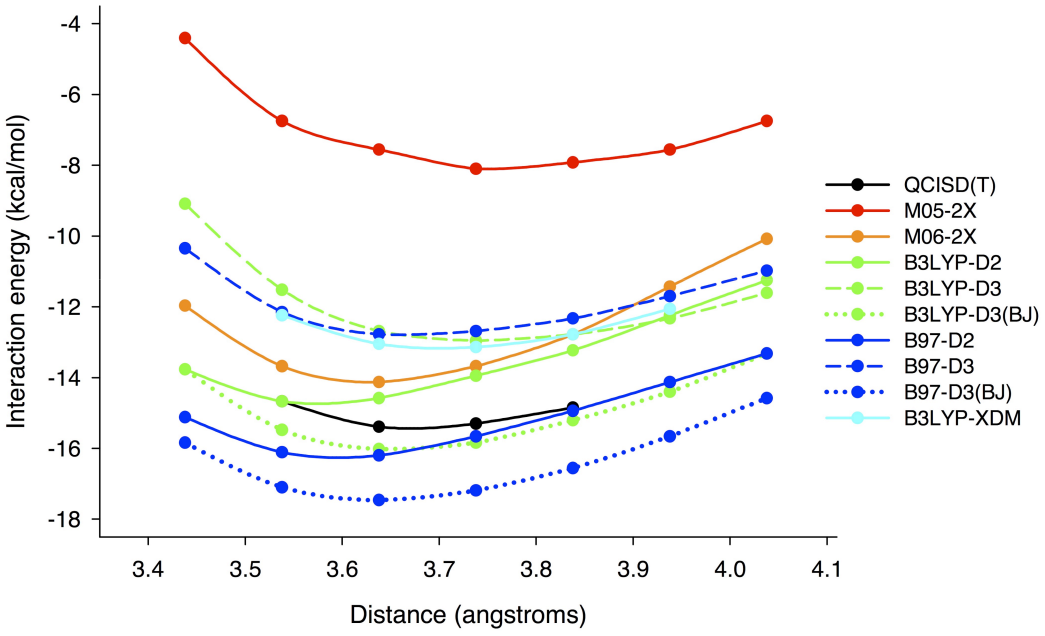


Figure 3.1: Counterpoise-corrected DFT/haDZ interaction energy for the corannulene dimer[24] compared to QCISD(T) reference values. Data taken from Reference 25.

Taking into account the above comments, the size of the studied systems and the software used (Turbomole), the choice of the B97-D2/TZVP level and the RI approximation seems appropriate. Therefore, this level calculation is employed in most calculations presented in this thesis.

3.2. Density functional theory (DFT)

The main strategy of this theory is to replace the wave function used for describing electrons in *ab initio* methods, by the electron density. While the wave function depends on 4*N* coordinates (three spatial coordinates and one spin coordinate for each electron), the electron density has the same number of variables (three spatial coordinates), independent the system size. So, the work is much easier both practically and conceptually.

The density functional theory began in the 20th century, with the works of Thomas and Fermi.[10, 31, 32] However, only in 1964, with the publication of two theorems by Hohenberg and Kohn,[33-35] DFT gained the status of theory based on solid physical basis.

3.2.1. Hohenberg and Kohn theorems

First theorem

"Any observable of a stationary non-degenerated ground state can be calculated, exactly in theory, from the electron density of the electron density of ground-state. In other words, any observable can be written as a functional of the electron density of the ground state."

The electron density must be *N*-representable, *i.e.*, must be a positive function defined in the entire space and its integral must be equal to the total number of electrons in the system:

$$\rho(\vec{r}) \geq 0 \quad \text{and} \quad \int \rho(\vec{r}) d\vec{r} = N \tag{3.1}$$

Furthermore, the electron density also should be *v*-representable, *i.e.*, there is an external potential from which density $\rho(\vec{r})$ can be derived.

Under these conditions, the electronic energy can be represented as:

$$E[\rho] = T[\rho] + V_{Ne}[\rho] + V_{ee}[\rho] \tag{3.2}$$

where $T[\rho]$ is the kinetic energy, $V_{Ne}[\rho]$ is the nuclear-electron attraction and $V_{ee}[\rho]$ is the interaction between electrons. $T[\rho]$ and $V_{ee}[\rho]$ are usually included within the Hohenberg-Kohn functional $F_{HK}[\rho]$.

The derivative of the nuclear-electron potential with respect to the electron density is the external potential $\upsilon(\vec{r})$:

$$\frac{\delta V_{Ne}}{\delta \rho} = \upsilon(\vec{r}) \tag{3.3}$$

Therefore, the electronic energy can be written as:

$$E[\rho] = \int \rho(\vec{r})\upsilon(\vec{r})d\vec{r} + F_{HK}[\rho] \tag{3.4}$$

Second theorem

"The electron density of a non-degenerate ground state can be calculated, exactly in theory, determining the density that minimizes the energy of the ground state."

The minimization of the functional of the energy with respect to the electron density provides the fundamental equation of the DFT:

$$\frac{\delta E[\rho]}{\delta \rho(\vec{r})} = \upsilon(\vec{r}) + \frac{\delta F_{HK}[\rho]}{\delta \rho(\vec{r})} = \mu \tag{3.5}$$

where μ is the chemical potential

Although these two theorems proved that the electronic energy of a system could be totally determined from its electronic density through the variational principle, there was still the difficulty to calculate accurately the kinetic energy term $T[\rho]$. Kohn and Sham[36] shortly after proposed a methodology able to solve these equations and obtain the total energy of the system.

3.2.2. Kohn-Sham method

To solve the problem of not knowing the connection between kinetic energy $T[\rho]$ and electron density, Kohn and Sham[36] suggested a method to calculate the energy from

the electron density employing the fact that if one knows the wavefunction ψ that describes the system, the kinetic energy $T[\psi]$ can easily be calculated.

So, the starting point of Kohn-Sham method is to suppose a reference system of N non-interacting electrons that is subjected to an external potential $\upsilon_s(\vec{r})$. This potential applied to the system generates a wave function, ψ_s, which has the same density that the real system. Since there are not interelectronic interactions, the Hartree-Fock method is accurate for this system and therefore the electronic Hamiltonian of this reference system is:

$$\hat{H}_s = \sum_{i=1}^{N} \hat{h}(i) = \sum_{i=1}^{N} -\frac{1}{2}\nabla^2(i) + \sum_{i=1}^{N} \hat{\upsilon}_s(i) \tag{3.6}$$

and the exact wave function of this system is the Slater determinant:

$$\psi_s = \frac{1}{\sqrt{N!}} \left| \chi_1(1)\chi_2(2)\chi_3(3)...\chi_N(N) \right| \tag{3.7}$$

The molecular orbitals of this determinant are obtained by solving the Hartree-Fock equations:

$$\left[-\frac{1}{2}\nabla^2 + \upsilon_s(\vec{r}) \right] \chi_i = E_i \chi_i \tag{3.8}$$

In addition, the exact electronic density and the exact kinetic energy for this system are as follows:

$$\rho(\vec{r}) = \sum_{i=1}^{m} \left| \chi_i(\vec{r}) \right|^2 \tag{3.9}$$

$$T_s[\rho] = \left\langle \sum_{i=1}^{m} \chi_i \left| -\frac{1}{2}\nabla_i^2 \right| \chi_i \right\rangle \tag{3.10}$$

where m is the number of occupied molecular orbitals and the subscript s indicates that the equation describes the reference system without interelectronic repulsions. Thereby, the fundamental DFT equation for this system is expressed as:

$$\frac{\delta E_s[\rho]}{\delta \rho(\vec{r})} = \upsilon_s(\vec{r}) + \frac{\delta T_s[\rho]}{\delta \rho(\vec{r})} = \mu \tag{3.11}$$

and the energy as:

$$E_s[\rho] = \sum_{i=1}^{m} E_i = T_s[\rho] + \int \rho(\vec{r}) \upsilon_s(\vec{r}) d\vec{r} \tag{3.12}$$

On the other hand, for the real system with electron-electron interactions, the total energy is given by:

$$E[\rho] = T_s[\rho] + \int \rho(\vec{r}) \upsilon(\vec{r}) d\vec{r} + J[\rho] + \left(T[\rho] - T_s[\rho]\right) + \left(V_{ee}[\rho] - J[\rho]\right) \tag{3.13}$$

where the Coulomb repulsion $J[\rho]$ between two electrons can be written as:

$$J[\rho] = \frac{1}{2} \iint \frac{\rho(\vec{r}_1)\rho(\vec{r}_2)}{\left|\vec{r}_1 - \vec{r}_2\right|} d\vec{r}_1 d\vec{r}_2 \tag{3.14}$$

The differences shown in equation 3.13 are defined as the following functionals:

$$T_c[\rho] = T[\rho] - T_s[\rho] \tag{3.15}$$

$$W_{XC}[\rho] = V_{ee}[\rho] - J[\rho] \tag{3.16}$$

where $T_c[\rho]$ is the correlation kinetic energy and $W_{XC}[\rho]$ is the exchange-correlation electronic energy.

Thus, the total exchange-correlation energy $E_{XC}[\rho]$ is the sum of these two energies:

$$E_{XC}[\rho] = T_c[\rho] + W_{XC}[\rho] \tag{3.17}$$

The exchange-correlation potential can be defined as the variation of $E_{XC}[\rho]$ with the electron density:

$$\upsilon_{XC}(\vec{r}) = \frac{\delta E_{XC}[\rho]}{\delta \rho(\vec{r})} \tag{3.18}$$

Therefore, replacing equations 3.14 and 3.17 into equation 3.13 one gets:

$$E[\rho] = T_s[\rho] + \int \rho(\vec{r}) \upsilon(\vec{r}) d\vec{r} + \frac{1}{2} \iint \frac{\rho(\vec{r}_1)\rho(\vec{r}_2)}{\left|\vec{r}_1 - \vec{r}_2\right|} d\vec{r}_1 d\vec{r}_2 + E_{XC}[\rho] \tag{3.19}$$

Applying the fundamental equation of DFT theory one obtains:

$$\frac{\delta E[\rho]}{\delta \rho(\vec{r})} = \frac{\delta T_s[\rho]}{\delta \rho(\vec{r})} + \upsilon(\vec{r}) + \int \frac{\rho(\vec{r}_2)}{|\vec{r}_1 - \vec{r}_2|} d\vec{r}_2 + \frac{\delta E_{XC}[\rho]}{\delta \rho(\vec{r})} = \mu \tag{3.20}$$

Since the Coulomb potential $\upsilon_c(\vec{r})$ is defined as:

$$\upsilon_c(\vec{r}) = \upsilon(\vec{r}) + \int \frac{\rho(\vec{r}_2)}{|\vec{r}_1 - \vec{r}_2|} d\vec{r}_2 \tag{3.21}$$

and the exchange-correlation potential following:

$$\upsilon_{XC}(\vec{r}) = \frac{\delta E_{XC}[\rho]}{\delta \rho(\vec{r})} \tag{3.22}$$

The fundamental equation of DFT for real systems can be written as:

$$\frac{\delta E[\rho]}{\delta \rho(\vec{r})} = \frac{\delta T_s[\rho]}{\delta \rho(\vec{r})} + \upsilon_e(\vec{r}) + \upsilon_{XC}(\vec{r}) = \mu \tag{3.23}$$

$$\frac{\delta T_s[\rho]}{\delta \rho(\vec{r})} + \upsilon_{eff}(\vec{r}) = \mu \tag{3.24}$$

If equations 3.24 and 3.11 are compared one can observe that the fundamental equation for a real system is equivalent to that of the reference system but substituting the external potential $\upsilon_s(\vec{r})$ by potential $\upsilon_{eff}(\vec{r})$. Since the equation to be solved is similar to equation 3.8, one can replace the monoelectronic Hamiltonian operator h_i by Kohn-Sham h_{KS}:

$$\hat{h}_{KS} = -\frac{1}{2}\nabla^2 + \upsilon_{eff}(\vec{r}) \tag{3.25}$$

Thereby, the equations to solve are very similar to Hartree-Fock equations:

$$\hat{h}_{KS}\chi_i = E_i\chi_i \tag{3.26}$$

In this case the orbitals are called Kohn-Sham orbitals, and they allow calculating the electronic density of a system:

$$\rho(\vec{r}) = \sum_{i=1}^{m} |\chi_i(\vec{r})|^2 \tag{3.27}$$

As for the Hartree-Fock method, the process to calculate the energy is iterative. The calculations start with a trial set of orbitals that are employed to compute the electron

density and with them the potential effective is obtained; then the effective potential is used to obtain the energy and wavefunctions. If these wavefunctions give rise to the same electron density the procedure has converged. Conversely, if the procedure has not converged the cycle will occur again until convergence is obtained.

The major bottleneck of DFT is the exchange-correlation energy, since an exact functional for its determination has not yet been proposed. Therefore, the different ways of approaching the exchange-correlation functional characterize the differences between the different DFT methods.

3.3. Exchange-correlation functionals

The exchange-correlation functionals can be classified in four generations depending on the approximations that are made to estimate $E_{XC}[\rho]$. The first one is the local density approximation (LDA). This approximation involves the exchange-correlation functional based on the atomic model of Thomas-Fermi-Dirac,[37] which assumes that the functional depends only on the electron density of a uniform gas. It is a very simple model and rarely gives rise to good results. A functional of this type is the VWN[38] developed by Vosko, Wilk and Nusair.

The second one is the generalized gradient approximation (GGA), with exchange-correlation functional $E_{XC}(\rho)$ depending not only on density ρ, but also of its gradient, and, therefore, the accuracy of the calculation increases. In general, these methods start with LDA and add gradient correction terms. There are several functionals of this kind, the most popular are those developed by Becke for exchange,[39] and Perdew[40] and Lee *et al.*[41] for correlation.

Another extension of GGA methods leads to the meta-GGA methods, which employ in their expression, in addition to the gradient, the second derivative (the Laplacian) of the density. These functionals achieve better results than the previous ones, but due to the complexity of their expressions also produce a large increase in computational cost. Functionals of these type are for example, B95,[42] τ-HCTH[43] and Minnesota functionals developed by Truhlar and co-workers.[13-15]

The last way to construct the functional is called hybrid or hyper-GGA methods, which include in their expression part of the exact Hartree-Fock exchange energy. As reference it can be cited the B3LYP, one of the hybrid functionals more widely used for DFT calculations. This functional contains a exchange term developed by Becke[39] (indicated by the letter B), and a correlation term developed by Lee, Yang and Parr[41] (indicated by the LYP abbreviation) and it also has three empirical parameters to optimize its performance (indicated by the number 3). This functional was employed for optimizations of the corannulene monomers in Chapter 4 due to it leads to a very similar geometry to that reported by X-ray for corannulene. [44]

Finally, it is noteworthy that most of the DFT functionals only provide local correlation effects that correspond with short-range effects. So, the last years have been

marked by the development of new DFT versions designed to overcome the failure of the standard DFT methods for describing the dispersive effects, as it will be explained in detail in the next section. Therefore, in this thesis the performance of several functionals for studying concave-convex π···π interactions was evaluated: B97-D,[19] PBE-D,[45] B-LYP-D,[39, 46] BP86-D,[39, 40] ωB97X-D,[47] M05-2X[15] and M06-2X.[14] These functionals can be arranged into three different groups based on the type of functional. The first four are GGA functionals with D2 empirical dispersion corrections; ωB97X-D is a long-range corrected GGA-hybrid functional with D2 empirical dispersion corrections; the latter two are Minnesota hybrid meta-GGA functionals specialized for the treatment of non-covalent interactions.

3.4. Dispersion-Corrected Density Functional Theory (DFT-D)

Despite the many applications of DFT methods, they cannot describe long-range electron correlations that are responsible for the dispersion forces. So, the use of dispersion-corrected DFT methods is mandatory to study concave-convex π···π interactions. Among them, perhaps the Grimme's empirical dispersion is the most popular. His original version (DFT-D),[18] was modified in 2006 (DFT-D2),[19] and further corrected in 2010 (DFT-D3)[20] and 2011 (DFT-D3(BJ)).[48]

As stated above (section 3.1), B97-D2 provides a good accuracy compared with the benchmark performed at the QCISD(T)/aug-cc-pVTZ level[25] for corannulene dimer. Therefore, the DFT-D2[19] version was employed in this thesis. For that reason along this manuscript, B97-D, or in general DFT-D, refers to the second implementation (-D2) of this kind of correction, unless otherwise specified.

3.4.1. DFT-D2

This approach enables taking into account the dispersive effects through the addition of an empirical C_6R^{-6} term to the standard density functionals.

In this method the total energy is given by

$$E_{DFT-D} = E_{KS-DFT} + E_{disp} \tag{3.28}$$

where $E_{KS\text{-}DFT}$ is the usual Kohn-Sham energy and E_{disp} is the empirical dispersion correction given by

$$E_{disp} = -S_6 \sum_{i=1}^{N-1} \sum_{j=i+1}^{N} \frac{C_6^{ij}}{R_{ij}^6} f_{dmp}(R_{ij}) \tag{3.29}$$

where, N is the number of atoms in the system, C_6^{ij} is the dispersion coefficient for the atom pair ij, S_6 is a global scaling factor that only depends on the functional used (1.25 for B97-D), R_{ij} is the interatomic distance between atoms i and j, and f_{dmp} is a damping (attenuating) function to suppress the emergence of a singularity when R approaches zero that is defined by

$$f_{dmp}(R_{ij}) = \frac{1}{1+e^{-d(R_{ij}/R_r-1)}} \tag{3.30}$$

where R_r is the sum of atomic van der Waals radii from atomic ROHF/TZVP computations and d is a constant set to 20.

As in the original DFT-D approach, too much weight is given to the smaller coefficient (lighter atom) when determining the dispersion coefficient for an atom pair. Grimme overcomes this problem in DFT-D2 by using a geometric mean of atomic contributions from C_6^i and C_6^j of the form

$$C_6^{ij} = \sqrt{C_6^i C_6^j} \tag{3.31}$$

where C_6 for a given atom a are calculated according to equation

$$C_6^a = 0.05 N I_p^a \alpha^a \tag{3.32}$$

where I_p^a and α^a are the ionization potential and the static dipole polarizabilities obtained from DFT/PBE0[49] calculations; N is the number of electrons in lattice corresponding to 2, 10, 18, 36 and 54 for atoms of 1-5 rows of Periodic Table. The value of the proportionality constant was selected to reproduce binding energies and bond distances of several complexes.

Finally, it is noteworthy that the DFT-D2 approach has showed a high accuracy for a large variety of applications such as fullerene inclusion complexes,[23] concave-convex interactions of corannulene[25] and a series of supramolecular structures and complexes of bio(organic) molecules.[21, 22]

3.5. *Reducing computational cost*

Unfortunately, conventional DFT methods reach their limit of applicability for systems with a maximum of 100-200 atoms. Therefore, methods that can include approximations to reduce even more the computational demand, without compromising the reliability of results, are still required. In this context, the use of "density fitting"

approximations, also known as the Resolution of the Identity (RI) approach, for the Coulomb (RI-*J*) energy is undoubtedly a very useful tool for treating large systems by means of DFT methods.[50]

3.5.1. Resolution of the identity density functional theory

The basic idea of the RI approximation is to decompose the four-centre two electron repulsion integrals into three- and two-centre integrals through the use of a second, or "auxiliary" basis set to represent the electron density.

As seen previously in Kohn-Sham equations, the contribution of the interelectronic repulsion is given by the exchange-correlation $Exc[\rho]$ and the Coulomb $J[\rho]$ functionals:

$$V_{ee}[\rho] = W_{XC}[\rho] + J[\rho] \tag{3.16}$$

While the evaluation of $Exc[\rho]$ represents a small percentage of the whole cost of a DFT calculation, the Coulomb term dominates the computational procedure. So, an approximate method for evaluation of the Coulomb term is crucial to study large systems.

As also seen previously, the Coulomb repulsion *J* term is given as:

$$J[\rho] = \frac{1}{2}\iint \frac{\rho(\vec{r}_1)\rho(\vec{r}_2)}{|\vec{r}_1 - \vec{r}_2|} d\vec{r}_1 d\vec{r}_2 \tag{3.14}$$

and the electron density can be computed from molecular orbitals by equation 3.9:

$$\rho(\vec{r}) = \sum_{i=1}^{m} |\chi_i(\vec{r})|^2 \tag{3.9}$$

Since the molecular orbitals are expressed as a linear combination of *m* basis functions θ_j, the electron density can be given as:

$$\rho(\vec{r}) = \sum_{i=1}^{m} |\chi_i(\vec{r})|^2 = \sum_{i=1}^{m}\sum_{j=1}^{m} (c_{ji}\theta_j)^2 \tag{3.33}$$

where c_{ji} are unknown coefficients.

So, expanding the square one obtains:

$$\rho(\vec{r}) = \sum_{i=1}^{m}\sum_{a=1}^{l}\sum_{b=1}^{l} c_{ai}c_{bi}\theta_a(\vec{r})\theta_b(\vec{r}) \tag{3.34}$$

The expansion coefficients are then collected in the density matrix *P* which contains all relevant information about the charge density

$$P_{ab} = \sum_{i=1}^{m} c_{ai} c_{bi} \tag{3.35}$$

Thus, the Coulomb contribution *J* can be represented in terms of the basis functions by replacing equation 3.34 into 3.14 as follows:

$$J = \sum_{a=1}^{l} \sum_{b=1}^{l} P_{ab} \iint \frac{\theta_a(\vec{r}_1)\theta_b(\vec{r}_1)\theta_c(\vec{r}_2)\theta_d(\vec{r}_2)}{r_{12}} d\vec{r}_1 d\vec{r}_2 = \sum_{a=1}^{l} \sum_{b=1}^{l} P_{ab} \langle ab|cd \rangle \tag{3.36}$$

As can be seen, the integral into equation 3.36 is a four-centre two-electron integral that is the bottleneck for DFT and *ab initio* calculations. So, Eichkorn *et al.*[51] have proposed an approximate method for expressing the electron density as a linear combination of an auxiliary basis g_α (or g_β) according to:

$$\rho(\vec{r}_2) \approx \tilde{\rho}(\vec{r}_2) = \sum_{\alpha} c_\alpha g_\alpha \tag{3.37}$$

where the tilde indicates that we are dealing with an approximate density (since in practice the auxiliary basis set will never be complete). $\tilde{\rho}(\vec{r}_2)$ is the *Fitted Density*. The coefficients c_α in previous equation is determined by minimizing the Coulomb repulsion of residual density:

$$\iint \frac{\left(\rho(\vec{r}_1) - \tilde{\rho}(\vec{r}_1)\right)\left(\rho(\vec{r}_2) - \tilde{\rho}(\vec{r}_2)\right)}{r_{12}} = \langle \rho - \tilde{\rho} | \rho - \tilde{\rho} \rangle \min \tag{3.38}$$

The condition 3.37 leads to a system of linear equations involving two and three-centre integrals.

$$\sum_{\beta} \langle \alpha | \beta \rangle c_\beta = \gamma_\alpha \tag{3.39}$$

with

$$\gamma_\alpha = \sum_{ab} \langle \alpha | ab \rangle P_{ab} \tag{3.40}$$

where α and β are the auxiliary basis and P_{ab} is the density matrix of the coefficients of the molecular orbitals.

The condition 3.38 is mathematically equivalent to the replacement

$$\langle ab|cd\rangle \approx \sum_{\alpha,\beta}\langle ab|\alpha\rangle\langle\alpha|\beta\rangle^{-1}\langle\beta|cd\rangle \tag{3.41}$$

This approximation formally resembles the resolution of the identity and is called RI-*J* because the RI approximation is applied on the Coulomb operator *J*.

Thus, the Coulomb operator can be expressed as

$$J[\rho] = \frac{1}{2}\langle\rho|\rho\rangle \approx \widetilde{J}[\rho] = \frac{1}{2}\langle\widetilde{\rho}|\rho\rangle \tag{3.42}$$

and replacing 3.34 and 3.37 into 3.41 one obtains:

$$J[\rho] = \frac{1}{2}c_\alpha\langle\alpha|ab\rangle = \frac{1}{2}c_\alpha\gamma_\alpha \tag{3.43}$$

where $\langle\alpha|ab\rangle P_{ab}$ is equal to γ_α by equation 3.38. So, the four-centre two-electron integral in equation 3.36 turns into a three-centre two-electron integral in 3.43 equation. This approach usually leads to a more than a tenfold speedup for non-hybrid DFT compared to the conventional method based on four-centre two-electron repulsion integrals.

Different sets of auxiliary basis functions are available in literature.[51-54] In this thesis the TZVP basis set was employed which shows a good performance for corannulene dimer.[25]

3.6. Density functional based tight-binding

Despite the RI-DFT method enables a considerable reduction of calculation time for large complexes, this approach is still quite time-consuming to be employed in the selection of suitable strategies to improve the efficiency and/or selectivity of buckycatchers. Therefore, density functional tight-binding (DFTB)[55-58], an approximate quantum chemistry method derived from DFT theory that shows an outstanding time/performance efficiency has been tested to study concave-convex π···π interactions.

The DFTB standard is based on the tight-binding method proposed by Slater and Koster in 1954.[59] The main idea behind this method is to describe the Hamiltonian eigenstates with an atomic-like basis set and replacing the Hamiltonian with a parameterized Hamiltonian matrix whose elements depend only on the internuclear distances; this implies to neglect all integrals of more than two centres.

Despite the Slater-Koster method was conceived for the calculation of band structures in periodic systems, it was later generalized to an atomistic model. The transition to atomistic has three main requirements, as discussed by Goringe *et al.* [60]

First, the elements of the Hamiltonian matrix must have a functional dependence on the interatomic distance. In the case of band structures one just has to know the matrix elements for discrete values of distance. This requirement was solved by Froyen and Harrison,[61] who proposed that the interatomic distance was related to the Hamiltonian elements by $1/r^2$.

The second requirement is to obtain an expression for the total energy and not only for the band energy. In 1979 Chadi[62] proposed that the total energy could be described as a sum of two contributions,

$$E = E_{bnd} + E_{rep} \tag{3.44}$$

where E_{bnd} is the sum over the energies of all occupied orbitals obtained by diagonalization of the parameterized Hamiltonian matrix, and E_{rep} is the repulsive contribution, obtained by the sum of the atomic-pair-terms,

$$E_{rep} = \sum_{\alpha,\beta}^{N} U_{\alpha\beta} \tag{3.45}$$

in which N is the number of atoms of system.

The last requirement is the possibility to derive the atomic forces from the total energy. This is especially important for geometry optimization and molecular dynamics. By assuming differentiability of $U_{\alpha\beta}$ in equation, the only difficulty is to derive E_{rep}, which depends on the parametrization method chosen for the Hamiltonian matrix.

The DFTB method attends these three requirements with the additional advantage of completely avoiding any empirical parameterization, since the Hamiltonian and overlap matrices are calculated using atom-like valence-orbitals, which are derived from DFT. Therefore, as commented above the DFTB method can be considered as a simplification of the Kohn-Sham method.

The starting point is the total energy expression as developed in DFT:

$$\begin{aligned} E[\rho] = \sum_{i}^{m} \left\langle \chi_i \left| -\frac{1}{2}\nabla^2 + \upsilon(\vec{r}) + \frac{1}{2}\int \frac{\rho(\vec{r}')}{\left|(\vec{r}) - (\vec{r}')\right|} d\vec{r}' \right| \chi_i \right\rangle \\ + E_{XC}[\rho] + \frac{1}{2}\sum_{\beta}^{N}\sum_{\alpha\neq\beta}^{N} \frac{Z_\alpha Z_\beta}{\left|\vec{R}_\alpha - \vec{R}_\beta\right|} \end{aligned} \tag{3.46}$$

Following Foulkes and Haydock[63] the electronic density is written as a reference density ρ_0 plus a small fluctuation in density $\delta\rho$,

$$\rho(\vec{r}) = \rho_0(\vec{r}) + \delta\rho(\vec{r}) \tag{3.47}$$

This electronic density is then inserted in equation 3.45:

where $\rho_0' = \rho_0(\vec{r}')$ and $\delta\rho' = \delta\rho(\vec{r}')$ are defined as shorthand notations. The second term in equation 3.48 corrects the double counting in the Coulomb term; the third term corrects the new exchange-correlation contribution; and the fourth term results from splitting the Coulomb energy into one part related to ρ_0 and another related to $\delta\rho$. E_{nn} *is* the nuclear repulsion.

$$\begin{aligned} E[\rho_0 + \delta\rho] = \sum_i^m \left\langle \chi_i \left| -\frac{1}{2}\nabla^2 + \upsilon(\vec{r}) + \int \frac{\rho_0'}{|\vec{r} - \vec{r}'|} d\vec{r}' + \upsilon_{XC}[\rho_0] \right| \chi_i \right\rangle \\ - \frac{1}{2}\iint \frac{\rho_0'(\rho_0 + \delta\rho)}{|\vec{r} - \vec{r}'|} d\vec{r} d\vec{r}' - \int \upsilon_{XC}[\rho_0](\rho_0 + \delta\rho) d\vec{r} \\ + \frac{1}{2}\iint \frac{\delta\rho_0'(\rho_0 + \delta\rho)}{|\vec{r} - \vec{r}'|} d\vec{r} d\vec{r}' + E_{XC}[\rho_0 + \delta\rho] + E_{nn} \end{aligned} \tag{3.48}$$

Afterwards, $E_{XC}[\rho_0 + \delta\rho]$ is expanded in a Taylor series up to a second-order term:

$$E_{\mathrm{XC}} = [\rho_0 + \delta\rho] = E_{\mathrm{XC}}[\rho_0] + \int \left.\frac{\delta E_{XC}}{\delta\rho}\right|_{\rho_0} \delta\rho d\vec{r} + \frac{1}{2}\iint \left.\frac{\delta^2 E_{XC}}{\delta\rho\delta\rho'}\right|_{\rho_0} \delta\rho\delta\rho' d\vec{r} d\vec{r}' \tag{3.49}$$

Substituting equation 3.49 into 3.48 and using the definition $\delta E_{XC}/\delta\rho)_{\rho_0} = \upsilon_{XC}[\rho_0]$ results in

$$\begin{aligned} E = \sum_i^m \left\langle \chi_i \left| -\frac{1}{2}\nabla^2 + \upsilon(\vec{r}) + \int \frac{\rho_0'}{|\vec{r} - \vec{r}'|} d\vec{r}' + \upsilon_{XC}[\rho_0] \right| \chi_i \right\rangle \\ - \frac{1}{2}\iint \frac{\rho_0'\rho_0}{|\vec{r} - \vec{r}'|} d\vec{r} d\vec{r}' + E_{XC}[\rho_0] - \int \upsilon_{XC}[\rho_0]\rho_0 d\vec{r} + E_{nn} \\ + \frac{1}{2}\iint \left(\frac{\delta\rho\delta\rho'}{|\vec{r} - \vec{r}'|} + \left.\frac{\delta^2 E_{XC}}{\delta\rho\delta\rho'}\right|_{\rho_0} \right) d\vec{r} d\vec{r}' \end{aligned} \tag{3.50}$$

From equation 3.50 it is possible to define four important terms. The first one is the reference Hamiltonian depending only upon ρ_0

$$\hat{H}^0 = -\frac{1}{2}\nabla^2 + \upsilon(\vec{r}\,) + \int \frac{\rho_0'}{|\vec{r} - \vec{r}'|} d\vec{r}' + \upsilon_{XC}[\rho_0] \tag{3.51}$$

The sum of terms given in the first line of equation 3.50 corresponds to the energy of the occupied atomic orbitals, analogue to E_{bnd} in equation 3.44. The terms in the second line of equation 3.50 define the repulsive contribution,

$$E_{rep}[\rho_0] = -\frac{1}{2}\iint \frac{\rho_0'\rho_0}{|\vec{r} - \vec{r}'|} d\vec{r} d\vec{r}' + E_{XC}[\rho_0] - \int \upsilon_{XC}[\rho_0]\rho_0 d\vec{r} + E_{nn} \tag{3.52}$$

Finally, the last term in equation 3.50 includes the correlation related to the fluctuations in the electronic density. This term is defined as

$$E_{2nd}[\rho_0, \delta\rho] = \frac{1}{2}\iint \left(\frac{\delta\rho\delta\rho'}{|\vec{r} - \vec{r}'|} + \left.\frac{\delta^2 E_{XC}}{\delta\rho\delta\rho'}\right|_{\rho_0} \right) d\vec{r} d\vec{r}' \tag{3.53}$$

Thus, considering the definitions of terms E_{bnd}, E_{rep}, and E_{2nd}, the equation 3.50 can be rewritten as:

$$E = \underbrace{\sum_i^m \left\langle \chi_i \middle| \hat{H}^0 \middle| \chi_i \right\rangle}_{E_{bnd}} + E_{rep}[\rho_0] + E_{2nd}[\rho_0, \delta\rho] \tag{3.54}$$

which becomes analogue to equation 3.44 when E_{2nd} contribution is neglected, as in tight-binding standard.

The energy of repulsion, E_{rep}, only considers the interactions of two centres and is parameterized through the DFT calculations considering only the interatomic distances between atoms in structures of reference. Thus, E_{rep} is fitted to the difference between DFT energy and E_{bnd} as a function of the interatomic distance $R_{\alpha\beta}$ using a suitable reference structure.

$$E_{rep}[\rho_0] \equiv E_{rep}(\vec{R}_{\alpha\beta}) = \left\{ E_{DFT}(\vec{R}_{\alpha\beta}) - E_{bnd}(\vec{R}_{\alpha\beta}) \right\}_{\text{ref.struct.}} \tag{3.55}$$

Within the two-centre approximation the matrix elements of Hamiltonian become

$$H^0_{\mu\upsilon} = \begin{cases} \varepsilon_\mu^{\text{free atom}}, & \mu = \upsilon \\ \left\langle \theta_\mu \left| \hat{T} + \hat{\upsilon}_{eff}[\rho_0^\alpha, \rho_0^\beta] \right| \theta_\upsilon \right\rangle, & \mu \in \{\alpha\},\ \upsilon \in \{\beta\},\ \alpha \neq \beta \\ 0, & \text{otherwise} \end{cases} \tag{3.56}$$

where the first term corresponds to the diagonal of the Hamiltonian matrix and corresponds to the energy value of the free atom. This value ensures a correct description of isolated atoms. The second term of the equation corresponds to the interaction between two atoms (indices α and β indicate the atom in which the atomic orbitals and potentials are centred), and $\hat{T}$ is the kinetic energy operator and the υ_{eff} represents an effective potential. The third line of the equation corresponds to interactions with more than two centres that are neglected in the standard DFTB method.

The different DFTB models are derived by expanding the DFT total energy functional around this density ρ_0 in first, second and third orders, respectively. The first-order terms constitute the standard DFTB1 model, which originally was called simply DFTB,[64-66] whereas the model based on second-order expansion, DFTB2,[57, 66-68] and the third-order terms constitute the DFTB3 model.[69-74]

The DFTB total energy can be explained in the respective orders as

$$E[\rho] = E^0[\rho_0] + E^1[\rho_0, \delta\rho] + E^2[\rho_0, (\delta\rho)^2] + E^3[\rho_0, (\delta\rho)^3] \tag{3.57}$$

E^0 and E^1 constitute the DFTB(1) model, the inclusion of E^2 defines DFTB2, and the inclusion of E^3 yields the DFTB3 model. In this thesis the DFTB2 model, also known as SCC-DFTB, was employed.

Despite the approximations made in the DFTB method, it provides good results for homonuclear systems or for those with strong covalent bonds, *i.e.*, fullerenes, nanotubes and WS_2. [65, 75-77] For heteroatomic systems with elements of similar electronegativities a more delicate charge balance between atoms must be considered. In this context, Elstner *et al.* [67, 78] developed a system with self-consistent correlation charge corrections, which allows a better description of heteronuclear systems, particularly large molecules.

3.6.1. The Self-Consistent Charge Correction: SCC-DFTB

As commented above, in self-consistent correlation charge corrections DFTB (SCC-DFTB), the electronic density is corrected through inclusion of E^{2nd} in equation 3.54, which are neglected in standard DFTB. The second-order terms in the density fluctuations are approximated by a simple distribution of atom-centred point charges estimated by a Mulliken population analysis $\left(\Delta q_\alpha = q_\alpha - q_\alpha^0\right)$,[79] *i.e.*, the difference between the atomic Mulliken population q_α of the atom in the molecule and in the neutral free atom, q_α^0.

Thus, in the SCC-DFTB method the energy is written as:

$$E_{scc} = \sum_{i}^{m} \left\langle \chi_i \middle| \hat{H}^0 \middle| \chi_i \right\rangle + \frac{1}{2} \sum_{\alpha\beta}^{N} \gamma_{\alpha\beta} \Delta q_\alpha \Delta q_\beta + E_{rep} \tag{3.58}$$

The first and second term of the equation correspond to the energy of standard DFTB method and the third term corresponds to the SCC correction.

The $\gamma_{\alpha\beta}$ parameter describes the electron-electron interaction within the atom α and can be related with the chemical hardness η_α,[80] or Hubbard parameter $\gamma_{\alpha\alpha} = 2\,\eta_\alpha = U_\alpha$ $I_\alpha - A_\alpha$, where I_α corresponds to ionization potential and A_α to electron affinity of atom α. Within monopole approximation, U_α can be calculated using a DFT procedure, as second derivative of the total atomic energy of atom α regarding to its atomic charge:

$$E_{2nd} \approx \frac{1}{2} \frac{\partial^2 E_\alpha[\rho_0]}{\partial q_\alpha^2} \Delta q_\alpha^2 = \frac{1}{2} U_\alpha \Delta q_\alpha^2 \rightarrow \frac{\partial \varepsilon_{\alpha,HOMO}}{\partial n_{\alpha,HOMO}} \tag{3.59}$$

where $\varepsilon_{\alpha,\,\mathrm{HOMO}}$ corresponds to the energy of the highest occupied molecular orbital (HOMO) and $n_{\alpha,\mathrm{HOMO}}$ to occupation number of the HOMO.

3.6.2. Dispersion-Corrected (SCC-) DFTB

Despite SCC correction significantly improves the treatment of heterogeneous systems by DFTB method, this method treats only short-range atomic potentials and terms with more than two centers are neglected. So, the Hamiltonian matrix elements fall off quickly and become negligible at interatomic distances typically found in the region of the van der Waals minimum, and therefore, the van der Waals interactions are completely disregarded, especially dispersion forces.

To solve this problem, two treatments to include dispersion interactions a *posteriori* have been proposed.[81, 82] In both cases the dispersion energy E_{disp} is calculated separately using empirical potentials and then added to the DFTB total expression energy. Since van der Waals forces are totally absent in DFTB, the addition of E_{disp} does not introduce any double-counting errors to the energy.

As both treatments are somewhat similar, only the treatment used in this thesis is discussed. This correction uses the UFF force field[83] and the dispersion potential for the DFTB method is given by

$$U_{\alpha\beta}(R) = \begin{cases} d_{\alpha\beta}\left[-2\left(\dfrac{R_{\alpha\beta}}{R}\right)^6 + \left(\dfrac{R_{\alpha\beta}}{R}\right)^{12}\right], & \forall R \geq 2^{-1/6} R_{\alpha\beta} \\ \dfrac{396}{25} d_{\alpha\beta} - 2^{5/6} \dfrac{672}{25} \dfrac{d_{\alpha\beta}}{R_{\alpha\beta}^5} R^5 + 2^{2/3} \dfrac{552}{25} \dfrac{d_{\alpha\beta}}{R_{\alpha\beta}^{10}} R^{10}, & \forall R \leq 2^{-1/6} R_{\alpha\beta} \end{cases} \tag{3.60}$$

At the top of the equation 3.60 is the potential of Lennard-Jones in which $R_{\alpha\beta}$ and $d_{\alpha\beta}$ correspond, respectively, to the van der Waals distance and well depth. Although widely used, the Lennard-Jones potential is not suitable for the description of the interaction between two very close atoms. Thus, Zhechkov and co-workers[82] proposed the polynomial at the bottom of this equation 3.60 for treating the dispersion at short distances. So, the energy of dispersion is then calculated as follows:

$$E_{disp} = \frac{1}{2}\sum_{\alpha,\beta}^{N} U_{\alpha\beta}(R) \tag{3.61}$$

This term can be then added to the total DFTB energy calculated either using standard DFTB or the SCC-DFTB scheme. In this thesis the dispersion corrected SCC-DFTB approach, also called SCC-DFTB-D, was employed.

3.7. Basis Sets

Quantum-mechanical methods begin the calculations with the choice of a basis set. The basis set is a collection of mathematical functions properly combined with the intention to emulate the behaviour of the molecular orbitals. Therefore, its appropriate use is an essential requirement to the success of calculations.

There are two types of basis functions commonly used in electronic structure calculations: Slater Type Orbitals (STO)[35, 84] and Gaussian Type Orbitals (GTO).[35, 85] Slater type orbitals have the functional form shown in equation 3.62

$$\chi(r,\theta,\varphi) = NY_{l,m}(\theta,\varphi)r^{n-1}e^{-\zeta r} \tag{3.62}$$

where r, θ, and ϕ are spherical coordinates, N is a normalization constant, n is a natural number that plays the role of principal quantum number, $Y_{l,m}$ are spherical harmonic functions, l and m are the angular momentum, r is the distance of the electron from the atomic nucleus and ζ (zeta) controls the width of the orbital (large ζ gives tight functions, small ζ gives diffuse functions).

Despite its exponential dependence ensures a fairly rapid convergence with increasing numbers of functions, there is no analytical solution for the three- and four-centre two-electron integrals generated, therefore they should be calculated by numerical methods. Unfortunately, these numerical methods in large systems have a high computational cost. To avoid the problem of numerical methods, in 1950 Boys[85] proposed the Gaussian type orbital (GTO) functions that have an analytical solution for the integrals.

$$\chi(r,\theta,\varphi) = NY_{lm}(\theta,\varphi)r^{2n-2-l}e^{-\zeta r^2} \tag{3.63}$$

Since single Gaussian function show a very poor description of the atomic orbital, conventionally there is trend to use Contracted Gaussian Type Orbital (CGTO)[86, 87] resulting of a lineal combination of the Gaussian functions GTO

$$\chi^{CGTO} = \sum_{i}^{N} a_i \chi_i \tag{3.64}$$

where a_i are the expansion coefficients and χ_i the Gaussian functions.

Another important point is the number of functions to be used.[88] The most commonly basis employed can be classified into the following groups:

Minimum basis set

It is the smallest number of functions possible that can be used to describe one atom, *i.e.*, one function for each atomic orbital (AO). In these basis sets, the same numbers of Gaussian primitives comprise core and valence orbitals. These basis set, developed by Pople group are denoted as STO-nG,[89] where *n* indicates the number of primitive Gaussian functions used in the development of an atomic orbital. The usual basis of this type is the STO-3G.[89, 90] The problem of this basis is that it is not flexible enough to describe the atom in a chemical environment. So, it leads to unsatisfactory results. In order to improve the results is necessary to expand the number of basis functions, using what is called extended or split valence basis set.

Extended basis set

This basis set employs more than one function per each minimum basis. An example is a double zeta type basis (DZ), where each atomic orbital is expressed as the sum of two Slater-type orbitals. The triple and quadruple-zeta basis sets work the same way, except using three and four Slater equations instead of two. The term zeta stems from the fact that the exponent of STO basis functions is often denoted by the Greek letter ζ. Of course, the better accuracy obtained with this basis implies more computational time required.

Split-valence basis set

The split-valence basis set employs a minimal basis for core orbitals and a value of zeta for valence orbitals. Despite this procedure has a small effect on the total energy, it practically does not affect most of the chemical properties, since valence electrons are those that principally take part in the bond.

Popular collections of basis sets are those developed by the groups of Pople, Dunning, and Ahlrichs, as seen in detail below.

Pople basis sets

These basis set comprise STO-nG and split-valence described above. The notation for split-valence basis set is typically X-YZG,[91] In this case, X represents the number of primitive Gaussians comprising each core atomic orbital basis function. The Y and Z indicate that the valence orbitals are composed of two basis functions each, the first one composed of a linear combination of Y primitive Gaussian functions, the other composed of a linear combination of Z primitive Gaussian functions. In this case, the presence of two numbers after the hyphens implies that this basis set is a split-valence double-zeta basis set. Split-valence triple- and quadruple-zeta basis set are also used, denoted as X-YZWG, X-YZWVG, and so on.

Furthermore, to each of these basis sets, polarization[92] and diffuse[93] functions (seen in detail below) can be added. Polarization is indicated by one asterisk (*) and two asterisks (**) after the G for heavy atoms and hydrogen, respectively. Diffuse functions are normally *s*- and *p*-functions and consequently go before the G. They are denoted by + or ++, with the first indicating one set of diffuse *s*- and *p*-functions on heavy atoms, and the second + indicating that a diffuse *s*-function is added also to hydrogen. So, the 6-31+G* is a split valence basis, where the core orbitals are a contraction of six primitive GTOs, the inner part of the valence orbitals is a contraction of three primitive GTOs and the outer part of the valence is represented by one primitive GTO. In addition, it has one set of diffuse *sp*-functions only on heavy atoms and a single *d*-type polarization function on heavy atoms.

Dunning basis sets[94]

These basis set are optimized using correlated wave functions (CISD). They are of the type cc-pVXZ, *i.e*, correlation consistent (cc), polarized in the valence shell and multiple Z (XZ) with X = D, T, Q, 5, 6, 7. Furthermore, if they have one set of diffuse functions for every angular moment present in the basis, the prefix "aug" (from augmented) is added, such as aug-cc-pVTZ. These basis sets are widely used, since they are designed to converge systematically to the complete basis set (CBS) limit using empirical extrapolation techniques.

Ahlrichs basis sets

The Ahlrichs group has developed the XVZ basis functions.[95, 96] The simplest basis is the SV (split valence) that doubles the number of valence basis, followed by the TZV that triples and by the QZV that quadruples. These basis sets describe the core electrons as a single contracted wave function and the valence as a combination of

functions. It is noteworthy that both TZV and QZV basis sets employ more contracted *s*-functions than indicated by the TZ and QZ acronyms.

Furthermore, basis functions even more flexible can be used if polarization and diffuse functions are introduced.

Polarization functions

Description of some chemical processes such as intermolecular interactions, requires an improvement in the basis set through the inclusion of polarization functions. In general, to polarize a basis function with angular momentum l, it mixes with basis functions of angular momentum $l + 1$. So, *p*-functions are added to hydrogen atoms, *d*-functions to Li-Ca atoms and *f*-functions to transition metals. This procedure enables to add some additional flexibility within the basis set, *i.e.*, it gives more room for the electrons to get away from each other to minimize electron-electron repulsion.

Diffuse functions

Diffuse functions are characterized by small ζ exponents; this means the electron is held far away from the nucleus. Therefore, it is very useful for an adequate description of anions, very electronegative atoms such as fluorine and binding energies of van der Waals complexes (bound by dispersion).

3.8. Supermolecule Method

The interaction energy is generally estimated using the approximation known as "supermolecule method". In this approximation the whole system is treated as a single molecule, and the energy is obtained by the difference between the energy of the supermolecule (whole system) and the energies of the isolated molecules. So, the interaction energy of a system $A\cdots B$ is calculated according to:

$$\Delta E_{int} = E_{AB}^{AB}(AB) - \left(E_{A}^{AB}(A) + E_{B}^{AB}(B)\right) \tag{3.65}$$

where the superscripts refer to the geometry (that of system AB), the subscripts denote the chemical species considered, and the symbols in parentheses denote the basis set used.

Unfortunately, the inevitable fact of having to use truncated basis for calculating energies causes an overestimation of the interaction energy known as basis set superposition error (BSSE).

3.9. Basis set superposition error (BSSE)

BSSE is a mathematical error that is present in all interaction energy calculations, as consequence of the unavoidable use of finite basis sets. This error constitutes one the major issues affecting the accuracy of calculations of interaction energies, especially those involving systems dominated by weak interactions. Therefore, all interaction energies evaluated in this thesis were corrected of BSSE.

When calculation of the interaction energy is performed by equation 3.65, the energy of each fragment within the dimer is artificially stabilized (with respect to the energy of the isolated fragments) because monomer *A* utilizes the extra basis functions from monomer *B* to describe its electron distribution, and vice versa. So, it leads to an overestimation of the magnitude of the interaction, *i.e.*, lower energies (more negative) than real are obtained.

The basis set superposition error was reported for the first time for the helium dimer in 1968.[97] However, Liu and McLean were the ones who introduced the term BSSE in 1973.[98] In the last decades this technique has been extensively studied and reviewed.[99-104] Nevertheless, it remains as a controversial subject.

The most common method to correct BSSE is the method of counterpoise (CP) developed by Boys and Bernardi.[105] According to this method, the interaction energy is obtained using the same basis sets for dimer and monomers, that is, the *AB* basis set. Thus, the counterpoise-corrected interaction energy is:

$$\Delta E_{int}^{CP} = E_{AB}^{AB}(AB) - \left(E_{A}^{AB}(AB) + E_{B}^{AB}(AB)\right) \tag{3.66}$$

where $E_{A}^{AB}(AB)$, represents the energy of *A* inside the dimer using its basis set and that of monomer *B*. For this purpose, the basis functions of *B* are placed on fictitious atoms ("ghost" atoms) specifying that the nuclear charge of the centres of *B* are zero. Similarly, $E_{B}^{AB}(AB)$, represents the energy of *B* in the presence of the basis of *A* on fictitious atoms.

The difference between the results of equation 3.66 and equation 3.65 is defined as the basis set superposition error (BSSE):

$$BSSE = \Delta E_{int}^{CP} - \Delta E_{int} \tag{3.67}$$

$$BSSE = E_{A}^{AB}(A) - E_{A}^{AB}(AB) + E_{B}^{AB}(B) - E_{B}^{AB}(AB) \tag{3.68}$$

From this definition, it follows that the error would be zero in the limit of complete basis, which is a virtually impossible case in almost all the *ab initio* calculations.

In summary, when very large basis sets are employed for each monomer, the presence of the other monomer basis sets does not provide a significant improvement in

the system description and the error made is small. However, when the bases are not sufficiently large, the error must be considered to obtain accurate values of interaction energy. Furthermore, this error is more important as weaker are the interaction forces between molecules.

3.9.1. Counterpoise correction including monomer deformation

It is noteworthy that monomers may be significantly deformed upon complexation.[5, 106-109] In these cases, the energy cost involved in the deformation of each monomer to adopt the geometry of complex must be incorporated through the deformation energy term:

$$\Delta E_{def} = \left(E_A^{AB}(A) - E_A^A(A)\right) + \left(E_B^{AB}(B) - E_B^B(B)\right) \tag{3.69}$$

Then, the full complexation energy is obtained as follows:

$$\Delta E_{complex} = \Delta E_{int}^{CP} + \Delta E_{def} \tag{3.70}$$

Other terms found in literature for the deformation energy are the relaxation energy (in the sense that if we consider the dissociation of the complex, the geometry has to relax to that of the isolated fragments)[106, 110, 111] or preparation energy (in the sense that this is the energy needed to prepare the fragments in order to form the complex at the final geometry).[112]

3.10. Pyramidalization angle (π-orbital axis vector, POAV)

The π-orbital direction for each tricordinate carbon atom in a nonplanar conjugated system is given by the pyramidalization POAV angle (π-orbital axis vector), proposed by Haddon.[113-115] This parameter can provide an adequate description of the local curvature of molecules of great interest such as fullerenes, carbon nanotubes and buckybowls.

In a planar molecule such as benzene, each of the π-orbitals is perpendicular to the molecular plane. However, in nonplanar systems like fullerenes or buckybowls, the sp^2-hybridized carbon atom is pyramidalized; the angle between its π-orbital and the three σ-bonds is larger than 90°. The pyramidalization angle θ_P for such a nonplanar carbon atom can be defined as the angle between its π-orbital and the σ-bonds, $\theta_{\sigma\pi}$, minus 90° (Figure 3.2). Thus, an sp^3-hybridized carbon atom (ideally tetrahedral) has a 19.5° pyramidalization angle, θ_P, while a regular sp^2 carbon (as in a fully planar benzene) has a θ_P of 0° (all carbon atoms in the icosahedral C_{60} have the same θ_P of ≈ 11.6°).

The pyramidalization angle provides a convenient index of the degree of nonplanarity at a conjugated carbon atom.

Finally, it is worth mentioning that data necessary for this analysis are only the atomic coordinates of the atoms in the molecule or fragment.

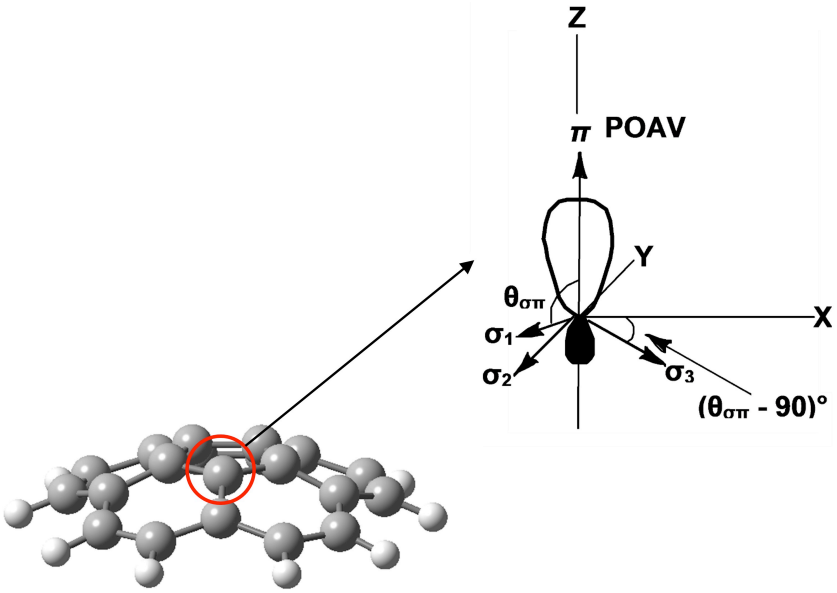


Figure 3.2: Representation of POAV. The angle is given by the pyramidalization $\theta p = \theta_{\sigma\pi} - 90°$.

3.11. Molecular Electrostatic Potential (MEP) Maps

This approach allows visualizing the three-dimensional charge distribution of molecular systems. Despite that molecular electrostatic potential (MEP) maps just provide primarily qualitative information, the knowledge of the charge distribution can be very useful to determine how molecules interact each other as well to guide the rational design of molecules.

MEP is a physical observable, although in practice it is rather difficult to design appropriate experiments to measure it.[34] Computationally, one can quantitatively compute the degree to which a positive or negative test charge is attracted to or repelled by a chemical species.

From Coulomb's law it follows that any distribution of electrical charge, such as the electrons and nuclei of a molecule, creates an electrical potential $V(\vec{r})$ in the surrounding space. $V(\vec{r})$ may be regarded as the potential of the molecule for interacting with an electrical charge located at the point $\vec{r}$. For example, an approaching point charge ±Q will interact with this electrical potential with interaction energy equal to

exactly $\pm QV(\vec{r})$, where $\vec{r}$ is the position of the point charge. Thus a positive point charge is attracted to those regions in which $V(\vec{r})$ is negative, since this leads to a negative (stabilizing) interaction energy, and it is repelled from regions of positive potential, in which the interaction energy is positive and destabilizing.

If a molecule has an electronic density function $\rho(\vec{r})$, then its electrostatic potential at any point $\vec{r}$ is given by equation 3.71

$$V(\vec{r}) = \sum_A \frac{Z_A}{\left|\vec{R}_A - \vec{r}\right|} - \int \frac{\rho(\vec{r}')}{\left|\vec{r}' - \vec{r}\right|} d\vec{r}' \tag{3.71}$$

where Z_A is the nuclear charge of atom A with position $\vec{R}_A$ and $\vec{r}'$ is an integration variable. The first term on the right side of equation 3.71 represents the contribution of the nuclei, which is positive; the second term brings the effect of the electrons, which is negative. For convenience, $V(\vec{r})$ is typically written in terms of atomic units, a.u.

The electrostatic potential $V(\vec{r})$ is a three-dimensional local property that can be evaluated at any or all points $\vec{r}$ in the space of a system (except for the positions $\vec{R}_A$ of the nuclei, at which the denominators in the summation in Equation (3.71) are zero).

It is noteworthy that equation 3.71 is an exact formula for the electrostatic potential due to the set of nuclei $\{Z_A\}$ and the electronic density $\rho(\vec{r})$. However, $\rho(\vec{r})$ is normally obtained by *ab initio* and density functional theory, and hence it is approximate, and, therefore, $V(\vec{r})$ is approximate too.

Basically, two steps are required to obtain electrostatic potential maps. The first one is to calculate the electrostatic potential in all the points of a three-dimensional grid. The second step is to choose a surface onto which MEP to be shown. Usually, for this purpose an arbitrary isosurface of electron density is chosen since this kind of surface defines approximately the size and shape of the molecule.

From its definition it is clear that electron-rich regions usually have negative potentials and the electron-poor regions usually have positive potentials. Typically the most negative potential is assigned to be red, the most positive potential is assigned to be blue, and the colour spectrum is mapped to all other values by linear interpolation.

Figure 3.3 shows the molecular electrostatic potential maps of the concave and convex faces of corannulene. As can be seen, the convex face (outside the bowl) is more negative than the concave face. Thereby, it is expected that the convex side is slightly favoured for interacting with cations such as Li^+ and Na^+.

Undoubtedly, the MEP is a useful interpretative and predictive tool in the study the intermolecular interactions. A more detailed explanation about molecular electrostatic potential is given in literature.[116-120]

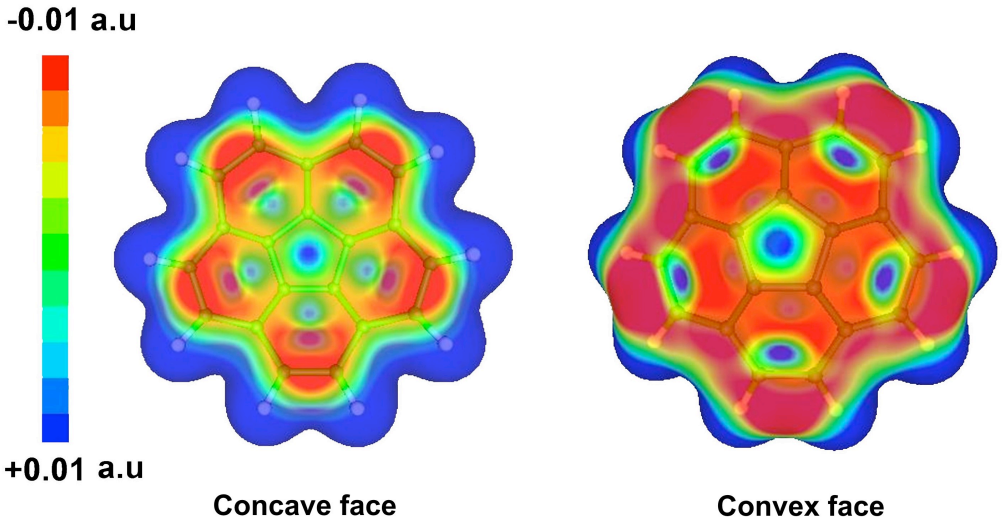


Figure 3.3: Molecular electrostatic potential onto an electron density isosurface of 0.005 a.u.

3.12. Non-covalent Interactions (NCI) Method

As commented previously, the study of non-covalent interactions are of crucial importance to many chemical, biological and technological systems. On other hand, the large size of some materials and structures of interest makes understanding non-covalent interactions to be a particularly hard task.

In this context, Johnson and co-workers has developed a non-covalent interactions (NCI) index to visualize non-covalent interactions.[121, 122] This approach has the dual advantages of being generally transferable to diverse chemical applications and being very fast to compute, since it can be calculated from promolecular densities.

Although the information provided by NCI plots is basically qualitative (which molecular regions interact) is of great importance in the study of non-covalent interactions.

The NCI index identifies interactions in a chemical system based on a 2D plot of the electron density (ρ) and the reduced density gradients (RDG, s), where

$$s = \frac{1}{2(3\pi^2)^{1/3}} \frac{|\nabla\rho|}{\rho^{4/3}} \tag{3.72}$$

Since in regions far from the molecule the density is decaying to zero exponentially, the reduced gradient will have very large positive values. On the contrary,

the reduced gradient will assume very small values, approaching zero, for regions of both covalent and non-covalent interactions.

3.12.1. Identifying non-covalent interactions

To differentiate between covalent and non-covalent bond the plot of *s versus* ρ is examined, where covalent bonds are identified by high density values, while non-covalent interactions show density values near to zero, since they are weaker than covalent ones. This behaviour can be observed in Figure 3.4: the covalent bonds are shown as a series of peaks that appear at a density of 0.28, while non-covalent appear from 0.00 to 0.05. In summary, regions of low reduced density gradient and low densities characterize the non-covalent interactions.

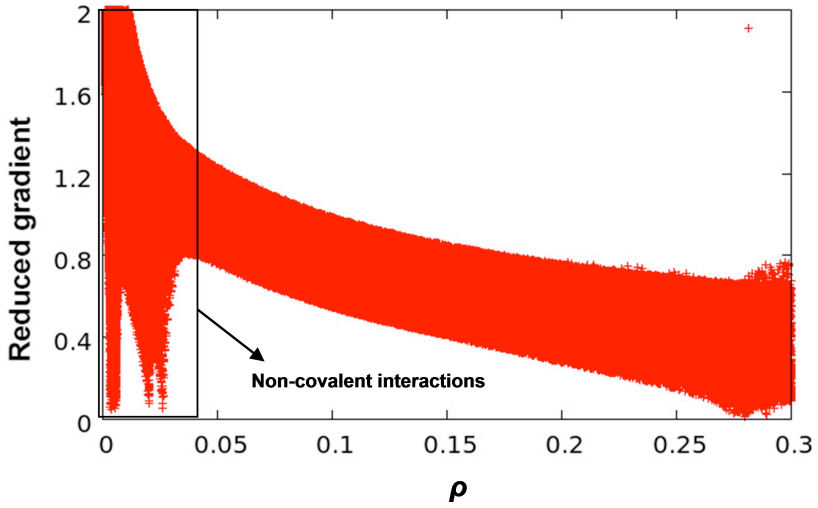


Figure 3.4: Identification of non-covalent interactions from graph of electronic density *vs.* reduced density gradient.

3.12.2. Identifying interaction types

Despite that localization of low-density and low-gradient regions enables identification of weak interactions in a molecular system, more specific interaction types cannot be determined from the density values alone, since both attractive and repulsive interactions appear in the same region of density/reduced gradient space. Therefore, to distinguish between attractive and repulsive interactions, it is necessary to consider the second derivative of the density.

The sign of the Laplacian ($\nabla^2\rho$) determines if density is concentrated or depleted at one point relative to surroundings. While, ($\nabla^2\rho < 0$) is characteristic of covalent interactions, ($\nabla^2\rho > 0$) is characteristic of weak interactions, both bonding and nonbonding.

To distinguish among the different types of weak interactions, the sign of the Laplacian itself cannot be used, because the sign is dominated by negative contributions from the nuclei. Instead, contribution to the Laplacian along the axes of its maximal variation must be analyzed. These contributions are eigenvalues λ_i of the electron density Hessian matrix,

$$\nabla^2\rho = \lambda_1 + \lambda_2 + \lambda_3 \,, (\lambda_1 < \lambda_2 < \lambda_3) \tag{3.73}$$

At the nuclei all the eigenvalues are negative, while away from them $\lambda_3 > 0$. In molecules, λ_3 values vary along the internuclear direction, while λ_1 and λ_2 report the variation of density in the plane normal to the λ_3 eigenvector. Through the sign of λ_2 it is possible to distinguish bonding and nonbonding interactions, since bonding interactions, such as hydrogen bonds, are characterized by an accumulation of density perpendicular to the bond ($\lambda_2 < 0$), nonbonded interactions, such as steric repulsion, produce density depletion ($\lambda_2 > 0$) and van der Waals interactions a negligible density overlap that gives $\lambda_2 \leq 0$. Figure 3.5 shows these interactions for phenol dimer.

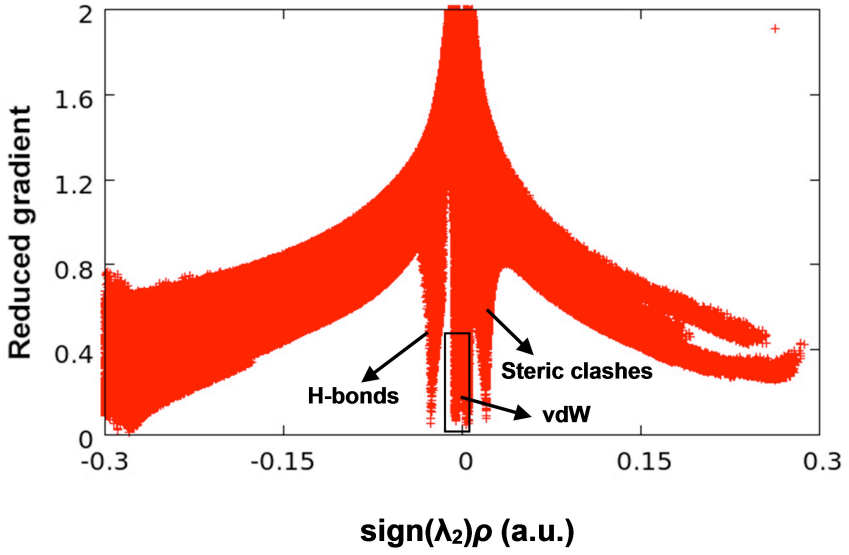


Figure 3.5: Identification of interaction types for phenol dimer from graph of sign $(\lambda_2)\rho$ *vs* reduced density gradient.

In summary, the NCI method enables identification of non-covalent interactions based on the peaks that appear in RDG at low densities. When an RDG isosurface for a low value of RDG is plotted, the non-covalent regions clearly appear in the supramolecular complex. These interactions correspond to both favourable and unfavourable interactions. To differentiate between them, the sign of the second density Hessian eigenvalue (λ_2), times the density (ρ) is colour-mapped onto the isosurfaces. These isosurfaces are the basis of NCI method. Figure 3.6 summarized the assumed values for sign λ_2 and ρ that characterize hydrogen bonds, steric clashes and van der Waals interactions.

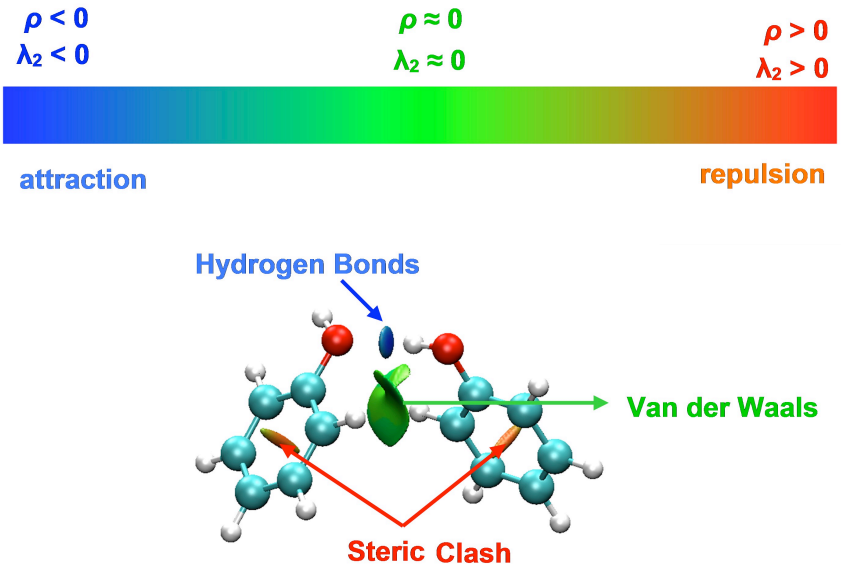


Figure 3.6: Schematic representation of values for sign λ_2 and ρ that characterize hydrogen bonds, steric clashes and van der Waals interactions for phenol dimer.

3.12.3. Type of calculations

To obtain the electron density and the reduced density gradient two different approaches can be used: the self-consistent field (SCF) and the promolecular.

The promolecular method is based in the sum of atomic densities:

$$\rho^{pro} = \sum_i \rho_i^{at} \tag{3.74}$$

Despite the lack of relaxation, introduced in a SCF Hartree-Fock or DFT calculation that use the complete wave function, the promolecular approach is very useful for describing large systems as proteins or DNA, since it only uses the atomic positions stored in a *xyz* coordinate file.

As can seen from Figure 3.7, both SCF and promolecular calculations give rise to qualitatively similar results; particularly for low electron density and low reduced density gradient that is what matters when working with weak interactions. The most significant difference between these approaches is observed for nonbonding interactions, where occurs an overestimation of repulsion by promolecular calculation, since electronic density does not fit well for these cases.

In general, reduced density gradient moves to higher values, and peaks shift toward more negative values, when the SCF approach is used.

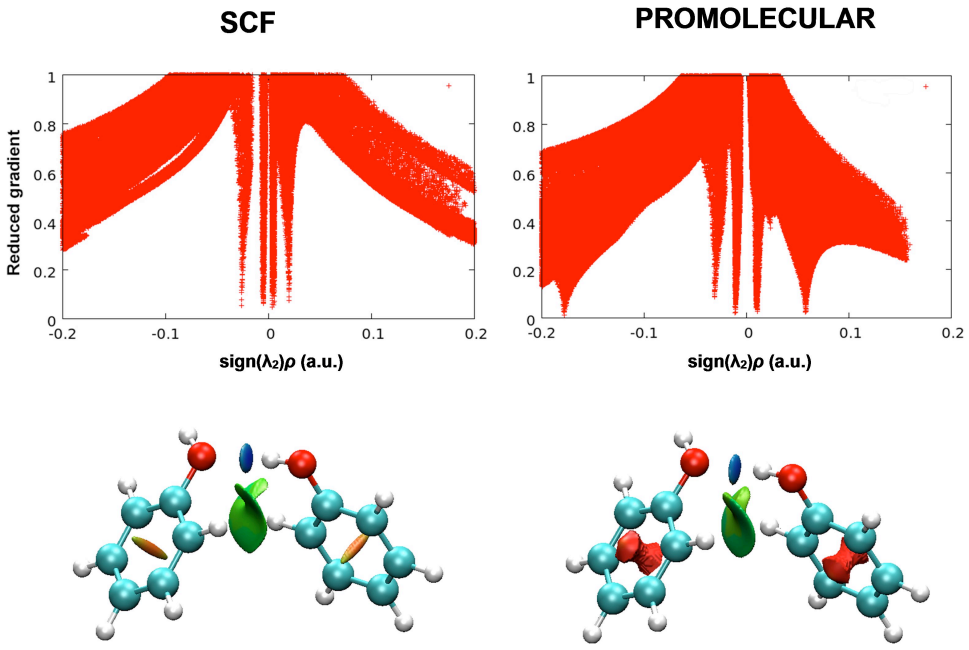


Figure 3.7: Comparison between NCI promolecular and SCF calculations for phenol dimer.

3.13. *References*

1. J. Cerny and P. Hobza, *Phys. Chem. Chem. Phys.*, 2007, **9**, 5291-5303.
2. K. E. Riley and P. Hobza, *WIREs: Comput. Mol. Sci.*, 2011, **1**, 3-17.
3. S. Tsuzuki, T. Uchimaru, K. Matsumura, M. Mikami and K. Tanabe, *Chem. Phys. Lett.*, 2000, **319**, 547–554.
4. P. Hobza, H. L. Selzle and E. W. Schlag, *J. Phys. Chem.*, 1996, **100**, 18790-18794.
5. E. M. Cabaleiro-Lago, A. Peña-Gallego and J. Rodríguez-Otero, *J. Chem. Phys.*, 2008, **128**, 194311/194311-194311/194318.
6. E. M. Cabaleiro Lago, J. Rodríguez Otero and A. Peña-Gallego, *J. Chem. Phys.*, 2008, **129**, 084305.
7. E. M. Cabaleiro Lago, J. Rodríguez Otero and A. Peña-Gallego, *J. Phys. Chem. A*, 2008, **112**, 6344–6350.
8. E. M. Cabaleiro Lago, J. Rodríguez Otero and A. Peña-Gallego, *J. Chem. Phys.*, 2011, **135**, 134310.
9. E. M. Cabaleiro Lago, J. Rodríguez Otero and A. Peña-Gallego, *Theor. Chem. Acc.*, 2011, **128**, 531–539.
10. *R. G. Parr and W. Yang, Density-Functional Theory of Atoms and Molecules,* Oxford University Press, Oxford, 1989.

11. *W. Koch and M. C. Holthausen, A Chemist's Guide to Density Fucntional Theory,* Wiley-VCH, New York, 2001.
12. A. D. Boese and J. M. L. Martin, *J. Chem. Phys.*, 2004, **121**, 3405-3416.
13. Y. Zhao, N. E. Schultz and D. G. Truhlar, *J. Chem. Phys.*, 2005, **123**, 161103.
14. Y. Zhao and D. G. Truhlar, *Theor. Chem. Acc.*, 2008, **120**, 215-241.
15. Y. Zhao, N. E. Schultz and D. G. Truhlar, *J. Chem. Theory Comput.*, 2006, **2**, 364-382.
16. B. M. Wong, *J. Comput. Chem.*, 2009, **30**, 51-56.
17. Y. Zhao and D. G. Truhlar, *Phys. Chem. Chem. Phys.*, 2008, **10**, 2813-2818.
18. S. Grimme, *J. Comput. Chem.*, 2004, **25**, 1463-1473.
19. S. Grimme, *J. Comput. Chem.*, 2006, **27**, 1787-1799.
20. S. Grimme, J. Antony, S. Ehrlich and H. Krieg, *J. Chem. Phys.*, 2010, **132**, 154104/154101-154104/154119.
21. R. Peverati and K. K. Baldridge, *J. Chem. Theory Comput.* , 2008, **4**, 2030–2048
22. S. Grimme, J. Antony, T. Schwabe and C. Muck-Lichtenfeld, *Org. Biomol. Chem.*, 2007, **5**, 741-758.
23. C. Mück-Lichtenfeld, S. Grimme, L. Kobryn and A. Sygula, *Phys. Chem. Chem. Phys.*, 2010, **12**, 7091-7097.
24. M. R. Kennedy, L. A. Burns and C. D. Sherrill, *J. Phys. Chem. A*, 2012, **116**, 11920-11926.
25. T. Janowski, P. Pulay, A. A. Sasith Karunarathna, A. Sygula and S. Saebø, *Chem. Phys. Lett.*, 2011, **512**, 155-160.
26. R. Ahlrichs, M. Bär, M. Häser, H. Horn and C. Kölmel, *Chem. Phys. Lett.*, 1989, **162**, 165-169.
27. D. Josa, J. Rodríguez Otero and E. M. Cabaleiro Lago, *Phys. Chem. Chem. Phys.*, 2011, **13**, 21139-21145.
28. S. Grimme, C. Mück-Lichtenfeld and J. Antony, *J. Phys. Chem. C*, 2007, **111**, 11199-11207.
29. D. Josa, J. Rodríguez-Otero, E. M. Cabaleiro-Lago and M. Rellán-Piñeiro, *Chem. Phys. Lett.*, 2013, **557**, 170-175.
30. I. Welsh and M. Lein, *J. Comput. Chem.*, 2014, **35**, 181-191.
31. L. H. Thomas, *Proc. Camb. Phil. Soc.*, 2008, **23**, 542.
32. E. Fermi, *Rend. Accad. Naz. Lincei* 1927, **6**, 602–607.
33. P. Hohenberg and W. Kohn, *Phys. Rev.* , 1964, **136**, B864-B871.
34. C. J. Cramer, *Essentials of Computational Chemistry: Theories and Models*, 2nd Edition, John Wiley & Sons Ltd, Chichester, 2004.
35. F. Jensen, *Introduction to computational chemistry,* John Wiley and Sons, Chichester, 2001.
36. W. Kohn and L. J. Sham, *Phys. Rev.*, 1965, **140**, A1133-A1138.
37. P. A. M. Dirac, *Proceedings of the Cambridge Philosophical Society*, 1930, **26**, 376-385.
38. S. H. Vosko, L. Wilk and M. Nusair, *Can. J. Phys.*, 1980, **58**, 1200-1211.
39. A. D. Becke, *Phys. Rev. A* 1988, **38**, 3098-3100.
40. J. Perdew, *Phys. Rev. B*, 1986, **33**, 8822-8824.
41. C. Lee, W. Yang and R. G. Parr, *Phys. Rev. B*, 1988, **37**, 785-789.
42. A. D. Becke, *J. Chem. Phys.*, 1996, **104**, 1040-1046.
43. A. D. Boese and N. C. Handy, *J. Chem. Phys.*, 2002, **116**, 9559-9569.

44. M. A. Petrukhina, K. W. Andreini, J. Mack and L. T. Scott, *J. Org. Chem.*, 2005, **70**, 5713-5716.
45. J. P. Perdew, K. Burke and M. Ernzerhof, *Phys.Rev.Lett.*, 1997, **78**, 1396.
46. B. Miehlich, A. Savin, H. Stoll and H. Preuss, *Chem. Phys. Lett.*, 1989, **157**, 200-206.
47. J.-D. Chai and M. Head-Gordon, *Phys. Chem. Chem. Phys.*, 2008, **10**, 6615–6620.
48. S. Grimme, S. Ehrlich and L. Goerigk, *J. Comput. Chem.*, 2011, **32**, 1456-1465.
49. C. Adamo and V. Barone, *J. Chem. Phys.*, 1999, **110**, 6158-6170.
50. C.-K. Skylaris, L. Gagliardi, N. C. Handy, A. G. Ioannou, S. Spencer and A. Willetts, *J. Mol. Struct: THEOCHEM*, 2000, **501-502**, 229–239.
51. K. Eichkorn, O. Treutler, H. Oehm, M. Haeser and R. Ahlrichs, *Chem. Phys. Lett.*, 1995, **240**, 283-290.
52. N. Godbout, D. R. Salahub, J. Andzelm and E. Wimmer, *Can. J. Chem.*, 1992, **70**, 560-571.
53. K. Eichkorn, F. Weigend, O. Treutler and R. Ahlrichs, *Theor. Chem. Acc.*, 1997, **97**, 119-124.
54. F. Weigend, *Phys. Chem. Chem. Phys.*, 2006, **8**, 1057-1065.
55. M. Elstner and M. Gaus, Self-Consistent-Charge Density Functional Tight-Binding Method: and Efficient Approximation of Density Functional Theory *in Computational Methods for Large Systems: Electronic Structure Approaches for Biotechnology and Nanotechnology*, First edition, Eddited by Reimers, J. R., John Wiley & Sons, Inc.,Hoboken, New Jersey, 2011.
56. T. Frauenheim, G. Seifert, M. Elstner, Z. Hajnal, G. Jungnickel, D. Porezag, S. Suhai and R. Scholz, *Comput. Simul. Mater. At. Level*, 2000, 41-62.
57. A. F. Oliveira, G. Seifert, T. Heine and H. A. Duarte, *J. Braz. Chem. Soc.*, 2009, **20**, 1193-1205.
58. P. Koskinen and V. Makinen, *Comput. Mater. Sci.*, 2009, **47**, 237–253.
59. J. C. Slater and G. F. Koster, *Phys. Rev.*, 1954, **94**, 1498-1524.
60. C. M. Goringe, D. R. Bowler and E. Hernandez, *Rep. Prog. Phys.*, 1997, **60**, 1447-1512.
61. S. Froyen and W. A. Harrison, *Phys. Rev. B: Condensed Matter Mater. Phys.*, 1979, **20**, 2420-2422.
62. D. J. Chadi, *Phy. Rev. Lett.*, 1979, **43**, 43-47.
63. W. Foulkes and R. Haydock, *Phys. Rev. B: Condensed. Matter Mater. Phys.* , 1989, **39**, 12520-12536.
64. D. Porezag, T. Frauenheim, T. Köhler, G. Seifert and R. Kaschner, *Phys. Rev. B*, 1995, **51**, 12947-12957.
65. G. Seifert, D. Porezag and T. Frauenheim, *Int. J. Quantum Chem.*, 1996, **58**, 185-192.
66. G. Seifert and J.-O. Joswig, *WIREs Comput Mol Sci.*, 2012, **2**, 456-465.
67. M. Elstner, D. Porezag, G. Jungnickel, J. Elsner, M. Haugk, T. Frauenheim, S. Suhai and G. Seifert, *Phys. Rev. B*, 1998, **58**, 7260-7268.
68. A. Kumar, M. Elstner and S. Suhai, *Int. J. Quantum Chem.*, 2003, **95**, 44-59.
69. M. Elstner, *Theor Chem Acc*, 2006, **116**, 316–325.
70. M. Elstner, T. Frauenheim, J. McKelvey and G. Seifert, *J. Phys. Chem. A*, 2007, **111**, 5607-5608.
71. Y. Yang, H. Yu, D. York, Q. Cui and M. Elstner, *J. Phys. Chem. A*, 2007, **111**, 10861-10873.

72. M. Gaus, Q. Cui and M. Elstner, *J. Chem. Theory Comput.*, 2011, **7**, 931-948.
73. M. Gaus, A. Goez and M. Elstner, *J. Chem. Theory Comput.*, 2013, **9**, 338-354.
74. M. Gaus, Q. Cui and M. Elstner, *WIREs: Comput. Mol. Sci.*, 2014, **4**, 49-61.
75. T. Heine, M. Buhl, P. W. Fowler and G. Seifert, *Chem. Phys. Lett.*, 2000, **316**, 373-380.
76. G. Seifert, H. Terrones, M. Terrones, G. Jungnickel and T. Frauenheim, *Solid State Commu.*, 2000, **114**, 245-248.
77. G. Seifert, H. Terrones, M. Terrones, G. Jungnickel and T. Frauenheim, *Phys. Rev. Lett.*, 2000, **85**, 146-149.
78. M. Elstner, T. Frauenheim and S. Suhai, *Phys. Status Solidi B*, 2000, **217**, 357-376.
79. R. S. Mulliken, *J. Chem. Phys.*, 1955, **23**, 1833.
80. R. G. Parr and R. G. Pearson, *J. Am. Chem. Soc.*, 1983, **105**, 7512-7516.
81. M. Elstner, P. Hobza, T. Frauenheim, S. n. Suhai and E. Kaxiras, *J. Chem. Phys.*, 2001, **114**, 5149.
82. L. Zhechkov, T. Heine, S. Patchkovskii, G. Seifert and H. A. Duarte, *J. Chem. Theory Comput.*, 2005, **1**, 841-847.
83. A. K. Rappe, C. J. Casewit, K. S. Colwell, W. A. Goddard, III and W. M. Skiff, *J. Am. Chem. Soc.*, 1992, **114**, 10024-10035.
84. J. Slater, *Physi. Rev.*, 1930, **36**, 57-64.
85. S. F. Boys, *Proc. R. Soc. (London) A*, 1950, **200**, 542-554.
86. E. Clementi, *IBM J. Res. and Dev.* , 1965, **9**, 2-19.
87. J. L. Whitten, *J. Chem. Phys.*, 1966, **44**, 359-364.
88. E. R. Davidson and D. Feller, *Chem. Rev.*, 1986, **86**, 681-696.
89. W. J. Hehre, R. F. Stewart and J. A. Pople, *J. Chem. Phys.*, 1969, **51**, 2657-2664.
90. J. B. Collins, P. v. R. Schleyer, J. S. Binkley and J. A. Pople, *J. Chem. Phys.*, 1976, **64**, 5142-5151.
91. R. Ditchfield, *J. Chem. Phys.*, 1971, **54**, 724.
92. M. M. Francl, W. J. Pietro, W. J. Hehre, J. S. Binkley, M. S. Gordon, D. J. DeFrees and J. A. Pople, *J. Chem. Phys.*, 1982, **77**, 3654-3665.
93. M. J. Frisch, J. A. Pople and J. S. Binkley, *J. Chem. Phys.*, 1984, **80**, 3265-3269.
94. T. H. Dunning, *J. Chem. Phys.*, 1989, **90**, 1007.
95. F. Weigend, F. Furche and R. Ahlrichs, *J. Chem. Phys.*, 2003, **119**, 12753-12762.
96. F. Weigend and R. Ahlrichs, *Phys. Chem. Chem. Phys.*, 2005, **7**, 3297.
97. N. R. Kestner, *J. Chem. Phys.*, 1968, **48**, 252-257.
98. B. Liu and A. D. McLean, *J. Chem. Phys.*, 1973, **59**, 4557-4558.
99. F. B. van Duijneveldt, J. G. C. M. van Duijneveldt-van de Rijdt and J. H. van Lenthe, *Chem. Rev.* , 1994, **94**, 1873-1885.
100. N. R. Kestner and J. E. Combariza, *Rev. Comput. Chem.*, 1999, **13**, 99-132.
101. D. Vijay, H. Sakurai and G. N. Sastry, *Int. J. Quantum Chem.*, 2011, **111**, 1893-1901.
102. B. Brauer, M. K. Kesharwani and J. M. L. Martin, *J. Chem. Theory Comput.*, 2014, **10**, 3791-3799.
103. L. A. Burns, M. S. Marshall and C. D. Sherrill, *J. Chem. Theory Comput.*, 2014, **10**, 49-57.
104. L. M. Mentel and E. J. Baerends, *J. Chem. Theory Comput.*, 2014, **10**, 252-267.
105. S. F. Boys and F. Bernardi, *Mol. Phys.*, 1970, **19**, 553-566.
106. S. S. Xantheas, *J. Chem. Phys.*, 1996, **104**, 8821-8824.

107. A. Campo-Cacharrón, E. M. Cabaleiro-Lago and J. Rodríguez-Otero, *ChemPhysChem*, 2012, **13**, 570-577.
108. P. A. Denis, *RSC Adv.*, 2013, **3**, 25296-25305.
109. D. Josa, L. Azevedo dos Santos, I. González-Veloso, J. Rodríguez-Otero, E. M. Cabaleiro-Lago and T. de Castro Ramalho, *RSC Adv.*, 2014, **4**, 29826-29833.
110. K. Szalewicz and B. Jeziorski, *J. Chem. Phys.*, 1998, **109**, 1198-1200.
111. G. Cha-lasinski and M.-l. M. Szczesniak, *Chem. Rev.* , 2000, **100**, 4227-4252.
112. M. v. Hopffgarten and G. Frenking, *WIREs Comput. Mol. Sci.*, 2012, **2**, 43-62.
113. R. C. Haddon, *J. Am. Chem. Soc.*, 1990, **112**, 3385-3389.
114. R. C. Haddon, *Acc. Chem. Res.*, 1988, **21**, 243-249.
115. R. C. Haddon, *J. Phys. Chem. A*, 2001, **105**, 4164-4165.
116. J. S. Murray and P. Politzer, *WIREs Comput Mol Sci.*, 2011, **1**, 153-163.
117. P. Politzer, P. R. Laurence and K. Jayasuriya, *Environ. Health Perspect.*, 1985, **61**, 191-202.
118. P. Polizer and M. J. S., Molecular Electrostatic Potentials in *Computational Medicinal Chemistry for Drug Discovery* (eds. P. Bultinck, H. De Winter, W. Langenaeker, J. P. Tollenare) Taylor & Francis e-Library, ch. 8, pp. 213-234, 2005, 2005.
119. *Molecular Electrostatic Potentials Concepts and Applications* (eds J. S. murray and K. Sen), Elsevier Science, 1996.
120. B. Galabov, V. Nikolova and S. Ilieva, *Chem. Eur. J.*, 2013, **19**, 5149-5155.
121. E. R. Johnson, S. Keinan, P. Mori-Sánchez, J. Contreras-García, A. J. Cohen and W. Yang, *J. Am. Chem. Soc.*, 2010, **132**, 6498–6506.
122. J. Contreras-Garcia, E. R. Johnson, S. Keinan, R. Chaudret, J. P. Piquemal, D. N. Beratan and W. Yang, *J.Chem. Theory Comput.*, 2011, **7**, 625-632.

Chapter 4

Substituent Effects in Corannulene Dimers

4.1. Introduction

Non-covalent intermolecular interactions are of great importance in modern chemical research, particularly in the area of molecular recognition, supramolecular chemistry, materials science and biochemistry.[1-4]

Several applications of fullerenes have generated a special interest in the chemistry of curved polycyclic aromatic hydrocarbons. Polyarenes including five and six membered rings, which correspond to a fragment of fullerene C_{60}, have been commonly called 'buckybowls'.[5] Buckybowl compounds differ from traditional aromatic hydrocarbons in that they are strained (curved) and they have both concave and convex surfaces.[6] As fragments of fullerenes, buckybowls are potential substrates for the synthesis of fullerenes and nanotubes. Therefore, the understanding of the interaction in these systems can be very important in the development of molecular engineering and materials science.

The smallest buckybowl, corannulene ($C_{20}H_{10}$, X=H Figure 4.1), has been the subject of intense experimental and theoretical research in recent years.[7-9] There is great interest in buckybowls because of their relation to the formation of intermolecular complexes of different natures. One of the most interesting types of interaction of these compounds is the concave-convex $\pi\cdots\pi$ interaction. These interactions can be established between two or more buckybowls and they are responsible for column packing in the crystal structure of buckybowls[10] and in the formation of dimers.[11] It is noteworthy that control of molecular stacking of polynuclear aromatic compounds is an important issue in the supramolecular chemistry.[12] Furthermore, these interactions may provide very important applications, as in the design of molecular tweezers like those synthesized by Sygula *et al.*[13] These authors showed that buckybowls seem ideal candidates for use as molecular receptors capable of recognizing fullerenes by concave-convex 'ball-and-socket' interactions. A different functionalization of buckybowls, which constitute the main part of tweezers, could provide a selective trapping of different species, thus obtaining a very efficient 'buckycatcher'.

While π···π interactions of planar aromatic compounds have been extensively investigated,[1,14,15] very few studies of the π···π interactions of curved systems have been published. Therefore, detailed studies of these kinds of interactions are required.

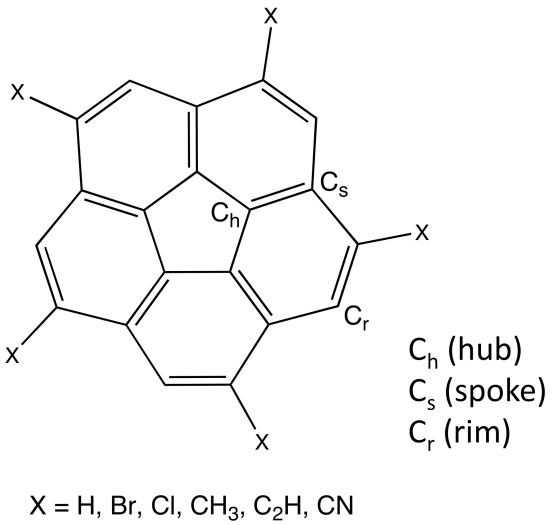


Figure 4.1: Corannulene and substituted corannulene studied in this work.

Recently, Sygula and Saebø performed an interesting research about π···π stacking of corannulene dimer.[11] Their calculations led to three important conclusions: 1) the interactions between curved π-systems are of comparable magnitude to those of planar systems of the same size, 2) at least, part of the interaction energy in the stacked curved systems can be attributed to electrostatic dipole-dipole interaction which is absent in planar dimers, 3) corannulene dimers prefer an eclipsed conformation, while planar dimers prefer a staggered conformation.

The aim of the present work is to investigate substituent effects in corannulene dimer. The introduction of substituents in the structure of corannulene is of great interest because it may exert a modulatory effect and enable a better concave-convex interaction with fullerenes. So, several works of Sherrill *et al.* have found important substituent effects for the planar π···π interaction in benzene dimers.[16-20]

Theoretical investigations of non-covalent interactions require an adequate treatment of delocalization and dispersion effects. Accurate *ab initio*-correlated wavefunction methods, such as CCSD(T), reach a good level of accuracy with a large basis set, but it is prohibitively expensive for large systems. Density functional theory (DFT), the most widely used method for electronic calculations in chemistry and physics,[21,22] offers the opportunity to study large systems at a reasonable computational cost. However, it is not appropriate for treatment of non-covalent interactions, because

conventional DFT techniques fail to treat dispersion effects completely. To solve this problem, nowadays, two types of strategies have been developed. The first of these is the development of new types of functionals such as BMK,[23] M05[24] or M06.[25] A variant of the latter two (M05-2X and M06-2X) was recently used to study the concave-convex interaction in the tweezers designed by Sygula *et al.* [13,26,27] The second strategy lies in trying to correct the deficiencies of the existing functionals, adding an empirical term for the dispersion: these are the so-called DFT-D methods.[28,29] Recently, Peverati and Baldridge have tried various methods based on both strategies for the study of a set of polynuclear hydrocarbons.[30] According to their results, both types of procedures can be very promising, especially the latter. Also, using DFT-D calculations, Grimme *et al*. have studied the anthracene dimer and the interaction of corannulene with small molecules (water, ammonia, methane).[31]

In the present work, DFT calculations were performed using both strategies as discussed above; specifically with ωB97XD,[32] B97D[29] and M06-2X[25] functionals. The results were compared with those obtained by Sygula and Saebø at the SCS-MP2/cc-pVTZ level.[11] Therefore, another objective of this work is to test the performance of both DFT strategies to solve the known limitations of 'standard' DFT methods regarding dispersion effects. This is an important issue due to the increasing size of systems of interest, which prevents the use of accurate *ab initio*-correlated wavefunction methods.

4.2. Computational details

The B3LYP/6-311G* geometry of monomers has been used to build the dimers (there is a justification for this choice in the next section). C_{60}like, corannulene with the curvature of buckminsterfullerene, C_{60}, was constructed by cutting the appropriate C_{20} fragment from the B3LYP/6-311G* optimized buckminsterfullerene, and attaching ten hydrogen atoms to the dangling bonds. The position of these hydrogen atoms was optimized keeping the carbon network frozen. The C_{60}like is a 'fullerene copy', and it was included in the study to imitate the concave-convex interaction between corannulene and buckminsterfullerene.

Corannulene monomers, with different curvature and substituents were used to build the dimers studied. The interaction energy and equilibrium distance between the monomers were calculated using M06-2X, B97D and ωB97XD functionals and 6-31+G* basis set. Counterpoise corrections were applied to all reported interaction energies to avoid basis set superposition error.[33] A series of single point calculations with frozen geometry of monomers and intermolecular separation between the monomers ranging from 3.0 to 4.0 Å with increases of 0.1 Å was carried out. Intermolecular separation between monomers was defined by the distance between the two pentagonal planes. The equilibrium distance for each dimer was found by fitting the points near the energy minimum to a quadratic function. Subsequently, interaction energies were obtained for the values of the equilibrium distance.

Quantum chemical calculations were carried out with the Gaussian09 program package.[34]

4.3. *Results and discussion*

4.3.1. Corannulene monomers

Figure 4.1 shows the monomers studied in the present work. For X=H, three different structures have been studied: the structure of minimum energy of corannulene, the C_{60}like, corannulene having the curvature of the buckminsterfullerene, and planar corannulene which corresponds to the transition state in the process of the bowl-to-bowl inversion. These latter two structures were chosen to test the performance of DFT functionals to assess the effect of curvature of the conjugated systems on their ability to form π···π stacked assemblies, by comparison with previous SCS-MP2 results.[11] According to studies by Petrukhina *et al.*, the B3LYP functional led to a geometry of corannulene very similar to that reported by X-ray diffraction.[35] In the present work a series of preliminary calculations using the B3LYP functional with basis sets of different sizes was carried out. The choice of the most appropriate level of calculation was based on the values of the *rms* (root mean square) obtained by superposition of heavy atoms of the structure obtained in our calculations with the structure of corannulene built using the arithmetic mean of the experimental geometrical data at 100° and 183°C.[35] So, *rms* values of 0.011, 0.013, 0.012 and 0.005 Å were obtained with the 6-31+G*, 6-31G*, 6-31G** and 6-311G* basis sets, respectively. These extremely small *rms* values show that agreement between experimental and calculated geometry is very good for any of these basis sets. The B3LYP/6-311G* geometry of monomers was chosen to study the interaction in dimers since it is slightly better, but knowing that this choice will not have much impact on the results obtained.

Both planar corannulene and C_{60}like monomers do not represent minimum energy structures and therefore they have greater energy than the fully optimized corannulene molecule. So, planar corannulene is less stable than corannulene by 10.09 kcal/mol and C_{60}like by 58.78 kcal/mol, at the B3LYP/6-311G* level. All substituted corannulene monomers are minimum energy structures and have a curvature similar to that of corannulene. Corannulene and C_{60}like have C_{5v} symmetry, while planar corannulene and substituted corannulene have D_{5h} symmetry and C_5 symmetry, respectively.

As a way of checking the changes introduced in the bowls by the substituents, Table 4.1 lists the values of some important geometric parameters. *R* is the interplanar distance between the planes formed by hub and rim atoms, respectively; it represents the bowl depth. R_1 is the longest distance between two carbon atoms of the rim of the bowl; it represents the bowl aperture or diameter. POAV is the pyramidalization angle (π-orbital axis vector) as proposed by Haddon.[36] The POAV angle allows the description of local curvature of a conjugated system and is defined as the angle between the C-C bond and the vector perpendicular to the pyramidal base of three idealized C-C bonds.

Furthermore, superimpositions of carbon atoms of corannulene and substituted corannulene were performed. *rms* values of 0.020, 0.016, 0.018, 0.015 and 0.014 Å were found for corannulene substituted with Br, Cl, CH_3, C_2H or CN units, respectively. Therefore, both these *rms* values and data from Table 4.1 show that the introduction of substituents causes only small changes in the corannulene bowl. In all cases these small changes consist of a decreasing of *R*, an increasing of R_1 and a decreasing of POAV; that is, the flattening of the corannulene bowl.

Table 4.1: Geometric parameters (*R* and R_1 in Å), and POAV angles at the hub position (degrees) obtained at the B3LYP/6-311G* level

	R	R_1	POAV
Corannulene	0.884	6.512	8.29
C_{60}like	1.495	6.074	11.64
Planar corannulene	0.000	6.723	0.00
Corannulene-5Br	0.845	6.526	7.99
Corannulene-5Cl	0.855	6.519	8.06
Corannulene-5CH_3	0.861	6.539	8.12
Corannulene-5C_2H	0.861	6.539	8.12
Corannulene-5CN	0.859	6.534	8.09

According to previous studies, one of the consequences of the curvature of corannulene is its substantial dipole moment; while the plane corannulene is nonpolar.[11] The electrostatic dipole-dipole attraction is responsible for a significant part of the interaction energies of the curved systems. However, the major electrostatic contribution in the planar dimers should come only from quadrupole-quadrupole interactions.[11]

Our calculations at the B3LYP/6-311G* led to a dipole moment of 2.22 D for corannulene and 3.90 D for C_{60}like. The convex side of the bowl is the more negative region of the bowl. Values of 0.36, 0.16, 2.29, 1.85, and 3.19 D were obtained for the pentasubstituted corannulene with Br, Cl, CH_3, C_2H, and CN, respectively. The dipole moment for corannulene substituted with Br and Cl is decreased because of the electron acceptor character of these atoms; this effect is much larger for the CN group, so dipole is fully reversed.

It is well documented in the literature that B3LYP functional can lead to a not very precise evaluation of dipole moments.[37-40] In order to verify the above dipole moments are not artifacts of the B3LYP functional, ωB97XD/6-311G** calculations were also performed. 2.37 and 4.13 D were obtained for corannulene and C_{60}like; 0.45, 0.23, 2.46, 2.00 and 3.12 D for the pentasubstituted corannulenes. That is, there are no very significant differences regarding B3LYP calculations and the trends are exactly the same.

4.3.2. Corannulene dimers

Figure 4.2 shows the corannulene dimers studied. A series of single-point calculations with B97D, ωB97XD and M06-2X functionals and 6-31+G* basis set with frozen monomer geometries was performed. All dimers were studied in the eclipsed

conformation, with all bonds in one monomer eclipsing the analogous bonds in the other monomer. For the planar corannulene we have also studied the staggered conformation, with one of the monomers rotated 36° around the axis defined by the center of both five-membered rings. According to previous studies realized by Sygula and Saebø, planar corannulene dimers in the staggered conformation are energetically more favorable than the eclipsed conformation. On the other hand, the eclipsed conformation is preferred for curved dimers.[11]

Corannulene dimer, planar corannulene dimer and corannulene···C_{60}like dimer were previously studied by Sygula and Saebø at the SCS-MP2/cc-pVTZ level of calculation.[11] Taking into account the reasonable quality of that level (and the lack of experimental data), our results were compared with those. In addition to these three dimer motifs, the planar corannulene···C_{60}like dimer has also been studied in order to get more information of the effect of curvature in the stack of bowls.

The calculated equilibrium distance and interaction energy for the dimers studied are showed in Table 4.2. Figure 4.3 shows the ωB97XD/6-31+G* calculated interaction energies of the dimers as a function of the distance between monomers.

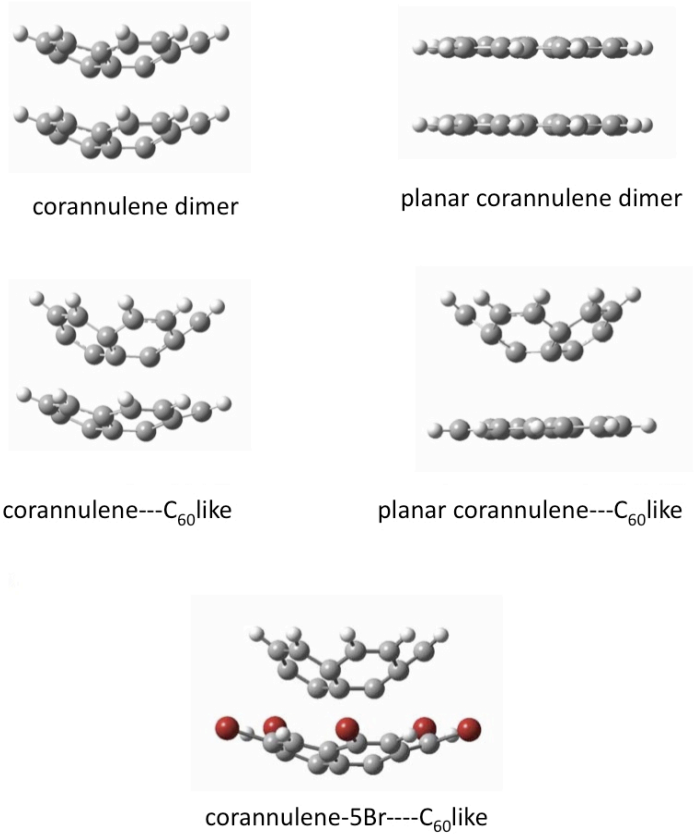


Figure 4.2: Corannulene dimers studied. A corannulene-5X···C_{60}like dimer was studied with X = Br, Cl, CH_3, C_2H, and CN.

Table 4.2: Equilibrium distance, d_{eq}, (Å) and interaction energy, E_{Int}, (kcal/mol) for the first four dimers shown in Figure 4.2. All calculations were performed with the basis set 6-31+G*

	B97D		ωB97XD		M06-2X		MP2[a]	
	d_{eq}	E_{Int}	d_{eq}	E_{Int}	d_{eq}	E_{Int}	d_{eq}	E_{Int}
Corannulene	3.67	-15.18	3.71	-17.55	3.66	-13.31	3.64	-17.20
Cora···C_{60}like	3.51	-14.16	3.59	-15.52	3.54	-11.70	3.45	-17.00
Pl. cora···C_{60}like	3.27	-10.83	3.33	-10.72	3.32	-6.09	-	-
Pl. cora (eclip.)	3.72	-11.64	3.69	-13.46	3.67	-7.03	3.67	-13.00
Pl. cora (stagg.)	3.41	-16.83	3.42	-18.84	3.43	-14.34	3.40	-18.40

[a]SCS-MP2/cc-pVTZ ref. 11.

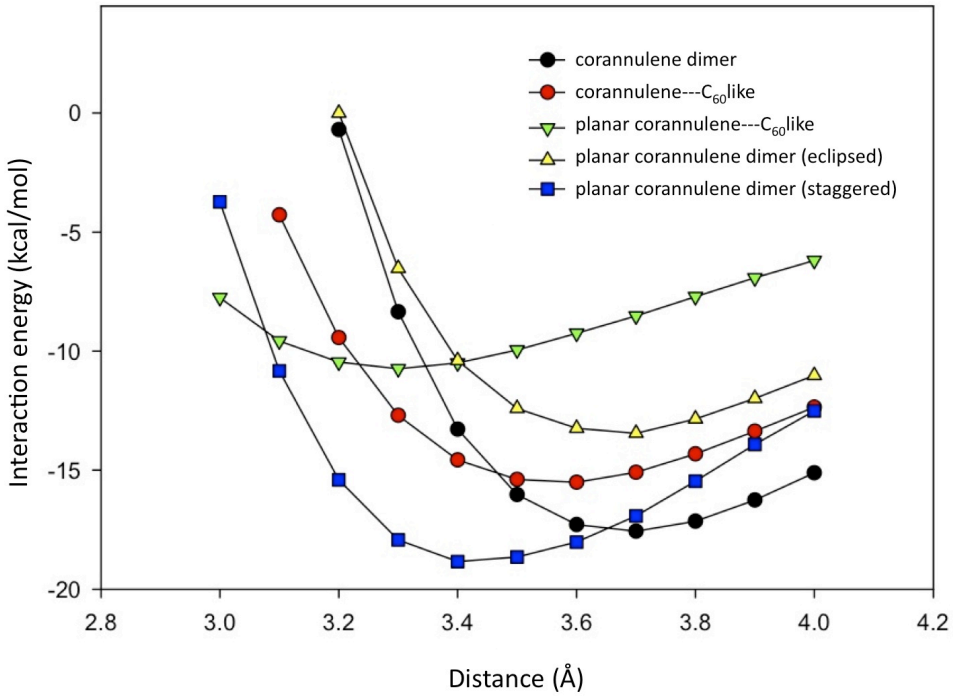


Figure 4.3: BSSE-corrected interaction energy calculated at the ωB97XD/6-31+G* level for the first four dimers shown in Figure 4.2.

Results of Table 4.2 show that DFT-D methods (B97D and ωB97XD) produce values closer to results obtained at the SCS-MP2/cc-pVTZ level than M06-2X method. In particular, ωB97XD functional works very well, with differences lower than 0.5 kcal/mol for the dimers studied by Sygula *et al.*[11] (except the corannulene···C_{60}like dimer which shows a difference of 1.48 kcal/mol). In general, B97D results led to a small underestimation. On the other hand, calculations with the M06-2X functional, developed for the treatment of non-covalent interactions, led to a considerable underestimation of the interaction energy. For example, an interaction energy of -13.31 kcal/mol was

obtained for the corannulene dimer, *i.e.* 23% smaller than the MP2 value (-12% and +2%, for B97D and ωB97XD, respectively). The underestimation of M06-2X results is similar or worse in the other dimers.

As expected, the smallest interaction energy takes place in the planar corannulene···C_{60}like dimer. So, the ability of planar corannulene to 'catch' curved compounds seems clearly poor.

In order to analyze in more detail the balance of energy contributions to the stability of the dimers, the interaction energy was decomposed according to a simple method. So, the two contributions of the model employed were taken into account; that is, the pure ωB97X interaction energy and the empirical dispersion contribution to the interaction energy. Results in Table 4.3 show that dispersion plays a very important role in the interaction energy of corannulene dimers. It is noteworthy that the small interaction energy for the planar corannulene···C_{60}like dimer is a direct consequence of the small dispersive stabilization. So, the dispersive effect is larger when two curved compounds or two planar compounds (especially in a staggered way) dimerize. These effects can be understood by the analysis of the values of distances between equivalent carbon atoms of the corannulene monomers (Table 4.4). Although the interaction of planar corannulene with C_{60}like produces the shortest equilibrium distance between monomers (3.33 Å, which corresponds to C_h-C_h distance), a significant increase between C_s, and especially C_r, carbon atoms was obtained. That explains the small dispersive effect of this dimer. Comparing Tables 4.3 and 4.4, almost a direct relationship between C_r-C_r distance and dispersion energy is observed: the larger C_r-C_r distance, the smaller dispersive stabilization.

Table 4.3: ωB97X interaction energy and dispersion contribution of the corannulene dimers obtained at the ωB97XD/6-31+G* level (kcal/mol)

	ωB97X	Dispersion
Corannulene	2.48	-20.03
Cora···C_{60}like	2.03	-17.55
Pl. cora···C_{60}like	1.92	-12.64
Pl. cora (eclip.)	6.17	-17.81
Pl. cora (stagg.)	4.27	-23.11

Table 4.4: Distance C_h-C_h, C_s-C_s and C_r-C_r between equivalent carbon atoms of the two monomers that form each dimer, calculated at the ωB97XD/6-31+G* level (Å)

	C_h-C_h	C_s-C_s	C_r-C_r
Corannulene	3.71	3.71	3.71
Cora···C_{60}like	3.59	3.79	4.21
Pl. cora···C_{60}like	3.33	4.06	4.84
Pl. cora (eclip.)	3.69	3.69	3.69
Pl. cora (stagg.)	3.48	3.75	3.47

4.3.3. Substituted corannulene dimers

In order to know the ability of substituted corannulene as 'buckycatcher', the interaction energy and equilibrium distance for the last dimer shown in Figure 4.2 (corannulene-5X···C_{60}like) were obtained with B97D, ωB97XD and M06-2X functionals (Table 4.5). Figure 4.4 shows the interaction energy (at the ωB97XD/6-31+G* level) of the dimer as a function of the separation distance between the monomers.

Table 4.5: Equilibrium distances, d_{eq}, (Å) and interaction energy, E_{Int}, (kcal/mol) for the last dimer shown in Figure 4.2: corannulene-5X···C_{60}like. All calculations were performed with the basis set 6-31+G*

	B97-D		ωB97X-D		M06-2X	
	d_{eq}	E_{Int}	d_{eq}	E_{Int}	d_{eq}	E_{Int}
Cora···C_{60}like	3.51	-14.16	3.59	-15.52	3.54	-11.70
Cora-5Br···C_{60}like	3.45	-20.44	3.52	-21.64	3.47	-16.41
Cora-5Cl···C_{60}like	3.47	-18.56	3.54	-19.92	3.48	-15.56
Cora-5CH_3···C_{60}like	3.44	-19.23	3.52	-20.11	3.47	-15.10
Cora-5C_2H···C_{60}like	3.47	-18.06	3.53	-19.32	3.48	-14.00
Cora-5CN···C_{60}like	3.43	-23.35	3.51	-24.64	3.47	-19.16

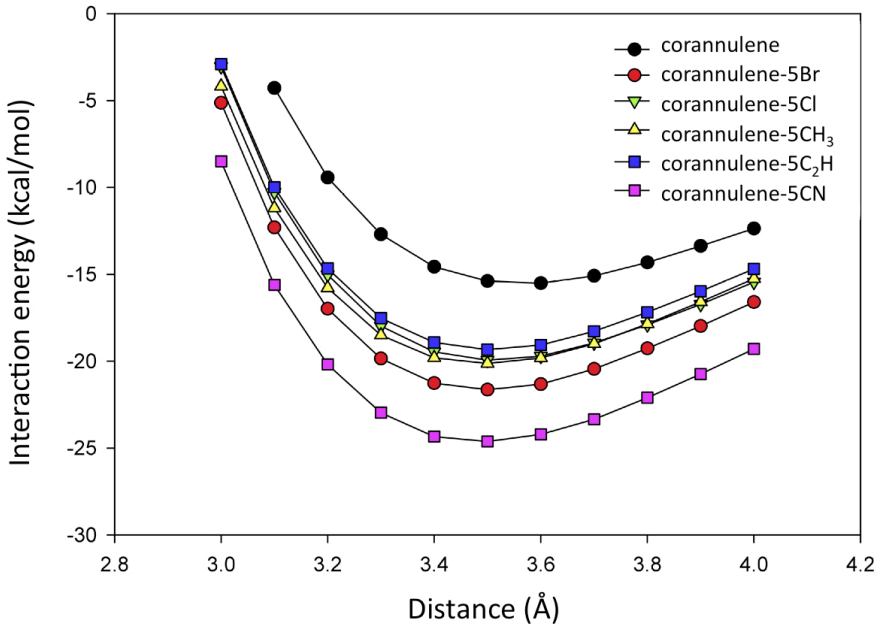


Figure 4.4: BSSE-corrected interaction energy calculated at ωB97XD/6-31+G* level for the last dimer shown in Figure 4.2: corannulene-5X···C_{60}like.

As can be seen in Figure 4.4 and in Table 4.5, there is a substantial increase in interaction energy of dimers when different substituents were placed in the corannulene monomer. However, only very small differences in the equilibrium distance were found.

The most significant increase in interaction energy was obtained for the corannulene substituted with five CN groups, with a gain of 9.19, 9.12 and 7.46 kcal/mol with B97D, ωB97XD and M06-2X functionals, respectively. For corannulene substituted with five Br atoms an increase ranging from 6.28 to 4.71 kcal/mol was obtained. In other cases (substitutions with Cl, CH_3 and C_2H) very similar increases were obtained: about 4-5 kcal/mol with DFT-D and about 3-4 kcal/mol with M06-2X. Regarding the equilibrium distance of the dimer, a slight shortening was obtained for all substituted dimers relative to the unsubstituted dimer, in accordance with the increase of interaction energy. In order to explain these findings, the contribution of dispersion was evaluated (Table 4.6) and molecular electrostatic potential maps of monomers were analyzed (Figure 4.5). In the dimer an interaction between the concave face of corannulene-5X (the catcher) and the convex face of C_{60}like (the fullerene C_{60} copy) takes place. From an electrostatic point of view (Figure 4.5) the convex face of C_{60}like is basically negative, and so interaction with a positive face will be favored. Under these circumstances, substitutions with Cl, Br and CN will be the most convenient. Corannulene-5C_2H would occupy an intermediate position; unsubstituted corannulene, and especially corannulene-5CH_3, would be the worse catchers. Moreover, these conclusions are in agreement with the expected acceptor/donor character of substituents. CN, Cl, Br and C_2H, as electron withdrawing groups, make a more positive MEP in both faces of the bowl. By contrast, the presence of CH_3 electron donating groups in the corannulene causes a slight increase in the electron density of the bowl, so MEP becomes more negative. Therefore, from the strictly electrostatic point of view of Figure 4.5, the ranking of catchers would be: 5CN > 5Cl > 5Br >> 5C_2H >> 5H > 5CH_3. However, the results of Table 4.5 show some outstanding differences with this ranking. The two most remarkable discrepancies are those of 5Br and 5CH_3. So, corannulene-5Br is better catcher than corannulene-5Cl, and corannulene-5CH_3 goes up several positions of the electrostatic ranking. These two discrepancies are adequately explained from the dispersion contributions included in Table 4.6. So, according to this table, corannulene-5CH_3···C_{60}like and corannulene-5Br···C_{60}like dimers are the most favored ones taking into account the dispersion contribution to stabilization: in both cases about -22.5 kcal/mol. By contrast, corannulene···C_{60}like dimer shows the smaller dispersion contribution: only -17.6 kcal/mol. It is noteworthy that among all the dimers studied in the present work, only corannulene-5CN···C_{60}like dimer has favorable pure ωB97X interaction energy; it does not need dispersion contribution to form a stable complex. Certainly, it is due to the huge electrostatic effect that takes place in this dimer.

In summary, substituted corannulene behave as a better catcher than the original corannulene, as a consequence of combination of electrostatic and dispersive effects. Moreover, the joint effects are responsible for the different ability (Table 4.5) of substituted corannulene to catch the fullerene copy. Therefore, the two contributions (electrostatic and dispersion) are important to analyze the effect of substituents in π···π stacked interactions in curved systems. That is in agreement with recent findings of Ringer and Sherrill for planar systems, which point out that substituent effects in face-to-face in π···π interactions are not governed solely by electrostatic control.[20]

Finally, in order to verify the trend pointed out by Sygula and Saebø,[11] according to that corannulene dimers prefer an eclipsed conformation, the interaction energy at the ωB97XD/6-31+G* level was computed for the staggered disposition of the dimers of Table

4.5. For this purpose, we have assumed that equilibrium distance of the staggered conformations is the same that the eclipsed ones (the difference for corannulene dimer[11] is less than 0.05 Å). The calculated values for the dimers of Table 4.5 were: -12.77, -19.27, -17.73, -17.60, -16.76, and -21.51 kcal/mol. So, the eclipsed disposition is favored by 2-3 kcal/mol and, therefore, the trend commented above is also true for the interaction between corannulene-5X and C_{60}like.

Table 4.6: ωB97X interaction energy and dispersion contribution of the corannulene-5X···C_{60}like dimers obtained at the ωB97XD/6-31+G* level (kcal/mol)

	ωB97X	Dispersion
Cora···C_{60}like	2.03	-17.55
Cora-5Br···C_{60}like	0.79	-22.43
Cora-5Cl···C_{60}like	0.84	-20.76
Cora-5CH_3···C_{60}like	2.40	-22.51
Cora-5C_2H···C_{60}like	2.32	-21.64
Cora-5CN···C_{60}like	-3.11	-21.53

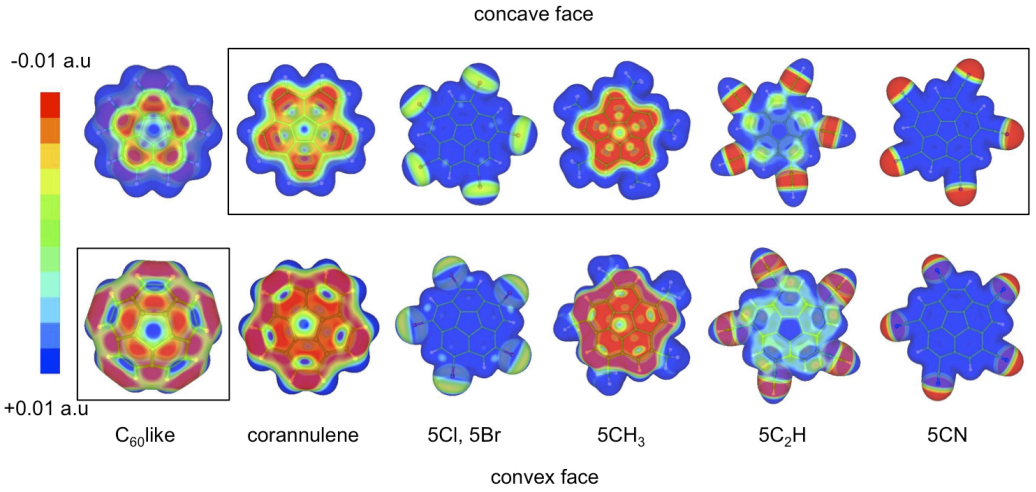


Figure 4.5: Molecular electrostatic potential onto an electron density isosurface of 0.005 a.u. Corannulene-5Br and corannulene-5Cl are virtually indistinguishable to the naked eye, although MEP for corannulene-5Cl is slightly more positive, as expected. In the corannulene-5X···C_{60}like dimer interaction takes place between the concave face of corannulene-5X and the convex face of C_{60}like.

4.4. Conclusions

The factors that control the stacking bowls have been investigated employing a series of dimers composed of corannulene monomers with different curvatures and substitutions.

Corannulene has a noticeable rigidity, so that inclusion of up to five substituents has a small effect on its structure: only a slight flattening of the bowl is observed.

Calculations with DFT-D methods using ωB97XD and B97D functionals give rise to better interaction energies for corannulene dimers than the M06-2X functional, compared with previous SCS-MP2 results. So, DFT-D (especially ωB97XD) seems to work better than M06-2X to obtain absolute interaction energies. However, to analyze the effect of substitution, the three functionals led to the same conclusions (in this case, both DFT-D functionals led to virtually the same differences).

All the pentasubstituted corannulenes behave as a better buckycatcher than the unsubstituted corannulene. The ability to catch the fullerene copy is directly related to the donor/acceptor character of substituents. So, electron-withdrawing groups give rise to a more positive MEP in the concave side (inside) of the bowl, which allows a better interaction with negative MEP of the convex side (outside) of the fullerene copy. Electron releasing groups have the opposite effect on MEP. However, not only electrostatic interactions are enough to explain the different ability of the catchers. So, it is necessary to take into account important dispersive effects to complete the explanation. For that reason, corannulene-5Br, and especially corannulene-5CH_3, have a better catcher ability than those predicted only from electrostatic considerations. Corannulene-5CN forms the most stable complex due to the huge electron withdrawing ability of cyano groups and, moreover, the dispersive effect is considerable too. Therefore this compound seems the best candidate for recognition of fullerenes by π···π concave-convex interaction.

4.5. References

1. C. A. Hunter and J. K. M. Sanders, *J. Am. Chem. Soc.*, 1990, **112**, 5525-5534.
2. E. A. Meyer, R. K. Castellano and F. Diederich, *Angew. Chem. Int. Ed.*, 2003, **42**, 1210-1250.
3. K. Müller-Dethlefs and P. Hobza, *Chem. Rev.*, 2000, **100**, 143-167.
4. P. Hobza and J. Sponer, *Chem. Rev.*, 1999, **99**, 3247-3276.
5. P. W. Rabideau, A. H. Abdourazak, H. E. Folsom, Z. Marcinow, A. Sygula and R. Sygula, *J. Am. Chem. Soc.*, 1995, **117**, 6410-6411.
6. P. A. Vecchi, C. M. Alvarez, A. Ellern, R. J. Angelici, A. Sygula, R. Sygula and P. W. Rabiedau, *Organometallics*, 2005, **24**, 4543-4552.
7. K. Kavitha, M. M. Manoharan and P. Venuvalingam, *J. Org. Chem.*, 2005, **70**, 2528-2536.
8. A. K. Kandalam, B. K. Rao and P. Jena, *J. Phys. Chem. A*, 2005, **109**, 9220-9225.
9. T. J. Seiders, K. K. Baldridge, G. H. Grube and J. S. Siegel, *J. Am. Chem. Soc.*, 2001, **123**, 517-525.
10. Y.-T. Wu, D. Bandera, R. Maag, A. Linden, K. K. Baldridge and J. S. Siegel, *J. Am. Chem. Soc.*, 2008, **130**, 10729-10739.
11. A. Sygula and S. Saebø, *Int. J. Quantum. Chem.*, 2009, **109**, 65-72.
12. D. M. Forkey, S. Attar, B. C. Noll, R. Koerner, M. M. Olmstead and A. L. Balch, *J. Am. Chem. Soc.*, 1997, **119**, 5766-5767.

13. A. Sygula, F. R. Fronczek, P. Sygula, M. M. Rabideau and M. M. Olmstead, *J. Am. Chem. Soc.*, 2007, **129**, 3842-3843.
14. F. Cozzi and J. S. Siegel, *Pure Appl. Chem.*, 1995, **67**, 683-689.
15. L. L. Miller and K. R. Mann, *Acc. Chem. Res.*, 1996, **29**, 417-423.
16. M. O. Sinnokrot and C. D. Sherrill, *J. Phys. Chem. A*, 2003, **107**, 8377-8379.
17. M. O. Sinnokrot and C. D. Sherrill, *J. Am. Chem. Soc.*, 2004, **126**, 7690-7697.
18. A. L. Ringer, M. O. Sinnokrot, R. P. Lively and C. D. Sherrill, *Chem. Eur. J.*, 2006, **12**, 3821-3828.
19. S. A. Arnstein and C. D. Sherrill, *Phys. Chem. Chem. Phys.*, 2008, **10**, 2646-2655.
20. A. L. Ringer and C. D. Sherrill, *J. Am. Chem. Soc.*, 2009, **131**, 4574-4575.
21. R. G. Parr and W. Yang, *Density-Functional Theory of Atoms and Molecules*, Oxford University Press, Oxford, 1989.
22. W. Koch and M. C. Holthausen, *A Chemist's Guide to Density Fucntional Theory*, Wiley-VCH, New York, 2001.
23. A. D. Boese and J. M. L. Martin, *J. Chem. Phys.*, 2004, **121**, 3405-3416.
24. Y. Zhao, N. E. Schultz and D. G. Truhlar, *J. Chem. Phys.*, 2005, **123**, 161103/1-161103/4.
25. Y. Zhao and D. G. Truhlar, *Theor. Chem. Acc.*, 2008, **120**, 215-241.
26. B. M. Wong, *J. Comput. Chem.*, 2009, **30**, 51-56.
27. Y. Zhao and D. G. Truhlar, *Phys. Chem. Chem. Phys.*, 2008, **10**, 2813-2818.
28. S. Grimme, *J. Comput. Chem.*, 2004, **25**, 1463-1473.
29. S. Grimme, *J. Comput. Chem.*, 2006, **27**, 1787-1799.
30. R. Peverati and K. K. Baldridge, *J. Chem. Theor. Comput.*, 2008, **4**, 2030-2048.
31. S. Grimme, J. Antony, T. Schwabe and C. Mück-Lichtenfeld, *Org. Bimol. Chem.*, 2007, **5**, 741-758.
32. J.-D. Chai and M. Head-Gordon, *Phys. Chem. Chem. Phys.*, 2008, **10**, 6615-6620.
33. S. F. Boys and F. Bernardi, Mol. Phys., 1970, **18**, 553-566.
34. M. J. Frisch *et al*. *GAUSSIAN 09 (Revision A.02)*, Gaussian, Inc., Wallingford CT, 2009.
35. M. A. Petrukhina, W. W. Anderini, J. Mack and L. T. Scott, *J. Org. Chem.*, 2005, **70**, 5713-5716.
36. R. C. Haddon, *J. Am. Chem. Soc.*, 1990, **112**, 3385-3389.
37. A. Dreuw and M. Head-Gordon, *J. Am. Chem. Soc.*, 2004, **126**, 4007-4016.
38. B. M. Wong and J. G. Cordaro, *J. Chem. Phys.*, 2008, **129**, 214703/1-214703/8.
39. B. M. Wong, M. Piacenza, and F. Dela Sala, *Phys. Chem. Chem. Phys.*, 2009, **11**, 4498-4508.
40. W. Liu, V. Settels, P. H. P. Harbach, A. Dreuw, R. F. Fink, and B. Engels, *J. Comput. Chem.*, 2011, **32**, 1971-1981.

Chapter 5

Analysis of the performance of DFT-D, M05-2X and M06-2X functionals for studying π···π interactions

5.1. Introduction

π···π interactions play an outstanding role in biochemistry, material science, molecular engineering, and packing of aromatic molecules in crystals.[1-5] However, an accurate description of the π···π interactions is a challenging task for quantum chemistry methods in general.[6,7] Accurate *ab initio*-correlated wavefunction methods, such as CCSD(T) in combination with a large basis set, reach a good level of accuracy, however they are prohibitively expensive for large systems. On the other hand, cheaper methods, such as MP2 remain unfeasible for large systems, and moreover tend to overestimate the interaction energy, especially for dispersive π···π interactions. [8-14]

Therefore, the more feasible option would be to use density functional theory (DFT) that allows to treat large systems with reasonable computational cost. Unfortunately, classical DFT methods fail completely to treat dispersion effects.

In this context, the last years have been marked by an intense research of new DFT variants for taking into account the dispersive effects. Two general pathways were developed to solve this problem: the first one was the development of a new type of functionals, such as the Truhlar's M05[15] and M06[16] suite of functionals. The second pathway was to include a term for the dispersion, termed as DFT-D methods. [17-23] The inclusion of empirical dispersion coefficients[17,18] is very simple, but these approaches have been successful in many applications. A different approach consists of calculating dispersion energies from dispersion coefficients: Becke and Johnson developed the XDM dispersion model,[19] Steinmann and Corminboeuf developed a GGA variant of the XDM model,[20] and there are other several methods. [21-23]

In the last years, the S22 database developed by Jurecka *et al.*[24] has been extensively used for evaluating the performance of methods for studying non-covalent

interactions.[25-29] However, one of the failures of the S22 database is to disregard sandwich complexes with eclipsed monomers. Although eclipsed conformations are not usually the most stable conformations for planar complexes as benzene and naphthalene dimer, they are very important for curved complexes.[30-32] Therefore, the S22 does not seem appropriate for evaluating the performance of functionals for studying the stacking interactions of curved conjugated systems. Nowadays, the stacking interactions between curved conjugated systems, also called concave-convex π···π interactions, have become a very attractive research field. A deep understanding of these interactions may be the key to obtaining new host-guest complexes, fullerene receptors and supramolecular architectures. However, an accurate level calculation is crucial for reliable results.

Currently, DFT-D, M05-2X and M06-2X functionals have been employed in the study of several concave-convex π···π complexes.[33-38] However, the performance of functionals seems to be substantially distinct than that expected from the S22 database validation. Thus, a considerably underestimation of the interaction energy was observed for the corannulene dimer using M06-2X functional,[31,32] despite this functional shows a good performance for S22 database complexes.[25] On the other hand, theoretical estimates of the interaction energy for the molecular tweezers designed by Sygula *et al.*[3] lead to a huge range (from 21 to 43 kcal/mol) depending on the DFT model used.[34,36,37] Therefore, a detailed evaluation of the functional performance would be very advisable, especially for curved conjugated systems.

The goal of this work is to evaluate the performance of DFT-D functionals with empirical dispersion correction: B97-D,[39] BLYP,[40,41] BP86,[40,42] PBE[43] and specialized functionals, M05-2X[44] and M06-2X[16] functionals for the treatment of non-covalent π···π interactions.

5.2. *Computational details*

Single-point energy calculations were performed on the geometry of S22 database complexes, obtained by Jurecka *et al.*[24] All other complexes evaluated were fully optimized. DFT-D calculations were carried out using resolution of identity approximation (RI) implemented in TURBOMOLE 5.10 program suite.[45]

DFT-D calculations were performed employing the B97-D, BLYP-D, BP86-D and PBE-D functionals, and the cc-pVTZ basis set.

Calculations employing the M05-2X and M06-2X functionals and cc-pVTZ basis set were carried out with Gaussian09 program package.[46]

Counterpoise corrections, CP, were applied to all reported interaction energies to avoid basis set superposition error, BSSE.

5.3. *Results and discussion*

The performance of DFT-D, M05-2X and M06-2X functionals for studying π···π interactions was evaluated employing four group of complexes: 1) dispersion-dominated complexes taken from the S22 database; 2) complexes with planar polycyclic aromatic hydrocarbons, PAHs; 3) complexes with curved PAHs; 4) mixed complexes made up by planar and curved PAHs. Table 5.1 summarizes interaction energy values and Table 5.2 equilibrium distances.

5.3.1. Complexes from the S22 benchmark database

The S22 database developed by Jurecka *et al*.[24] has been widespread used to benchmark existing and new quantum chemistry methods for studying non-covalent interactions. However, the S22 database is not fully representative. Despite recent enlargement of S22 database, the S66 database[47] also does no take into account concave-convex π···π interactions.

Table 5.1, and Figure 5.1 in a more visual manner, shows interaction energies obtained using DFT-D, M05-2X and M06-2X functionals on the geometry of five complexes with predominant dispersion from the S22 benchmark database. As can be seen, all functionals studied, except M05-2X, give a good performance for the S22 database complexes.[48,49]

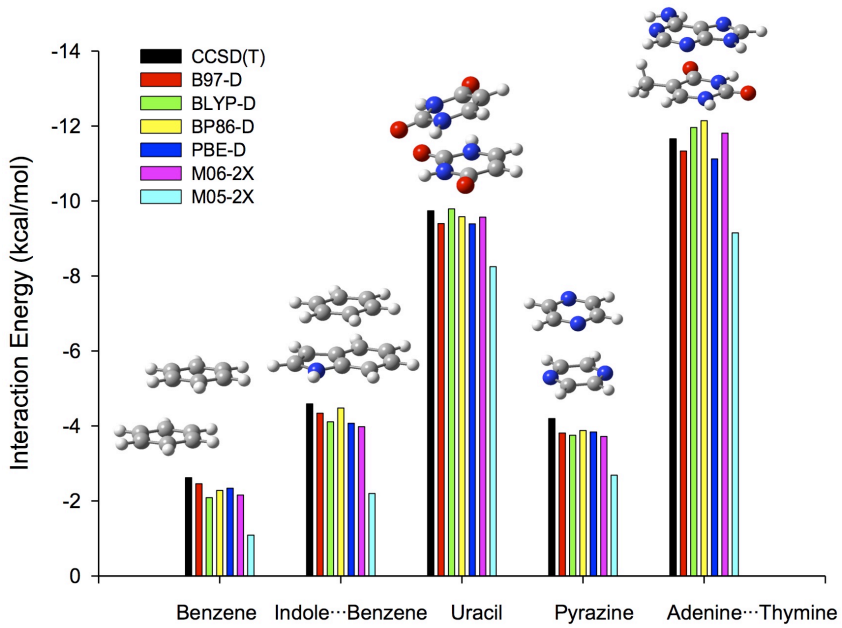


Figure 5.1: Interactiions energies of the S22 database complexes.

Table 5.1: Interaction energies (kcal/mol) for different complexes with π···π interactions. Reference CCSD(T) and QCISD(T) interactions energies are given for comparison (Ref)

Complex (symmetry)	Ref	B97-D	B-LYP-D	BP86-D	PBE-D	M06-2X	M05-2X
			S22 database complexes				
Benzene dimer (C_{2h})	-2.62[a],-2.65[b]	-2.46	-2.09	-2.28	-2.34	-2.16	-1.09
Indole···benzene stack (C_1)	-4.59[a],-4.52[b]	-4.34	-4.11	-4.48	-4.07	-3.98	-2.20
Uracil dimer (C_2)	-9.74[a],-9.78[b]	-9.40	-9.79	-9.58	-9.39	-9.57	-8.25
Pyrazine dimer (C_s)	-4.20[a],-4.26[b]	-3.81	-3.75	-3.88	-3.84	-3.72	-2.69
Adenine···thymine stack (C_1)	-11.66[a],-11.86[b]	-11.33	-11.96	-12.14	-11.12	-11.81	-9.15
			Planar complexes				
Benzene dimer (D_{6h})	-1.48[c],-1.70[d]	-1.60	-0.88	-0.78	-1.26	-0.62	-0.20
Naphthalene dimer (D_{2h})	-3.78[e]	-4.12	-3.08	-2.99	-3.10	-1.91	-1.09
Anthracene dimer (D_{2h})		-6.83	-5.47	-5.40	-5.04	-3.29	-1.94
Pyrene dimer (D_{2h})		-8.93	-7.49	-7.47	-6.50	-4.37	-2.55
Coronene dimer (D_{6h})	-14.73[f]	-16.30	-14.35	-14.48	-11.64	-7.98	-4.66
			Curved complexes				
Corannulene···corannulene (C_{5v})	-15.50[g]	-16.06	-15.05	-16.70	-12.67	-12.27	-7.05
Sumanene···sumanene (C_{3v})		-21.09	-21.09	-23.91	-17.64	-16.42	-10.04
Corannulene···sumanene (C_s)		-16.89	-16.10	-17.82	-13.28	-12.06	-7.10
Sumanene···corannulene (C_s)		-18.18	-17.79	-19.85	-14.90	-12.92	-7.87
			Curved and planar complexes				
Coronene···corannulene (C_s)		-17.17	-15.71	-17.67	-12.89	-11.23	-6.28
Coronene···sumanene (C_{3v})		-17.10	-15.74	-17.25	-12.66	-10.85	-6.10

[a]Takatani *et al*. (Ref. 48).

[b]Podeszwa *et al*. (Ref. 49).

[c]Tsuzuki *et al*. (Ref. 52).

[d]Sinnkrot *et al*. (Ref. 4).

[e]Tsuzuki *et al*. (Ref. 53).

[f]Janowski *et al*. (Ref. 54).

[g]Janowski *et al*. (Ref. 32).

It is interesting to note that the S22 database does not include any example of dimer with eclipsed monomers. For that reason, in the next section sandwich complexes with eclipsed conformation are evaluated.

5.3.2. Complexes with eclipsed planar complexes

All complexes of this section show an eclipsed conformation with all bonds of a monomer eclipsing the analogous bond in the other monomer. As can be seen in Table 5.1 and Figure 5.2, the performance of functionals evaluated is not so good as expected by S22 database validation (Figure 5.1). So, not only M05-2X but also to a lesser extent M06-2X, lead to a clear underestimation of interaction energies.

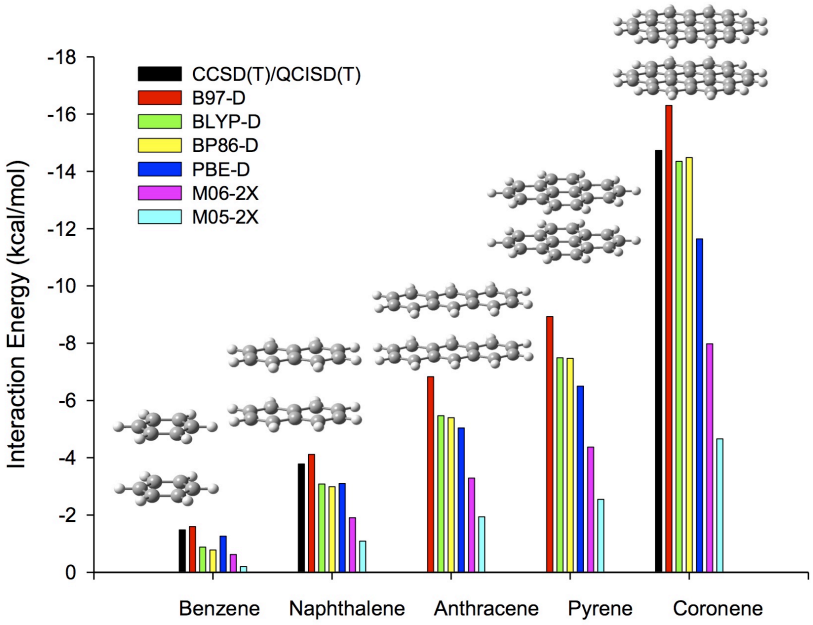


Figure 5.2: Interactions energies of complexes with eclipsed planar monomers.

In order to stress the difference between results of B97-D functional, which seems to give rise to the best results, and those of M06-2X functional, which works well for displaced complexes, but not so well for eclipsed ones, Figure 5.3 depicts the comparison of the interaction energy for benzene dimer as a function of the displacement of monomers. The largest difference between the curves (almost 1 kcal/mol) corresponds to $R_2 = 0$, *i.e.* when monomers are fully eclipsed.

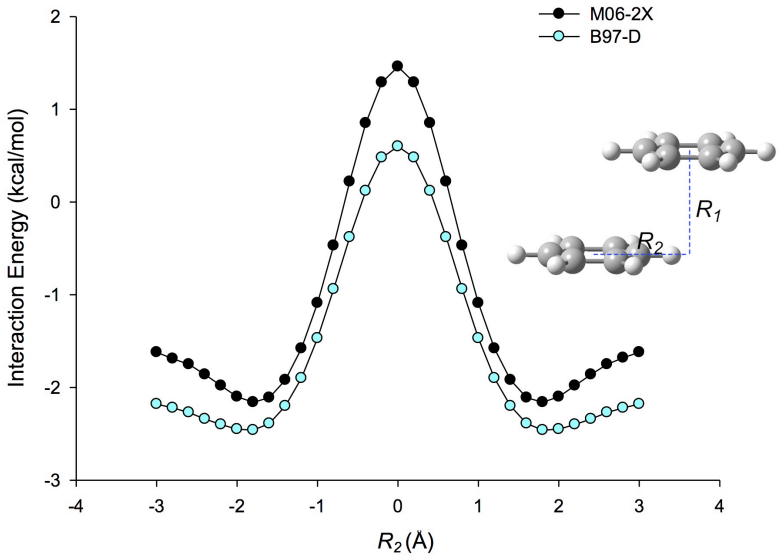


Figure 5.3: Interaction energy of the benzene dimer as a function of the displacement distance R_2, with interplane spacing R_1=3.35 Å, which corresponds to the optimized structure.[24]

The results obtained in this work seem to justify the excessive difference between the staggered and the eclipsed conformation obtained at the M06-2X level. So, for coronene dimer a difference of about 8 kcal/mol was obtained by Zhao and Truhlar[25] employing M06-2X functional, and however, SAPT(DFT)[50] and c-DFTB-D[51] calculations led to differences of only 2.92 and 1.20 kcal/mol, respectively.

Consequently, the M06-2X functional provides a considerable underestimation of the interaction energy values for planar eclipsed complexes. Therefore, it does not seem a good choice to obtain accurate interaction energies for these systems. In general, DFT-D functionals show more accurate interaction energies.

B97-D shows a good performance for benzene and naphthalene dimer with a difference of about 0.1 kcal/mol and 0.3 kcal/mol, respectively, compared to CCSD(T) calculations.[4,52,53] A difference of 1.57 and 2.39 kcal/mol was observed for coronene dimer regarding to QCISD(T)[54] and SAPT-DFT[50] reference results, respectively.

PBE-D also shows good interaction energies for benzene and naphthalene dimers compared to CCSD(T) calculations. However, its accuracy decreases significantly with the increase of the size of the complex.

On the other hand, BLYP-D and BP86-D give rise to virtually the same results, with differences of about 0.1 kcal/mol between them. They give rise to a slight underestimation of interaction energy for the smaller complexes, but supply the best energetic result for coronene.

Regarding equilibrium distances (Table 5.2), not very noticeable differences are found between functionals: only a slight shortening of the BP86-D values and a slight lengthening of the M05-2X ones.

5.3.3. Complexes with curved monomers

Concave-convex π···π interactions are a subject of great interest and important future applications. Therefore, the goal of this section is to evaluate the performance of six functionals for studying concave-convex π···π interactions. Interaction energies were obtained on the most stable complexes (Table 5.1, Figure 5.4).

According to the only available reference value (corannulene dimer), B97-D and B-LYP-D calculations provide the best result compared to that of the QCISD(T)/aug-cc-pVTZ level,[32] with a difference only of about 0.50 kcal/mol. BP86-D gives a slight overestimation of interaction energy, and PBE-D and M06-2X, and especially M05-2X, give a noticeable underestimation.

For the corannulene dimer the most stable structure is the eclipsed one.[32] For that reason, we might think that the poor result of M06-2X functional was based on the bad behavior (which was showed in the previous section) of this functional for eclipsed complexes. However, this is not probable since the behavior of M06-2X functional is very similar for curved complexes without eclipsed bonds, as corannulene···sumanene and sumanene···corannulene.

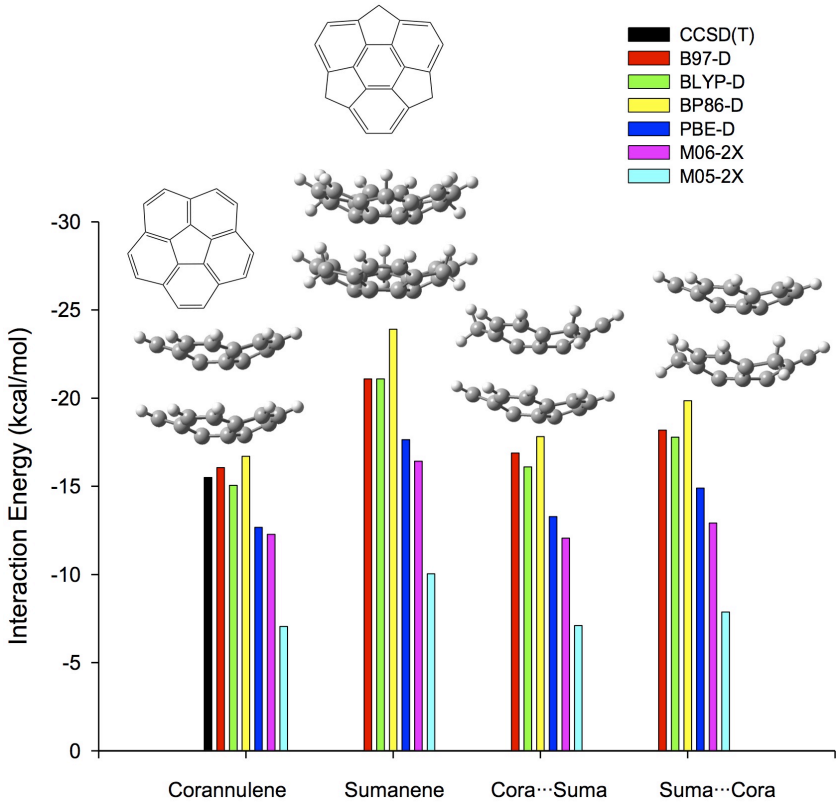


Figure 5.4: Interactions energies of complexes with curved complexes.

Recently, a theoretical investigation of the stacking interaction between three buckybowls (corannulene, sumanene, and pentaindenocorannulene) with fullerenes C_{60} and C_{70} has been reported.[38] The study was performed at the M06-2X/6-311G level and BSSE corrections were not included. However, probably these results are acceptable due an error cancellation by using a small basis set and not including BSSE corrections. An evidence for this cancellation error is the fact that the best interaction energy for the corannulene dimer was obtained using the M06-2X with the very small 6-31G basis set: 15.1 kcal/mol. This value becomes 17.8 kcal/mol by increasing the basis set to 6-311G. In its work Denis says: 'Thus, for very large systems the not inclusion of BSSE and use the 6-31G basis set is a good compromise between accuracy and computational cost'. Maybe this assertion could be true, but working under the support of error cancellation is a risk that must be avoided, whenever possible. In fact, the results of the present work suggest that energy underestimation of M06-2X is not due to the BSSE correction. It is due to the weakness of M06-2X for studying sandwich complexes with planar eclipsed monomers and complexes with curved monomers; on the contrary it works very well for complexes with displaced planar monomers, as S22 complexes evaluated in this work. Therefore, disregarding of the BSSE correction for these complexes may lead to unreliable interaction energies.

For the other curved complexes the trends are fully comparable to that for corannulene dimer: B97-D and BLYP-D give rise to very similar interaction energies, and

assuming that these were good values, BP86-D give a slight overestimation, PBE-D and M06-2X give a noticeable underestimation, and M05-2X gives a huge underestimation.

The study of the stacking between different buckybowls can produce important advances in host-guest chemistry of fullerene. As can be seen in Table 5.1, the sumanene dimer shows an increase of about 5 kcal/mol in the value of interaction energy compared with that of corannulene dimer at the B97-D/cc-pVTZ level of calculation. The CH···π interactions in sumanene dimer are largely responsible for this increase.[38] On the other hand, replacement of the corannulene monomer for sumanene monomer give rise to higher interaction energy compared with that of corannulene dimer for both cases: in the concave and in the convex side; however, the sumanene in the concave side is slightly preferred.

Finally, regarding equilibrium distances (Table 5.2), not very noticeable differences are found between functionals: only a slight shortening of the BP86-D values and a slight lengthening of the M05-2X ones; *i.e.* exactly the same behavior that observed in the previous section of planar complexes.

Table 5.2: Equilibrium distances (Å) for the studied complexes. All optimizations were performed using the cc-pVTZ basis set. Reference CCSD(T) and QCISD(T) distances are given for comparison (Ref)

Complex (symmetry)	Ref	B97-D	B-LYP-D	BP86-D	PBE-D	M06-2X	M05-2X
			Planar complexes				
Benzene dimer (D_{6h})	3.80[a], 3.90[b]	3.90	3.85	3.77	3.87	3.78	3.88
Naphthalene dimer (D_{2h})	3.80[c]	3.77	3.72	3.66	3.78	3.73	3.92
Anthracene dimer (D_{2h})		3.73	3.69	3.61	3.75	3.71	3.91
Pyrene dimer (D_{2h})		3.69	3.68	3.57	3.72	3.70	3.90
Coronene dimer (D_{6h})	3.69[d]	3.64	3.58	3.52	3.68	3.67	3.74
			Curved complexes				
Corannulene···corannulene (C_{5v})	3.69[e]	3.62	3.62	3.51	3.63	3.62	3.80
Sumanene···sumanene (C_{3v})		3.62	3.60	3.49	3.63	3.69	3.83
Corannulene···sumanene (C_s)		3.63	3.62	3.52	3.67	3.66	3.82
Sumanene···corannulene (C_s)		3.70	3.66	3.55	3.72	3.73	3.91
			Curved and planar complexes				
Coronene···corannulene (C_s)		3.25	3.24	3.16	3.25	3.35	3.47
Coronene···sumanene (C_{3v})		3.18	3.16	3.07	3.18	3.20	3.28

[a]Tsuzuki *et al.* (Ref. 52).

[b]Sinnkrot *et al.* (Ref. 4).

[c]Tsuzuki *et al*. (Ref. 53).

[d]Janowski *et al.* (Ref. 54).

[e]Janowski *et al.* (Ref. 32).

5.3.4. Mixed Complexes

Finally, we have studied two cases presenting an interaction between a planar compound (coronene) and a curved one (corannulene and sumanene), although for both cases no reference value is available (Table 5.1, Figure 5.5). The performance of functionals is a kind of intermediate case between the two groups above, as it would be expected. So, B97-D and BP86-D give very similar results, since for planar complexes B97-D gives the highest values of interaction energy, and for curved complexes BP86-D gives the highest values. BLYP-D gives values slightly lower than the two previous functionals, and PBE-D, M06-2X and M05-2X, give rise to a small, medium and large, respectively, underestimation of interaction energy, just as in the previous two groups (planar and curved).

It is worth noting that coronene···corannulene complex shows an increase of about 1 kcal/mol in the interaction energy compared with that of the corannulene dimer at the B97-D/cc-pVTZ level. So, surprisingly, the ability of planar coronene to 'catch' curved compounds is better than expected. The increase in the interaction energy could be due to monomer displacement, not observed for corannulene dimer. The displacement of corannulene monomer contributes for an increase of contact between carbon atoms of the monomers, increasing the dispersion interaction (Figure 5.5, top view).

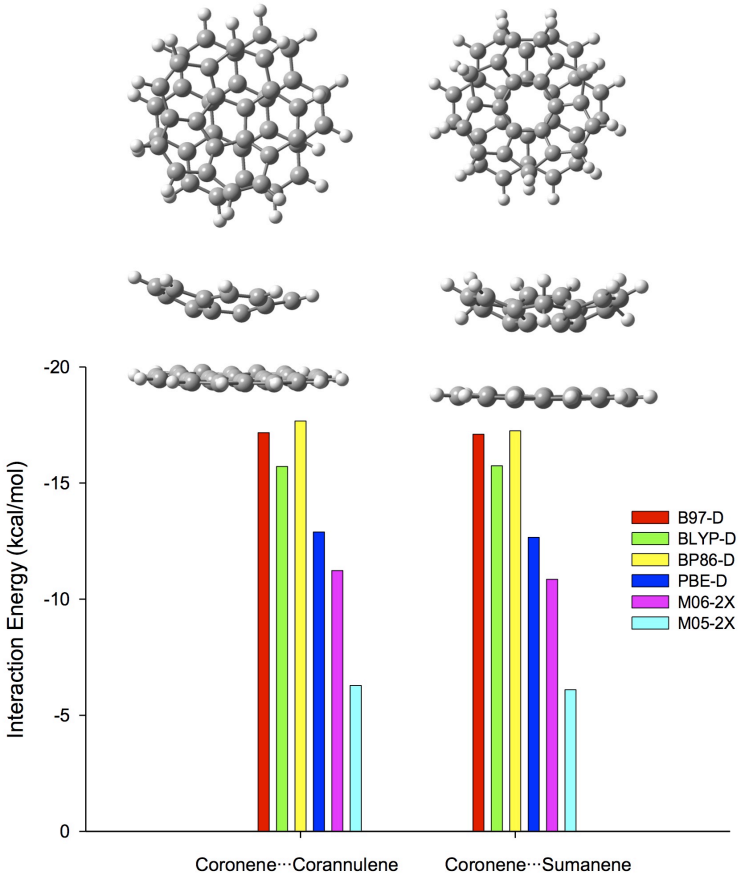


Figure 5.5: Interactions energies of the mixed complexes (top and side view).

On the other hand, the coronene···sumanene complex shows an interaction energy very similar to that obtained for coronene···corannulene complex. In this case the sumanene monomer does not show any displacement, but it rotates to reach a fully staggered conformation between monomers (Figure 5.5, top view).

Finally, regarding equilibrium distances (Table 5.2), the same behavior that observed in the two previous sections is found again: only a slight shortening of the BP86-D values and a slight lengthening of the M05-2X ones.

5.4. *Conclusions*

The performance of B97-D, B-LYP-D, BP86-D, PBE-D, M05-2X and M06-2X functionals was evaluated on four representative groups of complexes with π···π interactions. According to the results, the next conclusions can be inferred.

M05-2X should be completely avoided: it give rise to an underestimation of the interaction energy, going from important for planar complexes with non-eclipsed monomers, to very serious for the rest of cases.

A second group of functionals comprises the M06-2X and PBE-D functionals. These two functionals only work well for planar complexes with non-eclipsed monomers, but give rise to a substantial underestimation of the interaction energy for the rest of cases. Among them, PBE-D is slightly better, especially for planar complexes with eclipsed monomers.

The best performance corresponds to the B97-D, BLYP-D and BP86-D functionals. These three functionals, especially the first two, give rise to acceptable interaction energies for all kind of complexes with π···π interactions. Reviewing the results in a more detailed manner, we could conclude that the best choice would be the B97-D functional, since BLYP-D slightly underestimates interaction energies for some cases, and BP86-D also slightly underestimates interaction energies for some cases and slightly overestimates interaction energies for curved complexes.

Regarding equilibrium distances, we clearly can conclude that all methods work acceptably well; only BP86-D distances slightly shortened and M05-2X distances slightly lengthened are found.

From the overall results, we can establish the clear advantage of the DFT-D functionals compared with the M0(5-6)-2X ones for studying complexes with π···π interactions. The reason of the systematic underbinding of the Truhlar functionals is that they do not actually include the correct C_6/R^6 dispersion term, but were parameterized to mimic short- and intermediate dispersion effects. The interaction potential provided by these functionals decay too fast and thus misses the asymptotically correct behavior; so, for large complexes, the long-range dispersion attraction is almost missing for distant atoms, which add up to a significant fraction of the overall binding.

Also, the results of this work clearly show that curved complexes should not be treated only as general complexes with predominant dispersion contribution. They have unique properties that must be taken into account in the study, and show a different behavior that occurs usually with standard PAHs.

We hope that results of this work help to get a significant progress on the study of curved complexes and on the development of new benchmarks and methods for curved complexes.

5.5. References

1. K. Tiefenbacher and J. Rebek, Jr., *J. Am. Chem.Soc.*, 2012, **134**, 2914-2917.
2. V. Spiwok, P. Hobza and J. Řezáč, *J. Phys. Chem. C*, 2011, **115**, 19455-19462.
3. A. Sygula, F. R. Fronczek, R. Sygula, P. W. Rabideau and M. M. Olmstead, *J. Am. Chem. Soc.*, 2007, **129**, 3842-3843.
4. M. O. Sinnokrot and C. D. Sherrill, *J. Phys. Chem. A*, 2006, **110**, 10656-10668.
5. C. A. Hunter and J. K. M. Sanders, *J. Am. Chem. Soc.*, 1990, **112**, 5525-5534.
6. J. Cerny and P. Hobza, *Phys. Chem. Chem. Phys.*, 2007, **9**, 5291-5303.
7. K. E. Riley and P. Hobza, *WIREs: Comput. Mol. Sci.*, 2011, **1**, 3-17.
8. S. Tsuzuki, T. Uchimaru, K. Matsumura, M. Mikami and K. Tanabe, *Chem. Phys. Lett.*, 2000, **319**, 547–554.
9. P. Hobza, H. L. Selzle and E. W. Schlag, *J. Phys. Chem.*, 1996, **100**, 18790-18794.
10. E. M. Cabaleiro Lago, J. Rodríguez Otero and A. Peña-Gallego, *J. Chem. Phys.*, 2008, **129**, 084305/1-084305/8.
11. E. M. Cabaleiro Lago, J. Rodríguez Otero and A. Peña-Gallego, *J. Phys. Chem. A*, 2008, **112**, 6344–6350.
12. E. M. Cabaleiro-Lago, A. Peña-Gallego and J. Rodríguez-Otero, *J. Chem. Phys.*, 2008, **128**, 194311/1-194311/8.
13. E. M. Cabaleiro Lago, J. Rodríguez Otero and A. Peña-Gallego, *J. Chem. Phys.*, 2011, **135**, 134310/1-134310/8.
14. E. M. Cabaleiro Lago, J. Rodríguez Otero and A. Peña-Gallego, *Theor. Chem. Acc.*, 2011, **128**, 531–539.
15. Y. Zhao, N. E. Schultz and D. G. Truhlar, *J. Chem. Phys.*, 2005, **123**, 161103/1-161103/4.
16. Y. Zhao and D. G. Truhlar, *Theor. Chem. Acc.*, 2008, **120**, 215-241.
17. S. Grimme, *J. Comput. Chem.*, 2004, **25**, 1463-1473.
18. S. Grimme, J. Antony, T. Schwabe and C. Mück-Lichtenfeld, *Org. Biomol. Chem.*, 2007, **5**, 741-758.
19. A. D. Becke and E. R. Johnson, *J. Chem. Phys.*, 2007, **127**, 154108/1-154108/6.
20. S. N. Steinmann and C. Corminboeuf, *J. Chem. Phys.*, 2011, **134**, 044117/1-044117/5.
21. A. Tkatchenko and M. Scheffler, *Phys. Rev. Lett.*, 2009, **102**, 073005/1-073005/4.
22. A. Krishtal, K. Vanommeslaeghe, A. Olasz, T. Veszpremi, C. Van Alsenoy and P. Geerlings, *J. Chem. Phys.*, 2009, **130**, 174101/1-174101/8.
23. T. Sato and H. Nakai, *J. Chem. Phys.*, 2010, **133**, 194101/1-194101/9.

24. P. Jurecka, J. Sponer, J. Cerny and P. Hobza, *Phys. Chem. Chem. Phys.*, 2006, **8**, 1985-1993.
25. Y. Zhao and D. G. Truhlar, *J. Phys. Chem. C*, 2008, **112**, 4061-4067.
26. R. A. Distasio Jr and M. Head-Gordon, *Mol. Phys.*, 2007, **105**, 1073-1083.
27. T. Schwabe and S. Grimme, *Phys. Chem. Chem. Phys.*, 2007, **9**, 3397-3406.
28. S. Grimme, J. Antony, S. Ehrlich and H. Krieg, *J. Chem. Phys.*, 2010, **132**, 154104/1-154104/19.
29. Y. Zhao and D. G. Truhlar, *J. Chem. Theory Comput.*, 2007, **3**, 289-300.
30. A. Sygula and S. Saebø, *Int. J. Quantum Chem.*, 2009, **109**, 65-72.
31. D. Josa, J. Rodríguez Otero and E. M. Cabaleiro Lago, *Phys. Chem. Chem. Phys.*, 2011, **13**, 21139-21145.
32. T. Janowski, P. Pulay, A. A. Sasith Karunarathna, A. Sygula and S. Saebø, *Chem. Phys. Lett.*, 2011, **512**, 155-160.
33. S. Grimme, C. Mück-Lichtenfeld and J. Antony, *J. Phys. Chem. C*, 2007, **111**, 11199-11207.
34. C. Mück-Lichtenfeld, S. Grimme, L. Kobryn and A. Sygula, *Phys. Chem. Chem. Phys.*, 2010, **12**, 7091-7097.
35. G. Casella and G. Saielli, *New J. Chem.*, 2011, **35**, 1453-1459.
36. B. M. Wong, *J. Comput. Chem.*, 2009, **30**, 51-56.
37. Y. Zhao and D. G. Truhlar, *Phys. Chem. Chem. Phys.*, 2008, **10**, 2813-2818.
38. P. A. Denis, *Chem. Phys. Lett.*, 2011, **516**, 82-87.
39. S. Grimme, *J. Comput. Chem.*, 2006, **27**, 1787-1799.
40. A. D. Becke, *Phys. Rev. A* 1988, **38**, 3098-3100.
41. B. Miehlich, A. Savin, H. Stoll and H. Preuss, *Chem. Phys. Lett.*, 1989, **157**, 200-206.
42. J. P. Perdew, *Phys. Rev. B.*, 1986, **33**, 8822-8824.
43. J. P. Perdew, K. Burke and M. Ernzerhof, *Phys. Rev. Lett.*, 1997, **78**, 1396.
44. Y. Zhao, N. E. Schultz and D. G. Truhlar, *J. Chem. Theory Comput.*, 2006, **2**, 364-382.
45. R. Ahlrichs, M. Bär, M. Häser, H. Horn and C. Kölmel, *Chem. Phys. Lett.*, 1989, **162**, 165-169.
46. M. J. Frisch *et al*., GAUSSIAN 09 (Revision A.02), Gaussian, Inc., Wallingford CT, 2009.
47. J. Rezac, K. E. Riley and P. Hobza, *J. Chem. Theory Comput.*, 2011, **7**, 2427-2438.
48. T. Takatani, E. G. Hohenstein, M. Malagoli, M. S. Marshall and C. D. Sherrill, *J. Chem. Phys.*, 2010, **132**, 144104/1-144104/5.
49. R. Podeszwa, K. Patkowski and K. Szalewicz, *Phys. Chem. Chem. Phys.*, 2010, **12**, 5974-5979.
50. R. Podeszwa, *J. Chem. Phys.*, 2010, **132**, 044704/1-044704/8.
51. M. Rapacioli, F. Spiegelman, D. Talbi, T. Mineva, A. Goursot, T. Heine and G. Seifert, *J. Chem. Phys.*, 2009, **130**, 244304/1-244304/10.
52. S. Tsuzuki, K. Honda, T. Uchimaru, M. Mikami and K. Tanabe, *J. Am. Chem. Soc.*, 2002, **124**, 104-112.
53. S. Tsuzuki, K. Honda, T. Uchimaru and M. Mikami, *J.Chem. Phys.*, 2004, **120**, 647-659.
54. T. Janowski, A. R. Ford and P. Pulay, *Mol. Phys.*, 2010, **108**, 249-257.

Chapter 6

Substituted corannulenes and sumanenes as fullerene receptors

6.1. Introduction:

The search for molecular receptors for fullerenes has been a very attractive field of research in recent years.[1] Several compounds have been explored with the goal of finding more effective and selective fullerene receptors.[2-8] A promising strategy to design new molecular receptors for fullerenes is using concave-convex complementarity. In this context, the curved polynuclear aromatic hydrocarbons, also known as buckybowls or fullerene fragments, seem to be ideal candidates because the concave surface of a buckybowl can fit adequately to the convex surface of fullerenes by concave-convex 'ball-and-socket' interactions.[4]

The interaction between substituted buckybowls and fullerenes was reported in 2005 by Georghiou *et al.* for complexes between penta- and decasubstituted corannulenes with C_{60} in toluene solution.[9] Despite the promising results, the experiments did not prove the existence of strong π···π interactions between corannulenes and fullerenes. The association constants obtained were relatively small and highly dependent on substituents, so it could be argued that the true interaction that bound the complex was that taking place between the fullerene and the edge substituents of corannulene and not the π···π interaction between corannulene and fullerene.

Fortunately, two years later, Sygula *et al*. synthesized the molecular tweezers (a buckycatcher, $C_{60}H_{28}$) made up by two units of corannulene that can trap one fullerene and they confirmed that the strength of the interaction comes indeed from pure concave-convex π···π interactions between convex faces of fullerene and concave faces of the two subunits of suitably oriented corannulene.[4] Thenceforth, predicting how to modify this buckycatcher to improve their efficiency and selectivity has become a subject of great interest.

Undoubtedly, the success in designing efficient systems requires deep knowledge of the characteristics of the π···π interactions. However, an accurate

description of π···π interactions is a challenging task for quantum chemistry methods in general.[10-12]

Although the development of new types of functionals[13, 14] and DFT-D methods[15, 16] taking into account the dispersion contribution allows the theoretical estimation of the interaction energy for the molecular tweezers designed by Sygula *et al.*,[4] a huge range in the estimates (from -21 to -43 kcal/mol) were obtained depending on the DFT model used.[17-19]

Recently, a detailed evaluation of the performance of DFT-D, M05-2X, and M06-2X functionals for studying π···π interactions was performed.[12] On the other hand, Janowski *et al.* have performed a benchmark study for corannulene dimers taking the QCISD(T)/aug-cc-pVTZ level as reference.[20] Both studies show that B97-D2 seems a good approach for studies of concave-convex π···π interactions. In addition, together with the resolution of identity (RI) approximation,[21] this approach enables excellent results with a noticeably small computational cost. Moreover, recently, for the corannulene dimer, Kennedy *et al*.[22] showed that the best results (compared with the benchmark performed at the QCISD(T)/aug-cc-pVTZ level)[20] correspond to B3LYP-D3(BJ), but with a very small advantage over B3LYP-D2, M06-2X, and B97-D2. Of these DFT methods, B97-D2 is the best to take advantage of the noticeable reduction of computational cost that allows the resolution of identity approximation, since for non-hybrid functionals the RI procedure speeds up calculations by a factor of 10 at least (as compared to conventional treatments) without sacrificing accuracy.

Recently, a DFT-D evaluation of the effect of substituents on the concave-convex π···π interaction that takes place between penta-substituted corannulenes (with Br, Cl, CH_3, C_2H, and CN) and fullerene, was performed by our research group.[23] For that purpose, C_{60}-like, a 'fullerene copy' of C_{60}, was used instead of the real buckminsterfullerene, C_{60}, in order to save computation resources. However, the above-mentioned success of the B97-D2 (plus RI) level allows carrying out a comprehensive study of the effects of substituents, using the whole structure of C_{60}. Moreover, the interaction with different faces of C_{60} is taken into account and the complete analysis is extended, including the fullerene C_{70}. In addition, a comprehensive study is carried out for the interaction between hexa-substituted sumanenes and fullerene, for both C_{60} and C_{70}.

6.2. *Computational details*

All complexes evaluated were fully optimized at the B97-D2/TZVP level using the resolution of identity approximation (RI) implemented in the Turbomole 5.10 program suite.[24]

Counterpoise corrections (CP) were applied to all reported interaction energies to avoid basis set superposition error (BSSE).[25] According to this method, the interaction energy of a system AB (buckybowl···fullerene in our case) is calculated according to

$$\Delta E_{int} = E_{AB}^{AB}(AB) - \left(E_{A}^{AB}(AB) + E_{B}^{AB}(AB)\right) \quad (6.1)$$

where superscript refers to the geometry (that of the system AB) and the parentheses indicates the basis set used. So, $E_{A}^{AB}(AB)$ is the energy of monomer A (buckybowl or fullerene) calculated using its geometry in the system AB and the full basis set of the system AB. CP correction was applied to only the optimized geometries of the complexes.

6.3. *Results and discussion*

A series of complexes made up by substituted buckybowls (corannulene and sumanene) with fullerenes (C_{60} and C_{70}) were evaluated at the B97-D2/TZVP level. Stacking interactions using both corannulene and sumanene faces of fullerenes were taken into account in this work in order to obtain the more favorable face of fullerenes for interacting with buckybowls. In Figure 6.1 the concepts *cora face* and *suma face* of fullerenes are defined. All complexes were constructed by aligning the central ring of the buckybowl with the central ring of corannulene or sumanene face of fullerenes given in Figure 6.1. The distance between the centers of these two rings is named d_{eq}.

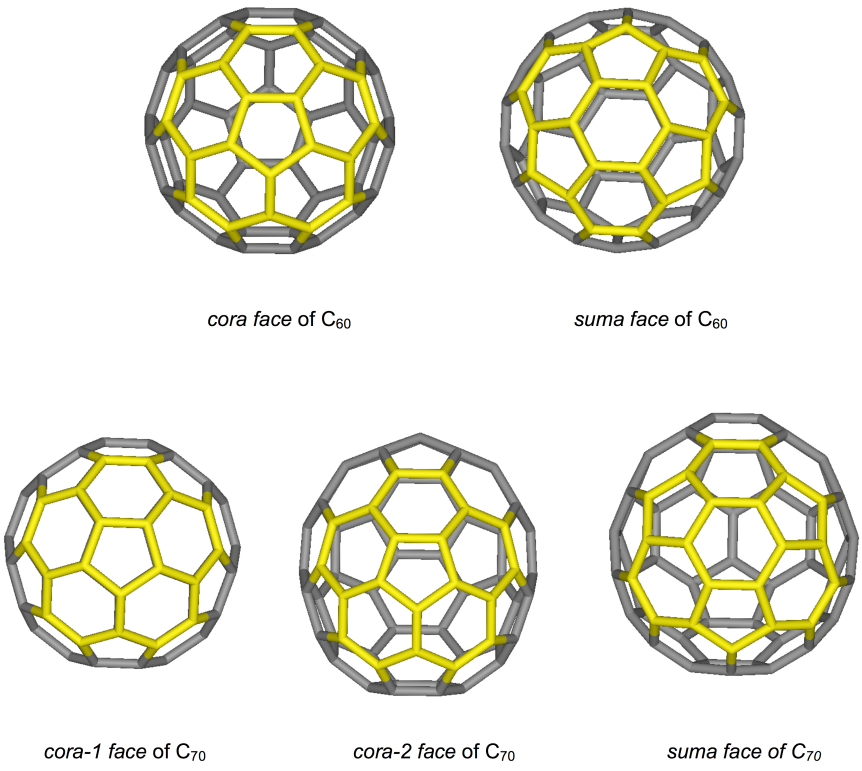


Figure 6.1: Faces of the fullerenes used to study the stacking interactions with buckybowls.

6.3.1. Unsubstituted complexes

As can be seen in Table 6.1, the larger interaction is related with the participation of sumanene structure. Thus, the largest interaction energy corresponds to the complex sumanene···$C_{60/70}$ (with the *suma face*) which amounts -20.40/-20.49 kcal/mol. Oppositely, the smallest interaction energy corresponds to the complex corannulene···$C_{60/70}$ (with the *cora face*) which amounts -17.03/-17.16 kcal/mol. Anyway, the participation of the sumanene structure is clearly more critical for the buckybowl than for the fullerene face chosen to form the complex. These results are similar to those obtained for complexes between corannulene and sumanene.[12] As reported previously by Denis,[26] sumanene shows three CH_2 groups (absent in corannulene) that can interact through CH···π interactions with fullerenes. So, CH···π interactions are of great importance for the better catching ability of sumanene compared to corannulene.

From Table 6.1 it is clear that interaction energies for C_{60} are very similar to those for C_{70}; only a very slight difference favors C_{70}. Therefore, unfortunately, it is not expected that the buckycatcher binds very specifically to one of the fullerenes when exposed to the C_{60}/C_{70} mixture.

6.3.2. Substituted complexes

Nowadays, predicting how to modify the traditional buckycatchers to improve their efficiency and selectivity is studied with great interest. Modification of tweezers by a different functionalization of buckybowls, which constitute the main part of tweezers, could improve their efficiency and selectivity. In this context, substituents may exert a modulatory effect and enable a better concave-convex interaction with fullerenes.

Recently, substituent effects on the concave-convex interaction between corannulene and C_{60} were studied by our research group (using C_{60}-like, a 'fullerene copy' to imitate C_{60}).[23] The results showed that introduction of substituents with different acceptor-donor character in the structure of buckybowls can substantially change the interaction. Thus, corannulenes substituted with five Br, Cl, CH_3, C_2H, and CN units behave as better buckycatchers than the unsubstituted corannulene. C_{60}-like proposed by Sygula *et al*.[27] provide a considerable computational cost reduction; however, according to Table 6.1, it seems clear that results obtained with this procedure (in parentheses in Table 6.1) are somewhat poor when compared with those using the whole C_{60} structure. Thus, not only absolute differences appear but also relative differences are remarkable. So, for instance, substitution with CH_3 is the most favorable when full C_{60} is used, whereas substitution with CN is the most favorable when C_{60}-like is used. So, C_{60}-like does not seem representative for imitating the concave-convex interaction between substituted corannulene and C_{60}. Therefore, a supplementary work using the whole C_{60} is very advisable. In the present work the study is fully completed as follows. First, not only the *cora face* of C_{60} is taken into account, but also the *suma face* is analyzed. Second, not only corannulene is studied, but also sumanene is used as a buckycatcher of fullerene. Finally, not only fullerene C_{60} is included, but also an almost parallel study for C_{70} is carried out.

Table 6.1: Interaction energies, E_{Int} (kcal/mol), and equilibrium distances, d_{eq} (Å), for complexes between buckybowls and fullerenes. All calculations were performed at the B97-D2/TZVP level. Calculations at the B97-D2/6-31+G* level using C_{60}-like[23] are given in parentheses for comparison

	X=C_{60}				X=C_{70}			
	cora face of C_{60}		*suma face* of C_{60}		*cora face* of C_{70}[a]		*suma face* of C_{70}	
	E_{Int}	d_{eq}	E_{Int}	d_{eq}	E_{Int}	d_{eq}	E_{Int}	d_{eq}
Corannulene···X	-17.03 (-14.16)	3.456 (3.51)	-17.26	3.563	-17.16 [-18.00]	3.447 [3.453]	-17.33	3.574
Corannulene-5Br···X	-23.06 (-20.44)	3.399 (3.45)	-22.90	3.523	-23.04	3.385		
Corannulene-5Cl···X	-20.60 (-18.56)	3.414 (3.47)	-20.49	3.534	-20.58	3.408		
Corannulene-5CH_3···X	-23.82 (-19.23)	3.394 (3.44)	-23.90	3.512	-23.87	3.378		
Corannulene-5C_2H···X	-22.31 (-18.06)	3.426 (3.47)	-22.17	3.554	-22.20	3.410		
Corannulene-5CN···X	-22.28 (-23.35)	3.442 (3.43)	-21.91	3.593	-22.10	3.434		
Sumanene···X	-18.47	3.502	-20.40	3.450	-18.57 [-19.53]	3.494 [3.489]	-20.49	3.453
Sumanene-6Br···X	-25.40	3.528	-26.50	3.507			-27.03	3.496
Sumanene-6Cl···X	-22.34	3.532	-23.40	3.512			-23.78	3.505
Sumanene-6CH_3···X	-26.43	3.511	-27.61	3.459			-28.10	3.446
Sumanene-6C_2H···X	-24.67	3.534	-25.88	3.510			-26.51	3.508
Sumanene-6CN···X	-25.51	3.521	-26.36	3.537			-27.02	3.511

[a]With cora-1 face and cora-2 (in square brackets).

In order to analyze the effect of substitution, corannulene and sumanene monomers were substituted with five and six Br, Cl, CH_3, C_2H, or CN units, respectively. Figure 6.2 shows one of the complexes investigated, and Table 6.1 summarizes interaction energies and equilibrium distances obtained. In order to save time and avoid a superfluous accumulation of data (since trends seem sufficiently clear), a full analysis of buckybowl substitution for the interaction with C_{70} is not performed; only the interaction of corannulenes with the *cora face* and the interaction of sumanene with the *suma face* are considered, *i.e*, only stacking interactions using a face of C_{70} equivalent to the buckybowl are evaluated. As stated above, very similar results are obtained for complexes with fullerenes C_{60} and C_{70}; therefore, an exhaustive study for C_{70} seems unnecessary. In the case of corannulene···C_{70} (*cora face*) only the *cora-1 face* is chosen, since this case leads to complexes with symmetry higher than the case of the *cora-2 face*, providing a considerable reduction of the computational cost.

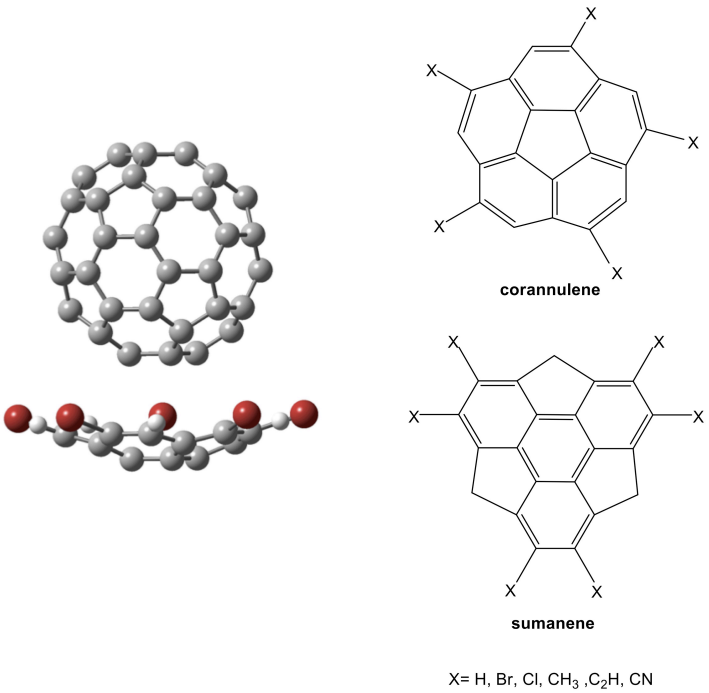


Figure 6.2: Structure of complex corannulene-5Br···C_{60} (cora face of C_{60}) (left panel). Substituted corannulene and sumanene studied (right panel).

According to values of Table 6.1, the ranking of buckybowls relative to the added substituents is CH_3 > Br > C_2H ≈ CN >> Cl >> H for all the corannulene···fullerene complexes. This ranking is rather different than that obtained previously using C_{60}-like:[23] CN >> Br > CH_3 > Cl > C_2H >> H.

When sumanene···fullerene complexes are considered, the ranking is mainly the same and suffers only a slight modification: CH_3 > Br ≈ CN > C_2H >> Cl >> H; that is to say, basically substitution with CN is strengthened and moves up, relative to corannulene complexes.

Sumanene substituted with six CH_3 groups is the best fullerene receptor (E_{int} = -28.10 kcal/mol), with an increase greater than 11 kcal/mol relative to the unsubstituted corannulene (about a 65% of increase of 'fullerene catching' ability). Almost certainly, the ability of sumanene-6CH_3 is directly related to the important role of CH···π interactions in this kind of complex.

As can be seen in Table 6.1, although there is a substantial increase in the interaction energy of complexes when different substituents are placed in corannulene and sumanene monomers, only very small differences in the equilibrium distance are found. For complexes with corannulene, in general, the introduction of substituents gives a slight decrease in the equilibrium distance values, with a vague trend in which an increase of interaction energy corresponds to a shortening of d_{eq} (with complexes with corannulene-5CN being the most notorious exception to this trend). For complexes with sumanene, differences in equilibrium distances are even more insignificant and exhibit a trend that is even more unclear.

As a way of checking the changes introduced in the bowls by the substituents, Table 6.2 lists the values of two important geometric parameters. *R* is the interplanar distance between the planes formed by *hub* and *rim* atoms of the buckybowl; it represents the bowl depth. POAV is the pyramidalization angle (π-orbital axis vector) as proposed by Haddon.[28] The POAV angle allows the description of local curvature of a conjugated system and is defined as the angle between the C–C bond and the vector perpendicular to the pyramidal base of three idealized C–C bonds. The greater depth of the bowl (greater *R*) is usually related to the greater curvature of carbons of the *hub* (greater POAV). According to results shown in Table 6.2, it is clear that substituents give rise to very small changes in the curvature of corannulene and sumanene bowls: no noteworthy difference relative to the unsubstituted buckybowl is found. So, there was not a clear relationship between the curvature of bowl and the changes in the interaction energy generated by addition of substituents in the bowl.

In order to analyze in more detail the balance of energy contributions to the stability of the complexes, the interaction energy was decomposed according to a simple method. So, the two contributions of the model employed were taken into account, that is, the pure B97 interaction energy and the empirical dispersion contribution to the interaction energy. Results in Table 6.3 show that dispersion plays a crucial role in the interaction energy of complexes. First, because the contribution of the pure B97 functional is clearly repulsive, so dispersion is responsible for the binding in the complexes. Second, and more noteworthy, because the ranking of interaction energies is directly related to the ranking of dispersion contributions. This fact is absolutely true for corannulene complexes and mainly true for sumanene complexes, with both C_{60} and C_{70}. It is worth noting that, regarding dispersion contributions, corannulene complexes behave exactly the same as sumanene complexes. The relationship between the dispersive contribution and the interaction energy can be clearly visualized in Figure 6.3, which includes all the complexes of Table 6.3 and shows a good correlation. Only in the cases of complexes with buckybowl-5(6)CN (hexagons in Figure 6.3), does a very slight deviation appear; interaction energies larger than those corresponding to their dispersion contributions are obtained.

Table 6.2: Geometric parameter *R* (in Å), and POAV angles at the *hub* position (degrees) of buckybowls obtained at the B97-D2/TZVP level. When different values of POAV are found, they are indicated

	X=C_{60}				X=C_{70}			
	cora face of C_{60}		*suma face* of C_{60}		*cora-1 face* of C_{70}		*suma face* of C_{70}	
	R	POAV	*R*	POAV	*R*	POAV	*R*	POAV
Corannulene···X	0.902	8.38	0.894	8.28, 8.31, 8.34	0.909	8.42		
Corannulene-5Br···X	0.882	8.26	0.871	8.11, 8.18, 8.19, 8.21	0.878	8.22		
Corannulene-5Cl···X	0.881	8.25	0.873	8.12, 8.17, 8.21	0.888	8.30		
Corannulene-5CH_3···X	0.914	8.51	0.904	8.36, 8.41, 8.42, 8.45, 8.48	0.915	8.51		
Corannulene-5C_2H···X	0.921	8.52	0.906	8.33, 8.42, 8.43, 8.44	0.910	8.44		
Corannulene-5CN···X	0.924	8.55	0.911	8.34, 8.46, 8.47, 8.49, 8.51	0.916	8.51		
Sumanene···X	1.093	8.42, 8.57, 8.64	1.067	8.43			1.076	8.46, 8.49, 8.51
Sumanene-6Br···X	1.096	8.63, 8.71	1.058	8.50			1.061	8.50, 8.52, 8.53
Sumanene-6Cl···X	1.098	8.61, 8.69, 8.70	1.063	8.49			1.065	8.50, 8.52
Sumanene-6CH_3···X	1.115	8.59, 8.74, 8.77	1.091	8.59			1.091	8.60, 8.61
Sumanene-6C_2H···X	1.138	8.79, 8.84	1.104	8.68			1.108	8.68, 8.70
Sumanene-6CN···X	1.126	8.75, 8.76, 8.79	1.101	8.68			1.102	8.66, 8.68, 8.70

Table 6.3: B97 interaction energy and dispersion contribution for complexes obtained at the B97-D2/TZVP level (kcal/mol)

	X=C_{60}				X=C_{70}			
	cora face of C_{60}		*suma face* of C_{60}		*cora-1 face* of C_{70}		*suma face* of C_{70}	
	B97	Dispersion	B97	Dispersion	B97	Dispersion	B97	Dispersion
Corannulene···X	16.17	-33.20	16.43	-33.69	16.21	-33.37		
Corannulene-5Br···X	21.07	-44.13	20.77	-43.67	21.10	-44.14		
Corannulene-5Cl···X	19.36	-39.96	19.12	-39.61	19.53	-40.11		
Corannulene-5CH_3···X	21.39	-45.21	21.44	-45.34	21.78	-45.65		
Corannulene-5C_2H···X	20.10	-42.41	19.71	-41.88	19.83	-42.03		
Corannulene-5CN···X	18.60	-40.88	18.33	-40.24	18.24	-40.34		
Sumanene···X	19.17	-37.64	20.47	-40.87			20.65	-41.14
Sumanene-6Br···X	23.66	-49.06	25.69	-52.19			26.22	-53.25
Sumanene-6Cl···X	21.70	-44.04	23.97	-47.37			24.23	-48.01
Sumanene-6CH_3···X	25.93	-52.36	26.94	-54.55			27.67	-55.77
Sumanene-6C_2H···X	22.98	-47.65	25.30	-51.18			25.30	-51.81
Sumanene-6CN···X	20.79	-46.30	22.16	-48.52			23.13	-50.15

Table 6.3 shows that these enhanced interaction energies are due to the small repulsion of the pure B97 functional (the least repulsive of the substituted corannulenes). Thus, if complexes with CN substitutions are not taken into account, the correlation is even better, R^2 going from 0.95 to 0.98 (see section A.1, Appendix A).

The partition of the interaction energy in two components (functional plus dispersion) could be questionable because B97-D was constructed as a whole, optimizing the functional form in the presence of a dispersion correction. However, this fact does not necessarily imply that the two components are unbalanced. In order to check that the partition used is appropriate and that it can lead to fully valid results, several single point calculations at the B3LYP-D3(BJ)/TZVP//B97-D2/TZVP level were carried out (see section A.2, Appendix A). The conclusions are the same as those obtained with B97-D2.

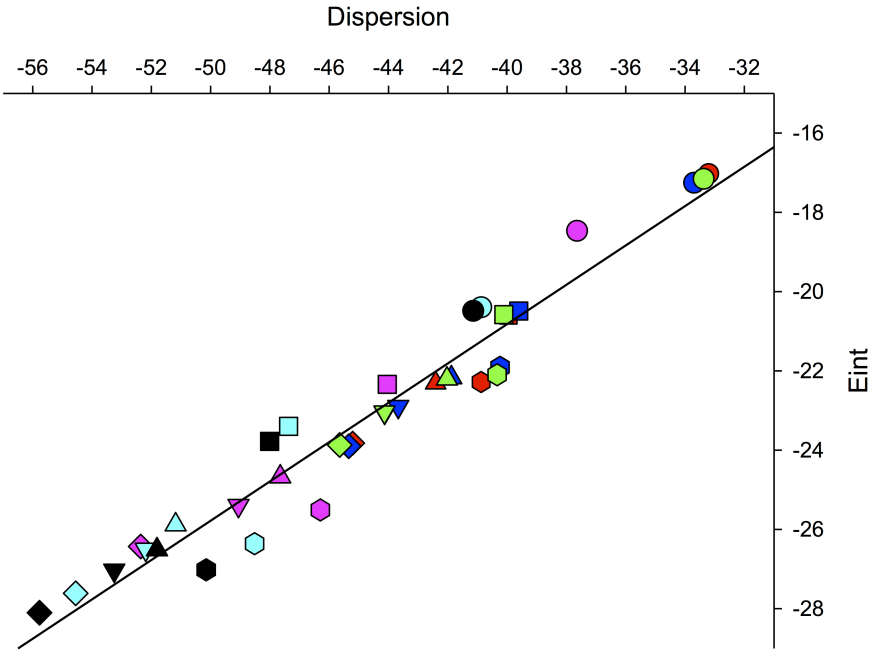


Figure 6.3: Dispersion contribution *vs.* interaction energy (in kcal/mol). Corannulene···C_{60} (*cora face*): red. Corannulene···C_{60} (*suma face*): dark blue. Corannulene···C_{70} (*cora-1 face*): green. Sumanene···C_{60} (*cora face*): pink. Sumanene···C_{60} (*suma face*): light blue. Sumanene···C_{70} (suma face): black. Buckybowl (corannulene or sumanene): circle. Buckybowl-5Br: triangle down. Buckybowl-5Cl: square. Buckybowl-5CH_3: diamond. Buckybowl-5C_2H: triangle up. Buckybowl-5CN: hexagon. E_{int} = 0.4960Disp – 0.9773, R^2 = 0.95.

As commented above, the buckycatcher ranking previously obtained using C_{60}-like[23] for mimicking the whole molecule fails. Where is the source of the error? As shown in the top panel of Figure 6.4, the fault does not lie in the dispersive contribution; the correlation between contributions obtained using the whole C_{60} and using C_{60}-like[23] is e xcellent.

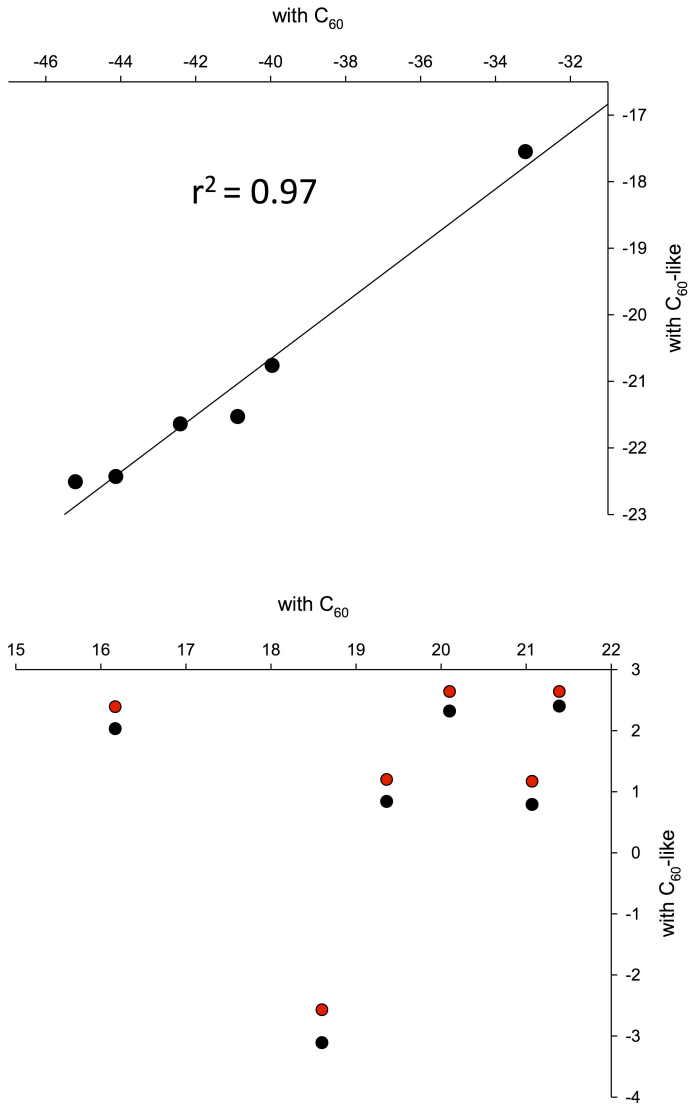


Figure 6.4: Top panel: dispersion contribution calculated with the whole C_{60} *vs.* dispersion contribution calculated previously with C_{60}-like.[23] Bottom panel: contribution of the functional calculated with the whole C_{60} *vs.* contribution of the functional calculated previously with C_{60}-like (the formerly calculated values in black,[23] and calculated values with the TZVP basis in red). Both figures refer to corannulene-5X$\cdots C_{60}$ complexes (X = H, Br, Cl, CH_3, C_2H, CN). Values in kcal/mol.

On the contrary, if contributions of the pure functional are compared, the correlation is awful, as shown in the bottom panel of Figure 6.4; the awful correlation occurs with the formerly calculated values for C_{60}-like[23] and also with the recalculated values with the TZVP basis set. The contribution of the pure functional includes the components corresponding to repulsion, electrostatics, and induction. Obviously, according to the bottom panel of Figure 6.4, these components are very different for C_{60} and for C_{60}-like. Without conducting an exhaustive analysis, it is clear that the electrostatic characteristics of these two species are rather different. While the convex face of C_{60}-like is basically negative,[23] the face of C_{60} shows an almost neutral molecular

electrostatic potential (MEP) and an even slightly positive MEP on top of the five-membered rings (see section A.3, Appendix A). C_{60}-like is a highly polar structure (μ = 4.13 D at the ωB97XD/6-311G* level[23]), while the first nonvanishing multipole moment is the 64-pole one for C_{60}. In summary, C_{60}-like reproduces rather well only the dispersive contribution in the complexes, failing completely from the electrostatic point of view. For complexes with C_{60} (and C_{70}), the interaction energies are almost fully controlled by dispersion (Table 6.3 and Figure 6.3); therefore, electrostatics plays a very secondary role. However, C_{60}-like erroneously confers to electrostatics much more importance than it actually has since its dipole leads to an important dipole-dipole interaction with buckybowls, all of them with non-zero dipole moment.

It is worth noting that corannulene-5CN clearly shows the highest dipolar moment among all substituted corannulenes: dipolar moments of 2.23, 0.29, 0.21, 2.47, 1.82, and 3.59 D at the B97-D2/TZVP level for corannulene-5X, with X = H, Br, Cl, CH_3, C_2H, and CN, respectively. This fact could explain the above-mentioned slight deviation suffered by the complexes formed between this buckybowl and fullerene (Figure 6.3). Its strong dipole makes perceptible the favorable electrostatic interaction with fullerene, which reduces the repulsive contribution of the pure B97 functional (Table 6.3). Moreover, the dipole moment of corannulene-5CN not only is the largest one in magnitude, but also has a clear difference with the other ones: the direction of $\vec{\mu}$ is exactly opposite to that of the others, going from the convex to the concave face of the bowl (from outside to inside). This is due to the huge electron acceptor character of CN groups, which are able to invert the electron distribution of corannulene (electron deficient at the *rim* of the bowl due to the electropositive character of the hydrogen atoms). On the other hand, in the case of sumanene derivatives, the dipole of the CN-substituted compound is even more different from the rest: 2.52, 0.53, 0.78, 3.14, 1.76, and 7.65 D for sumanene-6X, with X = H, Br, Cl, CH_3, C_2H, and CN, respectively. Therefore, this more relevant electrostatic interaction with sumanene-6CN could explain the above commented ranking for sumanene···fullerene complexes in which substitution with CN is strengthened and moves up.

Finally, in order to obtain more information about the interaction in the buckybowl···fullerene complexes, the plotting of non-covalent interaction regions was performed using the recently developed NCIPLOT program.[29,30] This method enables identification of non-covalent interactions and it is based on the peaks that appear in the reduced density gradient (RDG) at low densities. When an RDG isosurface for a low value of RDG is plotted, the non-covalent regions clearly appear in the supramolecular complex. These interactions correspond to both favorable and unfavorable interactions. In order to differentiate between them, the sign of the second density Hessian eigenvalue times the density is color-mapped onto the isosurface: bonding interactions can be identified by the negative sign. Figure 6.5 shows several NCI plots using an isosurface of 0.3 a.u.; blue, green, and red indicate strongly attractive, weak and strongly repulsive interactions, respectively (with a scale running from -0.040 to 0.040 a.u.). In order to save computation time, promolecular densities have been used[30] after checking in a couple of complexes that results are very similar to those obtained with SCF densities. According to NCI plots, the common interaction that takes place in all the complexes is the π···π interaction between the *spokes* of buckybowl and fullerene. This interaction is clearly the most important one in the complex corannulene···C_{60} (*cora face*). In the complex

sumanene···C_{60} (*suma face*) an additional interaction appears: that between CH_2 groups and the fullerene π cloud. Specifically, these are the so-called C-H···π interactions, found in different molecular systems including organic crystals, proteins, and nucleic acids.[31] One of the substituents that results in larger interaction energy is Br (Table 6.1), and this is shown in Figure 6.5 (according to Table 6.1, the increase of dispersion is the source of this fact). The largest effect corresponds to the inclusion of CH_3 groups in the buckybowl. It increases dispersion, but an additional interaction also emerges: the C-H···π interaction. The H atom of the CH_3 group that points to fullerene is responsible for this interaction, as shown in Figure 6.5. In the complex sumanene-6CH_3···C_{60} (*suma face*), nine such interaction take place: six are from the CH_3 groups, and three are from the sumanene itself, all of which can be observed in Figure 6.5.

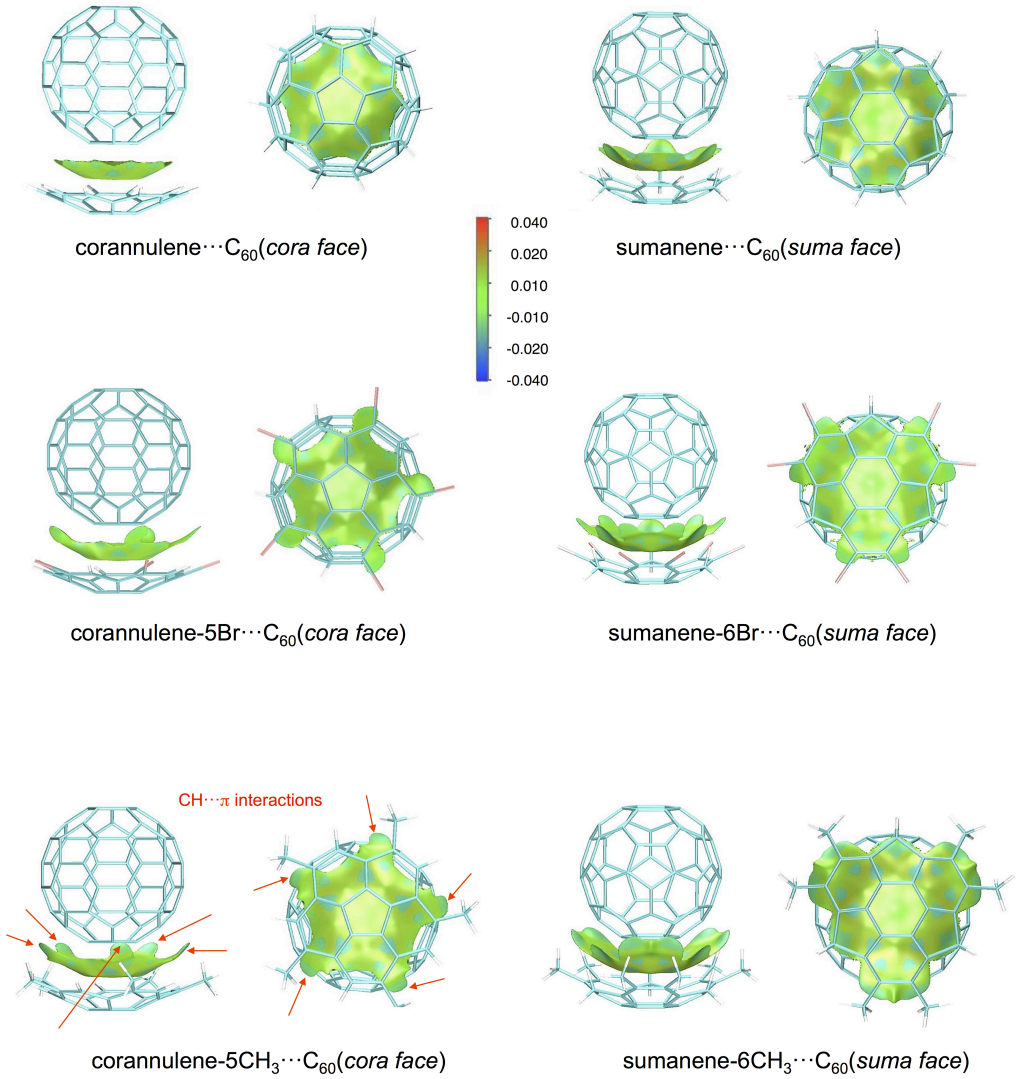


Figure 6.5: Front and bottom views of the NCIPLOT gradient isosurface (0.3 a.u.). The surfaces are colored on a blue-green-red scale according to the strength and type (attractive or repulsive) of interaction. Blue indicated strong attractive interactions, green weak vdW interactions, and red (they do not appear in the current cases) indicates strong non-bonded overlap.

6.4. Conclusions

Stacking interactions between substituted buckybowls (corannulene and sumanene) with fullerenes (C_{60} and C_{70}) were studied at the B97-D2/TZVP level in order to known the ability of these substituted buckybowls as 'buckycatchers'.

All substituted buckybowls evaluated behave as better buckycatchers than the unsubstituted buckybowls. Sumanene substituted with six CH_3 groups was the most favorable complex. CH···π interactions are largely responsible for this result; up to nine interactions of this kind can be found.

Regarding the face of fullerene involved in the interaction, overall, corannulenes prefer to bind by the *cora face* of fullerene, whereas sumanenes prefer to bind by the *suma face* of fullerene. This preference is weak for corannulenes (differences smaller than 1 kcal/mol), but it is considerably larger for sumanenes (about 3 kcal/mol).

Stacking interactions between buckybowls and fullerene C_{70} show interaction energies quite similar to those obtained with C_{60}. Therefore, it is not expected that buckybowls evaluated bind very specifically to one of the fullerenes when exposed to the C_{60}/C_{70} mixture.

According to our results, the interaction energy of the complexes is directly related to the dispersion contribution. Only very small deviations of this behavior are found for buckybowls substituted with CN groups: in this case a significant electrostatic effect emerges that modulates the strong dispersive effect.

The results of this work show that C_{60}-like, used in our previous work, does not seem representative for reproducing the concave···convex interactions between buckybowls and fullerenes. The weakness of the C_{60}-like comes from the inability of this structure to reproduce the electrostatic characteristics of the whole C_{60}. However, results using C_{60}-like are not too bad because C_{60}-like is able to reproduce rather well the dispersive effect (which is the most important contribution) of the real C_{60}.

6.5. References

1. E. M. Pérez and N. Martín, *Pure Appl. Chem.*, 2010, **82**, 523-533.
2. Y. Shoji, K. Tashiro and T. Aida, *J. Am. Chem. Soc.*, 2010, **132**, 5928–5929.
3. E.-X. Zhang, D.-X. Wang, Q.-Y. Zheng and M.-X. Wang, *Org. Lett.*, 2008, **10**, 2565-2568.
4. A. Sygula, F. R. Fronczek, R. Sygula, P. W. Rabideau and M. M. Olmstead, *J. Am. Chem. Soc.*, 2007, **129**, 3842-3843.
5. E. Huerta, H. Isla, E. M. Pérez, C. Bo, N. Martín and J. de Mendoza, *J. Am. Chem. Soc.*, 2010, **132**, 5351–5353.
6. K. Tashiro and T. Aida, *Chem. Soc. Rev.*, 2007, **36**, 189-197.

7. D. Canevet, M. Gallego, H. Isla, A. de Juan, E. M. Pérez and N. Martín, *J. Am. Chem. Soc.*, 2011, **133**, 3184-3190.
8. E. M. Pérez and N. Martín, *Chem. Soc. Rev.*, 2008, **37**, 1512-1519.
9. P. E. Georghiou, A. H. Tran, S. Mizyed, M. Bancu and L. T. Scott, *J. Org. Chem.*, 2005, **70**, 6158-6163.
10. J. Cerny and P. Hobza, *Phys. Chem. Chem. Phys.*, 2007, **9**, 5291-5303.
11. K. E. Riley and P. Hobza, *WIREs Comput. Mol. Sci.*, 2011, **1**, 3-17.
12. D. Josa, J. Rodríguez-Otero, E. M. Cabaleiro-Lago and M. Rellán-Piñeiro, *Chem. Phys. Lett.*, 2013, **557**, 170-175.
13. Y. Zhao, N. E. Schultz and D. G. Truhlar, *J. Chem. Phys.*, 2005, **123**, 161103/1-161103/4.
14. Y. Zhao and D. G. Truhlar, *Theor. Chem. Acc*, 2008, **120**, 215-241.
15. S. Grimme, *J. Comput. Chem.*, 2004, **25**, 1463-1473.
16. S. Grimme, J. Antony, T. Schwabe and C. Muck-Lichtenfeld, *Org. Biomol. Chem.*, 2007, **5**, 741-758.
17. C. Mück-Lichtenfeld, S. Grimme, L. Kobryn and A. Sygula, *Phys. Chem. Chem. Phys.*, 2010, **12**, 7091-7097.
18. B. M. Wong, *J. Comput. Chem.*, 2009, **30**, 51-56.
19. Y. Zhao and D. G. Truhlar, *Phys. Chem. Chem. Phys.*, 2008, **10**, 2813-2818.
20. T. Janowski, P. Pulay, A. A. Sasith Karunarathna, A. Sygula and S. Saebø, *Chem. Phys. Lett.*, 2011, **512**, 155-160.
21. C.-K. Skylaris, L. Gagliardi, N. C. Handy, A. G. Ioannou, S. Spencer and A. Willetts, *J. Mol. Struct.:THEOCHEM*, 2000, **501-502**, 229–239.
22. M. R. Kennedy, L. A. Burns and C. D. Sherrill, *J. Phys. Chem. A*, 2012, **116**, 11920-11926.
23. D. Josa, J. Rodríguez Otero and E. M. Cabaleiro Lago, *Phys. Chem. Chem. Phys.*, 2011, **13**, 21139-21145.
24. R. Ahlrichs, M. Bär, M. Häser, H. Horn and C. Kölmel, *Chem. Phys. Lett.*, 1989, **162**, 165-169.
25. S. F. Boys and F. Bernardi, *Mol. Phys.*, 1970, **19**, 553-566.
26. P. A. Denis, *Chem. Phys. Lett.*, 2011, **516**, 82-87.
27. A. Sygula and S. Saebø, *Int. J. Quantum Chem.*, 2009, **109**, 65-72.
28. R. C. Haddon, *J. Am. Chem. Soc.*, 1990, **112**, 3385-3389.
29. E. R. Johnson, S. Keinan, P. Mori-Sánchez, J. Contreras-García, A. J. Cohen and W. Yang, *J. Am. Chem. Soc.*, 2010, **132**, 6498–6506.
30. J. Contreras-Garcia, E. R. Johnson, S. Keinan, R. Chaudret, J. P. Piquemal, D. N. Beratan and W. Yang, *J. Chem. Theory Comput.*, 2011, **7**, 625-632.
31. M. Nishio, *Phys. Chem. Chem. Phys.*, 2011, **13**, 13873-13900.

Chapter 7

Ring-annelated corannulenes as fullerene receptors

7.1. Introduction

Since the discovery of fullerenes by Kroto *et al.* in 1985[1] the interest in buckybowls, bowl-shaped polycyclic aromatic hydrocarbons (PAHs) has increased. Buckybowls show a unique bowl-shaped architecture that provides two different faces, one concave and one convex, which significantly increases its potential with respect to standard PAHs. Thus, buckybowls can exhibit intermolecular interactions with a wide range of different species, such as transition metals[2-5], metal cations[6-9] and anions.[10] Also, the interaction with other curved surfaces can lead to an interesting type of interaction known as concave-convex π···π interaction. This interaction may have a huge practical value as in the case of molecular tweezers for trapping species of interest, such as fullerene, in which case buckybowls can be used as one the most efficient buckycatchers.[11]

The two most popular fullerenes, C_{60} and C_{70} are quite similar but show unique properties.[12-14] It would be interesting to know how to separate these similar structures, and some findings suggest strategies to do this task through molecular tweezers with corannulene pincers.[15, 16] The idea is to find molecular tweezers capable to discriminate C_{60} from C_{70}. However, recent research shows that binding energies of C_{60} complexes are very similar to those of C_{70} ones.[15, 17] In this context, understanding the factors that govern the concave-convex π···π interactions has become an attractive field of research. In the last years, several theoretical studies have been performed to investigate the curved π systems, mainly using the smallest buckybowl, corannulene $C_{20}H_{10}$ (compound 1, Figure 7.1).[17-21] Undoubtedly, the knowledge of curvature and substituent effects of buckybowls could give an important insight into the design of more effective and/or selective fullerene receptors. Recently, Kennedy *et al*.[21] have explored the effects of curvature on

π···π interactions. Their results indicated that curvature affects to all four major components of non-covalent interactions (dispersion, electrostatics, exchange and induction) and that an increase of curvature in concave-convex π···π interactions leads to more favourable interaction energies, except at short distances where the most highly curved systems are less favourable as exchange repulsion terms begin to dominate the interaction.

In order to evaluate the effect of substitution on concave-convex π···π interactions, our group has studied a series of corannulene dimers substituted with five alternating Br, Cl, CH_3, C_2H and CN units.[19] The results showed that all substituted corannulenes evaluated behave as a better catcher than the unsubstituted corannulene as a consequence of the contribution of electrostatic and dispersive effects. However, not clear relationship between the curvature of bowls and the interaction energy was observed. Corannulene shows a noticeable rigidity, so that inclusion of up to five substituents has a small effect on its structure, and only a slight flattening of the bowl was observed.[19]

Nowadays, ring-annelated corannulenes have attracted the attention of researchers because the correlation between the bowl depth and the bowl-to-bowl inversion barrier.[22, 23] Ring annelation to the *rim* of corannulene gradually flattens the bowl and, moreover, it introduces CH_2 groups in the bowl structure that can interact with fullerenes through CH···π interactions. Undoubtedly, the introduction of CH_2 groups in the bowl structure seems a good strategy to enhance convex π···π interactions. So, according to Denis results, the three CH_2 groups in sumanene structure are the great responsible for the stronger sumanene dimer interaction compared to that of corannulene dimer.[17] In addition, a recent study performed by Mahesh Kumar *et al*.[24] reveals that CH···π interaction from methylene (-CH_2) group of adamantane molecule with benzene is stronger than that of methine (-CH) group.

For the above reasons, ring-annelated corannulenes seem suitable structures for the further study of the interaction ability of corannulenes in the recognition of fullerenes, by concave-convex π···π interactions. Therefore, the aim of this work is to evaluate the stacking interactions between ring-annelated corannulenes with fullerenes C_{60} and C_{70}. In addition, for the ring-annelated corannulene with five saturated five-membered rings, the substitution effect of NH, O and S units was also evaluated.

7.2. *Computational details*

Since dispersion effects are crucial to study π···π interactions, dispersion-corrected DFT methods seem mandatory. Among them, perhaps the Grimme's empirical dispersion correction is the most popular. His original version (DFT-D),[25] was modified in 2006 (DFT-D2),[26] and further corrected in 2010 (DFT-D3),[27] and 2011 (DFT-D3(BJ)).[28]

Recently, for the corannulene dimer, Kennedy *et al*.[21] showed that the best results (compared with the benchmark performed at the QCISD(T)/aug-cc-pVTZ level)[29] correspond to B3LYP-D3(BJ), but with a very small advantage over B3LYP-D2, M06-2X and B97-D2. Of these DFT methods, B97-D2 is the best to take advantage of the noticeable reduction of computational cost that allows the resolution of identity approximation (RI) implemented in Turbomole program suite,[30] since for non-hybrid functionals the RI procedure speeds up calculations by a factor 10 at least (as compared to conventional treatments) without sacrificing accuracy. In addition, calculations using B97-D2 method also provide very good results as can be observed in several previous works.[15, 19, 26, 31, 32] Taking into account the above comments, the size of the studied systems and the software used (Turbomole), the choice of the B97-D2/TZVP (henceforth B97-D for simplicity) and the RI approximation seems appropriate. All the complexes were fully optimized at this level.

Counterpoise corrections, CP, were applied to all reported interaction energies to avoid basis set superposition error, BSSE.[33] According to this method, the interaction energy of a system A···B is calculated according to:

$$\Delta E_{int} = E_{AB}^{AB}(AB) - \left(E_{A}^{AB}(AB) + E_{B}^{AB}(AB)\right) \tag{7.1}$$

where superscript refers to the geometry (that of the system AB) and the parenthesis indicates the basis set used (the full basis set of the system A···B). If, in addition, the energy cost involved in the deformation of each monomer to adopt the geometry of the dimer is considered:

$$\Delta E_{def} = \left(E_{A}^{AB}(A) - E_{A}^{A}(A)\right) + \left(E_{B}^{AB}(B) - E_{B}^{B}(B)\right) \tag{7.2}$$

then, the full complexation energy is obtained as follows:

$$\Delta E_{complex} = \Delta E_{int} + \Delta E_{def} \tag{7.3}$$

Finally, to quantify the curvature of curved structures, POAV angle is an efficient tool. POAV is the pyramidalization angle proposed by Haddon;[34] it allows the description of local curvature of a conjugated system and is defined as the angle between de C-C bond and the vector perpendicular to the pyramidal base of three idealized C-C bonds.

7.3. *Results and discussion*

Stacking interactions between ring-annelated corannulenes with fullerenes C_{60} and C_{70} were studied at the B97-D level. Figure 7.1 shows all ring-annelated corannulenes used: three-membered rings were annelated in 2, four-membered rings were annelated in 3 and 4 (saturated and unsaturated), and five-membered rings were annelated in 5 and 6 (saturated and unsaturated). Finally, bowls 7, 8, and 9 were added to the study to analyse

the effect of including heteroatoms (for this purpose bowl 5 was chosen since in this case the effect of the heteroatom is more isolated from other possible effects).

The complexes were built by stacking the ring-annelated corannulenes with the corannulene face of fullerenes. Although for the corannulene dimer it is known that eclipsed conformation is the most favourable one,[29] both eclipsed and staggered conformations were studied. For the eclipsed conformation, the five *spoke* C-C bonds of corannulenes 1-9 were eclipsed with analogue bonds of the corannulene face of fullerenes C_{60}/C_{70}. For the staggered conformation, one of the monomers was rotated 36° around the axis defined by the centre of both *hub* five-membered rings. So, all complexes evaluated have C_{5v} symmetry.

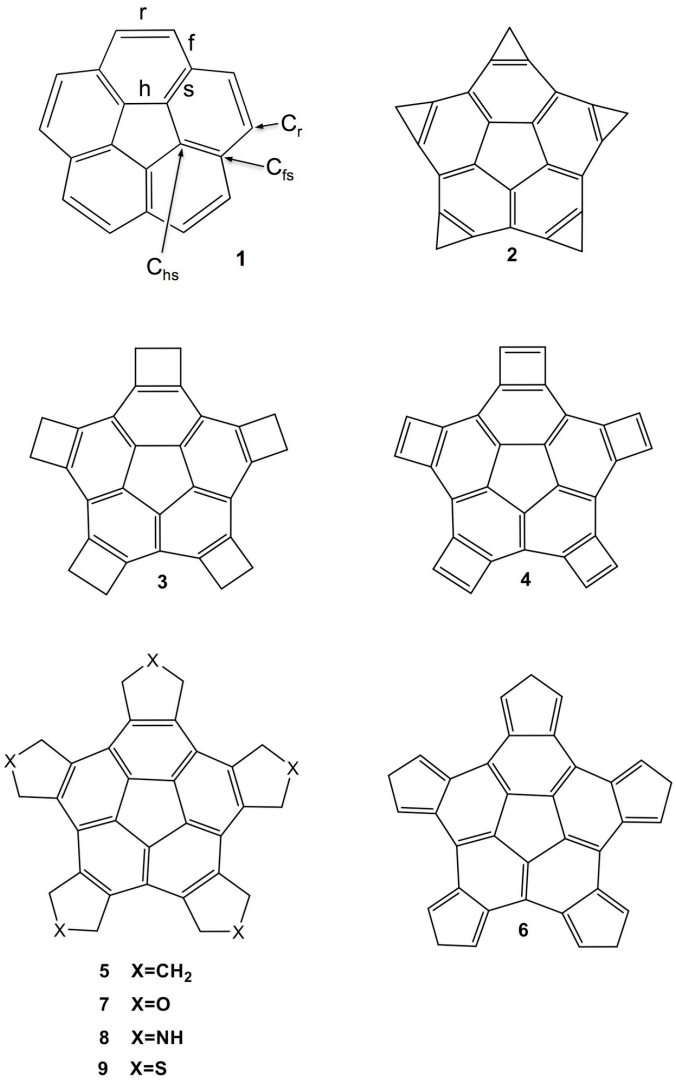


Figure 7.1: Ring-annelated corannulenes studied. Bonds (h=*hub*, s=*spoke*, f=*flank*, r=*rim*). C atom types (hs=*hub-spoke*, fs=*flank-spoke*, r=*rim*).

Table 7.1 summarizes interaction energies for eclipsed and staggered conformations. First, it is worth noting that all the annelated corannulenes led to an important increase of the interaction energy (ranging from about 5 to 16 kcal/mol) relative to that of the $C_{20}H_{10}$ corannulene (compound 1). Second, the difference of interaction between C_{60} and C_{70} is very small: it does not reach 1 kcal/mol at best, always in favour of C_{70} except for the staggered complex with compound 4. Given the huge similarity between the geometric and electronic characteristics (both without dipole moment) of C_{60} and C_{70} it is reasonable to think that the small energy advantage of C_{70} is justified by the fact that it has a non-zero quadrupole moment, which favours the electrostatic contribution of interaction. On the contrary, for C_{60} the first nonvanishing multipole moment is the 64-pole moment. Unfortunately, the complexation energy for complexes with C_{60} and C_{70} are very similar. Therefore, it is not expected that the substituted buckybowls to specifically bind one of the fullerenes when exposed to the C_{60}/C_{70} mixture.

In all cases the preferred conformation is the eclipsed one (with differences ranging from about 1 to 3 kcal/mol), with two exceptions: complex 2···X where both conformations are virtually isoenergetic, and complex 4···X where unexpectedly the staggered conformation is about 4 kcal/mol more favourable than the eclipsed one. Clearly, there is an effect that substantially favours the staggered conformation of 4···X. Although there are not conclusive evidences, that effect could be explained as follows: in the staggered conformation of complex 4···X both π bonds of the cyclobutadiene (which owns an extremely localized π clouds) are directly facing the *spoke* bond of fullerene, which is precisely the bond with the largest π character of fullerene (the largest bond order, the shortest bond length, the largest double-bond character). Thus, this additional π···π interaction, that takes place in the staggered conformation in a more appropriate way, not only offsets the advantage of the general trend favouring the eclipsed conformation, but it also overcomes it (section B.1 from Appendix B includes several calculations for supporting the previous hypothesis). On the other hand, it seems that this effect is somewhat less pronounced with C_{70}, since only for the staggered conformation of complex 4···X the interaction energy with C_{70} is smaller than that with C_{60}.[35]

Table 7.1: Interaction energies in kcal/mol obtained at the B97-D2/TZVP level calculation for complexes in eclipsed conformations (staggered conformations results in parentheses)

	X = C_{60}	X = C_{70}
1···X	-17.03 (-14.57)	-17.16 (-14.72)
2···X	-22.20 (-22.22)	-22.48 (-22.37)
3···X	-28.45 (-27.65)	-28.84 (-27.97)
4···X	-24.09 (-28.22)	-24.84 (-28.09)
5···X	-32.01 (-30.69)	-32.54 (-31.19)
6···X	-30.05 (-26.76)	-30.15 (-26.98)
7···X	-30.04 (-28.51)	-30.46 (-28.77)
8···X	-33.27 (-30.41)	-33.78 (-30.99)
9···X	-32.02 (-29.89)	-32.36 (-30.09)

Complexation energies given in Table 7.2 represent the value of interaction energy taking into account the fragment deformation (for each complex the preferred conformation, eclipsed or staggered, was chosen). Except for compound 6, deformation energies are rather modest. The deformation energy must be directly related with the geometric changes suffered by corannulenes derivatives upon complexation with C_{60} and C_{70}. Two main geometrical parameters provide a measure of the curvature of the corannulene bowls: *h* represents the bowl depth (taken as the distance between the plane of the *hub* carbons and that of the *rim* carbons) and POAV is the pyramidalization angle (POAV angle of the *hub-spoke* carbons of the bowl was used for our purposes). Table 7.3 shows the geometrical parameters of the isolated corannulenes, and Table 7.4 shows the values of these parameters after complexation. As can it be seen in Table 7.3, ring-annelated corannulenes optimized at the B97-D level show more curved structures (which is reflected in higher values of POAV and bowl depth *h*) than those obtained previously by Dynadayalane *et al.*[22] at the B3LYP/6-31G* level. The largest difference is observed for compound 6 that show a virtually flat structure at the B3LYP/6-31G* level while our calculations at the B97-D level indicate a slightly curved structure with POAV angle of 4.17° and a bowl depth of 0.447 Å. In order to check the discrepancy between both calculations, a MP2/TZVP optimization of compound 6 was performed: the results were very similar to those obtained at the B97-D level, with POAV angle of 4.09° and bowl depth of 0.436 Å. The failure of the B3LYP calculations comes mainly from the inadequate description of the intramolecular van der Waals interactions.[36] In any case, our goal is not to rigorously obtain the absolute curvature of the isolated corannulenes.

As expected from deformation energies, compound 6 undergoes the largest deformation of the bowl after complexation. So it substantially increases its curvature, which is reflected in an increase of about of 2 degrees in POAV and about of 2 tenths of Å in depth *h*. In the other cases the change of curvature of the bowl is rather small.

Table 7.2: Complexation energy (E_{comp}) and deformation energy (E_{def}) in kcal/mol. Calculations were performed at the B97-D2/TZVP level

	X = C_{60}		X = C_{70}	
	E_{def}	E_{comp}	E_{def}	E_{comp}
1···X	0.20	-16.83	0.16	-17.00
2···X	0.28	-21.94	0.12	-22.36
3···X	0.45	-28.00	0.46	-28.38
4···X	0.63	-27.59	0.60	-27.49
5···X	0.60	-31.41	0.55	-31.99
6···X	1.95	-28.10	1.95	-28.20
7···X	0.62	-29.42	0.60	-29.86
8···X	1.29	-31.98	1.38	-32.40
9···X	1.13	-30.89	1.17	-31.19

Table 7.4 also includes the equilibrium distance in the complex, D_{eq}, taken as the distance between the centres of the five membered rings of corannulene and fullerene. In all cases ring annelation to the *rim* of corannulene decreases the equilibrium distances

compared to unsubstituted corannulene 1; however, the trend is very vague, so there is no clear relationship between the complexation energy and the decrease of equilibrium distance. A relationship between the curvature of bowls and the changes on complexation energy generated by ring annelation to the *rim* of corannulene does not exist either.

Table 7.3: POAV angle (in degrees) and bowl depth (Å) for the isolated ring-annelated corannulenes studied in this work at the B97-D2/TZVP level and at the B3LYP/6-31G* previously obtained[22]

	B97-D2/TZVP		B3LYP/6-31G*	
	POAV	*h*	POAV	*h*
1	8.63	0.928	8.1	0.864
2	7.60	0.838	6.6	0.674
3	6.67	0.725	5.3	0.572
4	7.53	0.808	6.5	0.678
5	8.04	0.855	7.1	0.738
6	4.17	0.447	0.0	0.093
7	8.15	0.873		
8	8.08	0.866		
9	7.50	0.784		

Table 7.4: Equilibrium distance (D_{eq}) (Å), POAV angle (in degrees) and bowl depth (Å) for complexes in the eclipsed conformations (staggered conformations results in parentheses). Calculations were performed at the B97-D2/TZVP level

	X = C_{60}			X = C_{70}		
	D_{eq}	POAV	*h*	D_{eq}	POAV	*h*
1···X	3.456 (3.535)	8.38 (8.09)	0.902 (0.868)	3.453 (3.543)	8.42 (8.11)	0.909 (0.870)
2···X	3.364 (3.396)	7.29 (7.18)	0.753 (0.740)	3.352 (3.384)	7.35 (7.22)	0.760 (0.744)
3···X	3.242 (3.315)	6.91 (6.90)	0.764 (0.763)	3.242 (3.301)	7.02 (7.01)	0.776 (0.776)
4···X	3.350 (3.365)	7.40 (8.07)	0.808 (0.880)	3.419 (3.374)	7.94 (8.15)	0.866 (0.889)
5···X	3.329 (3.404)	8.10 (8.13)	0.871 (0.880)	3.363 (3.397)	8.35 (8.20)	0.876 (0.937)
6···X	3.123 (3.181)	6.02 (5.72)	0.673 (0.637)	3.112 (3.170)	6.03 (5.73)	0.674 (0.639)
7···X	3.363 (3.433)	8.28 (8.21)	0.895 (0.891)	3.353 (3.429)	8.32 (8.30)	0.899 (0.901)
8···X	3.351 (3.410)	8.29 (8.20)	0.900 (0.896)	3.360 (3.409)	8.42 (8.28)	0.916 (0.905)
9···X	3.286 (3.337)	7.95 (7.71)	0.846 (0.825)	3.274 (3.328)	7.97 (7.77)	0.849 (0.832)

In order to analyse in more detail the balance of energy contribution to the stability of the complexes, the interaction energy was decomposed according to a simple method. So, the two contributions of the model employed were taken into account: the pure B97 interaction energy and the empirical dispersion contribution to the interaction energy. As it can be seen from Table 7.5, dispersion is mainly responsible for the attraction of the complexes evaluated, being clearly repulsive the contribution of the pure

B97 functional. The annelation of corannulene led in all cases to an increase of the repulsive contribution, which is amply offset by the increase of the dispersive attraction, so the final balance is always favourable to ring annelation. Table 7.5 also shows that dispersion is responsible for the advantage of the eclipsed conformations, in all cases except for the above commented case of compound 4: in this case, dispersion is also responsible for preference but it clearly favours the staggered conformation.

Table 7.5: B97 interaction energy and dispersion contribution of the complexes obtained at the B97-D2/TZVP level (kcal/mol) for complexes in eclipsed conformations (staggered conformations results in parentheses)

	X = C_{60}		X = C_{70}	
	B97	Dispersion	B97	Dispersion
1···X	16.17 (14.94)	-33.20 (-29.51)	16.21 (14.23)	-33.37 (-28.95)
2···X	20.32 (18.40)	-42.52 (-40.60)	20.54 (18.53)	-43.02 (-40.90)
3···X	25.34 (23.07)	-53.79 (-50.72)	25.13 (23.99)	-53.97 (-51.96)
4···X	21.31 (21.82)	-45.40 (-50.04)	20.14 (21.28)	-44.98 (-49.37)
5···X	28.18 (26.86)	-60.19 (-57.55)	28.00 (26.73)	-60.54 (-57.92)
6···X	21.33 (20.49)	-51.38 (-47.25)	21.27 (20.46)	-51.42 (-47.44)
7···X	27.96 (26.18)	-58.00 (-54.69)	27.77 (26.74)	-58.23 (-55.51)
8···X	28.40 (28.04)	-61.67 (-58.45)	27.88 (27.54)	-61.66 (-58.53)
9···X	27.30 (24.80)	-59.32 (-54.69)	27.28 (25.97)	-59.64 (-56.06)

Table 7.5 also shows that in terms of dispersion, annelation with saturated rings is more favourable that annelation with unsaturated ones: differences about of 8-10 kcal/mol appear when the behaviour of compound 3 is compared with that of compound 4, and that of compound 5 with that of compound 6. In the final balance, the difference is much less noticeable, since compounds 4 and 6 partly offset their dispersive disadvantage with a more favourable behaviour in the contribution of the pure functional.

As regard inclusion of heteroatoms, a rather small effect is observed. So, values from Table 7.5 for compounds 7, 8, and 9, are not very different of those for compound 5, both for dispersion contribution and for that of the pure functional: differences are smaller than 2 kcal/mol.

The relationship between the dispersive contribution and the total complexation energy can be clearly visualized in Figure 7.2. Undoubtedly, the increase of the complexation energy is related to the increase of the dispersion energy, being the correlation excellent, with $r^2 = 0.98$. Only compounds 4 and 6, and to a lesser extent compound 7, deviate very slightly of the linear behaviour. In order to explain these minimum discrepancies, a qualitative analysis of the contribution of electrostatic energy to interaction energy has been carried out. Obviously, that contribution cannot be too large since compounds 1-9 have a substantial dipole moment but, however, as commented above, the first nonvanishing multipole moment is the 64-pole one for C_{60} and the quadrupole one for C_{70}. Therefore, the interaction must be negligible at a certain distance, especially in the case of C_{60}. However, the multipolar expansion does not work

satisfactorily at short distances and local effects must be taken into account. In order to analyse that question, Figure 7.3 shows maps of molecular electrostatic potential, MEP, of C_{60} and the concave side of compounds 1-9. C_{60} (C_{70} virtually has the same map) shows an almost neutral MEP, but slightly positive on top of the five-membered rings. In the complexes studied, these five-membered rings face the central five-membered ring of corannulenes 1-9. Consequently, a negative MEP above the central ring of corannulenes will favour a larger electrostatic interaction between corannulene and fullerene. Examining Figure 7.3 and taking as reference the MEP of the central region of compound 5 (compound that shows the best fitting in Figure 7.2), it can be observed that compounds 4 and 6 clearly show a more favourable MEP (more negative) for interacting with C_{60}. This fact agrees with Figure 7.2, where these two compounds obtain larger complexation energy than that predicted by its dispersion contribution. On the contrary, compounds 1, 2, 7, 8, and 9 show a less favourable MEP (more positive) in the central region; all of them are found over the straight line of Figure 7.2 (this conclusion is especially adequate for compound 7, and in a much lesser extent for the other four compounds). That is to say, these five compounds obtain a smaller complexation energy than that predicted by its dispersion contribution. In summary, MEP maps can help to explain (in a rather qualitative way) the small deviations of Figure 7.2.

Obviously, the above discussion is rather limited since the electrostatic is not the only contribution to the pure B97 interaction energy; it also includes repulsion and induction components. However, it seems that the electrostatic contribution constitutes an important differentiating factor inside the B97 interaction since the two larger deviations in Figure 7.2 (compounds 4 and 6) correspond to the most favourable MEPs; it clearly gives rise to a smaller repulsion in the B97 term (4-7 kcal/mol lower than the similar structures 3, 5, 7, 8, and 9).

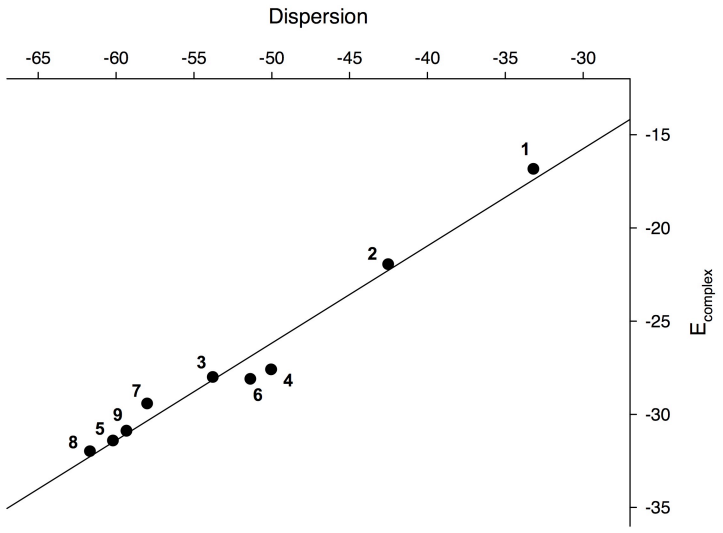


Figure 7.2: Dispersion contribution *vs.* complexation energy (in kcal/mol): $E_{complex} = 0.522E_{disp} - 0.08256$. $R^2 = 0.98$.

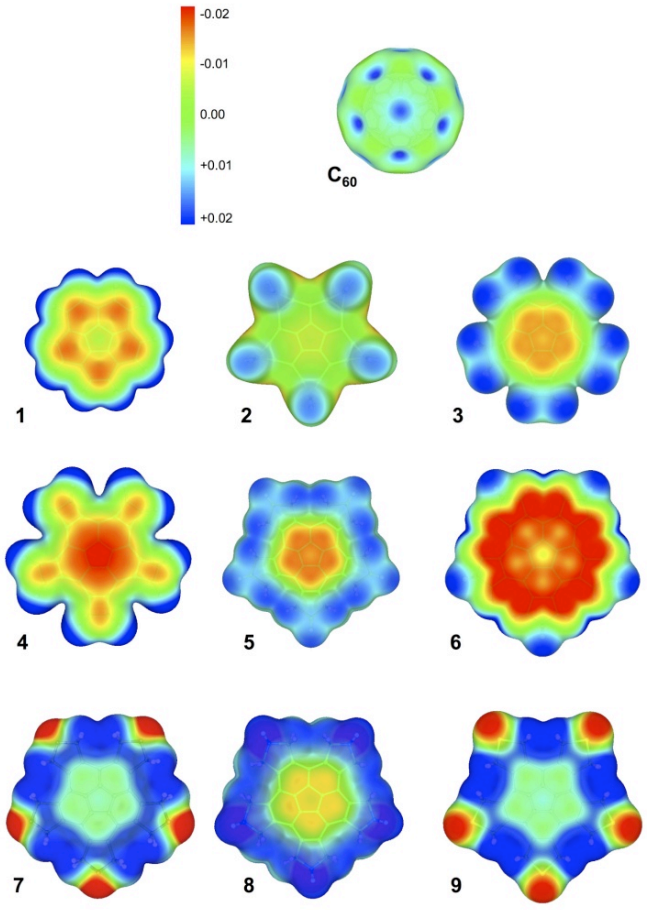


Figure 7.3: Molecular electrostatic potential, MEP, onto an electron density isosurface of 0.001a.u.

In order to obtain more information about the π···π interaction in the corannulene···fullerene complexes, the plotting of non-covalent interaction regions was performed using the recently developed NCIPLOT program.[37,38] This method enables identification of non-covalent interactions and it is based on the peaks that appear in the reduced density gradient (RDG) at low densities. Plotting an RDG isosurface for a low value of RDG, the non-covalent regions clearly appear in the supramolecular complex. These interactions correspond to both favourable and unfavourable interactions. In order to differentiate between them, the sign of the second density Hessian eigenvalue times the density is color-mapped onto the isosurface: bonding interactions can be identified by the negative sign. Figure 7.4 shows the NCI plots for the interaction between C_{60} and compounds 1-6 (figures for compounds 7-9 are almost the same that for compound 5) using an isosurface of 0.4 a.u.; blue, green and red indicate strongly attractive, weak and strongly repulsive interactions, respectively (with a scale running from -0.015 to 0.015 a.u.). In all cases a rather strong π···π interaction takes place between the *spokes* of corannulene and fullerene (except for compound 4, where the favourable conformation is the staggered one). Moreover, in complexes with compounds 2, 3, and 5, an additional

important interaction takes place: that between the CH_2 groups and the π cloud of fullerene. Specifically, these are the so called C-H···π interactions, found in different molecular systems including organic crystals, proteins and nucleic acids.[39] They can be either electrostatic- or dispersion- dominated depending upon the acidity of the C-H group; dispersion energy is the most important in typical cases where an aliphatic or aromatic CH is the hydrogen donor.[40] Moreover, the proportion of electrostatic energy decreases on going from sp^2-CH to sp^3-CH. Thus, according to values of Table 7.5, C-H···π interactions of compound 2, and especially those of 3, 5, 7, 8, and 9, are mainly of dispersive character. In this six compounds an important interaction of the internal hydrogen atoms of the CH_2 groups belonging to the annelated ring, is the main responsible for the increase of complexation energy with fullerene, relative to what happens with compound 1. For compound 4 (the only one with a favourable staggered conformation) the increase of complexation energy comes from the additional π···π interaction that takes place with the π bonds of the annelated cyclobutadiene rings, as commented above. Compound 6 has CH_2 groups, but too far from the π cloud of fullerene (as it happens for the external CH_2 group of compound 5). However, an additional weak interaction arises between the external π bonds of cyclopentadiene and the π cloud of fullerene, which partially offsets the lack of strong C-H···π interactions. Thus, compound 6 shows the smaller complexation energy of corannulene compounds with annelated five-membered rings.

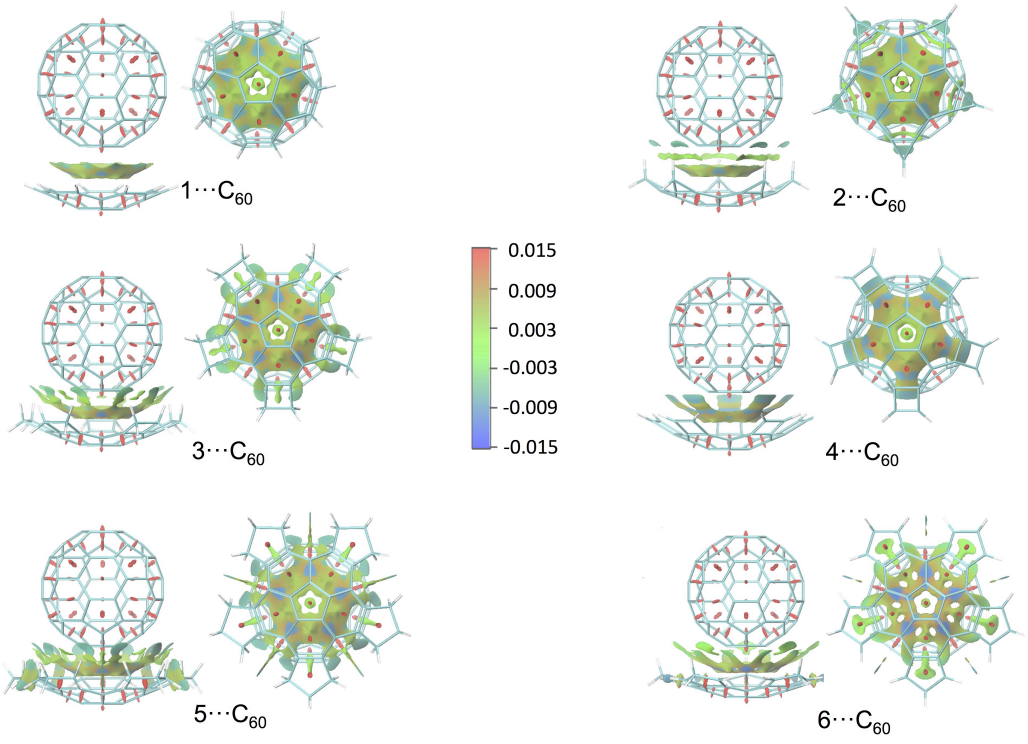


Figure 7.4: Front and bottom views of the NCIPLOT gradient isosurface (0.4 a.u.). The surfaces are colored on a blue-green-red scale according to the strength and type (attractive or repulsive) of interaction. Blue indicates strong attractive interactions, green indicate weak VdW interactions, and red indicates strong nonbonded overlap. Nonbonding regions only appear at the centre of all the rings, but they are irrelevant for the intermolecular analysis. More views of NCIPLOT are available in the section B.2 from Appendix B.

Finally, an attempt to confirm that interactions between corannulenes and fullerenes really come from π···π interactions is carried out. For this purpose a Natural Bond Analysis (NBO) was performed.[41] Effectively, the results of the second order perturbation analysis confirm that the main contribution for all corannulene···C_{60} complexes (except for 4···C_{60}, staggered) corresponds to the interaction between the π orbitals of the *spokes* of both monomers. However, that is not the only relevant contribution (see section B.3, Appendix B).

7.4. Conclusions

According to our results, ring annelation to the *rim* bonds of corannulene looks a good strategy to enhance the interaction with fullerenes C_{60} and C_{70}. The increase of complexation energy is linearly correlated to the increase of dispersion energy. The very small deviations of this behaviour can be explained by electrostatic considerations. In all the complexes the eclipsed conformation is the more favourable since it maximizes the π···π interaction between the *spoke* bonds of corannulenes and fullerene. Compound 4 constitutes the only exception; in this case the staggered conformation offsets (and overcomes) that trend by an additional π···π interaction that emerges between the double bonds of the cyclobutadiene annelated rings and the *spoke* bonds of fullerene; this interaction takes place in the staggered conformation in a more suitable way.

NCI calculations allow us showing that C-H···π interactions play a fundamental role in the increase of dispersion. This kind of interaction takes place especially for compounds with saturated annelated rings, where the internal hydrogen atom of the CH_2 groups points directly to the π cloud of fullerene, establishing a strong contact which is pretty evident in the NCI maps. Compounds 4 and 6, with unsaturated annelated rings, offset the lack of strong C-H···π interactions by better electrostatic characteristics: their *hubs* show an enhanced negative MEP that give rise to a better interaction with the slightly positive MEP of the bottom of fullerenes.

Inclusion of heteroatoms in the structure 5 has a rather small effect, so that C-H···π interactions remain as the main feature.

Stacking interactions between ring-annelated corannulenes and fullerene C_{70} show interaction energy values quite similar to that obtained for fullerene C_{60}: only slightly larger, but 1 kcal/mol at best. Therefore, it is not expected that the substituted buckybowls to specifically bind one of the fullerenes when exposed to the C_{60}/C_{70} mixture.

In summary, our results show that CH···π interactions can contribute significantly to enhance the interaction with fullerenes. So, the design of new molecular receptors that take into account the increase (and the proper orientation) of these interactions, could provide a considerable improvement in the task of fullerene recognition.

7.5. References

1. H. W. Kroto, J. R. Heath, S. C. O'Brien, R. F. Curl and R. E. Smalley, *Nature*, 1985, **318**, 162-163.
2. M. A. Petrukhina and L. T. Scott, *Dalton trans.*, 2005, 2969-2975.
3. P. A. Vecchi, C. M. Alvarez, A. Ellern, R. J. Angelici, A. Sygula, R. Sygula and P. W. Rabideau, *Organometallics*, 2005, **24**, 4543-4552.
4. H. Sakane, T. Amaya, T. Moriuchi and T. Hirao, *Angew. Chem.*, 2009, **48**, 1640-1643.
5. A. S. Filatov and M. A. Petrukhina, *Coord. Chem. Rev.*, 2010, **254**, 2234-2246.
6. U. D. Priyakumar and G. N. Sastry, *Tetrahedron Lett.*, 2003, **44**, 6043-6046.
7. J. R. Green and R. C. Dunbar, *J. Phys. Chem. A*, 2011, **115**, 4968-4975.
8. J. A. Carrazana-García, J. Rodríguez-Otero and E. M. Cabaleiro-Lago, *J. Phys. Chem. B*, 2011, **115**, 2774-2782.
9. M. Rellán Piñero, J. Rodríguez Otero, E. M. Cabaleiro Lago and D. Josa, *J. Mol. Model.*, 2013, **19**, 2049-2055.
10. P. García-Novo, A. Campo-Cacharrón, E. M. Cabaleiro-Lago and J. Rodríguez-Otero, *Phys. Chem. Chem. Phys.*, 2012, **14**, 104-112.
11. A. Sygula, F. R. Fronczek, R. Sygula, P. W. Rabideau and M. M. Olmstead, *J. Am. Chem. Soc.*, 2007, **129**, 3842-3843.
12. W. Zha, D. Chen and W. Fei, *J. Liq. Chrom. & Rel. Technol.*, 1999, **22**, 2443-2453.
13. T. C. Wu, M. K. Chen, Y. W. Lee, M. Y. Kuo and Y. T. Wu, *Angew. Chem.*, 2013, **52**, 1289-1293.
14. N. Martín, *Chem. Commun.*, 2013, **49**, 1039-1041.
15. C. Mück-Lichtenfeld, S. Grimme, L. Kobryn and A. Sygula, *Phys. Chem. Chem. Phys.*, 2010, **12**, 7091-7097.
16. A. Sygula and W. E. Collier, Molecular Clips and Tweezers with Corannulene Pincers, in *Fragments of Fullerenes and Carbon Nanotubes: Designed Synthesis, Unusual Reactions, and Coordination Chemistry* (eds M. A. Petrukhina and L. T. Scott), John Wiley & Sons, Inc., Hoboken, NJ, USA., 2011, ch. 1, pp. 1-40.
17. P. A. Denis, *Chem. Phys. Lett.*, 2011, **516**, 82-87.
18. A. Sygula and S. Saebø, *Int. J. Quantum Chem.*, 2009, **109**, 65-72.
19. D. Josa, J. Rodríguez Otero and E. M. Cabaleiro Lago, *Phys. Chem. Chem. Phys.*, 2011, **13**, 21139-21145.
20. G. Casella and G. Saielli, *New J. Chem.*, 2011, **35**, 1453-1459.
21. M. R. Kennedy, L. A. Burns and C. D. Sherrill, *J. Phys. Chem. A*, 2012, **116**, 11920-11926.
22. T. C. Dinadayalane, S. Deepa and G. N. Sastry, *Tetrahedron Lett.*, 2003, **44**, 4527-4529.
23. T. C. Dinadayalane, S. Deepa, A. S. Reddy and G. N. Sastry, *J. Org. Chem.*, 2004, **69**, 8111-8114.
24. R. Mahesh Kumar, M. Elango, R. Parthasarathi, D. Vijay and V. Subramanian, *J. Chem. Sci.*, 2012, **124**, 193–202.
25. S. Grimme, *J. Comput. Chem.*, 2004, **25**, 1463-1473.
26. S. Grimme, *J. Comput. Chem.*, 2006, **27**, 1787-1799.

27. S. Grimme, J. Antony, S. Ehrlich and H. Krieg, *J. Chem. Phys.*, 2010, **132**, 154104/1-154104/19.
28. S. Grimme, S. Ehrlich and L. Goerigk, *J. Comput. Chem.*, 2011, **32**, 1456-1465.
29. T. Janowski, P. Pulay, A. A. Sasith Karunarathna, A. Sygula and S. Saebø, *Chem. Phys. Lett.*, 2011, **512**, 155-160.
30. R. Ahlrichs, M. Bär, M. Häser, H. Horn and C. Kölmel, *Chem. Phys. Lett.*, 1989, **162**, 165-169.
31. D. Josa, J. Rodríguez-Otero, E. M. Cabaleiro-Lago and M. Rellán-Piñeiro, *Chem. Phys. Lett.*, 2013, **557**, 170-175.
32. S. Grimme, C. Mück-Lichtenfeld and J. Antony, *J. Phys. Chem. C*, 2007, **111**, 11199-11207.
33. S. F. Boys and F. Bernardi, *Mol. Phys.*, 1970, **19**, 553-566.
34. R. C. Haddon, *J. Am. Chem. Soc.*, 1990, **112**, 3385-3389.
35. In order to explain this fact, geometric reasons could be argued: the corannulene face of both fullerenes is very similar; however, in the case of C_{70} this face shows a slightly more pronounced curvature. This fact causes that π bonds of cyclobutadiene rings of 4 (especially, the outer ones) are more distant from the *spokes* of fullerene, and thus, π···π contacts are weakened. To quantify the difference in curvature of the corannulene face of C_{60} and C_{70}, POAV is an efficient tool. So, POAV angle of the *hub-spoke* carbons of the corannulene face (the carbons of the five-membered ring) is 11.64° and 11.84° for C_{60} and C_{70}, respectively. This difference may seem insignificant, but it is enough to increase the distance between the outer double bonds of cyclobutadiene and the *flank-spoke* carbons of fullerene from 3.217 to 3.230 Å (this small increase takes place in five contacts and it seems plausible to explain the decrease of a few tenths of kcal/mol in the interaction energy).
36. When the Grimme's empirical dispersion correction is added to B3LYP calculations (B3LYP-D), the geometry of compound 6 becomes no fully planar, with a curvature rather similar to that obtained with B97-D2 and MP2: POAV = 3.33°.
37. E. R. Johnson, S. Keinan, P. Mori-Sánchez, J. Contreras-García, A. J. Cohen and W. Yang, *J. Am. Chem. Soc.*, 2010, **132**, 6498–6506.
38. J. Contreras-Garcia, E. R. Johnson, S. Keinan, R. Chaudret, J. P. Piquemal, D. N. Beratan and W. Yang, *J.Chem. Theory Comput.*, 2011, **7**, 625-632.
39. M. Nishio, *Phys. Chem. Chem. Phys.*, 2011, **13**, 13873-13900.
40. M. Nishio, *J. Mol. Struct.*, 2012, **1018**, 2-7.
41. A. E. Reed, L. A. Curtiss and F. Weinhold, *Chem. Rev.*, 1988, **88**, 899-926.

Chapter 8

In search of buckybowls for fullerene recognition

8.1. Introduction

The discovery of a new form of elemental carbon, buckminsterfullerene (C_{60}),[1] in the mid-80s of last century has promoted a lot of research activities in the fields of physics, chemistry and materials science. In addition, this discovery has led to special interest on bowl-shaped polycyclic aromatic hydrocarbons (PAHs), commonly known as *buckybowls* or fullerene fragments. In contrast to other PAHs previously discovered, the curvature of buckybowls is not a consequence of addition bulky substituents, but of the impossibility of placing contiguous pentagons and hexagons in a planar sheet. Besides their pure scientific interest, buckybowls also represent chemical entities with future potential applications, especially for host-guest chemistry, such as the *buckycatcher* $C_{60}H_{28}$[2] made up by two corannulene units that can encapsulate fullerenes, or its more flexible analogue ($C_{52}H_{28}$) that can encapsulate solvating molecules of nitrobenzene in the solid state.[3]

The smallest buckybowl, corannulene (1, Figure 8.1) has been the subject of intense experimental and theoretical research in the last years.[4-17] Recently, Butterfield *et al.* have developed a process for synthesis of corannulene on a kilogram scale that reduces material costs by over 2 orders of magnitude compared to those of the published gram-scale synthesis.[16] Undoubtedly, this find represents a significant step for its future industrial commercialisation.

Nowadays, the design and synthesis of fullerene receptors is a very important field of research. Besides their great importance in the development of new materials in nanotechnology and nanoscience, they could also be crucial for the separation of fullerenes. This is because recent studies show that fullerenes and their derivatives represent potential health risks,[18, 19] and therefore, in the coming years, the need for chromatographic separation of fullerenes and their detection at low concentration will surely grow.[20]

As dispersion plays a major role in π···π interactions, maximising the host-guest complementarity is particularly important in molecular recognition of fullerenes, in terms of both the stability and the selectivity of complexes formed. In this context, the design and synthesis of molecular receptors for fullerenes incorporating buckybowls is very attractive, given that the concave surface of buckybowls can fit adequately to the convex surface of the fullerenes through concave-convex "ball-and-socket" π···π interactions.[2]

Although several buckybowls with different geometric and electronic properties have been synthesised in recent years, most studies of stacking interaction between buckybowls and fullerenes have focused on corannulene and its derivatives;[11, 13, 21] To the best of our knowledge, studies with sumanene,[11] pentaindenocorannulene[11] and bowl-shaped hexabenzocoronene derivatives have been reported.[21-23]

On the other hand, it is quite likely that changing the corannulene pincers of the double-concave hydrocarbon buckycatcher[2] by other buckybowls could be a good strategy to improve its efficiency. In this sense, recently, Denis has shown that changing these corannulene pincers by pentaindenocorannulene increases the interaction energy about 15 kcal/mol.[21, 24] Therefore, the aim of this work is to carry out a comprehensive theoretical study of stacking interactions between a series of buckybowls with different sizes and structures, and fullerenes. Our ultimate goal is finding the best buckybowl to improve the efficiency and/or selectivity of future *buckycatchers*.

8.2. Computational details

All complexes evaluated were optimised by the self-consistent charge density functional tight-binding method using an empirical correction to the dispersion (SCC-DFTB-D). The DFTB+ code was applied for this method, together with mio-1-1 parameter set.[25-28] Interaction energies were obtained at the B97-D2/TZVP level using the resolution of identity approximation (RI) as implemented in TURBOMOLE 5.10 program suite.[29] This level seems appropriate for this kind of study.[17]

Counterpoise corrections were applied to all reported interaction energies to avoid basis set superposition error (BSSE).[30] Furthermore, some selected complexes were also optimised at the B97-D2/TZVP level, in order to assess the performance of the B97-D2/TZVP//SCC-DFTB-D calculations for studying π···π interactions.

Visualisation of non-covalent interactions regions was performed using the NCIPLOT-3.0 program,[31, 32] and then graphics of the concave-convex π···π interactions were obtained using the VMD 1.9.1 software.[33] NCI enables identification of non-covalent interactions and is based on the peaks that appear in the reduced density gradient (RDG) at low densities. When an RDG isosurface for a low value of RDG is plotted, non-covalent regions clearly appear in the supramolecular complex. These interactions correspond to both favourable and unfavourable interactions. To differentiate between them, the sign of the second density Hessian eigenvalue times the density is colour-mapped onto the isosurface; bonding interactions can be identified by a negative

sign. To save computation time, promolecular densities have been used, as has been done previously with good results.[34]

8.3. Results and discussion

A series of stacking interactions between buckybowls and fullerenes (C_{60}, C_{70} and C_{40}) were evaluated in this work. Figure 8.1 shows the buckybowls studied, most of them previously synthesised.[22, 35-46] The first group (compounds 1-4) comprises the most popular buckybowl, corannulene (1), and three structures built from the central unit of corannulene. The second group includes sumanene (5) and three structures built from its central unit (6-8).

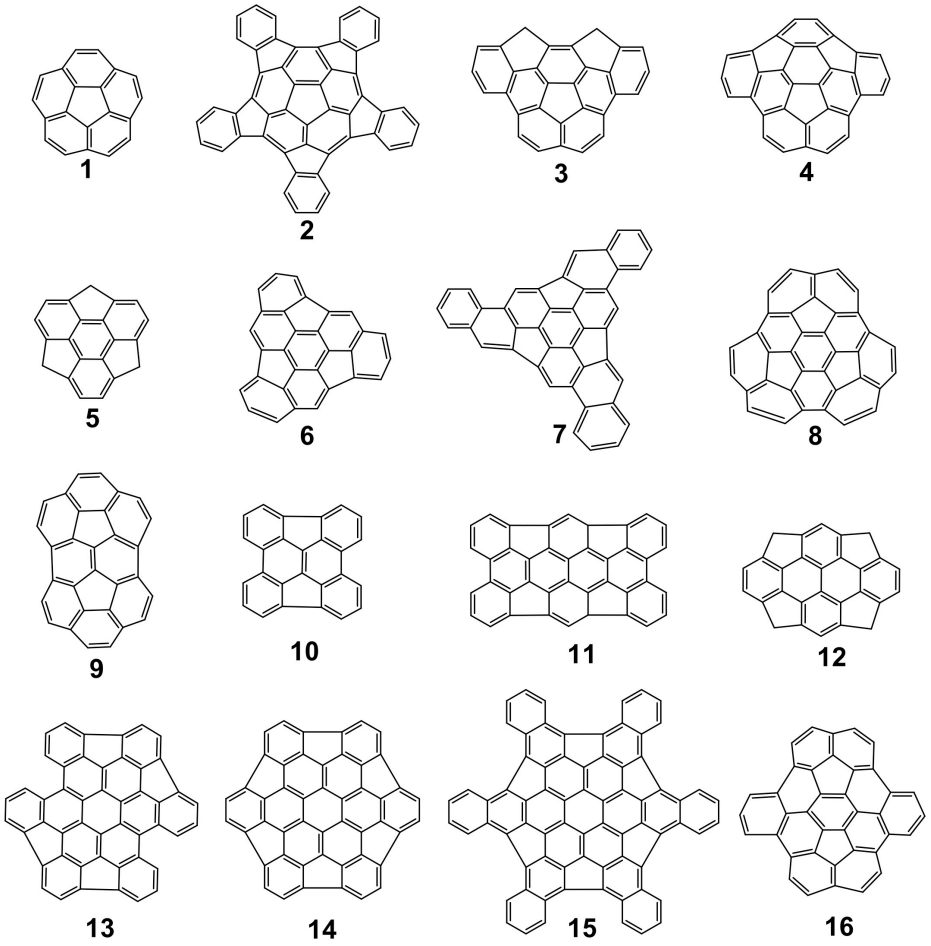


Figure 8.1: Buckybowls evaluated in this work.

In the third group, the geometrical centre of the structure is not a ring but a C-C bond; the central unit is a pyracyclene and it is expanded from its central position (compounds 9 and 10) or in a lateral position (compounds 11 and 12). The fourth group has a central unit of coronene. Coronene is a fully planar structure, but the addition of five-membered external rings leads to a bowl-shaped geometry (compounds 13-15). Finally, a slightly different kind of buckybowl was taken into account: compound 16. The prototypical buckybowls (such as corannulene or sumanene) corresponds to a fragment of fullerene C_{60}. However, compound 16 corresponds to a fragment of C_{70}. The structure of this latter compound could be considered as a fusion of two corannulene units, and it would be interesting to analyse its ability to supply a different environment for binding to fullerene. To the best of our knowledge, only compound 15 has not yet been synthetised; this compound was devised by us for trying to improve the "catching ability" of 14.

Complexes were optimised at the SCC-DFTB-D level and interaction energy calculations were performed at the B97-D2/TZVP level. Different faces of fullerenes and spatial dispositions were also taken into account in this study. All complexes were constructed by aligning of the central ring of the buckybowl with the central ring of the faces of fullerene, as shown in section C.1 (Appendix C). Section C.2 (Appendix C) explains the "building" and the naming of complexes.

8.3.1. Performance of B97-D2//SCC-DFTB-D for studying π···π interactions

According to several studies, B97-D2 seems a good approach for studying π···π interactions.[10, 12, 13, 17, 47-50] However, B97-D2 is still quite time-consuming to be employed in a systematic search for suitable strategies for improving the efficiency and/or selectivity of fullerene receptors, especially for studying complexes without any symmetry.

Recently, Sygula and Collier have suggested the use of molecular mechanics (MM) methods as rapid screening tool for designing molecular tweezers and clips.[20] Although their results are fairly acceptable, a most accurate description of concave-convex π···π interactions could be very useful in the selection of suitable strategies to design new fullerene receptors. On the other hand, the recent SCC-DFTB-D approach has not only shown outstanding time/performance efficiency in several studies, but also does not require large number of empirical parameter fields to describe molecular properties.[51, 52] Therefore, taking into account the limitations of MM methods, we believe that SCC-DFTB-D approach could be a more balanced and suitable screening tool.

Thus, the performance of the B97-D2//SCC-DFTB-D method regarding the full B97-D2 was evaluated for four groups of complexes with π···π interactions: (1) complexes with eclipsed PAHs; (2) complexes with curved PAHs; (3) mixed complexes made up by planar and curved PAHs; and (4) complexes made up by curved PAHs and C_{60}. Table 8.1 shows the results for the first three groups, obtained previously by us at the B97-D2/cc-pVTZ level[49] and Table 8.2 shows the results for the last group performed at the B97-D2/TZVP level. The complexes in Table 8.2 were chosen by trying to select a diverse set of buckybowls and including several faces of fullerenes.

Table 8.1: Interaction energies, E_{int}, (kcal/mol) and equilibrium distances, d_{eq}, (Å) for different complexes with π···π interactions studied previously.[49] The percentage of error in the B97-D2/TZVP//SCC-DFTB-D interaction energy (less favourable interaction) regarding to the B97-D2/cc-pVTZ value is shown in parentheses

	B97-D2/cc-pVTZ[a]		B97-D2/TZVP//SCC-DFTB-D	
	d_{eq}	E_{int}	d_{eq}	E_{int}
		Planar complexes		
Benzene dimer	3.90	-1.60	3.55	-0.53 (67%)
Naphthalene dimer	3.77	-4.12	3.54	-2.70 (35%)
Anthracene dimer	3.73	-6.83	3.54	-5.12 (25%)
Pyrene dimer	3.69	-8.93	3.53	-7.20 (19%)
Coronene dimer	3.64	-16.30	3.53	-14.13 (13%)
		Curved complexes		
1···1	3.62	-16.06	3.73	-14.95 (7%)
5···5	3.62	-21.09	3.94	-18.02 (15%)
1···5	3.63	-16.89	3.80	-15.20 (10%)
5···1	3.70	-18.18	3.94	-16.40 (10%)
		Curved and planar complexes		
Coronene···1	3.25	-17.17	3.36	-15.65 (9%)
Coronene···5	3.18	-17.10	3.28	-14.85 (13%)

[a] Data from reference 49.

Table 8.2: Interaction energies, E_{int}, (kcal/mol) and equilibrium distances, d_{eq}, (Å) for different cases of curved complexes with C_{60}. The percentage of error in the B97-D2/TZVP//SCC-DFTB-D interaction energy (less favourable interaction) regarding to the B97-D2/TZVP value is shown in parentheses

	B97-D2/TZVP		B97-D2/TZVP//SCC-DFTB-D	
	d_{eq}	E_{Int}	d_{eq}	E_{Int}
1···C_{60}(F_1-e)	3.456	-17.03	3.636	-16.42 (4%)
2···C_{60}(F_1-s_{36})	4.086	-37.95	4.313	-36.56 (4%)
5···C_{60}(F_2-s_{60})	3.450	-20.40	3.856	-17.77 (13%)
6···C_{60}(F_2-e)	4.005	-22.53	4.206	-21.52 (5%)
6···C_{60}(F_2-s_{30})	4.091	-22.29	4.221	-21.62 (3%)
6···C_{60}(F_2-s_{60})	3.977	-22.96	4.238	-21.70 (6%)
8···C_{60}(F_2-e)	5.054	-19.76	5.062	-19.53 (1%)
8···C_{60}(F_2-s_{30})	4.885	-22.69	5.011	-22.26 (2%)
8···C_{60}(F_2-s_{60})	5.094	-19.41	5.063	-19.13 (2%)
10···C_{60}(F_1-1)	3.529	-22.58	3.786	-21.12 (7%)
10···C_{60}(F_1-2)	3.527	-22.63	3.786	-21.12 (7%)
10···C_{60}(F_2-1)	3.637	-22.58	3.873	-21.60 (4%)
10···C_{60}(F_2-2)	3.599	-22.91	3.867	-21.40 (7%)
14···C_{60}(F_1)	4.483	-29.54	4.729	-27.98 (5%)
14···C_{60}(F_2-1)	4.463	-30.30	4.685	-28.77 (5%)
14···C_{60}(F_2-2)	4.577	-26.55	4.641	-25.06 (6%)
15···C_{60}(F_2-1)	4.130	-49.80	4.223	-49.47 (1%)
$C_{60}H_{28}$···C_{60}		-39.92		-38.55 (4%)

Regarding the geometry of dimers, the results in Tables 8.1 and 8.2 show a moderate increase in the equilibrium distance between the monomers (taken as the distance between the centre of the buckybowl´s central ring and the centre of the ring of the fullerene directly facing it) obtained at the SCC-DFTB-D level, relative to that obtained at the B97-D2 level. There are only two clear exceptions to this trend: planar complexes, where the trend is opposite, and complexes 8···C_{60}, where equilibrium distances are very similar at the two calculation levels (a difference of only about a tenth of an Ångström arises). As will be discussed later, this distinctive feature of compound 8 is related to its particular structure (closed and deep): this fact leads to very distant fullerenes, regardless of the level of calculation.

Obviously, the quality of the interaction energies obtained using the SCC-DFTB-D geometries is directly related to the quality of these geometries, which do not seem too bad, as they lead to rather satisfactory interaction energies. The worst results correspond to complexes formed from planar monomers, but even in this case the results improve as the size increases, reaching a moderate error (about 2 kcal/mol, 13%) for the coronene dimer. Therefore, B97-D2/TZVP//SCC-DFTB-D calculations could also seem appropriate for studying large π···π planar complexes. For complexes with curved monomers the energy results are much better and even errors of only 1% are obtained. Moreover, the correlation between interaction energies is excellent (R^2 = 0.995) as shown in Figure 8.2, which includes the results for the complexes with C_{60} in Table 8.2. Only complex 5···C_{60} deviates slightly from linear behaviour, although not by much. This is also directly related to the outstanding energetic error in Table 8.2 (13%), which in turn is a consequence of the largest difference in equilibrium distance (more than 4 tenths of an Ångström). On the other hand, complexes 8···C_{60} are found to have very small errors of 1-2%, as expected from their good geometries. It certainly appears somewhat similar with the complex 15···C_{60}, with an error of 1%, as a result of a difference smaller to a tenth of an Ångström in the equilibrium distance.

As already mentioned, the worst results in Table 8.2 and Figure 8.2 corresponds to the 5···C_{60} complex (the complex between sumanene and fullerene), but if Table 8.1 is analysed at the same time (for complexes with curved monomers), it is easy to realise that the worst results correspond to those cases involving sumanene, especially when it is doubly involved (5···5, 15%). However, the participation of corannulene leads to clearly better results: an error of between 7% (corannulene dimer) and 10%. In the same way the complex designed by Sygula *et al.*,[2] $C_{60}H_{28}$···C_{60} (which incorporates two corannulene units), shows an error of only 4%.

In summary, for complexes with curved monomers B97-D2/TZVP//SCC-DFTB-D calculations lead to very reasonable interaction energies if compared with the full B97-D2 values. With the only exception being complexes with sumanene, the difference in interaction energy ranges from 0.23 to 1.56 kcal/mol (which corresponds to an error of 1-7%). When sumanene is involved, the results are slightly worse, with a difference of 2.63 kcal/mol (13%) for the complex with C_{60}. At first sight, inspection of the structure of buckybowls in Table 8.2 leads to a first hypothesis: only sumanene includes sp^3 carbon atoms, *i.e.*, only this buckybowl has the ability to establish C-H···π interactions with fullerene. This kind of interaction can play a quite important role, as shown recently, since it especially takes place for compounds with saturated rings, where the internal

hydrogen atom of a CH_2 group points directly at the π cloud of fullerenes.[17] It would not be surprising that the SCC-DFTB-D method was not able to account for this subtle effect. For that reason, the monomers are not close enough and the reproduction of the interaction energy is slightly less accurate when sumanene participates.

In brief, despite some limitations, the B97-D2/TZVP//SCC-DFTB-D approach provides sufficiently accurate results, so that it can be used as a useful tool for a rapid selection of suitable strategies for rational design of molecular clips and tweezers. Moreover, the SCC-DFTB-D method can also be very useful to provide start guess for more accurate calculations of the largest π···π complexes.

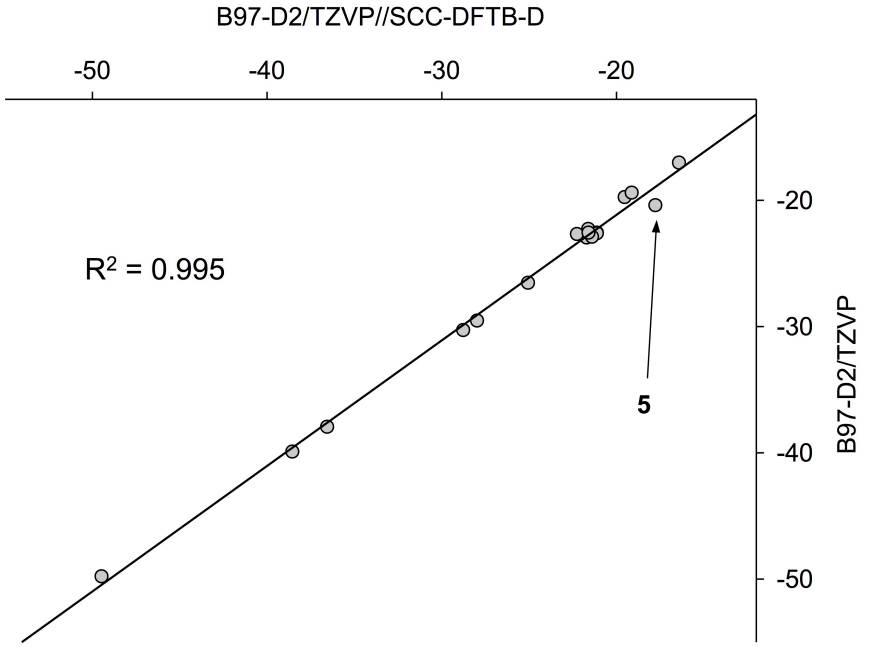


Figure 8.2: B97-D2/TZVP *vs.* B97-D2/TZVP//SCC-DFTB-D interaction energy (kcal/mol). Linear fit gave $E_{int\ (B97\text{-}D2/TZVP)} = 0.9942E_{int\ (B97\text{-}D2/TZVP//SCC\text{-}DFTB\text{-}D)} - 1.271$ with an R^2 value of 0.995.

8.3.2. Stacking interactions between buckybowls and fullerenes C_{60}, C_{70}, and C_{40}

Dispersion interactions play the most prominent role in the association of buckybowls with fullerenes.[17] So, it seems very obvious that increasing the buckybowl size will lead to an enhancement of the interaction with the fullerene. However, the key question is: how to increase the buckybowl size to maximise fullerene recognition? In

order to answer this question, the stacking interactions between a series of buckybowls and fullerene C_{60} has been evaluated.

First, the stacking interaction, taking into account different faces of fullerene C_{60}, was evaluated in order to obtain the most favourable face for interacting with buckybowls. According to our results, the stacking interaction with different faces of C_{60} leads to energy differences ranging from 0.31 to 3.71 kcal/mol (section C.3, Appendix C). Therefore, it seems that the choice of the face is not relevant in some cases, but it is crucial to get the correct results in others. A similar analysis was performed with fullerenes C_{70} and C_{40}, but only with some selected buckybowls: 1 and 5, the most popular buckybowls, corannulene and sumanene; 2 and 6, variants of the above two; 8, a very particular buckybowl (a highly enclosed bowl with a very large depth); 10, the most simple example of buckybowls derived from pyracyclene; and 15, an example of the coronene derived structures, and clearly the best buckycatcher for C_{60}. According to our results (section C.3, Appendix C), comparable conclusions to those obtained with C_{60} were drawn. The main difference is that, for complexes with these two fullerenes, the choice of the face is more critical: there are no cases where this selection is irrelevant, since it always leads to differences higher than 1 kcal/mol in interaction energy. In general these differences (especially with C_{70}, ranging from 1.61 to 3.93 kcal/mol) are always higher if compared with those for the analogous complexes with C_{60}. This is a fairly reasonable result, since C_{60} is the most spherical fullerene and therefore the particular face for binding to the bowl should be less relevant.

Taking into account only the best case (largest interaction energy) for each buckybowl···fullerene complex, Table 8.3 summarises the equilibrium distances, d_{eq}, at the SCC-DFTB-D level, and Figure 8.3 shows a comparison of the calculated interaction energies.

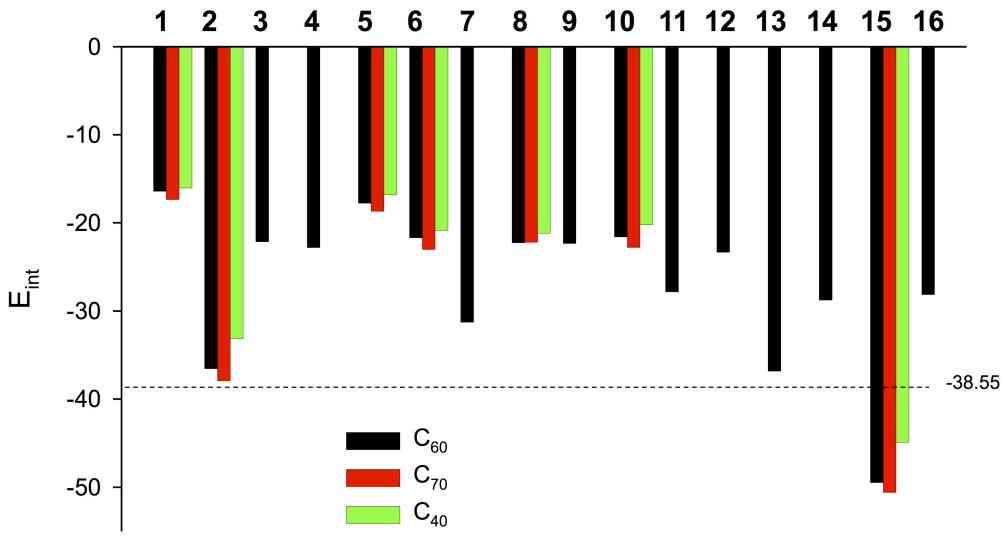


Figure 8.3: B97-D2/TZVP//SCC-DFTB-D interaction energy (kcal/mol) for complexes buckybowl···fullerene.

Table 8.3: Equilibrium distances (Å) for the most stable conformation of the studied complexes. All optimisations were performed at the SCC-DFTB-D level

	X = C_{60}	X = C_{70}	X = C_{40}
1···X	3.636	3.644	3.649
2···X	4.313	4.361	4.328
3···X	4.075[a]		
4···X	3.862[a]		
5···X	3.856	3.912	3.596[a]
6···X	4.238	4.047[a]	4.128
7···X	4.197		
8···X	5.011	5.003	4.907
9···X	4.412		
10···X	3.873	3.907	3.804
11···X	4.300[a]		
12···X	4.084		
13···X	3.373[a]		
14···X	4.685		
15···X	4.223	4.096[a]	3.836
16···X	4.101		

[a] In these complexes the buckybowl's central ring is significantly displaced from the centre of the face of the fullerene used to build the complex; therefore, d_{eq} is taken to be the distance between the centre of the buckybowl's central ring and the closest atom of the fullerene.

As expected, none general correlation between equilibrium distance and interaction energy was found (section C.4, Appendix C), because differences in the structure of the buckybowls are too large. Only in the case of compound 13 with C_{60} was a significantly shorter equilibrium distance found than for 1, corannulene. Compound 8 leads to the complexes with the largest d_{eq}, which is a consequence of the enclosed and deep structure of this buckybowl, as already commented above.

Figure 8.3 shows that, in general, interaction with C_{70} is slightly more favourable than that with C_{60}; however, the interaction with C_{40} is significantly less favourable. Consequently, it is not expected that these buckybowls will specifically bind either of the fullerenes when exposed to a C_{60}/C_{70} mixture, since the major difference between binding to C_{60} and C_{70} is only about 1.3 kcal/mol, for compounds 2 and 6. With C_{40} the differences, relative to C_{60}, are higher, reaching 3.43 and 4.56 kcal/mol for compounds 2 and 15; thus some selectivity could be found, especially when compound 15 is exposed to a C_{60}/C_{40} mixture (but this combination is not very common, since C_{60} is usually mixed with larger fullerenes).

According to Figure 8.3, compounds 2, 7, 13, and 15 lead to the most favourable cases (interaction energies stronger than -30 kcal/mol). Compounds 2, 7, and 15 show a rather interesting particularity: they are the only ones that have a ring that shares only one bond with the *rim* of the bowl; that external ring might be called a *flap*. As can be seen, these three buckybowls show a noteworthy improvement in fullerene recognition

compared to buckybowls of the same group without *flaps*. It could be argued that this improvement might simply be caused by the increase in the size of the bowl, with a subsequent increase in dispersion. This issue has no simple answer, but, if the behaviours of compounds 14 and 15 are compared (the only case where the same structure is available with and without *flaps*), then it can be observed that a increase in the bowl size (from 48 to 72 carbon atoms, 50%) leads to a significantly higher increase in the interaction energy with C_{60} (from -28.77 to -49.47 kcal/mol, 72%). Compound 13 leads to one of the highest interaction energies (-36.26 kcal/mol with C_{60}) but it does not have *flaps*, as these are described above. However, this compound has four external hexagonal rings that act in a similar manner. They are less able to bend as in the case of the real *flaps* (anchoring to the *rim* of the bowl takes place by sharing two bonds), but its structure is flexible enough for "embracing" the fullerene to some extent. This ability leads to an increase in the interaction energy with C_{60} of 26% if compared with that of compound 14, both compounds having very similar sizes. Moreover, it is worth noting that only for this compound 13 is the equilibrium distance in its complex with C_{60}, d_{eq}, smaller than that of corannulene, 1.

As already noted, a possible way to measure the efficiency of a receptor is comparing its size with the interaction energy that it causes. This is because simply by increasing the size of a receptor an increase in dispersion energy is achieved when this receptor binds to a fullerene. Although the number of C atoms in a structure is not a very reliable measure of the size of this structure, it may account for the relevance of dispersion. As expected, Figure 8.4 shows a rather good correlation between the number of C atoms in a bowl and its interaction energy with C_{60} (R^2 = 0.937). Nevertheless, the most important thing is detecting deviations from linear behaviour when looking for the most efficient receptors; that is to say, the receptors that produce large interaction energies without a large increase in size. In this respect, it seems clear that compounds 2, 7, 10, 12, 15, and especially 13, are efficient receptors with larger interaction energy than predicted by their size. Compounds 2, 7, 13, and 15 (with some kind of *flaps*) have already been commented on above, and thus Figure 8.4 reinforces the previous conclusions. Compounds 10 and 12 also work rather well, with larger interaction energy than predicted from their size. However, due to their small size, this good performance in relative terms is not so good in absolute terms. Compounds 3, and especially 8 and 14 are found in the opposite situation, with smaller interaction energies than predicted from their size. They are very rigid and compact structures with little ability to "embrace" fullerenes. Especially poor is the performance of compound 14, a large bowl with rather modest "catching" aptitude. Addition of *flaps* to this structure leads to buckybowl 15 (proposed here, but not yet synthesised): clearly the strongest fullerene receptor obtained. It almost triples the interaction produced by corannulene, 1, and leads to an increase of about 11 kcal/mol in the interaction energy if compared with that of the tweezers designed by Sygula *et al*.[2] These tweezers (shown in red in Figure 8.4) do not have high efficiency relative to their number of C atoms, but this is not surprising since, in this case, not all the C atoms face directly the fullerene (as it is the case of a significant part of the tetrabenzocyclooctatetraene tether).

In summary, an important conclusion could be that addition of *flaps* to the bowl *rim* seems a promising strategy for designing more effective fullerene receptors. The addition of these *flaps* not only increases the size of the π-system, but does so in an

advantageous manner, since the slight flexibility of the *flaps* favours the "embrace" of fullerenes. Although this flexibility is rather small, it is strong enough to modify significantly the distance between the external rings and the fullerene, thereby modifying the dispersion effects (see Section C.5 from Appendix C). If the bowl does not have any kind of *flaps*, it should at least have some flexibility in order to be an efficient fullerene receptor. Therefore, in general, large rigid structures can be good receptors but with an efficiency much less than predicted from their size.

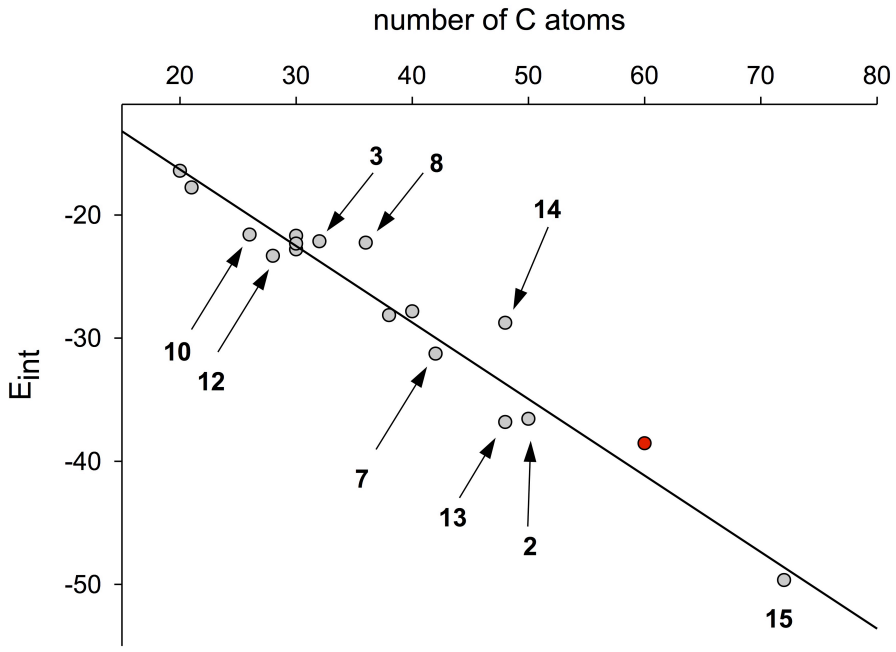


Figure 8.4: Relationship between the bowl size (given by the number of carbons, N_C) and the interaction energy (kcal/mol): $E_{int} = -0.6218N_C - 3.859$ with an R^2 value of 0.937. The red point corresponds to the tweezers designed by Sygula *et al.*[2]

In order to analyse in more detail the balance of energy contributions to the stability of the complexes, the interaction energy was decomposed according to a very simple method. So, the two main contributions from the model employed were taken into account: that is, the pure B97 interaction energy and the empirical dispersion contribution to the interaction energy. Results in Table 8.4 show that dispersion plays a crucial role in the interaction energy of complexes. First, because the contribution from the pure B97 functional is clearly repulsive, so dispersion is responsible for the binding in complexes. Secondly, and more noteworthy, as can be seen in Figure 8.5, there is an excellent correlation between the dispersion and interaction energies for the complexes evaluated (with R^2 = 0.985, 0.996, and 0.996 for complexes with C_{60}, C_{70}, and C_{40}, respectively). Only bowls 3, 10, and 11 when complexed with C_{60} deviate from perfectly linear behaviour by a somewhat appreciable difference: compound 10 leads to a larger interaction energy than that predicted from dispersion; compounds 3 and 11 lead to the

opposite situation. In order to explain these minimal discrepancies, a qualitative analysis based on the contribution of electrostatics to interaction energy (similar to that performed previously in a recent paper[17]) has been carried out (see section C.6, Appendix C).

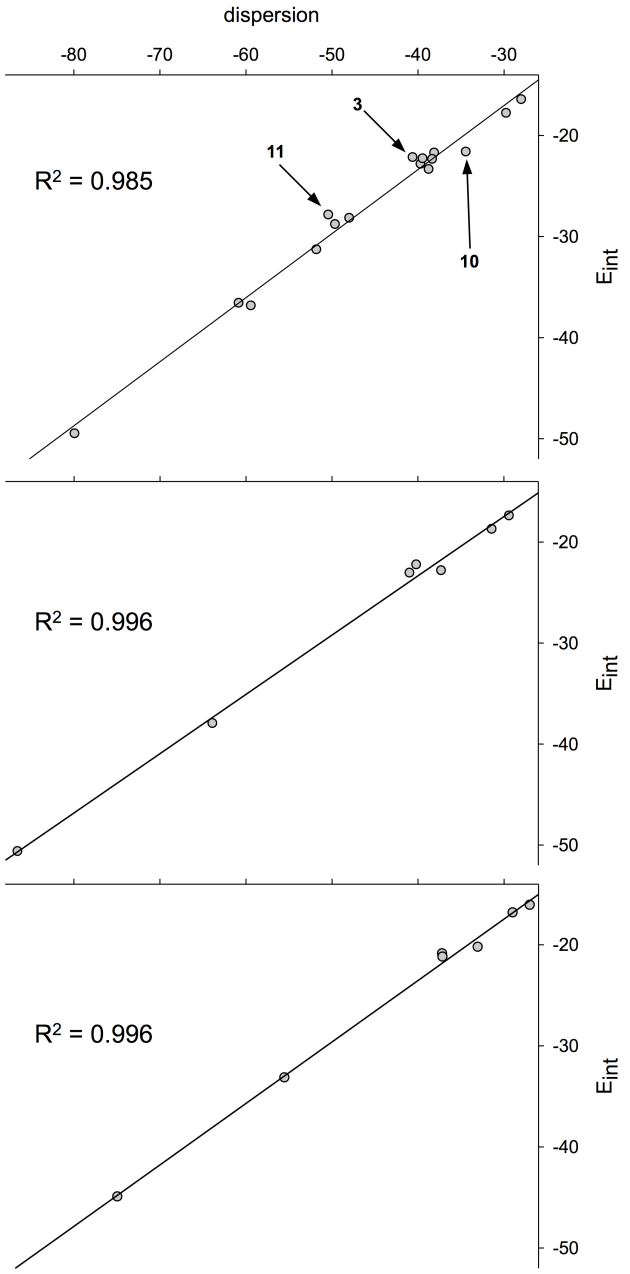


Figure 8.5: Interaction energy *vs.* dispersion component (kcal/mol). Top: complexes with C_{60}; $E_{int} = 0.6337E_{disp} + 1.983$, $R^2 = 0.985$. Middle: complexes with C_{70}; $E_{int} = 0.5867E_{disp} + 0.1327$, $R^2 = 0.996$. Bottom: complexes with C_{40}; $E_{int} = 0.6082E_{disp} + 0.8041$, $R^2 = 0.996$.

Table 8.4: B97 component of the interaction energy and dispersion contribution (kcal/mol) for the most stable complexes (optimised at the SCC-DFTB-D level) calculated at the B97-D2/TZVP level

	X = C_{60}		X = C_{70}		X = C_{40}	
	B97	Dispersion	B97	Dispersion	B97	Dispersion
1···X	11.59	-28.01	12.05	-29.41	10.97	-27.02
2···X	24.30	-60.86	26.00	-63.92	22.41	-55.54
3···X	18.48	-40.63				
4···X	16.90	-39.71				
5···X	12.00	-29.77	12.73	-31.42	12.19	-29.00
6···X	16.43	-38.13	17.96	-40.99	16.35	-37.21
7···X	20.55	-51.82				
8···X	17.22	-39.48	17.99	-40.20	15.98	-37.16
9···X	16.04	-38.37				
10···X	12.85	-34.45	14.52	-37.31	12.86	-33.06
11···X	22.60	-50.43				
12···X	15.44	-38.77				
13···X	22.61	-59.43				
14···X	20.89	-49.66				
15···X	30.46	-79.93	35.99	-86.59	30.04	-74.95
16···X	19.85	-48.00				

Finally, a qualitative non-covalent interactions (NCI) analysis was performed to obtain more information about π···π interactions and more data about the behaviour of the different bowls. The visualisation of π···π interactions between the two monomers in the real space was drawn using VMD software[33] with an isosurface of 0.4 a.u. and scale running from -0.020 (min) to 0.020 a.u. (max): blue, green and red indicate strongly attractive, weak and strongly repulsive interactions, respectively. Figure 8.6 shows the NCI plots for complexes with C_{60} (section C.7 from Appendix C includes more views of the NCI plots). The first thing that catches the eye in this figure is that compounds 8 and 14 (which are the most inefficient ones in relation to their size, as discussed above) are precisely those that show the most significant discontinuities in their RDG isosurfaces. This is undoubtedly related to the fact, as previously commented, that these two bowls have very compact and deep structures, which leads to the longest equilibrium distances (4.685 Å for 14···C_{60}, and especially 5.011 Å for 8···C_{60}). For this reason, for these two compounds the interaction with fullerene is much more important with the walls than with the bottom of the bowl. Even so, for compound 14 the interaction is still rather important due to the considerable size of its surface (a consequence of the size of compound) and the significant attractive zones. In general, the best receptors in absolute terms, such as 2, 7, 11, 13, 15, and 16 or in relative terms (in relation to their size) also including 10 and 12, are indicated by large and continuous RDG surfaces with important attractive zones (blue). Compound 7 is the only exception to this trend: in this case, the small discontinuity in the surface is compensated for by the presence of three strong attractive areas. The surface of 11···C_{60} clearly shows the displacement of fullerene to the right side of the bowl, weakening the interaction in the other side. Comparison of NCI plots of 14···C_{60} and 15···C_{60} shows the huge difference between these two cases: the addition of *flaps* not only increases the interaction surface but it also removes its

discontinuities. This causes a huge shortening in the equilibrium distance: 0.462 Å. In summary, NCI plots reinforce the conclusion that shape of a buckybowl plays a fundamental role for the enhancement of fullerene recognition.

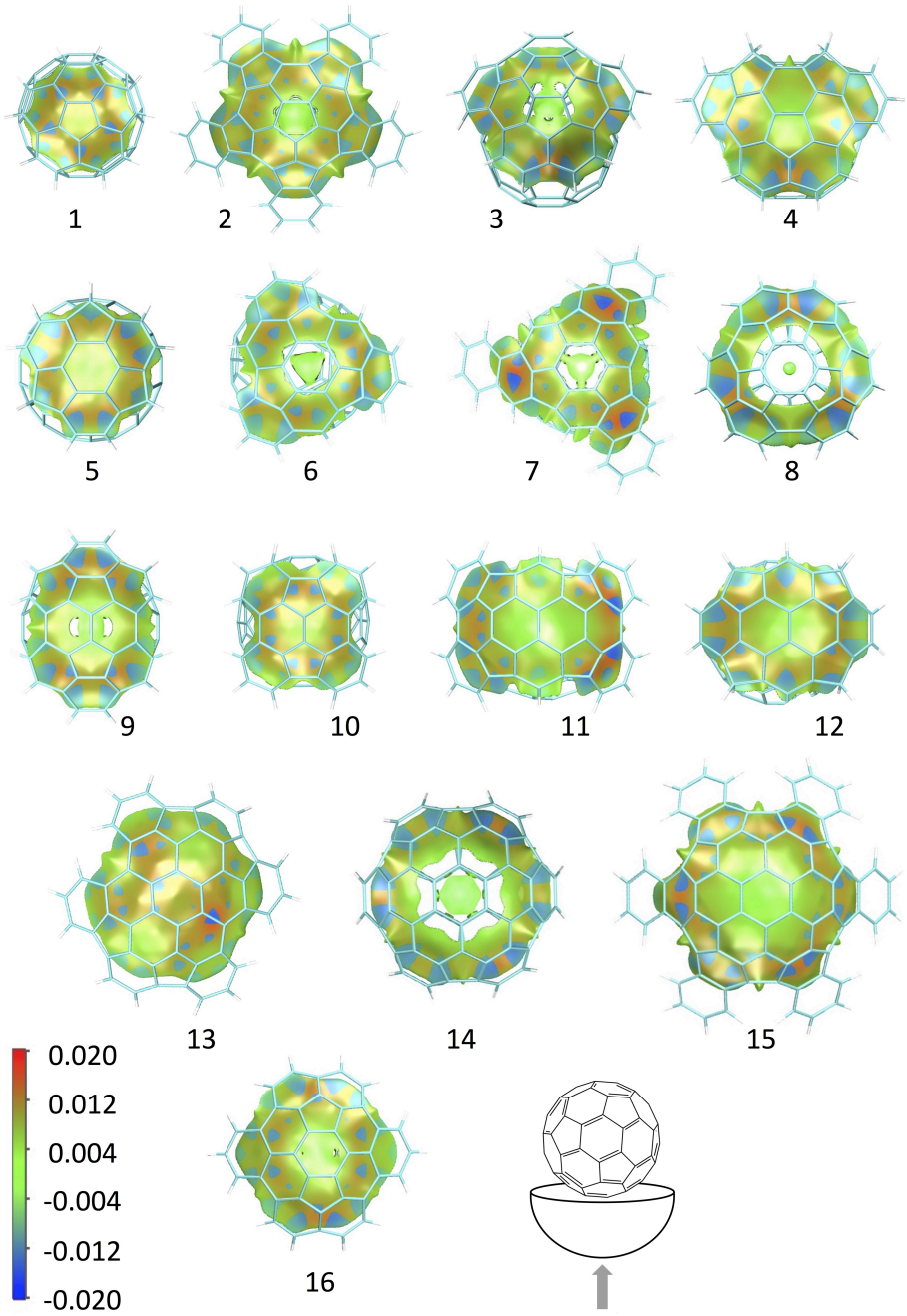


Figure 8.6: Bottom views (following the arrow) of the NCIPLOT gradient isosurface (0.4 a.u.). The surfaces are coloured on a blue-green-red scale according to the strength and type (attractive or repulsive) of interaction. Blue indicates strong attractive interactions, green indicate weak VdW interactions, and red indicates strong nonbonded overlap. Front and top views of NCIPLOT are available in section C.7 from Appendix C.

8.4. Conclusions

According to our results, the B97-D2/TZVP//SCC-DFTB-D approach seems to be a useful tool for a rapid selection of suitable strategies for rational evaluation and design of fullerene receptors. Fullerene orientation relative to the bowl has very little importance in some cases, but in others it is essential to get proper results (differences of almost 4 kcal/mol can be obtained).

Dispersion plays a crucial role on the interaction energy in these complexes: it is responsible for the binding in them, showing an excellent correlation with the interaction energies (the minimal deviations can be explained by a qualitative analysis based on the contribution of electrostatics to interaction energy). As expected, an increase in dispersion energy shows a fairly good correlation with an increase on bowl size. However, there are some substantial deviations, which can be attributed to the shape of the bowl. In this way, compounds whose structure possesses *flaps* at the *rim* of the bowl show an enhanced ability to interact with fullerenes. On the contrary, compounds with very rigid and compact structures show little ability to "embrace" fullerenes.

The largest interaction corresponds to complexes with the devised compound 15, a bowl-shaped hexabenzocoronene derivative. This buckybowl has a large size and added *flaps*, which allows obtaining interaction energies of about 50 kcal/mol (triple than that achieved with corannulene). However, in relation to its size, the most efficient receptor is compound 13, which also has a kind of *flap*. This type of appendix not only increases the size of the π-system, but also does so in an advantageous manner since their slight flexibility favours the "embrace" of fullerenes. If the bowl does not have any kind of *flap*, it should at least have some flexibility in order to be an efficient fullerene receptor. For this reason, large compounds with a very rigid structure can be good receptors but with an efficiency much smaller than predicted from their size.

NCI plots reinforce the conclusion that the shape of the buckybowl plays a fundamental role for the enhancement of fullerene recognition. The best receptors are indicated by large and continuous RDG surfaces with important attractive zones.

Finally, it is worth mentioning that the interaction energies for the complexes with C_{70} only show small increases with respect to those obtained with C_{60}. On the other hand, complexes with C_{40} show a significant decrease in their interaction energy regarding to C_{60} and C_{70}. The greatest differences take place for buckybowls 2 and 15, which show a decrease of 3.43 and 4.56 kcal/mol regarding to C_{60}, respectively. Curiously, buckybowls 2 and 15 are the only ones (studied with C_{40}) having *flaps* in their structure. So, the addition of *flaps* on the *rim* of the bowl could perhaps also be a useful strategy for designing buckybowls for the selective separation of fullerenes from mixtures.

8.5. References

1. H. W. Kroto, J. R. Heath, S. C. O'Brien, R. F. Curl and R. E. Smalley, *Nature*, 1985, **318**, 162-163.
2. A. Sygula, F. R. Fronczek, R. Sygula, P. W. Rabideau and M. M. Olmstead, *J. Am. Chem. Soc.*, 2007, **129**, 3842-3843.
3. L. Kobryn, W. P. Henry, F. R. Fronczek, R. Sygula and A. Sygula, *Tetrahedron Lett.*, 2009, **50**, 7124-7127.
4. T. J. Seiders, K. K. Baldridge, G. H. Grube and J. S. Siegel, *J. Am. Chem. Soc.*, 2001, **123**, 517-525.
5. K. Kavitha, M. Manoharan and P. Venuvanalingam, *J. Org. Chem.*, 2005, **70**, 2528-2536.
6. A. K. Kandalam, B. K. Rao and P. Jena, *J. Phys. Chem. A*, 2005, **109**, 9220-9225.
7. P. A. Denis, *THEOCHEM*, 2008, **865**, 8-13.
8. M. A. Petrukhina, K. W. Andreini, J. Mack and L. T. Scott, *J. Org. Chem.*, 2005, **70**.
9. A. Sygula and S. Saebø, *Int. J. Quantum Chem.*, 2009, **109**, 65-72.
10. T. Janowski, P. Pulay, A. A. Sasith Karunarathna, A. Sygula and S. Saebø, *Chem. Phys. Lett.*, 2011, **512**, 155-160.
11. P. A. Denis, *Chem. Phys. Lett.*, 2011, **516**, 82-87.
12. D. Josa, J. Rodríguez Otero and E. M. Cabaleiro Lago, *Phys. Chem. Chem. Phys.*, 2011, **13**, 21139-21145.
13. I. Welsh and M. Lein, *J. Comput. Chem.*, 2014, **35**, 181-191.
14. M. Rellán Piñero, J. Rodríguez Otero, E. M. Cabaleiro Lago and D. Josa, *J. Mol. Model.*, 2013, **19**, 2049-2055.
15. M. R. Kennedy, L. A. Burns and C. D. Sherrill, *J. Phys. Chem. A*, 2012, **116**, 11920-11926.
16. A. M. Butterfield, B. Gilomen and J. S. Siegel, *Org. Process Res. Dev.*, 2012, **16**, 664-676.
17. D. Josa, L. Azevedo dos Santos, I. González-Veloso, J. Rodríguez-Otero, E. M. Cabaleiro-Lago and T. de Castro Ramalho, *RSC Adv.*, 2014, **4**, 29826-29833.
18. J. Gao, H. L. Wang, A. Shreve and R. Iyer, *Toxicol. Appl. Pharmacol.*, 2010, **244**, 130-143.
19. E. J. Park, H. Kim, Y. Kim, J. Yi, K. Choi and K. Park, *Toxicol. Appl. Pharmacol.*, 2010, **244**, 226-233.
20. A. Sygula and W. E. Collier, Molecular Clips and Tweezers with Corannulene Pincers, in *Fragments of Fullerenes and Carbon Nanotubes: Designed Synthesis, Unusual Reactions, and Coordination Chemistry* (eds M. A. Petrukhina and L. T. Scott), John Wiley & Sons, Inc., Hoboken, NJ, USA, 2012, ch.1, pp. 1-40.
21. P. A. Denis, *RSC Adv.*, 2013, **3**, 25296-25305.
22. A. C. Whalley, K. N. Plunkett, A. A. Gorodetsky, C. L. Schenck, C.-Y. Chiu, M. L. Steigerwald and C. Nuckolls, *Chem. Sci.*, 2011, **2**, 132-135.
23. G. Casella and G. Saielli, *New J. Chem.*, 2011, **35**, 1453-1459.
24. P. A. Denis, *Chem. Phys. Lett.*, 2014, **591**, 323–327.
25. M. Elstner, D. Porezag, G. Jungnickel, J. Elsner, M. Haugk, T. Frauenheim, S. Suhai and G. Seifert, *Phys. Rev. B*, 1998, **58**, 7260-7268.
26. M. Elstner, T. Frauenheim and S. Suhai, *Phys. Status Solidi B*, 2000, **217**, 357-376.

27. M. Elstner, P. Hobza, T. Frauenheim, S. n. Suhai and E. Kaxiras, *J. Chem. Phys.*, 2001, **114**, 5149-5155.
28. M. Elstner, K. J. Jalkanen, M. Knapp-Mohammady, T. Frauenheim and S. Suhai, *Chem. Phys.*, 2001, **263**, 203-219.
29. R. Ahlrichs, M. Bär, M. Häser, H. Horn and C. Kölmel, *Chem. Phys. Lett.*, 1989, **162**, 165-169.
30. S. F. Boys and F. Bernardi, *Mol. Phys.*, 1970, **19**, 553-566.
31. E. R. Johnson, S. Keinan, P. Mori-Sánchez, J. Contreras-García, A. J. Cohen and W. Yang, *J. Am. Chem. Soc.*, 2010, **132**, 6498–6506.
32. J. Contreras-Garcia, E. R. Johnson, S. Keinan, R. Chaudret, J. P. Piquemal, D. N. Beratan and W. Yang, *J.Chem. Theory Comput.*, 2011, **7**, 625-632.
33. W. Humphrey, A. Dalke and K. Schulten, *J. Mol. Graphics*, 1996, **14**, 33-38.
34. D. Josa, J. Rodriguez-Otero, E. M. Cabaleiro-Lago, L. A. Santos and T. C. Ramalho, *J. Phys. Chem. A*, 2014, **118**, 9521-9528.
35. W. E. Barth and R. G. Lawton, *J. Am. Chem. Soc.*, 1966, **88**, 380-381.
36. E. A. Jackson, B. D. Steinberg, M. Bancu, A. Wakamiya and L. T. Scott, *J. Am. Chem. Soc.*, 2007, **129**, 484-485.
37. T. C. Wu, H. J. Hsin, M. Y. Kuo, C. H. Li and Y. T. Wu, *J. Am. Chem. Soc.*, 2011, **133**, 16319-16321.
38. H. Sakurai, T. Daiko and T. Hirao, *Science*, 2003, **301**, 1878.
39. S. Hagen, M. S. Bratcher, M. S. Erickson, G. Zimmermann and L. T. Scott, *Angew. Chem. Int. Ed. Engl.*, 1997, **36**, 406-408.
40. S. Higashibayashi and H. Sakurai, *Chem. Lett.*, 2011, **40**, 122-128.
41. L. T. Scott, M. S. Bratcher and S. Hagen, *J. Am. Chem. Soc.*, 1996, **118**, 8743-8744.
42. G. Mehta and G. Panda, *Chem. Commun.*, 1997, 2081-2082.
43. L. T. Scott, *Pure & Appl. Chem.*, 1996, **68**, 291-300.
44. A. Sygula, *Eur. J. Org. Chem.*, 2011, **2011**, 1611-1625.
45. G. Mehta, G. Panda, R. D. Yadav and K. Ravikumar, *Indian J. Chem.*, 1997, **36**, Sec B, 301-302.
46. T. C. Wu, M. K. Chen, Y. W. Lee, M. Y. Kuo and Y. T. Wu, *Angew. Chem. Int. Ed.*, 2013, **52**, 1289-1293.
47. C. Mück-Lichtenfeld, S. Grimme, L. Kobryn and A. Sygula, *Phys. Chem. Chem. Phys.*, 2010, **12**, 7091-7097.
48. S. Grimme, *J. Comput. Chem.*, 2006, **27**, 1787-1799.
49. D. Josa, J. Rodríguez-Otero, E. M. Cabaleiro-Lago and M. Rellán-Piñeiro, *Chem. Phys. Lett.*, 2013, **557**, 170-175.
50. S. Grimme, C. Mück-Lichtenfeld and J. Antony, *J. Phys. Chem. C*, 2007, **111**, 11199-11207.
51. G. Zheng, S. Irle and K. Morokuma, *Chem. Phys. Lett.*, 2005, **412**, 210-216.
52. M. Gaus, Q. Cui and M. Elstner, *WIREs: Comput. Mol. Sci.*, 2014, **4**, 49-61.

Chapter 9

Fullerene recognition with molecular tweezers made up of efficient buckybowls

9.1. Introduction

Nearly 30 years after their discovery, fullerenes, the third allotrope of carbon, still attract the attention of many researchers worldwide due to their unique properties and their applications in a wide range of fields such as material science or medicine.[1-3] Nowadays, one of the most active fields in fullerene chemistry is the search for molecular receptors capable to form stable associates with them. These receptors not only are useful for isolating fullerenes of the soot, but also for developing new materials for solar energy conversion, optoelectronics, catalysis and switching.[2, 4, 5]

Since dispersion forces are predominant in the stabilization of fullerene complexes, a key strategy to design new molecular receptors is to make use of concave-convex complementarity to maximize these forces. Nevertheless, the examples of concave fullerene receptors are relatively scarce given that curved molecules are not always an easy synthetic target due to their tensioned structures.[6] In this context, bowl-shaped polycyclic aromatic hydrocarbons, commonly known as buckybowls or fullerene fragments, seem very attractive because several buckybowls have been synthesized in the last few years,[7-16] their concave surface being highly suitable for fitting to the convex surface of fullerenes through concave-convex "ball-and-socket" π···π interactions.[17]

The first strong evidence of π···π interactions between buckybowls and C_{60} was published in 2007 by Sygula and co-workers,[17] with the synthesis of the molecular tweezers (a buckycatcher, $C_{60}H_{28}$) made up by two units of corannulene and a tetrabenzocyclooctatetraene tether (1a, Figure 9.1). Thenceforth, the interest in concave-convex π···π interactions has revitalized and several studies have been performed.[18-30] The usefulness of molecular tweezers with buckybowls pincers could be very noticeable. So, Sygula and Collier envisioned future applications for buckycatchers as stationary phases in liquid chromatography for the separation of fullerenes or as buckycatcher-fullerene complexes in photovoltaic devices.[31]

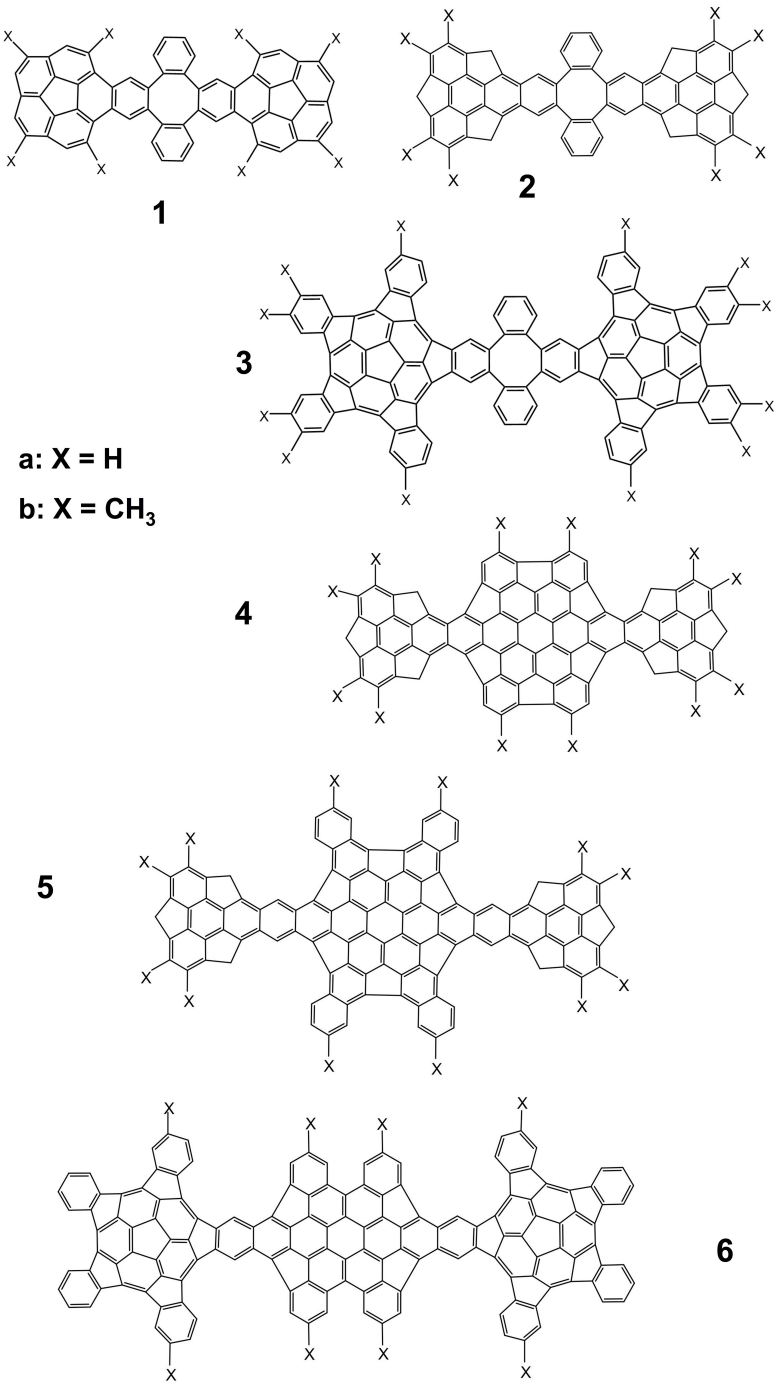


Figure 9.1: Buckycatchers studied in this work. (1-6)a, X = H. (1-6)b, X = CH_3.

Moreover, some theoretical studies have already predicted potential applications for the host-guest complex 1a···C_{60}, such as two-photon absorption (TPA) active material at near-IR wavelengths[32] that shows application in photodynamic cancer therapy (PDCT)

and as a charge-transfer mediator for applications in nanoelectronic devices.[33] In addition, recent studies show that crystallization of supramolecular complexes made up of buckycatcher 1a and endohedral nitrogen fullerene ($N@C_{60}$) provides a solid material with a columnar alignment of fullerene cages that can be candidates for quantum-information processing (QIP) as qubits.[34]

Undoubtedly, the design and synthesis of buckycatchers with more ability and/or selectivity than 1a is a task of great interest. In order to obtain these buckycatchers, the classic approach would be a hard and expensive job that would include: selecting tethers and pincers to be potential candidates to maximize interactions with fullerenes, synthesizing several molecular tweezers, and then testing their recognition ability in solution and in the solid state. In this context, the utilization of computational models to design and identify synthetic targets with desired π···π interactions could be crucial for saving cost and time. In 2008, Zhao and Truhlar reported the first theoretical modification of traditional tweezers 1a. In that study, corannulene pincers were changed by a π-extended tetrathiafulvalene (TTF), in particular 9,10-bis(1,3-dithiol-2-ylidene)-9,10-dihydroanthracene (TTFAQ, $C_{20}H_{10}S_4$).[29] Unfortunately, their results indicate that complexes between a buckycatcher with TTFAQ pincers and fullerene C_{60} show an interaction energy smaller than that obtained for complex 1a···C_{60}.

Recently, Yanney and Sygula[26] have synthesized a molecular clip made up three corannulene pincers and one cyclotriveratrylene (CTV) tether. Although the new clip consists of one more corannulene pincer than that of buckycatcher 1a, the results showed association constants lower than those reported for complexes of buckycatcher 1a with fullerenes C_{60} and C_{70}. According to these authors, the results could be due to the high conformational flexibility of this molecular clip; it not only results in the larger association entropy penalty in comparison with 1a, but also introduces the possible internally stacked conformers of the free clip competing with the formation of the fullerene inclusion complexes. In addition, a recent theoretical study pointed out that this molecular clip has a very high deformation energy that is even larger than their complexation energy.[24]

Despite that most of modifications carried out on buckycatcher 1a involve the change of the tether fragment of the tweezers,[21,26,31] to the best of our knowledge, no study has been attempted with a buckybowl working as a tether. Furthermore, it is noteworthy that in only one theoretical study the corannulene pincers were changed by a pentaindenocorannulene.[35]

In the last few years, our group has been devoted to the study of a series of concave-convex interactions between buckybowls and fullerenes in order to find the factors that maximize their interactions.[36-38] In particular, a buckybowl that shows an increase of interaction energy of about 11 kcal/mol regarding to buckycatcher 1a has been proposed.[38] So, the use (as a tether or a pincer fragment) of this kind of buckybowls could be very useful for designing new molecular tweezers.

In this context, the theoretical study of new molecular tweezers with different buckybowls used as pincers and/or tether could be very desirable. Therefore, the goal of this work is to carry out a detailed study of three different strategies that can give rise to more effective fullerene receptors: 1) changing the corannulene pincers by others

buckybowls; (2) changing the tetrabenzocyclooctatetraene tether by a buckybowl; and (3) introducing methyl substituents on the buckycatcher (since they favour the emergence of C-H···π interactions contributing to the stability of the complexes as was shown).[36]

9.2. *Computational details*

First, complexes are optimized by the self-consistent charge density functional tight-binding method using an empirical correction to the dispersion (SCC-DFTB-D). The DFTB+ code is applied for this method together with the mio-1-1 parameter set.[39-41] According to our previous work, the SCC-DFTB-D method can be very useful to provide starting guesses for more accurate calculations of the largest π···π complexes.[38] Afterwards, re-optimization is performed at the B97-D2/TZVP level using resolution of identity (RI) approximation implemented in the TURBOMOLE 6.3.1 program suite.[42] The latter seems to be a good calculation level as explained in a recent work of us.[36] For the corannulene dimer (for which high quality QCISD(T) results are available[30]), B97 with the more recent dispersion corrections, D3 and D3(BJ), led to slightly worse results (from an energetic point of view) than the D2 correction.[22] Anyway, some exploratory calculations suggest that the choice of the dispersion correction has a little effect on the conclusions of the study, given the high correlation between the results obtained by the different methods (section D.1, Appendix D).

Counterpoise corrections are applied to all reported interaction energies to avoid basis set superposition error (BSSE).[43] According to this method, the interaction energy of an A···B system is calculated according to:

$$\Delta E_{int} = E_{AB}^{AB}(AB) - \left(E_{A}^{AB}(AB) + E_{B}^{AB}(AB)\right) \tag{9.1}$$

where superscript refers to the geometry (of the AB system) and the parenthesis indicates the basis set used (the full basis set of the A···B system). If, in addition, the energetic cost involved in the deformation of each monomer to adopt the geometry of the dimer is considered:

$$\Delta E_{def} = \left(E_{A}^{AB}(A) - E_{A}^{A}(A)\right) + \left(E_{B}^{AB}(B) - E_{B}^{B}(B)\right) \tag{9.2}$$

then, the full complexation energy is obtained as follows:

$$\Delta E_{complex} = \Delta E_{int} + \Delta E_{def} \tag{9.3}$$

According to our calculations (section D.2, Appendix D), the BSSE correction represents around a 10% of the interaction energy in all cases, with very small differences between complexes ranging from 9.7 to 10.8%.

The visualization of non-covalent interactions is conducted using the NCIPLOT-3.0 program.[44, 45] Graphic displays of concave-convex π···π interactions are obtained using the VMD 1.9.1 software.[46] NCI enables identification of non-covalent

interactions and is based on the peaks that appear in the reduced density gradient (RDG) at low densities. When an RDG isosurface for a low value of RDG is plotted, the non-covalent regions clearly appear in the supramolecular complex. These interactions correspond to both favourable and unfavourable interactions. To differentiate between them, the sign of the second eigenvalue of the density Hessian times the density is colour-mapped onto the isosurface; bonding interactions can be identified by the negative sign. To save computation time, promolecular densities have been used, as was done previously with good results.[36]

9.3. Results and discussion

A series of molecular tweezers are devised (Figure 9.1) and their supramolecular complexes with C_{60} are studied at the B97-D2/TZVP//SCC-DFTB-D and B97-D2/TZVP levels. C_{2v} symmetry is kept to save computation time. These tweezers are devised using three strategies in order to improve the ability of the buckycatcher designed by Sygula (1a).[17] First, the corannulene pincers are changed by other buckybowls: sumanene in 2, and for an efficient buckybowl (studied in our previous work)[38] in 3. Second, the tetrabenzocyclooctatetraene tether is changed by buckybowls, specifically bowl-shaped hexabenzocoronene derivatives (studied in our previous work);[38] with sumanene pincers (4 and 5) and with efficient buckybowl pincers (6). Finally, methyl substituents have been added on the buckycatcher structure to favour the development of C-H···π interactions, buckycatchers "b".

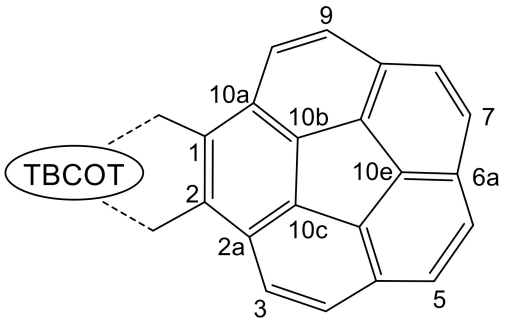
9.3.1. Analysis of B97-D2/TZVP//SCC-DFTB-D performance regarding to B97-D2/TZVP

Calculations at the B97-D2/TZVP level seem to be a reasonable choice for studying concave-convex π···π interactions.[20, 28, 30, 47, 48] Although this level is chosen in the present work, it is noteworthy that this level is still quite expensive for large complexes. For that reason, assessing the accuracy of "cheaper" procedures could be a very important task for future investigations involving even greater systems. In this context, B97-D2/TZVP//SCC-DFTB-D calculations seem to be a good alternative as screening tool for studying concave-convex π···π interactions, as observed in our previous study.[38] So, B97-D2/TZVP//SCC-DFTB-D calculations are performed to verify their usefulness.

First, the X-ray geometrical data for complex 1a···C_{60} is compared with both theoretical (B97-D2/TZVP and SCC-DFTB-D) results. According to Table 9.1, SCC-DFTB-D calculations reproduce the experimental data reasonably well. In general, the calculated distances are slightly larger than the experimental data, with average deviation of 0.07 Å, due to more opened pincers that corresponds to an increase of the aperture from 12.81 to 13.08 Å. Previously reported B97-D2/TZVP calculations behave oppositely, with distances slightly shorter than the experimental data, with average deviation of 0.08Å.[28] Thus, both theoretical methods seem to give rise to results of similar quality; in one case the error is excess and in another is shortage, regarding distances in

Table 9.1. However, if only distances involving the central regions of the pincers (the central five-membered rings of the corannulene pincers that are more directly "catching" the fullerene) are taken into account, the B97-D2/TZVP results are much closer to the experimental, which clearly is manifested by an aperture of pincers practically equal to the experimental one (12.80 *vs.* 12.81 Å).

Table 9.1: Distances (in Å) between the centroid of the fullerene cage and the pincer carbon atoms of the buckycatcher in 1a···C_{60}.[a] Tetrabenzocyclooctatetraene tether is represented as TBCOT



	X-Ray[b]	B97-D[c]	SCC-DFTB-D
C1(C2)	6.77	6.68	6.78
C2a(C10a)	6.71	6.63	6.75
C3(C10)	6.73	6.65	6.76
C4(C9)	6.76	6.68	6.80
C4a(C8a)	6.77	6.69	6.84
C5(C8)	6.83	6.73	6.88
C6(C7)	6.85	6.74	6.90
C6a	6.80	6.71	6.87
C10b(C10c)	6.85	6.80	6.98
C10d(C10f)	6.88	6.82	7.02
C10e	6.90	6.84	7.04
R_p[d]	12.81	12.80	13.08

[a] Distances averaged over C_{2v} symmetry-related carbon atoms of the corannulene subunits of 1a.

[b] Ref. 17

[c] Ref. 28

[d] Defined as the distance between carbon atoms C10e and C10e'.

Table 9.2 shows three important geometrical parameters in order to obtain a more detailed evaluation of the performance of SCC-DFTB-D geometries regarding to B97-D2/TZVP ones. R_{pc} and R_{pi} are inter-pincer distances for buckycatcher···C_{60} complexes and for isolated buckycatchers, respectively. The inter-pincer distance is defined as the distance between the centroids of the buckybowl pincers, and *R* is defined as the distance between the centroid of the C_{60} cage and the centroid of the tether (see Figure 9.2).

Table 9.2: Inter-pincer distance for buckycatcher···C_{60} (R_{pc}) complex, inter-pincer distance for isolated buckycatchers (R_{pi}) and distances between the centroid of the C_{60} cage and the centroid of tether part of buckycatchers (R) (in Å). The calculations were performed at the B97-D2/TZVP level. SCC-DFTB-D results are given in parentheses for comparison

	R_{pc}	R_{pi}	R
1a···C_{60}	11.539 (11.736)	10.661 (9.872)	7.840 (7.988)
1b···C_{60}	11.267 (11.447)	11.140 (10.962)	8.114 (8.278)
2a···C_{60}	11.983 (12.394)	10.360 (6.663)	7.382 (7.661)
2b···C_{60}	12.030 (12.360)	9.270 (7.991)	7.340 (7.689)
3a···C_{60}	13.800 (14.055)	11.071 (10.800)	7.831 (7.920)
3b···C_{60}	13.821 (14.032)	13.496 (11.893)	7.772 (7.997)
4a···C_{60}	13.406 (13.910)	14.694 (15.424)	7.545 (7.782)
4b···C_{60}	13.380 (13.852)	14.635 (15.441)	7.413 (7.700)
5a···C_{60}	13.468 (14.159)	17.603 (17.712)	7.529 (7.702)
5b···C_{60}	13.532 (14.150)	17.794 (17.843)	7.530 (7.656)
6a···C_{60}	14.400 (14.692)	20.698 (20.759)	6.547 (6.740)
6b···C_{60}	14.489 (14.714)	20.742 (20.797)	6.550 (6.760)

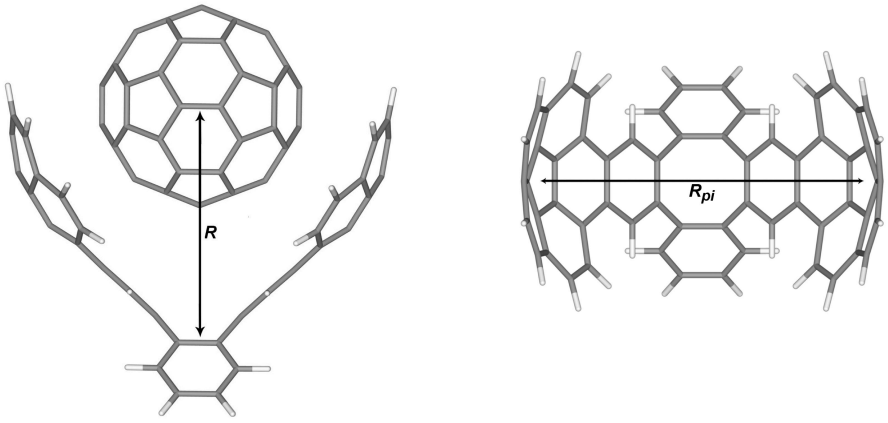


Figure 9.2: *R* is defined as the distance between the centroid of the C_{60} cage and the centroid of the tether. The inter-pincer distance is defined as the distance between the centroid of buckybowl pincers. R_{pi} is the inter-pincer distance for isolated buckycatchers.

If only R_{pc} and R are taken into account (*i.e.* parameters corresponding to complexes), the SCC-DFTB-D results could be considered rather acceptable, with differences in the B97-D2/TZVP results ranging from 0.18 to 0.69 Å and from 0.09 to 0.35 Å, for R_{pc} and R, respectively. In all cases SCC-DFTB-D distances are larger than B97-D2/TZVP ones. Thus, SCC-DFTB-D predicts complexes where the fullerene is less "embraced" by the tweezers: pincers are less closed and fullerene does not enter so much inside the catcher. As expected, differences between both methods are much larger for isolated buckycatchers because the tweezers bend more easily when not joined to the fullerene. Thus, buckycatchers with a tetrabenzocyclooctatetraene tether (1, 2, and 3) show shorter R_{pi} distances obtained at the SCC-DFTB-D level than those obtained at B97-D2/TZVP level (especially in the case of 2a, where the difference is almost 3.7 Å).

However, the opposite is true for buckycatchers with a buckybowl tether (4, 5, and 6). In any case, it is worth mentioning that both calculation levels give rise to the same qualitative picture: buckycatchers with a tetrabenzocyclooctatetraene tether open the pincers after complexation and buckycatchers with a buckybowl tether close them.

As can be seen in Figure 9.3, complexation energy obtained at the B97-D2/TZVP//SCC-DFTB-D level shows an acceptable correlation with that obtained at the B97-D2/TZVP level. The correlation is much better for the interaction energy (section D.3, Appendix D), since the discrepancy between both methods mainly comes from the deformation energy values (section D.4, Appendix D, includes the B97-D2/TZVP//SCC-DFTB-D data).

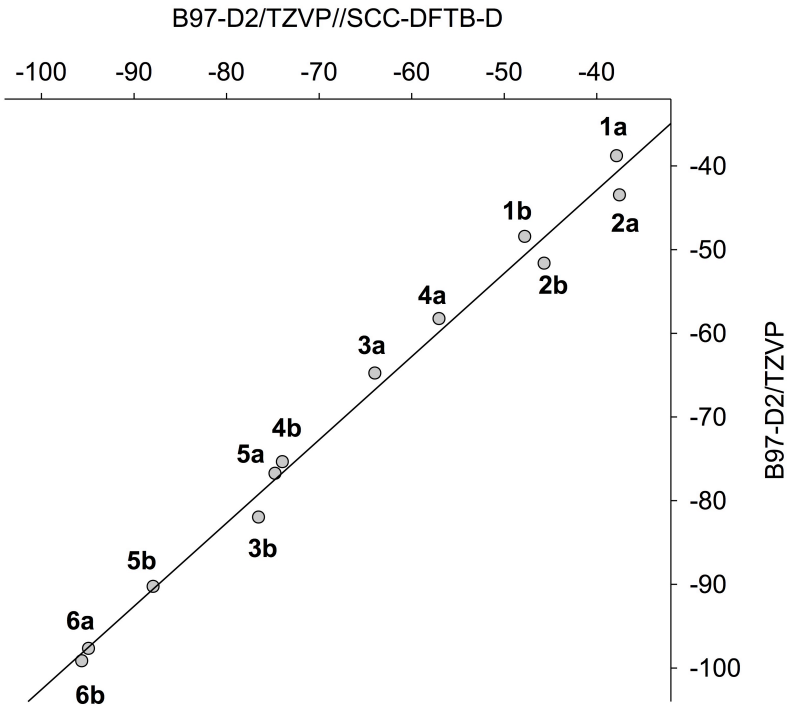


Figure 9.3: B97-D2/TZVP//SCC-DFTB-D *vs.* B97-D2/TZVP complexation energy (in kcal/mol): $E_{\text{complex (B97-D2/TZVP)}} = 0.9948 \times E_{\text{complex (B97-D2/TZVP//SCC-DFTB-D)}} - 3.0762$. $R^2 = 0.991$.

In summary, our results show that the B97-D2/TZVP//SCC-DFTB-D approach could be a fast screening tool for designing new molecular tweezers. So, reasonable geometries and interaction energies are obtained. However, the mediocre reproduction of deformation energies prevents getting very good complexation energies. The source of this weakness is the considerable difference in the inter-pincer distance, R_{pi}, of the isolated buckycatchers obtained with low and high level calculations. For more rigid monomers (where deformation is more irrelevant), the B97-D2/TZVP//SCC-DFTB-D approach leads to very good results, as happened in our previous work.[38]

However, for flexible monomers (such as tweezers) this approach can be used for a preliminary searching, but re-optimization at the high level would be highly recommended. This is precisely what has been done in the present work, and results will be discussed below.

9.3.2. Improving the ability of buckycatcher $C_{60}H_{28}$ for catching C_{60}

As shown in Table 9.2, the inter-pincer distance value for the complex (R_{pc}) differs significantly from its isolated value (R_{pi}). Therefore, deformation energies are very important, as shown in Table 9.3. Deformation plus interaction energies give rise to complexation energies, also shown in this table. Regarding their corresponding interaction energies, deformation energies range from an almost insignificant 1% (for complex 5a···C_{60}) to an important 11% (for complex 3a···C_{60}). As expected, most of deformation (80-98%) corresponds to the buckycatcher, since fullerene is very rigid. The only exception to this trend is the complex 5a···C_{60} (37%) where deformation is very small, both for the buckycatcher and for the fullerene: 0.29 and 0.50 kcal/mol, respectively. In the complex with the largest deformation energy (3a···C_{60} with 8.10 kcal/mol) it almost entirely corresponds to the buckycatcher: 7.94 kcal/mol. As fully expected, there is some relationship between the magnitude of the deformation energy and the difference in the aperture of the tweezers, before and after complexation, which is manifested by the difference between R_{pc} and R_{pi}. As commented above, this difference is positive in some cases (tweezers that open after complexation) and negative in other cases (tweezers that close after complexation). The former occurs for buckycatchers with tetrabenzocyclooctatetraene tether, and the latter for buckycatchers with a buckybowl tether. In general, according to results of Tables 9.2 and 9.3, it seems that closure of tweezers is energetically an easier process than opening. For example, for complex 6a···C_{60} the deformation energy is 6.05 kcal/mol with a huge closure of 6.298 Å (R_{pc} - R_{pi} = -6.298 Å), whereas for complex 3a···C_{60} the deformation energy is 8.10 kcal/mol with a much smaller opening of 2.729 Å. The only exceptions to this trend are the complexes with buckycatchers 4a and 4b; in these cases a small closure (1.29, 1.26 Å) leads to a substantial deformation energy (5.6, 5.2 kcal/mol).

The first strategy employed herein in order to increase the catching ability of tweezers 1a has been to change the corannulene pincers by other buckybowls. Recently, our studies have shown that buckybowls with CH_2 groups[37] or *flaps*[38] can improve considerably the recognition of fullerenes. In this context, buckycatcher 2a includes two sumanene pincers with CH_2 groups, and buckycatcher 3a includes two efficient buckybowls (with *flaps*) as pincers. According to the results of Table 9.3, both options (especially the latter) lead to complexes with an important enhancement in their complexation energy, which increases from -38.80 to -43.48 and -64.76 kcal/mol, respectively. Thus, for complex 3a···C_{60} an extraordinary increase is obtained (67%), even though this complex exhibits the largest deformation penalty (the increase in interaction energy is 83%).

Table 9.3: Complexation energy ($E_{complex}$) and deformation energy (E_{def}) in kcal/mol. Calculations are performed at the B97-D2/TZVP level. Percentage of deformation of the buckycatcher is given in parentheses

	$E_{complex}$	E_{def}
1a···C_{60}	-38.80	1.12 (91%)
1b···C_{60}	-48.44	0.74 (87%)
2a···C_{60}	-43.48	3.78 (93%)
2b···C_{60}	-51.64	5.59 (96%)
3a···C_{60}	-64.76	8.10 (98%)
3b···C_{60}	-81.97	3.76 (91%)
4a···C_{60}	-58.26	5.57 (95%)
4b···C_{60}	-75.35	5.17 (91%)
5a···C_{60}	-76.74	0.79 (37%)
5b···C_{60}	-90.25	1.94 (80%)
6a···C_{60}	-97.67	6.05 (97%)
6b···C_{60}	-99.17	7.59 (97%)

A recent study of Yanney and Sygula showed that a molecular clip with three corannulene pincers[26] is not better than the original tweezers 1a[17] with two pincers. However, molecular tweezers with three buckybowls, two as pincers and one as tether, could be a possible strategy worthy of testing for the design of new fullerene receptors, especially using rigid pincers such as Klärner's molecular tweezers.[49] Obviously, the main reason for designing buckycatchers using a buckybowl as a tether is supported by the fact that its concave surface offers a natural advantage for interacting with the convex surface of fullerenes. This strategy was checked by means of three buckycatchers (4a, 5a and 6a). Bowl-shaped hexabenzocoronene derivatives are employed as tether because in our previous study they showed excellent ability for recognition of fullerenes.[38] If the behaviour of complex 4a···C_{60} is compared with that of 2a···C_{60}, a moderate increase in complexation energy (-14.78 kcal/mol, 34%) is observed, which is only due to introduction of a buckybowl as a tether. However, the effect is much larger for buckycatcher 5a, with an increase of -33.26 kcal/mol (76%) relative to 2a. Thus, the hexabenzocoronene used as tether in 5a is much better than that used in 4a. This is not surprising considering the results of our previous work: the difference in behaviour of the two buckybowls was very large, which was attributed to the action of the *flaps* of the latter buckybowl.[38] A comparison of complexes 3a···C_{60} and 6a···C_{60} allows determining the behaviour of a third hexabenzocoronene (which is used in 6a) as a tether. In this case the increase is -32.91 kcal/mol (51%), *i.e.* very similar in absolute terms to that obtained for the tether used in 5a.

As a summary of the results commented above, it can be concluded that the best pincers are those used in the buckycatcher 3a (and 6a). In the same way, the best tether is a bowl-shaped hexabenzocoronene. However, it is difficult to choose which one because those used in 5a and in 6a give rise to a similar enhancement of the complexation energy; that used in 5a lead to somewhat better results, but at the expense of a huge increase in size. Moreover, in our previous study, it was already showed that bowl-shaped hexabenzocoronene used in 6a as a tether was a very efficient buckybowl.[38] For these reasons, the biggest buckycatcher devised in the present study is 6a, with the best pincers

and a very efficient tether: an enhancement in complexation energy of -58.87 kcal/mol (152%) is obtained compared to original tweezers 1a.

Finally, the third strategy for improving fullerene recognition could be the addition of methyl substituents on the buckycatchers, because according to previous theoretical studies the alkylation of buckybowls seems to be a promising method for the synthesis of better new fullerene receptors.[24,36,37] Addition of alkyl groups increases dispersion as well as the number of hydrogen atoms that can interact with fullerenes through CH···π interactions. As shown in Table 9.3, the addition of methyl groups on buckycatchers leads to a considerable increase in the complexation energy values that can be greater than 17 kcal/mol (for 3a and 4a). The smallest effect takes place precisely on the best buckycatcher: only 1.5 kcal/mol, (6a *vs.* 6b).

In summary, all devised tweezers behave as better receptors of C_{60} than the original one designed by Sygula (1a).[17] The best results correspond to buckycatcher 6b, where the three above commented strategies are combined. Thus, complexation energy 2.6 times larger than that for the original 1a is obtained (from -38.80 to -99.17 kcal/mol, an increase of -60.37 kcal/mol, a 156% increase).

In order to analyse in more detail the balance of energy contributions to the stability of the complexes, the interaction energy is decomposed according to a simple method. So, the two contributions of the model employed are taken into account; that is, the pure B97 interaction energy and the empirical dispersion contribution to the interaction energy. As it can be seen from Table 9.4, dispersion is mainly responsible for the attraction of all the complexes evaluated. Furthermore, an excellent relationship between the dispersion contribution and the total complexation energy can be clearly visualized in Figure 9.4, with a very good correlation (R^2 = 0.975).

As shown in Table 9.4 and Figure 9.4, the increase of complexation energy is directly related to the increase of dispersion energy. It could be argued that this latter increase might be simply caused by the increase of the size of the buckycatcher. For that reason, it could be interesting to know the efficiency of a buckycatcher relative to its size. In this context, although the number of carbon atoms of a compound is not a very reliable measure of its size, it is an easy-to-use parameter closely related to the size of that compound. Figure 9.5 shows a rather good correlation between the number of C atoms of the buckycatcher and its complexation energy with C_{60} (R^2 = 0.951, the linear regression is done using the unmethylated buckycatchers, 1-6a). However, the most important thing is detecting the deviations of the linear behaviour looking for the most efficient receptors; that is to say, the best receptors that produce large complexation energies without a large increase of size. In this respect, and taking into account the unmethylated buckycatchers, 1-6a, it seems clear that buckycatchers 5a and 6a are efficient fullerene receptors with larger complexation energy than predicted by their size. It is worth noting that the original tweezers, 1a, shows a mediocre efficiency, only beaten (in the bad sense) by 3a. When methyl groups are added to the buckycatcher (compounds 1-6b, red circles in Figure 9.5) the efficiency undergoes an important increase, except for compound 6 which suffers a slight decrease, which is due to the above commented small effect of methylation (only 1.5 kcal/mol in complexation energy) that takes place for 6a. According to Figure 9.5 the best efficiency corresponds to buckycatchers 4b and 5b (both with added

methyl groups). On the contrary, methylation of the best buckycatcher (in absolute terms), 6a, is not worthwhile.

Table 9.4: B97 interaction energy and dispersion contribution of the complexes obtained at the B97-D2/TZVP level (kcal/mol)

	B97	*Disp*
1a···C_{60}	36.27	-76.19
1b···C_{60}	42.48	-91.66
2a···C_{60}	49.46	-96.72
2b···C_{60}	57.77	-115.00
3a···C_{60}	66.44	-139.30
3b···C_{60}	75.22	-160.95
4a···C_{60}	54.31	-118.14
4b···C_{60}	71.77	-152.29
5a···C_{60}	72.65	-150.18
5b···C_{60}	81.96	-174.15
6a···C_{60}	81.54	-185.26
6b···C_{60}	78.53	-185.29

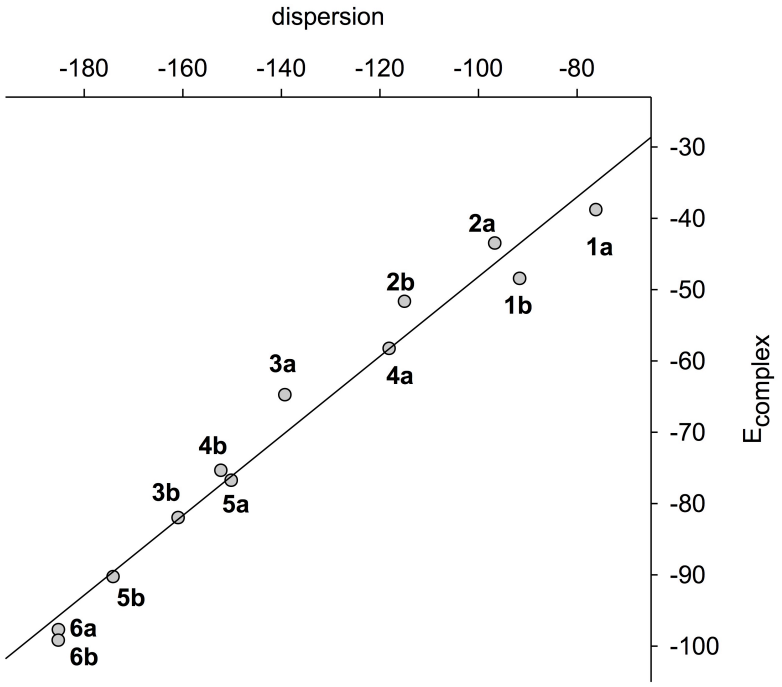


Figure 9.4: Dispersion contribution *vs.* complexation energy (in kcal/mol): $E_{complex} = 0.5583 \times E_{disp} + 7.6635$. $R^2 = 0.975$.

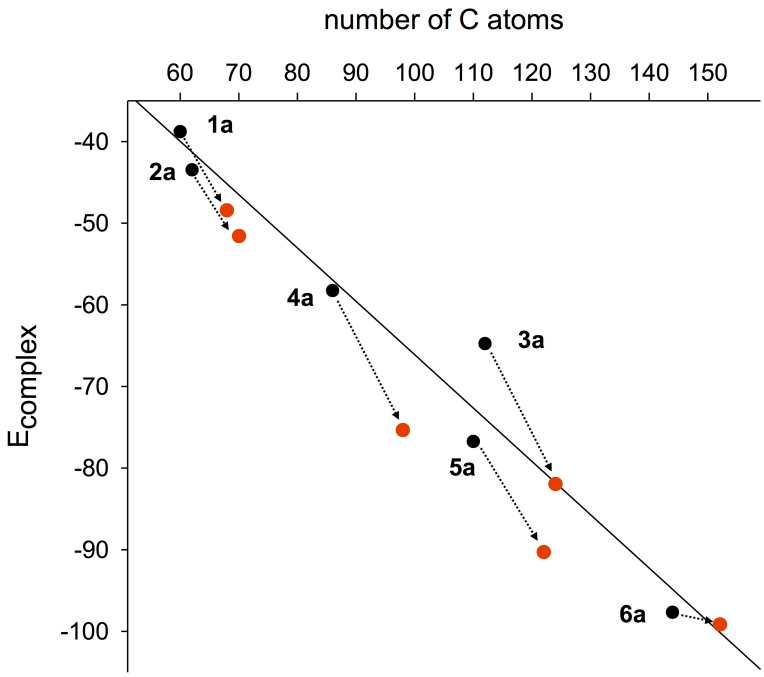


Figure 9.5: Number of C atoms *vs.* complexation energy. $E_{complex}$ = –0.6533 × (number of C atoms) – 0.7815. R^2 = 0.951. Arrows point to methylated buckycatchers (1-6)b, red points.

Finally, a non-covalent interactions (NCI) analysis has also been performed in order to obtain more information about π···π interactions. The visualization of π···π interactions between the two monomers in the real space is drawn using VMD software[46] with an isosurface of 0.35 a.u. and scale running from -0.030 (min) to 0.030 (max); blue, green and red indicate strongly attractive, weak and strongly repulsive interactions, respectively. Figure 9.6 shows the front view of the NCI plots (more detailed views are available in the section D.5 from Appendix D). As shown in Figure 9.5, all modifications proposed herein display an enhancement of C_{60} recognition regarding to the buckycatcher 1a: both weak and strongly attractive interactions grow substantially. The change of the tetrabenzocyclooctatetraene tether by a bowl-shaped hexabenzocoronone is especially evident, since the former seems to play a small role in fullerene recognition. It is also apparent that the best pincers are those used in the buckycatcher 3a (and 6a). Figure 9.6 also displays clearly the effect of adding methyl groups on the buckycatchers: the C-H···π contacts are readily observable by the emergence of new regions on the RDG surface of strong attractive character (blue). In this context, as expected (according to complexation energies of Table 9.3) the smallest effect is observed for buckycatcher 6b. Figure 9.6 allows an understanding of this small effect; in the complex 6b···C_{60} methyl groups of pincers are very far from fullerene; the same applies largely to methyl groups on the tether (only for the complex 4b···C_{60} the effect of methyl groups placed on the tether is important).

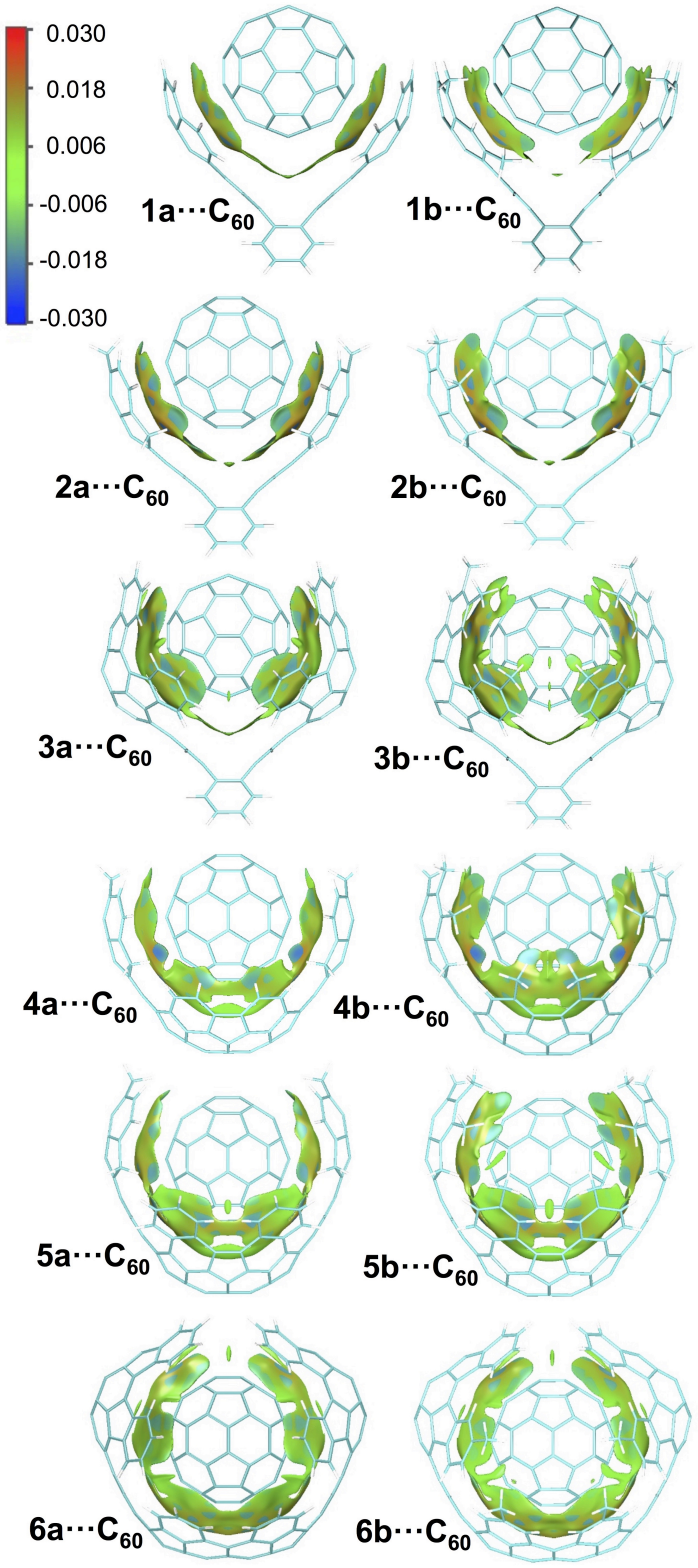


Figure 9.6: Front views of the NCIPLOT gradient isosurface (0.35 a.u.). The surfaces are colour-mapped in a blue-green-red scale according to the strength and type (attractive or repulsive) of interaction. Blue indicates strongly attractive interactions, green indicates weak VdW interactions, and red indicates strong non-bonded overlap.

9.4. Conclusions

Our results show that the B97-D2/TZVP//SCC-DFTB-D approach could be a rapid screening tool for designing of new molecular tweezers. In this way, this methodology leads to reasonable results for buckycatcher···C_{60} complexes, both for the geometry and the energetic values. Its main failure is the deficient description of the deformation energy, since considerable deviations in the inter-pincer distance of the isolated buckycatchers are found. As shown in our previous results,[38] the B97-D2/TZVP//SCC-DFTB-D results can be of high quality when the receptor has a quite rigid structure; this is not the case of tweezers, and thus can be used only as starting point for a higher level re-optimization. Since for tweezers the deformation energy represents an important contribution to the total complexation energy, re-optimization at the full B97-D2/TZVP level is performed herein.

To improve the ability for fullerene recognition of the original buckycatcher designed by Sygula *et al.*,[17] three different strategies are tried. The first one is to change the corannulene pincers by other buckybowls. The results show an important improvement when sumanene and, especially an efficient buckybowl, are used as pincers. The second strategy consists of replacing the tether part of the tweezers by a buckybowl. For this purpose, a bowl-shaped hexabenzocoronene is employed and good results are also obtained. Finally, methyl substituents have been added on the buckycatcher structure to favour the development of C-H···π contacts: as with the other two strategies, the improvements achieved are outstanding.

A combination of the three above commented strategies leads to several enhanced buckycatchers, with complexation energies of the complex buckycatcher···C_{60} up to 2.6 times larger than that of the original buckycatcher (from -38.80 to -99.17 kcal/mol, an increase of -60.37 kcal/mol, a 156%).

Dispersion plays a crucial role in the interaction in all the complexes: it is responsible for the binding in them and shows an excellent correlation with the complexation energies. As expected, the increase on dispersion energy shows a fairly good correlation with the increase on bowl size. However, there are several deviations that mark differences in efficiency between the different buckycatchers. Thus, the best buckycatcher in absolute terms (6b) possesses only a mediocre efficiency, clearly overtaken by its unmethylated precursor, 6a. Only for this case the methylation is not worthwhile, since for the remaining cases it does have an important effect both in absolute terms and in relation to efficiency.

In summary, according to our results, and taking into account a balance between the absolute "catching" ability and the efficiency, the best tweezers could be 6a, 4b, and 5b. The first one is a strong fullerene receptor with considerable efficiency. The last two, having a rather moderate size, possess a considerable ability as fullerene receptors that lead to a high efficiency. In any case, all three clearly overtake the features of the original buckycatcher 1a as fullerene receptors. Another issue is to know whether these receptors are easy to synthesize or not. Anyway, the theoretical contribution presented herein leads to the fact that the tweezers synthesized by Sygula *et al*.[17] have much room for

improvement. Some possible strategies for achieving this improvement are the three strategies analysed here, which represent promising possibilities.

9.5. References

1. A. Bianco and T. Da Ros, Biological Applications of Fullerenes, in *Fullerenes Principles and Applications.* Ed. F. Langa and J. F. Nierengarten. Cambridge: RSC Publ., 2008, ch. 10, pp. 301-328.
2. P. Hudhomme and J. Cousseau, Plastic Solar Cells Using Fullerene Derivatives in the Photoactive Layer, in *Fullerenes Principles and Applications.* Ed. F. Langa and J. F. Nierengarten. Cambridge: RSC Publ., 2008, ch. 8, pp. 221-265.
3. R. Bakry, R. M. Vallant, M. Najam-ul-Haq, M. Rainer, Z. Szabo, C. W. Huck and K. B. Günther, *Int. J. Nanomedicine*, 2007, **2**, 639-649.
4. F. D'Souza and O. Ito, *Chem. Commun.*, 2009, 4913-4928.
5. H. Imahori and S. Fukuzumi, *Adv. Funct. Mater.*, 2004, **14**, 525-536.
6. E. M. Pérez and N. Martín, *Chem. Soc. Rev.*, 2008, **37**, 1512-1519.
7. W. E. Barth and R. G. Lawton, *J. Am. Chem. Soc.*, 1966, **88**, 380-381.
8. E. A. Jackson, B. D. Steinberg, M. Bancu, A. Wakamiya and L. T. Scott, *J. Am. Chem. Soc.*, 2007, **129**, 484-485.
9. T. C. Wu, M. K. Chen, Y. W. Lee, M. Y. Kuo and Y. T. Wu, *Angew. Chem. Int. Ed.*, 2013, **52**, 1289-1293.
10. T. C. Wu, H. J. Hsin, M. Y. Kuo, C. H. Li and Y. T. Wu, *J. Am. Chem. Soc.*, 2011, **133**, 16319-16321.
11. H. Sakurai, T. Daiko and T. Hirao, *Science*, 2003, **301**, 1878.
12. S. Hagen, M. S. Bratcher, M. S. Erickson, G. Zimmermann and L. T. Scott, *Angew. Chem. Int. Ed. Engl.*, 1997, **36**, 406-408.
13. L. T. Scott, M. S. Bratcher and S. Hagen, *J. Am. Chem. Soc.*, 1996, **118**, 8743-8744.
14. L. T. Scott, *Pure Appl. Chem.*, 1996, **68**, 291-300.
15. A. Sygula, *Eur. J. Org. Chem.*, 2011, 1611-1625.
16. A. C. Whalley, K. N. Plunkett, A. A. Gorodetsky, C. L. Schenck, C.-Y. Chiu, M. L. Steigerwald and C. Nuckolls, *Chem. Sci.*, 2011, **2**, 132-135.
17. A. Sygula, F. R. Fronczek, R. Sygula, P. W. Rabideau and M. M. Olmstead, *J. Am. Chem. Soc.*, 2007, **129**, 3842-3843.
18. A. Sygula and S. Saebø, *Int. J. Quantum Chem.*, 2009, **109**, 65-72.
19. D. Josa, J. Rodríguez Otero and E. M. Cabaleiro Lago, *Phys. Chem. Chem. Phys.*, 2011, **13**, 21139-21145.
20. D. Josa, J. Rodríguez-Otero, E. M. Cabaleiro-Lago and M. Rellán-Piñeiro, *Chem. Phys. Lett.*, 2013, **557**, 170-175.
21. L. Kobryn, W. P. Henry, F. R. Fronczek, R. Sygula and A. Sygula, *Tetrahedron Lett.*, 2009, **50**, 7124-7127.
22. M. R. Kennedy, L. A. Burns and C. D. Sherrill, *J. Phys. Chem. A*, 2012, **116**, 11920-11926.
23. P. A. Denis, *Chem. Phys. Lett.*, 2011, **516**, 82-87.
24. P. A. Denis, *RSC Adv.*, 2013, **3**, 25296-25305.
25. G. Casella and G. Saielli, *New J. Chem.*, 2011, **35**, 1453-1459.

26. M. Yanney and A. Sygula, *Tetrahedron Lett.*, 2013, **54**, 2604-2607.
27. I. Welsh and M. Lein, *J. Comput. Chem.*, 2014, **35**, 181-191.
28. C. Mück-Lichtenfeld, S. Grimme, L. Kobryn and A. Sygula, *Phys. Chem. Chem. Phys.*, 2010, **12**, 7091-7097.
29. Y. Zhao and D. G. Truhlar, *Phys. Chem. Chem. Phys.*, 2008, **10**, 2813-2818.
30. T. Janowski, P. Pulay, A. A. Sasith Karunarathna, A. Sygula and S. Saebø, *Chem. Phys. Lett.*, 2011, **512**, 155-160.
31. A. Sygula and W. E. Collier, Molecular Clips and Tweezers with Corannulene Pincers, in *Fragments of Fullerenes and Carbon Nanotubes: Designed Synthesis, Unusual Reactions, and Coordination Chemistry* (eds M. A. Petrukhina and L. T. Scott), John Wiley & Sons, Inc., Hoboken, NJ, USA, 2012, ch.1, pp. 1-40.
32. S. Chakrabarti and K. Ruud, *J. Phys. Chem. A*, 2009, **113**, 5485–5488.
33. A. A. Voityuk and M. Duran, *J. Phys. Chem. C*, 2008, **112**, 1672-1678.
34. J. Yang, P. Feng, A. Sygula, W. Harneit, J.-H. Su and J. Du, *Phys. Lett. A*, 2012, **376**, 1748-1751.
35. P. A. Denis, *Chem. Phys. Lett.*, 2014, **591**, 323–327.
36. D. Josa, J. Rodríguez-Otero, E. M. Cabaleiro-Lago, L. A. Santos and T. C. Ramalho, *J. Phys. Chem. A*, 2014, **118**, 9521-9528.
37. D. Josa, L. Azevedo dos Santos, I. González-Veloso, J. Rodríguez-Otero, E. M. Cabaleiro-Lago and T. de Castro Ramalho, *RSC Advances*, 2014, **4**, 29826-29833.
38. D. Josa, I. González-Veloso, J. Rodríguez-Otero and E. M. Cabaleiro-Lago, *Phys. Chem. Chem. Phys.*, 2015, **17**, 6233-6241.
39. M. Elstner, D. Porezag, G. Jungnickel, J. Elsner, M. Haugk, T. Frauenheim, S. Suhai and G. Seifert, *Phys. Rev. B*, 1998, **58**, 7260-7268.
40. M. Elstner, T. Frauenheim and S. Suhai, *Phys. Status Solidi B*, 2000, **217**, 357-376.
41. M. Elstner, K. J. Jalkanen, M. Knapp-Mohammady, T. Frauenheim and S. Suhai, *Chem. Phys.*, 2001, **263**, 203-219.
42. R. Ahlrichs, M. Bär, M. Häser, H. Horn and C. Kölmel, *Chem. Phys. Lett.*, 1989, **162**, 165-169.
43. S. F. Boys and F. Bernardi, *Mol. Phys.*, 1970, **19**, 553-566.
44. E. R. Johnson, S. Keinan, P. Mori-Sánchez, J. Contreras-García, A. J. Cohen and W. Yang, *J. Am. Chem. Soc.*, 2010, **132**, 6498–6506.
45. J. Contreras-García, E. R. Johnson, S. Keinan, R. Chaudret, J. P. Piquemal, D. N. Beratan and W. Yang, *J. Chem. Theory Comput.*, 2011, **7**, 625-632.
46. W. Humphrey, A. Dalke and K. Schulten, *J. Mol. Graphics*, 1996, **14**, 33-38.
47. S. Grimme, *J. Comput. Chem.*, 2006, **27**, 1787-1799.
48. S. Grimme, C. Mück-Lichtenfeld and J. Antony, *J. Phys. Chem. C*, 2007, **111**, 11199-11207.
49. F. G. Klärner and B. Kahlert, *Acc. Chem. Res.*, 2003, **36**, 919-932.

Chapter 10

General Conclusions

In this thesis a series of supramolecular systems involving concave-convex π···π interactions have been studied in order to gain insight about the main factors controlling stacking bowls. The general conclusions are summarized in six sections for clarity. Figure 10.1 depicts the thesis overview and the promising strategies for future design of new fullerene receptors.

i. Reducing calculation time

Our results show that C_{60}-like, a "fullerene copy", (a corannulene with the curvature of buckminsterfullerene, C_{60}) employed in our first study in order to save calculation time does not seem representative for reproducing concave···convex interactions between buckybowls and fullerenes. The weakness of C_{60}-like comes from the inability of this structure to reproduce the electrostatic characteristics of the whole C_{60}. However, results using C_{60}-like are not too bad because C_{60}-like is able to reproduce rather well the dispersive effects (which are the most important contribution) of the real C_{60} in complexes with buckycatchers.

On the other hand, B97-D2/TZVP//SCC-DFTB-D approach can be a rapid screening tool for testing new molecular tweezers. However, since this approach does not correctly reproduce the deformation energy and this energy represents an important contribution to the total complexation energy, a subsequent higher-level re-optimization is compulsory to achieve reliable results. This re-optimization could be superfluous when quite rigid buckycatchers are involved.

Finally, it is noteworthy that utilization of the SCC-DFTB-D method as starting guess enables considerable savings of the calculation time (almost 50% regarding the full B97-D2/TZVP optimization of the emblematic $C_{60}H_{28}$···C_{60} complex).

ii. Performance of DFT variants to study concave-convex π···π interactions

DFT-D functionals (B97-D, PBE-D, B-LYP-D, BP86-D) show a clear advantage over the M0(5-6)-2X ones for studying complexes with concave-convex π···π interactions.

It is noteworthy that despite M06-2X functional shows a good performance for S22 database complexes, it gives a noticeable underestimation of the interaction energy for sandwich complexes with planar eclipsed monomers and for complexes with curved monomers. On the other hand, M05-2X functional should be completely avoided, since it gives rise to a very serious underestimation of the interaction energy.

Specifically, B97 together with the Grimme's semiempirical dispersion corresponding to the 2006 implementation (-D2), *i.e.*, B97-D2, seems appropriate to study concave-convex π···π interactions. This model shows a good performance for corannulene dimer regarding to QCISD(T)/aug-cc-pVTZ calculations and it also enables the use of the RI approximation that takes advantage of the noticeable reduction of computational cost.

iii. Effect of curvature in fullerene recognition

A clear relationship between the curvature of bowl and the changes of the interaction energy was not observed in any of the cases studied.

iv. Effect of substituents in fullerene recognition

All the substituted corannulenes and sumanenes (with Br, Cl, CH_3, C_2H, and CN units) behave as better buckycatcher than the unsubstituted ones. According to our results, the increase of complexation energy is directly related to the increase of the dispersion contribution; the very small deviations from this behaviour can be explained by electrostatic considerations.

CH···π interactions play a very important role in fullerene recognition. So, the design of new molecular receptors that take into account the increase (and the proper orientation) of these interactions could provide a considerable improvement in the task of fullerene recognition.

v. Effect of buckybowl shape in fullerene recognition

The shape of the buckybowl plays a crucial role on its ability for fullerene recognition. Compounds whose structure possess *flaps* at the *rim* of the bowl show an enhanced capability for interacting with fullerenes. The addition of these *flaps* not only increases the size of the π-system, but also does so in an advantageous manner since the

slight flexibility of the *flaps* favours the "embrace" of fullerenes. On the contrary, compounds with very rigid and compact structures show little ability to "catch" fullerenes.

vi. Selectivity

All the stacking interactions between buckybowls and fullerene C_{70} show interaction energy values quite similar to those obtained with fullerene C_{60}. Therefore, it is not expected for buckybowls to specifically bind to one of the fullerenes when exposed to a C_{60}/C_{70} mixture.

On the other hand, buckybowls with *flaps* in their structure show a significant decrease on the interaction with C_{40} regarding to C_{60} and C_{70}. So, the addition of *flaps* on the *rim* of the bowl maybe could also be a useful strategy for designing buckybowls for the selective separation of C_{40} from mixtures.

Future Outlook

Undoubtedly, the novelty of buckybowls and their unique properties will continue to attract the attention of chemists and material scientists. It is noteworthy that the recent progresses in computational and theoretical chemistry in last years have opened the door for the systematic exploration of concave-convex π···π interactions. On the other hand, synthesis of buckybowls is no longer an extremely limiting factor for research, since several buckybowls have been synthesized in last years, even in kilogram scale (corannulene). In this context, there is a stimulating scenery to continue studying concave-convex π···π interactions. Therefore, a noticeable increase in the study of these systems and exciting results of future researches are expected.

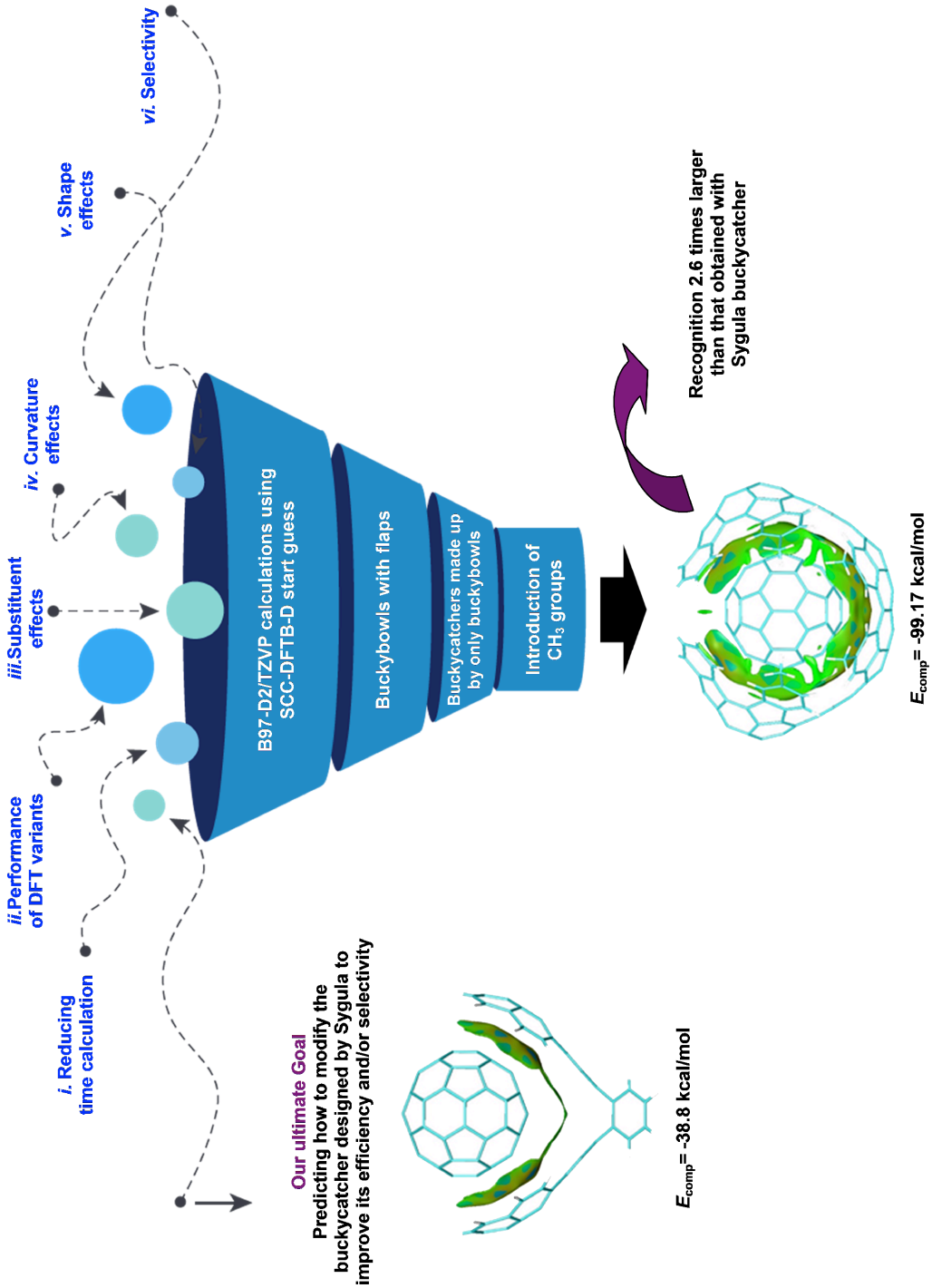


Figure 10.1: Funnel diagram with main thesis conclusions and strategies to design efficient buckycatchers.